Alma Mater Studiorum – University of Bologna

DEPARTMENT OF ELECTRICAL, ELECTRONIC AND INFORMATION ENGINEERING "GUGLIELMO MARCONI"

Ph.D. in Electrical Engineering

XXV Cycle

Electrical Energy Engineering (09/E2)

Power electronic converters, electrical machines and drives (ING-IND/32)

Non-Linear Analysis and Design of Synchronous Bearingless Multiphase Permanent Magnet Machines and Drives

Ph.D. Thesis

of

STEFANO SERRI

Tutor:

Prof. Eng. Giovanni Serra

Coordinator:

Prof. Eng. Domenico Casadei

July 2013, Bologna, Italy

Table of contents

CHAPTER 2

AN ALGORITHM FOR NON-LINEAR ANALYSIS OF MULTIPHASE BEARINGLESS SURFACE-MOUNTED PM SYNCHRONOUS MACHINES

Appendix A2.1

The Programming Code - Part 1

Appendix A2.2

The Programming Code - Part 2

CHAPTER 3

PRINCIPLES OF BEARINGLESS MACHINES

CHAPTER 5

DESIGN AND DEVELOPMENT OF A CONTROL SYSTEM FOR MULTIPHASE SYNCHRONOUS PERMANENT MAGNET BEARINGLESS MACHINES

Introduction

The use of multiphase motors over conventional three-phase motors gives a series of benefits that can be summarized as follows: possibility of dividing the power between multiple phases, higher reliability in case of failure of a phase, use of various harmonic orders of airgap magnetic field to obtain better performances in terms of electromagnetic torque and possibility to create multi-motor drives by connecting several machines in series controlled by a single power converter [1]-[9]. These features are appreciated when high power, high reliability and low dc bus voltage are requested as it happens in ship propulsion, electrical vehicles and aerospace applications. In recent years, suitable techniques have been applied in order to reduce the power losses in multiphase IGBT inverters [10].

Bearingless motors are spreading because of their capability of producing rotor suspension force and torque avoiding the use of mechanical bearings and achieving in this way much higher maximum speed. There are two typologies of winding configurations: dual set and single set of windings. The first category comprises two separated groups of three-phase windings, with a difference in their pole pair numbers equal to one: the main one carries the ‘motor currents’ for driving the rotor, while the other carries the ‘levitation currents’, to suspend the rotor [11].

The windings belonging to the latter category produce torque and radial forces by means of injecting different current sequences to give odd and even harmonic orders of magnetic field, using the properties of multiphase current systems, which have multiple orthogonal d-q planes. One of them can be used to

control the torque. The additional degrees of freedom can be used to produce levitation forces [12].

The main advantages of bearingless motors with a single set of windings (i.e., the assets of bearingless and multiphase motors together) lead to a simpler construction process, better performances in control strategy and torque production with relatively low power losses [13]. This kind of technology is expected to have very large developments in the future, particularly in the design of high power density generators, actuators and motors of More Electric Aircraft (MEA), mainly for the ability of achieving higher speed in comparison to conventional electrical machines [14]. In addition, it can be supposed that the cooperation of bearingless control techniques and the adoption of magnetic bearing could be of large interest in the MEA field.

An important target in the design of electrical machines is the analysis and comparison of a large number of solutions, spending less time than is possible but also providing an accurate description of electromagnetic phenomena. The main problems are related to the calculation of global and local quantities like linkage fluxes, output torque, flux densities in various areas of the device. The difficulties increase especially in presence of magnetic saturation, in fact in the case of non-linear magnetic problems it would be necessary to provide in-depth analyses by using complex software based on accurate analytical methods, like Finite Element Analysis (FEA). Simultaneously, it would be useful to save time, not only in terms of reducing computing time, but mainly for the need of re-designing the model of the machine in a CAD interface when changing some electrical or geometrical parameter. In order to solve this problems, some authors present analyses based on equivalent magnetic or lumped parameter circuit models [15], [16], [17].

In this thesis, a method for non-linear analysis and design of Surface-Mounted Permanent Magnet Synchronous Motors (SPMSM) is presented. The

relevant edge consists in the possibility of defining the machine characteristics in a simple user interface. Then, by duplicating an elementary cell, it is possible to construct and analyze whatever typology of windings and ampere-turns distribution in a pole-pair. Furthermore, it is possible to modify the magnet width-to-pole pitch ratio analyzing various configurations or simulating the rotor movement in sinusoidal multiphase drives or in a user-defined current distribution. Previous papers proposed the analysis of open-slot configurations with prefixed structure of the motor, with given number of poles and slots, or for only a particular position of the rotor with respect to the stator. The performances of the proposed non-linear model of SPMSM have been compared with those obtained by FEA software in terms of linkage fluxes, co-energy, torque and radial force. The obtained results for a traditional three-phase machine and for a 5-phase machine with unconventional winding distribution showed that the values of local and global quantities are practically coinciding, for values of the stator currents up to rated values. In addition, they are very similar also in the non-linear behavior even if very large current values are injected.

When developing a new machine design the proposed method is useful not only for the reduction of computing time, but mainly for the simplicity of changing the values of the design variables, being the numerical inputs of the problem obtained by changing some critical parameters, without the need for re-designing the model. For a given rotor position and for given stator currents, the output torque as well as the radial forces acting on the moving part of a multiphase machine can be calculated. The latter feature makes the algorithm particularly suitable in order to design and analyze bearingless machines. For these reasons, it constitutes a useful tool for the design of a bearingless multiphase synchronous PM machines control system.

Another important section of this thesis concerns an analytical model for radial forces calculation in multiphase bearingless SPMSM. It allows to predict

amplitude and direction of the force, depending on the values of the torque current, of the levitation current and of the rotor position. It is based on the space vectors method, letting the analysis of the machine not only in steady-state conditions but also during transients.

When designing a control system for bearingless machines, it is usual to consider only the interaction between the main harmonic orders of the stator and rotor magnetic fields. In multiphase machines, this can produce mistakes in determining both the module and the spatial phase of the radial force, due to the interactions between the higher harmonic orders. The presented algorithm allows to calculate these errors, taking into account all the possible interactions; by representing the locus of radial force vector, it allows the appropriate corrections.

In addition, the algorithm permits to study whatever configuration of SPMSM machine, being parameterized as a function of the electrical and geometrical quantities, as the coil pitch, the width and length of the magnets, the rotor position, the amplitude and phase of current space vector, etc.

The design of a control system for bearingless machines constitutes another contribution of this thesis. It implements the above presented analytical model, taking into account all the possible interactions between harmonic orders of the magnetic fields to produce radial force and provides in this way an accurate electromagnetic model of the machine.

This latter is part of a three-dimensional mechanical model where one end of the motor shaft is constrained, to simulate the presence of a mechanical bearing, while the other is free, only supported by the radial forces developed in the interactions between magnetic fields, to simulate a bearingless system with three degrees of freedom. The complete model represents the design of the experimental system to be realized in the laboratory.

References

[1] D. Casadei, D. Dujic, E. Levi, G. Serra, A. Tani, and L. Zarri, “General Modulation Strategy for Seven-Phase Inverters with Independent Control of Multiple Voltage Space Vectors”, *IEEE Trans. on Industrial Electronics*, Vol. 55, NO. 5, May 2008, pp. 1921-1932.

[2] Fei Yu, Xiaofeng Zhang, Huaishu Li, Zhihao Ye, “The Space Vector PWM Control Research of a Multi-Phase Permanent Magnet Synchronous Motor for Electrical Propulsion”, *Electrical Machines and Systems (ICEMS)*, Vol. 2, pp. 604-607, Nov. 2003.

[3] Ruhe Shi, H.A.Toliyat, “Vector Control of Five-phase Synchronous Reluctance Motor with Space Pulse Width Modulation for Minimum Switching Losses”, *Industry Applications Conference, 36th IAS Annual Meeting*. Vol. 3, pp. 2097-2103, 30 Sept.-4 Oct. 2001.

[4] M. A. Abbas, R.Christen, T.M.Jahns, “Six-phase Voltage Source Inverter Driven Induction Motor”, *IEEE Trans. on IA*, Vol.IA-20, No. 5, pp. 1251-1259, 1984.

[5] E. E. Ward, H. Harer, “Preliminary Investigation of an Inverter fed 5-phase Induction Motor”, *IEE Proc*, June 1969, Vol. 116(B), No. 6, pp. 980-984, 1969.

[6] Y. Zhao, T. A. Lipo, “Space Vector PWM Control of Dual Three-phase Induction Machine Using Vector Space Decompositon”, *IEEE Trans. on IA*, Vol. 31, pp. 1177-1184, 1995.

[7] Xue S, Wen X.H, “Simulation Analysis of A Novel Multiphase SVPWM Strategy”, *2005 IEEE International Conference on Power Electronics and Drive Systems (PEDS)*, pp. 756-760, 2005.

[8] Parsa L, H. A. Toliyat, “Multiphase Permanent Magnet Motor Drives”, *Industry Applications Conference, 38th IAS Annual Meeting.* Vol. 1, pp. 401-408, 12.-16 Oct. 2003.

[9] H. Xu, H.A. Toliyat, L.J. Petersen, “Five-Phase Induction Motor Drives with DSP-based Control System”, *IEEE Trans. on IA*, Vol. 17, No. 4, pp. 524-533, 2002.

[10] L. Zarri, M. Mengoni, A. Tani, G. Serra, D. Casadei: "Minimization of the Power Losses in IGBT Multiphase Inverters with Carrier-Based Pulsewidth Modulation," *IEEE Trans. on Industrial Electronics*, Vol. 57, No. 11, November 2010, pp. 3695-3706.

[11] A. Chiba, T. Deido, T. Fukao and et al., "An Analysis of Bearingless AC

Motors," *IEEE Trans. Energy Conversion*, vol. 9, no. 1, Mar. 1994, pp. 61-68.

[12] M. Kang, J. Huang, H.-b. Jiang, J.-q. Yang, “Principle and Simulation of a 5-Phase Bearingless Permanent Magnet-Type Synchronous Motor”, *International Conference on Electrical Machines and Systems*, pp. 1148 – 1152, 17-20 Oct. 2008.

[13] S. W.-K. Khoo, "Bridge Configured Winding for Polyphase Self-Bearing Machines" *IEEE Trans. Magnetics*, vol. 41, no. 4, April. 2005, pp. 1289-1295.

[14] B. B. Choi, “Ultra-High-Power-Density Motor Being Developed for Future Aircraft”, in NASA TM—2003-212296, *Structural Mechanics and Dynamics Branch 2002 Annual Report*, pp. 21–22, Aug. 2003.

[15] Y. Kano, T. Kosaka, N. Matsui, “Simple Nonlinear Magnetic Analysis for Permanent-Magnet Motors”, *IEEE Trans. Ind. Appl.*, vol. 41, no. 5, pp. 1205–1214, Sept./Oct. 2005.

[16] B. Sheikh-Ghalavand, S. Vaez-Zadeh and A. Hassanpour Isfahani, “An Improved Magnetic Equivalent Circuit Model for Iron-Core Linear Permanent-Magnet Synchronous Motors”, *IEEE Trans. on Magnetics*, vol. 46, no. 1, pp. 112–120, Jan. 2010.

[17] S. Vaez-Zadeh and A. Hassanpour Isfahani, “Enhanced Modeling of Linear Permanent-Magnet Synchronous Motors”, *IEEE Trans. on Magnetics*, vol. 43, no. 1, pp. 33–39, Jan. 2007.

Chapter 1

TWO-DIMENSIONAL ANALYSIS OF MAGNETIC FIELD DISTRIBUTIONS IN THE AIRGAP OF ELECTRICAL MACHINES

1.1 Introduction

The aim of this chapter is the development of a method proposed in literature [1] to study the distributions of the magnetic vector potential, magnetic field and flux density in the airgap of axial flux permanent magnet electrical machines by applying a two-dimensional model. With respect to [1], the contribution of this chapter consists in the execution of the complete calculations, not reported in the original work, to get the solution of the problem. They were conducted by using the techniques of mathematical analysis applied to physical

and engineering problems, with particular reference to [2].

In the origin, the method has been applied to the design of axial flux PM machines, but it can be generalized to the analysis of any typology of electrical machine in the case of neglecting slotting effects and with the assumption of developing the machine linearly in correspondence of the mean airgap radius.

1.2 Analytical methods in literature

The works [3]-[6] represent a series of papers for a complete 2-d analysis of the magnetic field distribution in brushless PM radial-field machines. In [3] is presented an analytical method for determining the open-circuit airgap field distribution in the internal and external rotor typologies. The solution is given by the governing field equations in polar coordinates applied to the annular magnets and airgap regions of a multi-pole slotless motor, with an uniform radial magnetization in the magnets.

In [4] the analysis is conducted to determine the armature reaction field produced by a 3-phase stator currents and to take into account the effect of winding current harmonic orders on the airgap field distribution.

In [5], the method developed in [3], [4] is integrated with a model to predict the effect of stator slotting on the magnetic field distribution, using a 2-d permeance function which realizes a much higher accuracy than the conventional 1-dimensional models.

Finally, [6] presents a model to analyze the load operating conditions of the motor, by combining the armature reaction field component with the open-circuit field component produced by the magnets, studied in [3]. All the cases [3]-[6] were compared with the results of FE analysis, showing an excellent agreement.

The paper [7] presents an analytical method to study magnetic fields in permanent-magnet brushless motors, taking into consideration the effect of stator

slotting, by studying the magnetic field distribution in the situations where the magnet passes over the slot opening. In such situations it is difficult to interpret the correct method for determining, with the properly accuracy, the flux density distribution and, consequently, the magnetic forces and cogging torque.

In [8] the effects of slotting in a brushless dc motor (BLDCM) are determined by calculating the airgap permeance distribution using the Schwarz-Christoffel transformation. The analytical calculations of no-load air-gap magnetic field distribution, armature field distribution, and phase electromotive force, are implemented. Then, a three-phase circuital model is realized for determining the phase current waveforms and the instantaneous magnetic field distribution in load conditions, during the actual operations of the drive. The computation of electromagnetic torque and the analysis of torque ripple complete the features of the algorithm.

The paper [9] presents a method for the accurate calculation of magnetic field distribution in the motors with big airgap, by means of the magnetic potential superimposed calculation, since in the examined case the computing error resulting by conventional formulas can’t be neglected as happens in the small airgap machines.

In [10] a general analytical method to predict the magnetic field distribution in surface-mounted brushless permanent magnet machines is presented, considering a two-dimensional model in polar coordinates which solves the Laplacian equations in the airgap and magnets areas, with no constraints about the recoil permeability of the magnets. The analysis is applicable to internal/external rotor typologies, to radial/parallel magnetization of the magnets, to slotless/slotted motors.

1.3 Main assumptions and case study

In the following, the main assumptions of the case study are presented:

I) The permeability of iron is infinite;

II) The considered model is a slotless machine, or a slotted one with slot-openings supposed of infinitesimal width, so that the slotting effects are negligible;

III) In correspondence of the rotor and stator boundary surfaces, the magnetic field lines have only normal component;

IV) The mean airgap radius is assumed infinite, so that the airgap path can be considered as having a linear development, ignoring curvature;

V) Extremity effects are neglected.

VI) The effects of the leakage fluxes are neglected.

The Ampere-turns distributions are analyzed by means of the current sheet technique; the innovative aspect of the analysis, presented in [1], is the process of solving the electromagnetic problem depending on a generalized current distribution, whatever be the generating source, and then applying to the general solution the current-sheet related to the particular case study (ampere-turns distribution of the stator, equivalent distribution of the magnets, etc.). Consider the 2-D model presented in Fig. 1.1:

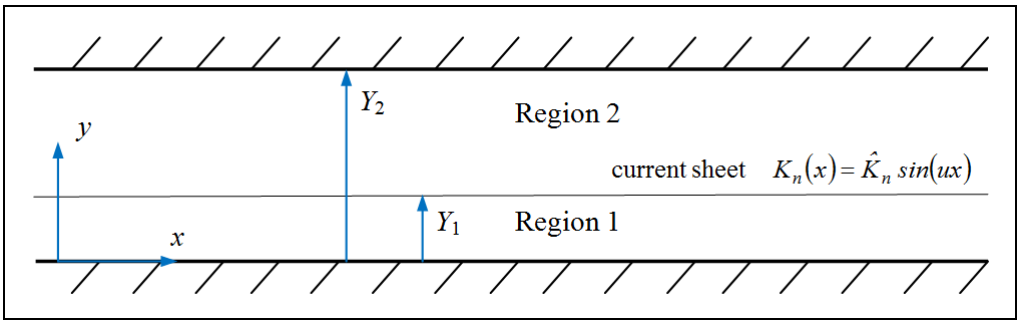

Fig. 1.1

The lower surface, placed at $y = 0$, represents the rotor iron; the higher one, placed at $y = Y_2$, represents the stator iron. A generalized current sheet distribution, given by $K_n(x) = \hat{K}_n \, sin(ux)$, is placed at $y = Y_1$ coordinate: this parameter can be assumed as a variable height, dividing the airgap in two areas and determining different solutions of the magnetic vector potential in everyone of them. In this way, the current sheet $K_n(x)$ can be considered in one case the stator current distribution (in the presented example, by substituting $Y_1 = Y_2$) in the other case the equivalent ampere-turns distribution produced by rotor magnets (in the presented example, by substituting $Y_1 = Y_m$, being this latter the magnet height). So, it is possible firstly to solve the problem for a generalized distribution and then to apply it to the particular case to represent.

1.4 Analytical solution of the problem

Consider by assumption that the magnetic vector potential $\overline{A}$ has the only non-zero component A_z, not dependent on z-coordinate (i.e., the analysis is carried out by operating on xy-planes where all the magnetic and electrical quantities are supposed invariant with respect to the z-axis). With these assumptions, the Laplace operator $\nabla^2\overline{A}$ can be written as:

$$\overline{A} = A_z(x,y)\hat{k} \tag{1.1}$$

$$\nabla^2\overline{A} = \nabla^2 A_z = \nabla\cdot(\nabla A_z) = \left(\frac{\partial}{\partial x}\hat{i} + \frac{\partial}{\partial y}\hat{j} + \frac{\partial}{\partial z}\hat{k}\right)\cdot\left(\frac{\partial A_z}{\partial x}\hat{i} + \frac{\partial A_z}{\partial y}\hat{j}\right) = \frac{\partial^2 A_z}{\partial x} + \frac{\partial^2 A_z}{\partial y} \tag{1.2}$$

The x- and y-components of flux density and magnetic field distributions can be determined as:

$$\overline{B} = \nabla\times\overline{A} = \begin{bmatrix} \hat{i} & \hat{j} & \hat{k} \\ \frac{\partial}{\partial x} & \frac{\partial}{\partial y} & \frac{\partial}{\partial z} \\ 0 & 0 & A_z \end{bmatrix} = \frac{\partial A_z}{\partial y}\hat{i} + \left(-\frac{\partial A_z}{\partial x}\right)\hat{j} \tag{1.3}$$

$$B_x = \frac{\partial A_z}{\partial y}, \quad B_y = -\frac{\partial A_z}{\partial x}, \quad H_x = \frac{B_x}{\mu_0} = \frac{1}{\mu_0}\frac{\partial A_z}{\partial y}, \quad H_y = \frac{B_y}{\mu_0} = -\frac{1}{\mu_0}\frac{\partial A_z}{\partial x}, \tag{1.4}$$

The equation to be solved in the domain of study (1.5), with its related boundary conditions (1.6), is the characteristic Laplace's equation considered in a two-dimensional domain:

$$\nabla^2\overline{A} = 0 \qquad \Rightarrow \qquad \frac{\partial^2 A_z}{\partial x^2} + \frac{\partial^2 A_z}{\partial y^2} = 0 \tag{1.5}$$

$$\begin{aligned} &1)\, H_{x1}(y=0)=0 \\ &2)\, H_{x2}(y=Y_2)=0 \\ &3)\, H_{x2}(y=Y_1)-H_{x1}(y=Y_1)=K_n(x) \\ &4)\, H_{y2}(y=Y_1)=H_{y1}(y=Y_1) \end{aligned} \tag{1.6}$$

Since the boundary conditions are homogeneous, it is possible to apply the method of separation of variables. Let us assume, therefore, that A_z is of the form:

$$A_z = X(x)Y(y) \qquad \Rightarrow \qquad \nabla^2 A_z = Y(y)\frac{\partial^2 X(x)}{\partial x^2} + X(x)\frac{\partial^2 Y(y)}{\partial y^2} = 0 \tag{1.7}$$

hence, multiplying both sides by $1/[X(x)Y(y)]$ and rewriting the second derivatives in a different way for brevity, we obtain:

$$\frac{1}{X(x)}\frac{\partial^2 X(x)}{\partial x^2} + \frac{1}{Y(y)}\frac{\partial^2 Y(y)}{\partial y^2} = 0 \qquad \Rightarrow \qquad \frac{1}{X(x)}X^{xx}(x) + \frac{1}{Y(y)}Y^{yy}(y) = 0 \tag{1.8}$$

By isolating in different members the terms respectively dependent on x and y we obtain:

$$\frac{Y^{yy}(y)}{Y(y)} = -\frac{X^{xx}(x)}{X(x)} \tag{1.9}$$

Note that the members of the equation are absolutely independent from each other, since the first one is a function of the variable x only, the second one of the y only: having to be equivalent for any value assumed by the two variables, it is deduced that they have to be both equal to a constant term, which we define as u^2, assumed positive. By further developing the calculations, two separate differential equations are obtained, each one as a function of a single variable:

$$-\frac{X^{xx}(x)}{X(x)} = u^2 \qquad \Rightarrow \qquad X^{xx}(x) + u^2 X(x) = 0 \tag{1.10}$$

$$\frac{Y^{yy}(y)}{Y(y)} = u^2 \qquad \Rightarrow \qquad Y^{yy}(y) - u^2 Y(y) = 0 \tag{1.11}$$

Are obtained from (1.10), (1.11) the respective characteristic equations and their solutions:

$$p^2 + u^2 = 0 \qquad \Rightarrow \qquad p_{1,2} = \pm\sqrt{j^2 u^2} = \pm ju \tag{1.12}$$

$$q^2 - u^2 = 0 \qquad \Rightarrow \qquad q_{1,2} = \pm\sqrt{u^2} = u \tag{1.13}$$

Recalling the general expression of the solutions associated with the characteristic equations (1.12), (1.13):

$$X(x) = A_x e^{jux} + B_x e^{-jux} \tag{1.14}$$

$$Y(y) = A_y e^{uy} + B_y e^{-uy} \tag{1.15}$$

where A_x, B_x, A_y, B_y, are constant terms to be evaluated using the boundary conditions. Recalling (1.7) is possible to write:

$$A_z(x,y) = X(x)Y(y) = \left(A_x e^{jux} + B_x e^{-jux}\right)\left(A_y e^{uy} + B_y e^{-uy}\right) \tag{1.16}$$

By introducing the Euler's formulas, presented in the follows:

$$e^{jux} = cos(ux) + j\,sin(ux), \qquad e^{-jux} = cos(ux) - j\,sin(ux) \tag{1.17}$$

$$e^{uy} = cosh(uy) + sinh(uy), \qquad e^{-uy} = cosh(uy) - sinh(uy) \tag{1.18}$$

and using (1.17) and (1.18) in (1.16), the general solution can be expressed in a trigonometric form:

$$A_z(x,y) = X(x)Y(y) = \left[A\,sin(ux) + B\,cos(ux)\right]\left[C\,sinh(uy) + D\,cosh(uy)\right] \tag{1.19}$$

1.4.1 Analysis in the Region 1

Assume for region 1 the following general expression for the magnetic vector

potential:

$$A_{z1}(x,y) = X(x)Y(y) = [A_1\, sin(ux) + B_1\, cos(ux)][A_2\, sinh(uy) + B_2\, cosh(uy)] \tag{1.20}$$

The value of the x-component of the magnetic field in the lower boundary of the region 1, leads to the first boundary condition:

$$H_{x1}(y=0) = 0 \tag{1.21}$$

$$H_{x1}(x,y) = \frac{1}{\mu_0}\frac{\partial A_{z1}}{\partial y} = \frac{u}{\mu_0}[A_1\, sin(ux) + B_1\, cos(ux)][A_2\, cosh(uy) + B_2\, sinh(uy)] \tag{1.22}$$

By applying the condition (1.21) in (1.22) and considering that the equation has to be verified for any value of x and y, we obtain (1.23):

$$H_{x1}(y=0) = \frac{u}{\mu_0}[A_1\, sin(ux) + B_1\, cos(ux)]A_2 = 0 \qquad \Rightarrow \qquad A_2 = 0 \tag{1.23}$$

By substituting the result of (1.23) into (1.20):

$$A_{z1}(x,y) = B_2\, cosh(uy)[A_1\, sin(ux) + B_1\, cos(ux)] \tag{1.24}$$

where, defining the constant terms $k_1 = B_2 A_1$ and $k_2 = B_2 B_1$:

$$A_{z1}(x,y) = cosh(uy)[k_1\, sin(ux) + k_2\, cos(ux)] \tag{1.25}$$

By substituting the result of (1.23) into (1.22):

$$H_{x1}(x,y) = \frac{u}{\mu_0} sinh(uy)[k_1\, sin(ux) + k_2\, cos(ux)] \tag{1.26}$$

By executing similar calculations is possible to write the H_{y1} component of the magnetic field as:

$$H_{y1}(x,y) = -\frac{1}{\mu_0}\frac{\partial A_{z1}}{\partial x} = \frac{u}{\mu_0} cosh(uy)[k_2\, sin(ux) - k_1\, cos(ux)] \tag{1.27}$$

1.4.2 Analysis in the Region 2

Assume for region 2 the following general expression for the magnetic vector potential:

$$A_{z2}(x,y) = X(x)Y(y) = [C_1\, sin(ux) + D_1\, cos(ux)][C_2\, sinh(uy) + D_2\, cosh(uy)] \tag{1.28}$$

The value of the x-component of the magnetic field in the higher boundary of the region 2, leads to the second boundary condition:

$$H_{x2}(y = Y_2) = 0 \tag{1.29}$$

$$H_{x2}(x,y) = \frac{1}{\mu_0}\frac{\partial A_{z2}}{\partial y} = \frac{u}{\mu_0}[C_1\, sin(ux) + D_1\, cos(ux)][C_2\, cosh(uy) + D_2\, sinh(uy)] \tag{1.30}$$

By applying the condition (1.29) in (1.30) and considering that the equation has to be valid for any value of x and u, we obtain (1.31), (1.32):

$$H_{x2}(y = Y_2) = \frac{u}{\mu_0}[C_1\, sin(ux) + D_1\, cos(ux)][C_2\, cosh(uY_2) + D_2\, sinh(uY_2)] = 0 \tag{1.31}$$

$$C_2\, cosh(uY_2) + D_2\, sinh(uY_2) = 0 \quad \Rightarrow \quad D_2 = -C_2\, coth(uY_2) \tag{1.32}$$

By substituting (1.32) in (1.28):

$$A_{z2}(x,y) = C_2[C_1\, sin(ux) + D_1\, cos(ux)][sinh(uy) - cosh(uy)coth(uY_2)] \tag{1.33}$$

where, in a similar way to what was done for the region 1, by introducing the constant terms $k_3 = C_1C_2$ and $k_4 = D_1C_2$, it gives:

$$A_{z2}(x,y) = [k_3\, sin(ux) + k_4\, cos(ux)][sinh(uy) - cosh(uy)coth(uY_2)] \tag{1.34}$$

which can be written, by explicating $coth(uY_2)$, as:

$$A_{z2}(x,y) = [k_3\ sin(ux) + k_4\ cos(ux)]\left[\frac{sinh(uy)sinh(uY_2) - cosh(uy)cosh(uY_2)}{sinh(uY_2)}\right] \tag{1.35}$$

By considering that:

$$cosh\ u(Y_2 - y) = cosh(uY_2 - uy) = cosh(uY_2)cosh(uy) - sinh(uY_2)sinh(uy) \tag{1.36}$$

The relationship (1.35) can be simplified as in (1.37):

$$A_{z2}(x,y) = -[k_3\ sin(ux) + k_4\ cos(ux)]\frac{cosh\ u(Y_2 - y)}{sinh(uY_2)} \tag{1.37}$$

and, by means of (1.38), the related components of the magnetic field in region 2 can be calculated as in (1.39), (1.40):

$$H_{x2}(x,y) = \frac{1}{\mu_0}\frac{\partial A_{z2}}{\partial y}, \qquad H_{y2}(x,y) = -\frac{1}{\mu_0}\frac{\partial A_{z2}}{\partial x} \tag{1.38}$$

$$H_{x2}(x,y) = \frac{u}{\mu_0}[k_3\ sin(ux) + k_4\ cos(ux)]\frac{sinh\ u(Y_2 - y)}{sinh(uY_2)} \tag{1.39}$$

$$H_{y2}(x,y) = \frac{u}{\mu_0}[k_3\ cos(ux) - k_4\ sin(ux)]\frac{cosh\ u(Y_2 - y)}{sinh(uY_2)} \tag{1.40}$$

1.4.3 Common boundary conditions

Considering a current sheet described by means of an harmonic distribution given in the generic form:

$$K_n(x) = \hat{K}_n\ sin(ux) \tag{1.41}$$

where $\hat{K}_n$ depends on the actual current distribution and has to be evaluated in

any particular considered case, while u is defined as follows:

$$u = \frac{\pi}{\tau_p} n \tag{1.42}$$

The discontinuity between the x-component values of the magnetic field in the current sheet region, leads to the third boundary condition:

$$H_{x2}(y = Y_1) - H_{x1}(y = Y_1) = K_n(x) \tag{1.43}$$

which can be expressed by calculating (1.26) and (1.39) in correspondence of the particular value $y = Y_1$. By substituting them in (1.43) it gives:

$$\frac{u}{\mu_0}\left[k_3 \sin(ux) + k_4 \cos(ux)\right]\frac{\sinh u(Y_2 - Y_1)}{\sinh(uY_2)} - \frac{u}{\mu_0}\left[k_1 \sin(ux) + k_2 \cos(ux)\right]\sinh(uY_1) = \\ = \hat{K}_n \sin(ux) \tag{1.44}$$

By collecting the common terms in (1.44):

$$\sin(ux)\left[k_3 \frac{\sinh u(Y_2 - Y_1)}{\sinh(uY_2)} - k_1 \sinh(uY_1) - \frac{\mu_0 \hat{K}_n}{u}\right] + \\ + \cos(ux)\left[k_4 \frac{\sinh u(Y_2 - Y_1)}{\sinh(uY_2)} - k_2 \sinh(uY_1)\right] = 0 \tag{1.45}$$

Note that (1.45) has to be verified for any value of u and x, so the only possibility is that both the coefficients of $\sin(ux)$ and $\cos(ux)$ are equal to zero:

$$k_3 \frac{\sinh u(Y_2 - Y_1)}{\sinh(uY_2)} - k_1 \sinh(uY_1) - \frac{\mu_0 \hat{K}_n}{u} = 0 \tag{1.46}$$

$$k_4 \frac{\sinh u(Y_2 - Y_1)}{\sinh(uY_2)} - k_2 \sinh(uY_1) = 0 \tag{1.47}$$

After a few steps (1.46) and (1.47) give, respectively, the relations $k_3 = f(k_1)$ and $k_4 = f(k_2)$:

$$k_3 = \frac{sinh(uY_2)\left[\mu_0 \hat{K}_n + uk_1\, sinh(uY_1)\right]}{u\, sinh\, u(Y_2 - Y_1)} \tag{1.48}$$

$$k_4 = \frac{sinh(uY_1)sinh(uY_2)}{sinh\, u(Y_2 - Y_1)} k_2 \tag{1.49}$$

Putting (1.48) and (1.49) in (1.40):

$$H_{y2}(x,y) = \frac{u\, cosh\, u(Y_2 - y)}{\mu_0}\left[\frac{\mu_0 \hat{K}_n + uk_1\, sinh(uY_1)}{u\, sinh\, u(Y_2 - Y_1)} cos(ux) + - \frac{sinh(uY_1)}{sinh\, u(Y_2 - Y_1)} k_2\, sin(ux)\right] \tag{1.50}$$

The continuity between the y-components of the magnetic field in the current sheet region, leads to the fourth boundary condition:

$$H_{y2}(y = Y_1) = H_{y1}(y = Y_1) \tag{1.51}$$

By calculating (1.50) and (1.27) in $y = Y_1$ it respectively gives (1.52) and (1.53); by substituting them in (1.51), it gives (1.54):

$$H_{y2}(y = Y_1) = \frac{u\, cosh\, u(Y_2 - Y_1)}{\mu_0}\left[\frac{\mu_0 \hat{K}_n + uk_1\, sinh(uY_1)}{u\, sinh\, u(Y_2 - Y_1)} cos(ux) + - \frac{sinh(uY_1)}{sinh\, u(Y_2 - Y_1)} k_2\, sin(ux)\right] \tag{1.52}$$

$$H_{y1}(y = Y_1) = \frac{u}{\mu_0} cosh(uY_1)\left[k_2\, sin(ux) - k_1\, cos(ux)\right] \tag{1.53}$$

$$\frac{u\, cosh\, u(Y_2 - Y_1)}{\mu_0}\left[\frac{\mu_0 \hat{K}_n + uk_1\, sinh(uY_1)}{u\, sinh\, u(Y_2 - Y_1)} cos(ux) - \frac{sinh(uY_1)}{sinh\, u(Y_2 - Y_1)} k_2\, sin(ux)\right] = = \frac{u}{\mu_0} cosh(uY_1)\left[k_2\, sin(ux) - k_1\, cos(ux)\right] \tag{1.54}$$

By collecting common terms in (1.54):

$$\left[\frac{\mu_0\hat{K}_n + uk_1\,sinh(uY_1)}{\mu_0}coth\,u(Y_2-Y_1)+k_1\frac{u}{\mu_0}cosh(uY_1)\right]cos(ux)= \\ =\left[uk_2\,sinh(uY_1)\frac{coth\,u(Y_2-Y_1)}{\mu_0}+\frac{u}{\mu_0}cosh(uY_1)k_2\right]sin(ux) \tag{1.55}$$

As seen before, (1.55) has to be verified for any value of u and x, so the only possibility is that both the coefficients of $sin(ux)$ and $cos(ux)$ are equal to zero. From (1.55) the equation (1.56):

$$\hat{K}_n\,coth\,u(Y_2-Y_1)+k_1\frac{u\,sinh(uY_1)}{\mu_0}coth\,u(Y_2-Y_1)+k_1\frac{u}{\mu_0}cosh(uY_1)=0 \tag{1.56}$$

which results after a few steps in (1.57):

$$k_1=-\frac{\mu_0\hat{K}_n}{u}\frac{coth\,u(Y_2-Y_1)}{sinh(uY_1)coth\,u(Y_2-Y_1)+cosh(uY_1)} \tag{1.57}$$

and also the equation (1.58):

$$k_2\left[u\,sinh(uY_1)\frac{coth\,u(Y_2-Y_1)}{\mu_0}+\frac{u}{\mu_0}cosh(uY_1)\right]=0 \tag{1.58}$$

which results in (1.59):

$$k_2=0 \tag{1.59}$$

Note that (1.57) can be simplified, by simplifying the term $coth\,u(Y_2-Y_1)$ in the numerator and denominator. After a few steps, it gives:

$$k_1=-\frac{\mu_0\hat{K}_n}{u}\frac{cosh\,u(Y_2-Y_1)}{sinh(uY_2)} \tag{1.60}$$

By substituting (1.60) in (1.48) and performing some similar calculations, a simplified form for k_3 can be obtained:

$$k_3=\frac{\mu_0\hat{K}_n}{u}cosh\,(uY_1) \tag{1.61}$$

Finally, using the result of (1.59) in (1.49), it gives:

$$k_4 = 0 \tag{1.62}$$

All the coefficients are now known; thus, is possible to determine the expression of magnetic vector potential and of magnetic field in the regions of the machine. By substituting (1.59) and (1.60) in (1.25), it immediately gives:

$$A_{z1}(x,y) = -\frac{\mu_0 \hat{K}_n}{u} \frac{cosh\, u(Y_2 - Y_1)}{sinh(uY_2)} sin(ux) cosh(uy) \tag{1.63}$$

Similarly, by substituting (1.61) and (1.62) in (1.37):

$$A_{z2}(x,y) = -\frac{\mu_0 \hat{K}_n}{u} \frac{cosh(uY_1)}{sinh(uY_2)} sin(ux) cosh\, u(Y_2 - y) \tag{1.64}$$

From (1.63) and (1.64) are derived the following relationships (1.65)-(1.68):

$$H_{x1}(x,y) = \frac{1}{\mu_0}\frac{\partial A_{z1}}{\partial y} = -\hat{K}_n \frac{cosh\, u(Y_2 - Y_1)}{sinh(uY_2)} sin(ux) sinh(uy) \tag{1.65}$$

$$H_{y1}(x,y) = -\frac{1}{\mu_0}\frac{\partial A_{z1}}{\partial x} = \hat{K}_n \frac{cosh\, u(Y_2 - Y_1)}{sinh(uY_2)} cos(ux) cosh(uy) \tag{1.66}$$

$$H_{x2}(x,y) = \frac{1}{\mu_0}\frac{\partial A_{z2}}{\partial y} = \hat{K}_n \frac{cosh(uY_1)}{sinh(uY_2)} sin(ux) sinh\, u(Y_2 - y) \tag{1.67}$$

$$H_{y2}(x,y) = -\frac{1}{\mu_0}\frac{\partial A_{z2}}{\partial x} = \hat{K}_n \frac{cosh(uY_1)}{sinh(uY_2)} cos(ux) cosh\, u(Y_2 - y) \tag{1.68}$$

1.5 Current sheet distribution of the magnets

As a particular example of a current sheet distribution $K_n(x)$, will be examined the equivalent current density distribution of the magnets. Each magnet is represented by two current pulses at its edges, assuming to flow in a tending to

zero thickness, having an angular width equal to $2\delta_m$.

$$J(x)=\sum_{n=1,3,5..}^{\infty}\hat{J}_n\,sin(n\theta)=\sum_{n=1,3,5..}^{\infty}\hat{J}_n\,sin\left(n\frac{\pi}{\tau_p}x\right)=\sum_{n=1,3,5..}^{\infty}\hat{J}_n\,sin(ux) \tag{1.69}$$

The function is represented by means of the Fourier harmonic series distribution, the coefficients of which are calculated in the following:

$$\begin{aligned}
\hat{J}_n &= \frac{1}{\pi}\int_{-\pi}^{\pi} j(\theta)sin(n\theta)d\theta = \frac{2}{\pi}\int_{0}^{\pi} j(\theta)sin(n\theta)d\theta = \\
&= \frac{2}{\pi}\int_{\theta_{mp}-\delta_m}^{\theta_{mp}+\delta_m} J\,sin(n\theta)d\theta + \frac{2}{\pi}\int_{\pi-\theta_{mp}-\delta_m}^{\pi-\theta_{mp}+\delta_m} J\,sin(n\theta)d\theta = \\
&= \frac{2}{\pi}\frac{1}{n}J\left\{\left[-cos(n\theta)\right]_{\theta_{mp}-\delta_m}^{\theta_{mp}+\delta_m}+\left[-cos(n\theta)\right]_{\pi-\theta_{mp}-\delta_m}^{\pi-\theta_{mp}+\delta_m}\right\}= \\
&= \frac{2J}{n\pi}\left\{2\,sin(n\theta_{mp})sin(n\delta_m)+2\,sin(n\pi-n\theta_{mp})sin(n\delta_m)\right\}= \\
&= \frac{4J}{n\pi}\left\{sin(n\delta_m)\left[sin(n\theta_{mp})+sin(n\pi-n\theta_{mp})\right]\right\}= \\
&= \frac{4J}{n\pi}\left\{2\,sin(n\delta_m)sin\left(\frac{n\pi}{2}\right)cos\left(\frac{2n\theta_{mp}-n\pi}{2}\right)\right\}
\end{aligned} \tag{1.70}$$

Considering that n is an odd number, the value of $cos(n\pi/2)$ in (1.71) is always zero:

$$cos\left(\frac{2n\theta_{mp}-n\pi}{2}\right)=cos(n\theta_{mp})cos\left(n\frac{\pi}{2}\right)+sin(n\theta_{mp})sin\left(n\frac{\pi}{2}\right)=sin(n\theta_{mp})sin\left(n\frac{\pi}{2}\right) \tag{1.71}$$

By substituting the result of (1.71) in (1.70), it gives:

$$\hat{J}_n=\frac{8J}{n\pi}sin(n\delta_m)sin^2\left(n\frac{\pi}{2}\right)sin(n\theta_{mp})=\frac{8J}{n\pi}sin(n\delta_m)sin(n\theta_{mp}) \tag{1.72}$$

The equivalent surface current density related to the magnets is expressed by (1.73):

$$J = \frac{H_c \pi}{2\delta_m \tau_p} = \frac{B_{rem}}{\mu_m} \frac{\pi}{2\delta_m \tau_p} \quad \left[A/m^2\right] \tag{1.73}$$

By substituting (1.73) in (1.72), is also necessary to calculate the limit as δ_m tends to zero, considering every edge of the magnet as a current pulse:

$$\hat{J}_n = \lim_{\delta_m \to 0} \frac{8}{\pi} \frac{B_{rem}}{\mu_m} \frac{\pi}{2\tau_p} \frac{sin(n\delta_m)}{n\delta_m} sin(n\theta_{mp}) \tag{1.74}$$

Being:

$$\lim_{\delta_m \to 0} \frac{sin(n\delta_m)}{n\delta_m} = 1 \quad \forall n \tag{1.75}$$

It results:

$$\hat{J}_n = \frac{4B_{rem}}{\mu_m \tau_p} sin(n\theta_{mp}) = \frac{4B_{rem}}{\mu_m \tau_p} sin\left(n \frac{\pi}{2} \frac{\tau_m}{\tau_p}\right) \tag{1.76}$$

By substituting the relationship (1.76) in (1.69), it gives:

$$J(x) = \sum_{n=1,3,5..}^{\infty} \frac{4B_{rem}}{\mu_m \tau_p} sin\left(n \frac{\pi}{2} \frac{\tau_m}{\tau_p}\right) sin(n\theta) \tag{1.77}$$

Considering that:

$$u = \frac{\pi}{\tau_p} n \quad \Rightarrow \quad n\theta = \left(n \frac{\pi}{\tau_p}\right) x = ux \tag{1.78}$$

By substituting (1.78) in (1.77), it results:

$$J(x) = \sum_{n=1,3,5..}^{\infty} \frac{4B_{rem}}{\mu_m \tau_p} sin\left(n \frac{\pi}{2} \frac{\tau_m}{\tau_p}\right) sin(ux) \tag{1.79}$$

To define the function of distribution $K_n(x)$, is important to note that the magnets are constituted by a succession of current sheets, each one of

infinitesimal width dy, thus characterized by a linear current density given as:

$$K_n(x) = \hat{J}_n dy \sin(ux) \quad [A/m] \tag{1.80}$$

The expression of magnetic vector potential in the region 2, given by the magnets distribution (1.80) can be obtained by integrating (1.64) over the magnet thickness Y_m:

$$\begin{aligned} A_{z2}(x,y) &= -\int_0^{Y_m} \frac{\mu_0 \hat{J}_n}{u} \frac{\cosh(uy_1)}{\sinh(uY_2)} \sin(ux) \cosh u(Y_2 - y) dy_1 = \\ &= -\frac{\mu_0 \hat{J}_n}{u^2} \frac{\sinh(uY_m)}{\sinh(uY_2)} \sin(ux) \cosh u(Y_2 - y) \end{aligned} \tag{1.81}$$

Note that the particular form of equation (1.80), which represents in this case the magnets distribution, replaces the general function $\hat{K}_n \sin(ux)$ in the equation (1.64).

1.6 Conclusion

In this chapter a method proposed in literature was developed to study the distributions of the magnetic vector potential, magnetic field and flux density in the airgap of axial flux permanent magnet electrical machines by applying a two-dimensional model.

The contribution of this chapter with respect to the examined work, consists in the execution of the complete calculations, which are not presented in the original paper, to get the solution of the problem. They were conducted by using the techniques of mathematical analysis applied to physical and engineering problems.

This method can be generalized to the analysis of any typology of electrical machine in the case of neglecting slotting effects and with the assumption of developing the machine linearly in correspondence of the mean airgap radius.

1.7 References

[1] J.R. Bumby, R. Martin, M.A Mueller, E. Spooner, N.L. Brown and B.J. Chalmers, "Electromagnetic design of axial-flux permanent magnet machines", *IEEE Proc.-Electr. Power Appl.*, Vol. 151, No. 2, March 2004

[2] P. Zecca, "Problemi al bordo per le Equazioni Differenziali", Dispense dei corsi universitari, *http://www.de.unifi.it/anum/zecca*.

[3] Z. Zhu, D. Howe, E. Bolte, and B. Ackermann, "Instantaneous magnetic field distribution in brushless permanent magnet dc motors, Part I: Open-circuit field" *IEEE Transactions on Magnetics*, vol. 29, no. 1, pp. 124-135, Jan. 1993.

[4] Z. Q. Zhu and D. Howe, "Instantaneous magnetic field distribution in brushless permanent magnet dc motors, Part II: Armature reaction field," *IEEE Trans. Magn.,* vol. 29, no. 1, pp. 136-142, Jan. 1993.

[5] Z. Q. Zhu and D. Howe, "Instantaneous magnetic-field distribution in brushless permanent magnet dc motors, Part III: Effect of stator slotting," *IEEE Trans. Magn.*, vol. 29, no. 1, pp. 143-151, Jan. 1993.

[6] Z. Q. Zhu and D. Howe, "Instantaneous magnetic field distribution in brushless permanent magnet dc motors, Part IV: Magnetic field on load," *IEEE Trans. Magn.*, vol. 29, no. 1, pp. 152-158, Jan. 1993.

[7] Z. J. Liu and J. T. Li, "Analytical solution of air-gap field in permanent-magnet motors taking into account the effect of pole transition over slots," *IEEE Trans. Magn.*, vol. 43, no. 10, pp. 3872-3883, Oct. 2007.

[8] X. Wang, Q. Li, S. Wang, and Q. Li, "Analytical calculation of air-gap magnetic field distribution and instantaneous characteristics of brushless dc motors," *IEEE Trans. Energy Convers.,* vol. 18, no. 3, pp. 424-432, Sep. 2003.

[9] G. Meng, H. Li and H. Xiong, "Calculation of big air-gap magnetic field in poly-phase multi-pole BLDC motor," *International Conference on Electrical Machines and Systems, ICEMS 2008*, pp. 3224-3227.

[10] Z.Q. Zhu, D. Howe and C.C. Chan, "Improved Analytical Model for Predicting the Magnetic Field Distribution in Brushless Permanent-Magnet Machines," *IEEE Trans. Magnetics,* vol. 38, no. 1, 2002, pp. 229-238.

Chapter 2

AN ALGORITHM FOR NON-LINEAR ANALYSIS OF MULTIPHASE BEARINGLESS SURFACE-MOUNTED PM SYNCHRONOUS MACHINES

2.1 Introduction

In recent years, more and more advanced technologies and an impressive rise in the use of electronics, both in civil as in the industrial sector, given a contribution to reduce the cost of the components, allowing the use of complex technologies which in the past had high costs and therefore of little industrial

interest. In the field of electrical machines this evolution led not only to the realization of power drives controlled by an inverter, capable of ensuring performance significantly better than those obtained with the previous control systems, but also the advent of a new type of machines with a different number of phases from the traditional three-phase, usually employed in generation and distribution of electric energy. This has reawakened the interest in the study of multi-phase electrical machines.

In [1], a general modulation strategy is presented to be used in multimotor drives and in multiphase motor drives for improving the torque density.

In [2] a scheme, functional to implement a space vector PWM control of a twelve-phase permanent magnet synchronous motor is analyzed, to reduce the switching losses without affecting performances.

A rotor field oriented based on the space vector PWM (SVPWM) technique for a 5-phase synchronous reluctance motor is developed in [3] and verified using a dedicated inverter.

In [4] the stator of an induction machine is rewound with two three-phase winding sets displaced from each other by 30 electrical degrees, showing that this winding configuration eliminates rotor copper losses and torque harmonics of particular orders and the sixth harmonic dominant torque ripple.

In [5] an invertor-fed 5-phase induction motor is compared with a corresponding 3-phase motor, showing that the amplitude of the torque fluctuation is reduced to approximately one third.

The space vector decomposition technique is presented in [6], where the analytical modeling and control of the machine are developed in three 2-dimensional orthogonal subspaces which permits to decouple the variables related to the control of harmonic contributions.

In [7] a novel multiphase SVPWM strategy is presented, able to synthesize the d-q subspace voltage vectors to accomplish the control requirements and

make null the resultant voltage vectors on other subspace, minimizing the switching losses.

The advantages of multiphase machines are explained and discussed in [8]: capability of improve the torque production by injecting harmonic of currents in the motor, a better torque and flux adjustment in DTC control, the fault resilient current control of multi phase drive under loss of phases and the possibility of controlling multi motors through a single inverter.

The space vector control and direct torque control (DTC) schemes are presented in [9], applied to the operation of a 5-phase induction motor and using a fully digital implementation. Experimental results show that an optimal control capability is obtained for both methods, further validating the theoretical concepts. In the last years, various techniques have been applied in order to reduce the power losses in multiphase IGBT inverters [10].

The multiphase feature results particularly suitable in bearingless machines, capable of producing rotor suspension force and torque avoiding the use of mechanical bearings and achieving in this way much higher maximum speed [11]. There are two typologies of winding configurations: dual set and single set of windings. The first category comprises two separated groups of three-phase windings, with a difference in their pole pair numbers equal to one: the main one carries the ‘motor currents’ for driving the rotor, while the other carries the ‘levitation currents’, to suspend the rotor [11].

The windings belonging to the latter category produce torque and radial forces by means of injecting different current sequences to give odd and even harmonic orders of magnetic field, using the properties of multiphase current systems, which have multiple orthogonal d-q planes. One of them can be used to control the torque, the additional degrees of freedom can be used to produce levitation forces [12], as will be explained in chapter 3. The main advantages of bearingless motors with a single set of windings (i.e. of multiphase type) consist

of a simpler construction process, better performances in control strategy and torque production with relatively low power losses [13]. This kind of technology is expected to have very large developments in the future, particularly in the design of high power density generators, actuators and motors of More Electric Aircraft (MEA), mainly for the ability of achieving higher speed in comparison to conventional electrical machines [14].

In addition, it can be supposed that the characteristics of bearingless control techniques and the use of magnetic bearing could be of large interest in the MEA field.

The possibility of making quick analyses, with the comparison of a large number of solutions, nevertheless providing an accurate calculation of electromagnetic quantities, represents a relevant goal in the design of electrical machines, by analyzing global and local quantities as output torque, magnetic energy and co-energy, linkage fluxes, magnetic fields and flux densities in many parts of the machine. The difficulties increase especially in presence of magnetic saturation; in order to solve these problems, the equivalent magnetic circuit method lets fast modifications of the geometrical and electrical parameters simply by varying numerical inputs and, at the same time, obtaining an high accuracy in calculations with respect to other software based on more in-depth analytical methods, as Finite Element Analysis (FEA).

Previous papers proposed the analysis of open-slot configurations with a prefixed structure of the motor, with a given number of poles and slots [15], or by studying only particular positions of the rotor with respect to the stator without relative movement [16], [17]. This chapter presents an algorithm for non-linear magnetic analysis of multiphase surface-mounted permanent-magnet machines with semi-closed slots. The relevant edge of the method consists in the possibility of defining the machine characteristics in a simple user interface. Then, by duplicating an elementary cell, it is possible to construct and analyze

whatever typology of windings and ampere-turns distribution in a pole-pair. Furthermore, it is possible to modify the magnet width-to-pole pitch ratio analyzing various configurations in order to minimize the cogging torque, or simulating the rotor movement in sinusoidal multiphase drives or in a user-defined current distribution.

Finally, the capability of radial forces calculation allows to determine the optimal ampere-turns distribution in the design of a bearingless control of the motor. The choice of using a software based on the equivalent magnetic circuit method allows relevant time saving for this kind of analysis with respect to a FEA software, not only due to the reduction of computing time, but mainly for the simple change of electrical and geometrical parameters (i.e. the numerical inputs of the problem), without the need of re-designing the model in a CAD interface.

2.2 The Magnetic Circuit Model

The basic element of the magnetic network is shown in Fig. 2.1, whose the related reluctances are highlighted.

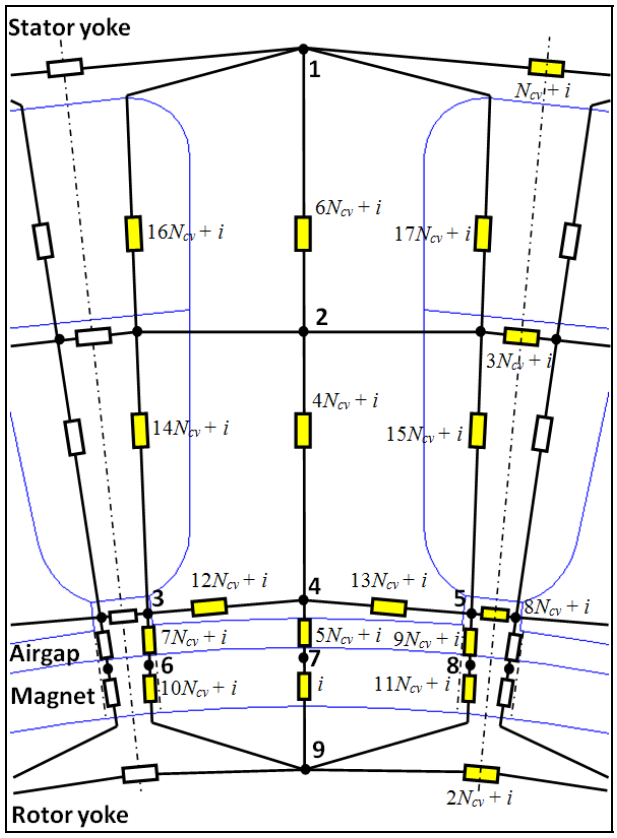

Fig. 2.1. The basic element of the magnetic network

It consists of one tooth and the adjacent two semi-slots, being composed of 18 reluctances representing sub-domains of the machine, i.e. volumes of teeth, sections of the airgap, of the magnets, branches of yokes, semi-slots, etc.

Beside of considering longitudinal components, in the model were provided transverse components of the magnetic fluxes as, for example, in the slot area and in the slot-opening to take into account the leakage paths [18], in the tips of the tooth and in the branches of stator and rotor yokes.

To construct the whole model of a motor, the i-th basic cell is connected to the previous one through four transverse reluctances: $N_{cv} + i - 1$, $2N_{cv} + i - 1$

(stator and rotor yokes), $3N_{cv} + i - 1$ (slot area), $8N_{cv} + i - 1$ (slot-opening area). Furthermore, the i-th basic cell is connected to the following one through the elements $N_{cv} + i$, $2N_{cv} + i$, $3N_{cv} + i$, and $8N_{cv} + i$.

Considering one pole pair of the model, that comprises two gaps between the magnets (each one of them provides 4 additional terms), the whole network results in a number of reluctances, i.e. unknown terms, equal to $18N_{cv} + 8$, being N_{cv} the number of slots per pole pair.

2.2.1 Analytical Models of the Reluctances

In this subsection some formulas and criteria used to determine the most relevant parameters of the magnetic circuit are described.

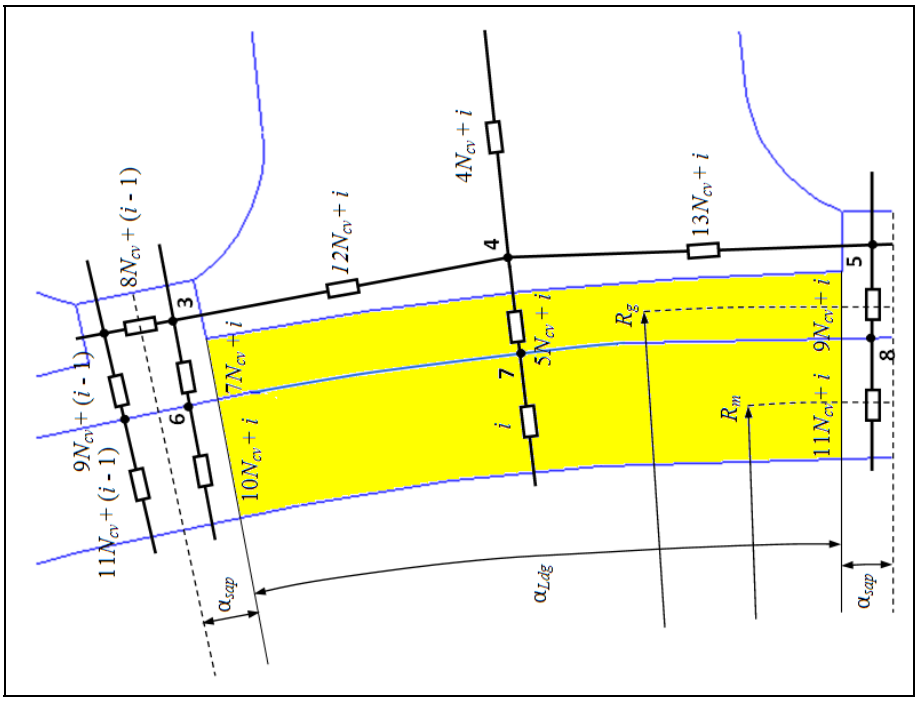

Fig. 2.2. Configuration of the network in the case of uniform magnet

Elements $i = 1$ to N_{cv}, $i = 5N_{cv}+1$ to $6N_{cv}$

To provide a more realistic representation of the flux lines crossing the airgap,

the total magnetic flux in a slot pitch, passing through the magnet, was divided into three tubes (Fig. 2.1): the one in the middle presents the tooth surface as cross-sectional area, depending on the mean radius R_m for the magnet zone (2.1) and on the mean radius R_g for the airgap zone (2.2). The related reluctances are respectively calculated as:

$$\Re_i = \frac{1}{\mu_m} \frac{L_m}{R_m \alpha_{Ldg} L} \tag{2.1}$$

$$\Re_i = \frac{1}{\mu_0} \frac{g}{R_g \alpha_{Ldg} L} \tag{2.2}$$

where the meaning of the symbols is shown in Fig. 4 and in Tab. I.

Elements $i = 7N_{cv}+1$ to $8N_{cv}$, $i = 9N_{cv}+1$ to $10N_{cv}$, elements $i = 10N_{cv}+1$ to $11N_{cv}$, $i = 11N_{cv}+1$ to $12N_{cv}$

The two tubes in left and right sideways positions with respect to the tooth, develop their paths across the airgap in a succession of a straight line and a circumferential arc, closing in the tooth tips [14], [18]. The related reluctances are calculated as:

$$\Re_i = \frac{1}{L\mu_0 \int_0^{h_{cl}} \frac{1}{g + \pi r/2} dr} = \frac{\pi}{2\mu_0 L \, ln\left(\frac{2g + \pi h_{cl}}{2g}\right)} \tag{2.3}$$

In the magnet, flux paths are developed in radial direction, using the simple conventional formula:

$$\Re_i = \frac{1}{\mu_m} \frac{L_m}{R_m \alpha_{sap} L} \tag{2.4}$$

Elements i = 12N_{cv}+1 to 14N_{cv}

Furthermore, a description of the leakage flux in the gap between the magnets is provided by using transverse reluctances. These create a closed loop including the magnets, the airgap and the tooth tips. This situation has a not negligible effect on PM machines [15] and is described in the literature [19]. The reluctance used to describe a tooth tip is given by the series of two elements, a rectangular-shaped one and a trapezoidal-shaped one (Fig. 2.3 *a*):

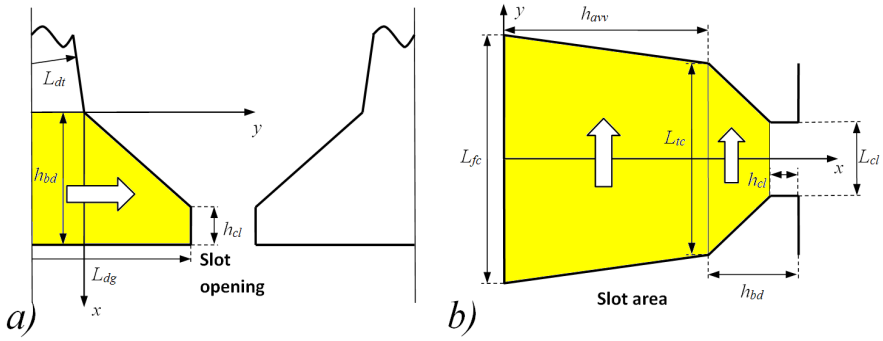

Fig. 2.3. Reference systems for calculating the transverse reluctance:
a) tooth tip, b) slot area.

$$\Re_i = \frac{1}{\mu_{i(B,H)}} \frac{L_{dt}}{2h_{bd}L} + \frac{1}{\mu_{i(B,H)}} \frac{L_{dg} - L_{dt}}{2(h_{cl} - h_{bd})L} ln\left(\frac{h_{cl}}{h_{bd}}\right) \tag{2.5}$$

Note that the reluctances placed in the iron have a value of the permeability which depends on the magnetic characteristic of the material, thus characterized as $\mu_{i(B,H)}$.

Elements i = 3N_{cv}+1 to 4N_{cv}, i = 8N_{cv}+1 to 9N_{cv}

For evaluating the leakage flux produced by the stator currents were used two transverse reluctances: one through the air of the slot (2.6), calculated as the

parallel connection of two reluctances (Fig. 2.3 *b*), the other across the slot opening (2.7):

$$\Re_i = \frac{1}{\mu_0 L \frac{h_{avv}}{(L_{tc} - L_{fc})} ln\left(\frac{L_{tc}}{L_{fc}}\right) + \mu_0 L \frac{(h_{bd} - h_{cl})}{(L_{cl} - L_{tc})} ln\left(\frac{L_{cl}}{L_{tc}}\right)} \tag{2.6}$$

$$\Re_i = \frac{1}{\mu_0} \frac{L_{cl}}{h_{cl} L} \tag{2.7}$$

Other elements

The reluctances related to other elements are not reported because of their simple form. Note that, in general, the non-linear sub-domains have a value of permeability that depends on the B-H curve, as in (2.5).

2.3 The Numerical Solving Process

The problem is described through a non-linear system of n equations ($n = 18N_{cv} + 8$) where the unknowns are the values of the magnetic fluxes $\varphi_1, \varphi_2, \ldots \varphi_n$ in every sub-domain of the machine.

Two principles of electromagnetism are used to write the equations: Hopkinson's law, applied along closed paths identified in the machine, and Gauss's law, i.e. conservation of the magnetic fluxes incoming in and outgoing from the nodes of the network (continuity equations).

Overall, the system includes $9N_{cv} + 5$ equations of the first typology and $9N_{cv} + 3$ of the second typology, with a matrix form defined as follows:

$$[A]\overline{\varphi} = \overline{F}_M \tag{2.8}$$

Matrix [*A*] in (2.8) can be seen as composed by some blocks depending on the following characterization: its coefficients a_{ij} represent magnetic reluctances in the rows related to Hopkinson's law equations, whereas they have the value ±1 in the rows related to Gauss' law equations, being essentially algebraic sum of fluxes:

$$\begin{aligned} a_{ij} &\equiv \Re(\mu, \theta_{xm}) \quad i = 1..5N_{cv}+1, 12N_{cv}+1..14N_{cv}, 16N_{cv}+1.. \\ &\quad ..18N_{cv}, 18N_{cv}+1, 18N_{cv}+2, 18N_{cv}+5, 18N_{cv}+6 \\ a_{ij} &\equiv \pm 1 \qquad i = 5N_{cv}+2..12N_{cv}, 14N_{cv}+1..16N_{cv}, \\ &\quad 18N_{cv}+3, 18N_{cv}+4, 18N_{cv}+7, 18N_{cv}+8 \end{aligned} \tag{2.9}$$

The system, divided in groups of equations according to the different areas of the machine, is specified in detail as follows (2.10 – 2.28). Note that the index *i* varies in every group from 1 to N_{cv} depending on the basic cell related to the examined equation, except for group (2.16), where the first equation of the group is substituted by (2.15):

Tooth to tooth across the airgap $(i = 1 \text{ to } N_{cv})$

$$\begin{aligned} &\Re_{(i)}\varphi_{(i)} - \Re_{(i+1)}\varphi_{(i+1)} - \Re_{(N_{cv}+i)}\varphi_{(N_{cv}+i)} - \Re_{(2N_{cv}+i)}\varphi_{(2N_{cv}+i)} + \\ &+ \Re_{(4N_{cv}+i)}\varphi_{(4N_{cv}+i)} - \Re_{(4N_{cv}+i+1)}\varphi_{(4N_{cv}+i+1)} + \Re_{(5N_{cv}+i)}\varphi_{(5N_{cv}+i)} + \\ &- \Re_{(5N_{cv}+i+1)}\varphi_{(5N_{cv}+i+1)} + \Re_{(6N_{cv}+i)}\varphi_{(6N_{cv}+i)} + \\ &- \Re_{(6N_{cv}+i+1)}\varphi_{(6N_{cv}+i+1)} = F_{M(i)} \end{aligned} \tag{2.10}$$

Higher slot area between two teeth $(i = N_{cv}+1 \text{ to } 2N_{cv})$

$$\begin{aligned} &- \Re_{(N_{cv}+i)}\varphi_{(N_{cv}+i)} - \Re_{(3N_{cv}+i)}\varphi_{(3N_{cv}+i)} + \Re_{(6N_{cv}+i)}\varphi_{(6N_{cv}+i)} + \\ &- \Re_{(6N_{cv}+i+1)}\varphi_{(6N_{cv}+i+1)} = F_{M(N_{cv}+i)} \end{aligned} \tag{2.11}$$

Tooth to tooth around the slot area $\left(i = 2N_{cv} + 1 \text{ to } 3N_{cv}\right)$

$$\begin{aligned} &-\Re_{(N_{cv}+i)}\varphi_{(N_{cv}+i)} + \Re_{(4N_{cv}+i)}\varphi_{(4N_{cv}+i)} - \Re_{(4N_{cv}+i+1)}\varphi_{(4N_{cv}+i+1)} + \\ &+\Re_{(6N_{cv}+i)}\varphi_{(6N_{cv}+i)} - \Re_{(6N_{cv}+i+1)}\varphi_{(6N_{cv}+i+1)} - \Re_{(8N_{cv}+i)}\varphi_{(8N_{cv}+i)} + \\ &-\Re_{(12N_{cv}+i+1)}\varphi_{(12N_{cv}+i+1)} - \Re_{(13N_{cv}+i)}\varphi_{(13N_{cv}+i)} = F_{M(2N_{cv}+i)} \end{aligned} \tag{2.12}$$

Right tooth tip across the airgap $\left(i = 3N_{cv} + 1 \text{ to } 4N_{cv}\right)$

$$\begin{aligned} &\Re_{(i)}\varphi_{(i)} + \Re_{(5N_{cv}+i)}\varphi_{(5N_{cv}+i)} - \Re_{(9N_{cv}+i)}\varphi_{(9N_{cv}+i)} + \\ &-\Re_{(11N_{cv}+i)}\varphi_{(11N_{cv}+i)} + \Re_{(13N_{cv}+i)}\varphi_{(13N_{cv}+i)} = 0 \end{aligned} \tag{2.13}$$

Left tooth tip across the airgap $\left(i = 4N_{cv} + 1 \text{ to } 5N_{cv}\right)$

$$\begin{aligned} &-\Re_{(i)}\varphi_{(i)} - \Re_{(5N_{cv}+i)}\varphi_{(5N_{cv}+i)} + \Re_{(7N_{cv}+i)}\varphi_{(7N_{cv}+i)} + \\ &+\Re_{(10N_{cv}+i)}\varphi_{(10N_{cv}+i)} + \Re_{(12N_{cv}+i)}\varphi_{(12N_{cv}+i)} = 0 \end{aligned} \tag{2.14}$$

Closing equation $\left(i = 5N_{cv} + 1\right)$

$$\sum_{i=1}^{N_{cv}} \Re_{(N_{cv}+i)}\varphi_{(N_{cv}+i)} = 0 \ . \tag{2.15}$$

Nodes (1-2-4-7-9-3-5)

$\left(i = 5N_{cv} + 2 \text{ to } 6N_{cv}\right)$

$$\varphi_{(N_{cv}+i-1)} - \varphi_{(N_{cv}+i)} - \varphi_{(6N_{cv}+i)} - \varphi_{(16N_{cv}+i)} - \varphi_{(17N_{cv}+i)} = 0 \tag{2.16}$$

$\left(i = 6N_{cv} + 1 \text{ to } 7N_{cv}\right)$

$$\varphi_{(3N_{cv}+i-1)} - \varphi_{(3N_{cv}+i)} + \varphi_{(4N_{cv}+i)} - \varphi_{(6N_{cv}+i)} + \varphi_{(14N_{cv}+i)} + \\ + \varphi_{(15N_{cv}+i)} - \varphi_{(16N_{cv}+i)} - \varphi_{(17N_{cv}+i)} = 0 \tag{2.17}$$

$\left(i = 7N_{cv} + 1 \text{ to } 8N_{cv}\right)$

$$\varphi_{(4N_{cv}+i)} - \varphi_{(5N_{cv}+i)} - \varphi_{(12N_{cv}+i)} + \varphi_{(13N_{cv}+i)} = 0 \tag{2.18}$$

$\left(i = 8N_{cv} + 1 \text{ to } 9N_{cv}\right)$

$$\varphi_{(i)} - \varphi_{(5N_{cv}+i)} = 0 \tag{2.19}$$

$\left(i = 9N_{cv} + 1 \text{ to } 10N_{cv}\right)$

$$\varphi_{(i)} - \varphi_{(2N_{cv}+i-1)} + \varphi_{(2N_{cv}+i)} + \varphi_{(10N_{cv}+i)} + \varphi_{(11N_{cv}+i)} = 0 \tag{2.20}$$

$\left(i = 10N_{cv} + 1 \text{ to } 11N_{cv}\right)$

$$\varphi_{(7N_{cv}+i)} + \varphi_{(8N_{cv}+i-1)} - \varphi_{(12N_{cv}+i)} - \varphi_{(14N_{cv}+i)} = 0 \tag{2.21}$$

$\left(i = 11N_{cv} + 1 \text{ to } 12N_{cv}\right)$

$$\varphi_{(8N_{cv}+i)} - \varphi_{(9N_{cv}+i)} - \varphi_{(13N_{cv}+i)} + \varphi_{(15N_{cv}+i)} = 0 \tag{2.22}$$

Right semi-slot area $\left(i = 12N_{cv} + 1 \text{ to } 13N_{cv}\right)$

$$\Re_{(4N_{cv}+i)}\varphi_{(4N_{cv}+i)} + \Re_{(6N_{cv}+i)}\varphi_{(6N_{cv}+i)} - \Re_{(13N_{cv}+i)}\varphi_{(13N_{cv}+i)} + \\ - \Re_{(15N_{cv}+i)}\varphi_{(15N_{cv}+i)} - \Re_{(17N_{cv}+i)}\varphi_{(17N_{cv}+i)} = F_{M(12N_{cv}+i)} \tag{2.23}$$

Lower tooth area between two slots $\left(i = 13N_{cv} + 1 \text{ to } 14N_{cv}\right)$

$$-\Re_{(12N_{cv}+i)}\varphi_{(12N_{cv}+i)} - \Re_{(13N_{cv}+i)}\varphi_{(13N_{cv}+i)} + \\ + \Re_{(14N_{cv}+i)}\varphi_{(14N_{cv}+i)} - \Re_{(15N_{cv}+i)}\varphi_{(15N_{cv}+i)} = F_{M(13N_{cv}+i)} \tag{2.24}$$

Nodes (6-8)

$\left(i = 14N_{cv} + 1 \text{ to } 15N_{cv}\right)$

$$\varphi_{(7N_{cv}+i)} - \varphi_{(10N_{cv}+i)} = 0 \tag{2.25}$$

$\left(i = 15N_{cv} + 1 \text{ to } 16N_{cv}\right)$

$$\varphi_{(9N_{cv}+i)} - \varphi_{(11N_{cv}+i)} = 0 \tag{2.26}$$

Higher left semi-slot area $\left(i = 16N_{cv} + 1 \text{ to } 17N_{cv}\right)$

$$-\Re_{(6N_{cv}+i)}\varphi_{(6N_{cv}+i)} + \Re_{(16N_{cv}+i)}\varphi_{(16N_{cv}+i)} = F_{M(16N_{cv}+i)} \tag{2.27}$$

Higher right semi-slot area $\left(i = 17N_{cv} + 1 \text{ to } 18N_{cv}\right)$

$$\Re_{(6N_{cv}+i)}\varphi_{(6N_{cv}+i)} - \Re_{(17N_{cv}+i)}\varphi_{(17N_{cv}+i)} = F_{M(17N_{cv}+i)} \tag{2.28}$$

The form of the remaining eight equations is described in the next sections: they are used for describing additional branches which are formed during the movement of the rotor. The known terms $F_{M(i)}$, i = 1 to n, represent the ampere-turns linked by the paths related to the Hopkinson's law equations.

Note that the row $5N_{cv}$+1 (14) represents the equation which makes the system

solvable: it can be seen as a boundary condition equation, closing the path along the branches of the stator yoke.

The solving process is based on the method of Gaussian elimination, for reducing the matrix of coefficients to a triangular one. It is applied iteratively k-times, being some coefficients dependent on the rotor position ($a_{ij(k)} = f(\theta_{xm})$), some other also dependent on the value of magnetic permeability of the i-th sub-domain ($a_{ij(k)} = f(\mu_{i(k)}, \theta_{xm})$). For a given rotor position θ_{xm} the length and thickness for the flux tubes that change dimensions or position are recalculated. Starting with initial random values of $\Re_{i(1)}$, i = 1 to n, the solution of the system in the k-th order of iteration is obtained in terms of $\varphi_{i(k)}$, i = 1 to n, by solving the system (2.8): it is then possible to determine the values of flux densities $B_{i(k)}$ being known the flux tubes cross-sectional areas S_i. An interpolation of the magnetic characteristic $H_i = f(B_i)$ is implemented for domains occupied by non-linear magnetic material, while a constant value of μ_i is used for linear domains. It is then possible to calculate the k-th value $\mu_{i(k)}$ by combining the actual value $\hat{\mu}_{i(k)}$ and the previous value $\mu_{i(k-1)}$ and, for every order of iteration, re-calculating the magnetic permeabilities $\mu_{i(k)}$ related to non-linear domains, following the general criterion, to facilitate the convergence process [15]:

$$\hat{\mu}_{i(k)} = \frac{B_{i(k)}}{H_{i(k)}} \tag{2.29}$$

$$\mu_{i(k)} = \hat{\mu}_{i(k)}^{d} \mu_{i(k-1)}^{1-d} \tag{2.30}$$

where the value of d, the damping constant, is chosen equal to 0.1. Consequently, the reluctances $\Re_{i(k)} = f(\mu_{i(k)}, \theta_{xm})$ are updated, leading to a further step for the Gauss method, until the following condition is satisfied [15]:

$$\left| \frac{\mu_{i(k)} - \mu_{i(k-1)}}{\mu_{i(k-1)}} \right| \leq \delta \tag{2.31}$$

being δ the requested accuracy. At this step, all the magnetic quantities related to each sub-domain of the machine are known: permeabilities μ_i, magnetic field H_i, fluxes φ_i, flux densities B_i.

2.4 Simulating the Movement

The analysis in the presence of movement proceeds with an external loop that sets the rotor angular position θ_{xm}, representing the N-magnet position in a generic time instant, with respect to a fixed reference system. The origin of the reference system lies on the axis of symmetry of a chosen slot.

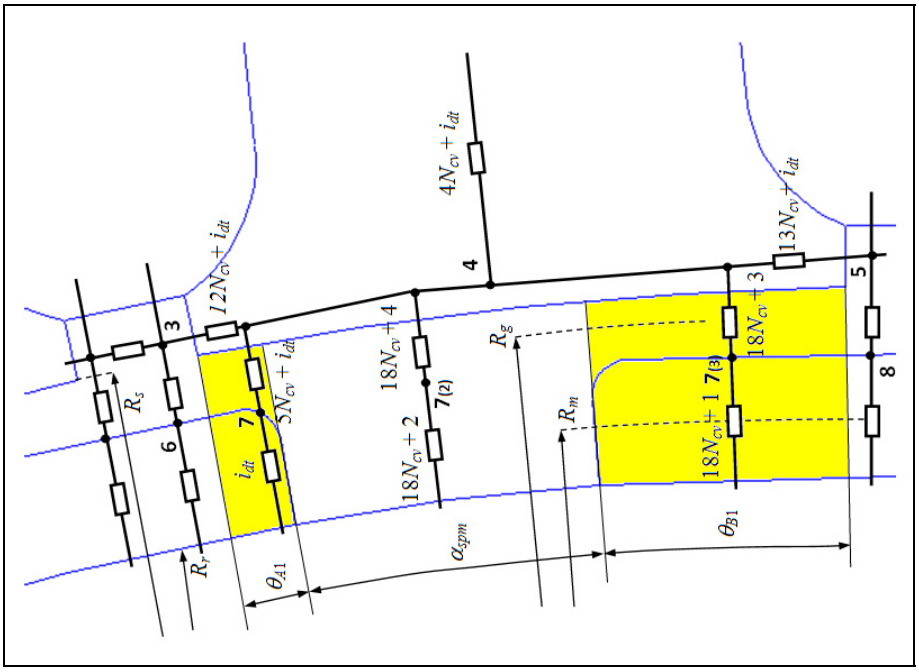

Fig. 2.4. Configuration of the network in presence of gap between N- and S- magnet.

By varying the value of θ_{xm}, the geometrical parameters of the flux tubes are modified. Consequently, the related coefficients $a_{ij}(k) = f(\mu_i(k), \theta_{xm})$ and the continuity equations in the nodes involved in changes are modified also. The solution process is then repeated by solving every step in the same way described in Section 2.3.When the gap between the magnets is comprised under a tooth, as

shown in Fig. 2.4, the software modifies the configuration of the magnetic network by adding two new branches and four new reluctances of variable cross section, depending on the value of θ_{xm} in a generic time instant. Consequently, there are four new unknowns per gap. Instead of only one flux tube, as in the case of uniform magnet (Fig. 2.2), in this situation the area under the tooth can be divided into three flux tubes related, respectively, to N-magnet portion, magnet gap and S-magnet portion, as shown in Fig. 2.4.The index i_{dt} assumes an integer value to identify the tooth that comprises the gap, so that the reluctances $\Re_{(idt)}$, $\Re_{(5Ncv+\ idt)}$, $\Re_{(18Ncv+1)}$, $\Re_{(18Ncv+3)}$ involved in the movement, change their reference angles $\theta_{A1} = f(\theta_{xm})$ and $\theta_{B1} = f(\theta_{xm})$, that subtend the related cross-sectional area, according to:

$$\theta_{A1} = \left\lfloor \theta_{xm} - \alpha_{sap} - (i_{dt} - 1)\alpha_{cv} \right\rfloor \tag{2.32}$$

$$\alpha_{spm} = s_{pm} / R_m \tag{2.33}$$

$$\theta_{B1} = \left\lfloor \alpha_{cv} - \alpha_{sap} - \theta_{xm} - \alpha_{spm} + (i_{dt} - 1)\alpha_{cv} \right\rfloor \tag{2.34}$$

The three flux tubes under the tooth are characterized by six reluctances: two of them also existing in the case of uniform magnet, $\Re_{(idt)}$ and $\Re_{(5Ncv+\ idt)}$, but in the present case modified in the cross-sections and four additional reluctances, from the $\Re_{(18Ncv+1)}$ to the $\Re_{(18Ncv+4)}$.

$$\Re_{(i_{dt})} = \frac{1}{\mu_m} \frac{L_m}{R_m \theta_{A1}(\theta_{xm}, i_{dt}) L} \tag{2.35}$$

$$\Re_{(5N_{cv}+i_{dt})} = \frac{1}{\mu_0} \frac{g}{R_g \theta_{A1}(\theta_{xm}, i_{dt}) L} \tag{2.36}$$

$$\Re_{(18N_{cv}+1)} = \frac{1}{\mu_m} \frac{L_m}{R_m \theta_{B1}(\theta_{xm}, i_{dt}) L} \tag{2.37}$$

$$\Re_{(18N_{cv}+3)} = \frac{1}{\mu_0}\frac{g}{R_g \theta_{B1}(\theta_{xm}, i_{dt})L} \tag{2.38}$$

$$\Re_{(18N_{cv}+2)} = \frac{1}{\mu_0}\frac{L_m}{R_m \alpha_{spm} L} \tag{2.39}$$

$$\Re_{(18N_{cv}+4)} = \frac{1}{\mu_0}\frac{g}{R_g \alpha_{spm} L} \tag{2.40}$$

The cross-sectional areas in the formulas are calculated at the reference radius of every sub-domain. Four additional equations (2.41)-(2.44) are added to the system for taking into account the new unknown fluxes with respect to the case of uniform magnet: the Hopkinson's law applied to *N*- and *S*-magnet, the continuity equations applied to nodes $7_{(2)}$ and $7_{(3)}$:

$$\begin{aligned}&\Re_{(i_{dt})}\varphi_{(i_{dt})} + \Re_{(5N_{cv}+i_{dt})}\varphi_{(5N_{cv}+i_{dt})} - \Re_{(18N_{cv}+2)}\varphi_{(18N_{cv}+2)} + \\ &- \Re_{(18N_{cv}+4)}\varphi_{(18N_{cv}+4)} = F_{M(18N_{cv}+1)}\end{aligned} \tag{2.41}$$

$$\begin{aligned}&-\Re_{(18N_{cv}+1)}\varphi_{(18N_{cv}+1)} + \Re_{(18N_{cv}+2)}\varphi_{(18N_{cv}+2)} - \Re_{(18N_{cv}+3)}\varphi_{(18N_{cv}+3)} + \\ &+ \Re_{(18N_{cv}+4)}\varphi_{(18N_{cv}+4)} = F_{M(18N_{cv}+2)}\end{aligned} \tag{2.42}$$

$$-\varphi_{(18N_{cv}+2)} + \varphi_{(18N_{cv}+4)} = 0 \tag{2.43}$$

$$-\varphi_{(18N_{cv}+1)} + \varphi_{(18N_{cv}+3)} = 0 \ . \tag{2.44}$$

Obviously, other equations already comprised in the system have to be modified according to the variations in the magnetic circuit, as for example in the node 4, where the continuity equation written in the presence of gap (2.45) is compared with the situation of uniform magnet (2.46):

$$\begin{aligned}&\varphi_{(4N_{cv}+i_{dt})} - \varphi_{(5N_{cv}+i_{dt})} - \varphi_{(12N_{cv}+i_{dt})} + \varphi_{(13N_{cv}+i_{dt})} + \\ &- \varphi_{(18N_{cv}+3)} - \varphi_{(18N_{cv}+4)} = 0\end{aligned} \tag{2.45}$$

$$\varphi_{(4N_{cv}+i)} - \varphi_{(5N_{cv}+i)} - \varphi_{(12N_{cv}+i)} + \varphi_{(13N_{cv}+i)} = 0 \tag{2.46}$$

The same logic can be applied to the other additional equations (with indexes from $18N_{cv} + 5$ to $18N_{cv} + 8$) considering the second gap between the magnets, depending on the related reference angles and on a new index i_{dt2} which identifies the tooth comprising the gap, with reluctances $\Re_{(idt2)}$, $\Re_{(5Ncv+\ idt2)}$, $\Re_{(18Ncv+5)}$, $\Re_{(18Ncv+6)}$, $\Re_{(18Ncv+7)}$, $\Re_{(18Ncv+8)}$.

2.5 Co-energy, Torque and Radial Forces

One of the features of the proposed algorithm is the capability of determining the total magnetic co-energy of the machine in a series of different rotor positions: this allows calculating the electromagnetic torque acting between stator and rotor. In order to do this, the volumes τ_i and flux paths of every sub-domain are developed in circular shape, based on the average radius of the related part of the machine [15], [18]. The equation used to determine the magnetic co-energy W_i' of the i-th sub-domain is [20]:

$$W_i' = \int_{\tau_i} \int_0^{\overline{H}} B_i(\overline{H})\, dH_i\, d\tau \tag{2.47}$$

To evaluate (2.47), in case of non-linear sub-domains, the algorithm uses the numerical integration method of trapezoids by interpolating the magnetic characteristic of the material in order to find the couples of consequent values B_{j+1} and B_j in m-1 steps, where m depends on the desired accuracy:

$$W'_{i(NL)} = \sum_{j=1}^{m-1} \frac{\left[B_{j+1}\left(H_{j+1}\right) + B_j\left(H_j\right)\right]\Delta H_j}{2}\, \tau_i \tag{2.48}$$

In the case of linear sub-domains, the following relationship is used:

$$W'_{i(L)} = \frac{1}{2}\frac{B_i^2}{\mu_i}\tau_i \tag{2.49}$$

The electromagnetic torque T is calculated through the finite difference approximation of the first derivative of the total co-energy W' obtained as summation of all the W_i' [21]:

$$T = \lim_{\Delta\theta_{rm}\to 0}\left.\frac{\Delta W'}{\Delta\theta_{rm}}\right|_{i_f=const.} \cong \left.\frac{\partial W'}{\partial\theta_{rm}}\right|_{i_f=const.} \tag{2.50}$$

where $\Delta\theta_{rm}$ is the angular rotor displacement between two different steps and the calculation is done by maintaining constant values of the phase currents.

The radial component F_r of the forces was determined by applying the Maxwell Stress Tensor method (42) on a closed surface enveloping the frontal cross sections of the teeth in the stator, taking into account the normal and tangential components of flux density and of magnetic field acting in every tooth.

$$\vec{T} = \vec{H}\left(\vec{B}\cdot\hat{n}\right) - \frac{1}{2}\left(\vec{B}\cdot\vec{H}\right)\hat{n} = H_t B_n \hat{t} + \frac{1}{2}\left(H_n B_n - H_t B_t\right)\hat{n} \tag{2.51}$$

Integrating (2.51) on the above described surface and considering the discretization of the model, the contribution related to the i-th tooth is given, for radial components acting along the axis of the tooth (normal to the surface), as

$$\begin{aligned} F_{rn(i)} = {} & \frac{1}{2\mu_0}\left(S_{dg}B^2_{5N_{cv}+i} + S_{sap}B^2_{7N_{cv}+i} + S_{sap}B^2_{9N_{cv}+i}\right) + \\ & - \frac{1}{2\mu_0}\left(S_{sap}B^2_{8N_{cv}+i-1} + S_{sap}B^2_{8N_{cv}+i}\right) \end{aligned} \tag{2.52}$$

and, for radial components acting perpendicularly to the axis of the tooth (tangential to the surface), is given as

$$F_{rt(i)} = \frac{1}{\mu_0}\left(S_{sap}B_{7N_{cv}+i}B_{8N_{cv}+i-1} + S_{sap}B_{9N_{cv}+i}B_{8N_{cv}+i}\right) \tag{2.53}$$

Note that, in (2.52) and (2.53), S_{dg} represents the frontal cross-sectional area of the tooth, S_{sap} the area related to a semi-slot opening, while the considered flux densities values are described in Figs. 2.2-2.4. The projections of the normal and tangential components on a reference system centered on the motor axis are finally given as

$$F_{xr(i)} = F_{rn(i)}\, cos\left(\alpha_{dt(i)}\right) + F_{rt(i)}\, sin\left(\alpha_{dt(i)}\right) \tag{2.54}$$

$$F_{yr(i)} = F_{rn(i)}\, sin\left(\alpha_{dt(i)}\right) - F_{rt(i)}\, cos\left(\alpha_{dt(i)}\right) \tag{2.55}$$

where $\alpha_{dt(i)}$ represents the angular position of the axis of the i-th tooth with respect to the x axis; by summing the terms in (2.54), (2.55) for all the teeth, it gives the components F_{xr} and F_{yr} of the resultant radial force applied on the rotor.

2.6 Results and Comparison with FEA Software

The 2D FEA software "FEMM 4.2" [22] was used in order to verify the accuracy of the proposed analysis. Two different typologies of synchronous PM machine were considered, as shown in Fig. 2.5, supplied by sinusoidal drives.

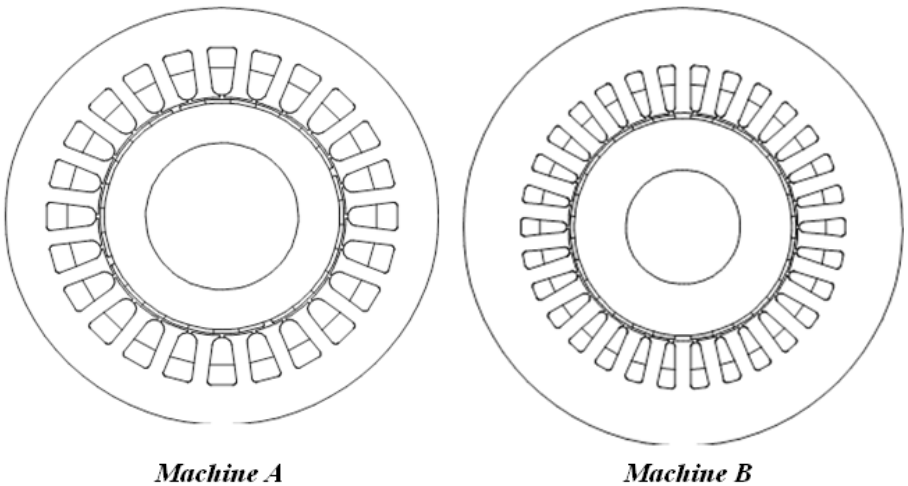

Fig. 2.5. The PMSM machines considered in the analysis

***Machine A*:** 2-pole pairs, 3-phase, 24 slots, traditional winding (only odd mmf harmonic components), 1 - 6 double layer shortened pitch.

Machine B: 1-pole pair, 5-phase, 30 slots, special winding (odd and even mmf harmonic components), 6 slots per phase per pole in each layer, one phase occupying 72° in angular space of the stator.

In order to obtain an accurate electromagnetic analysis, about 108˙000 nodes were used for meshing the models in FEMM. In Tab. I the main geometrical dimensions of the machines are given.

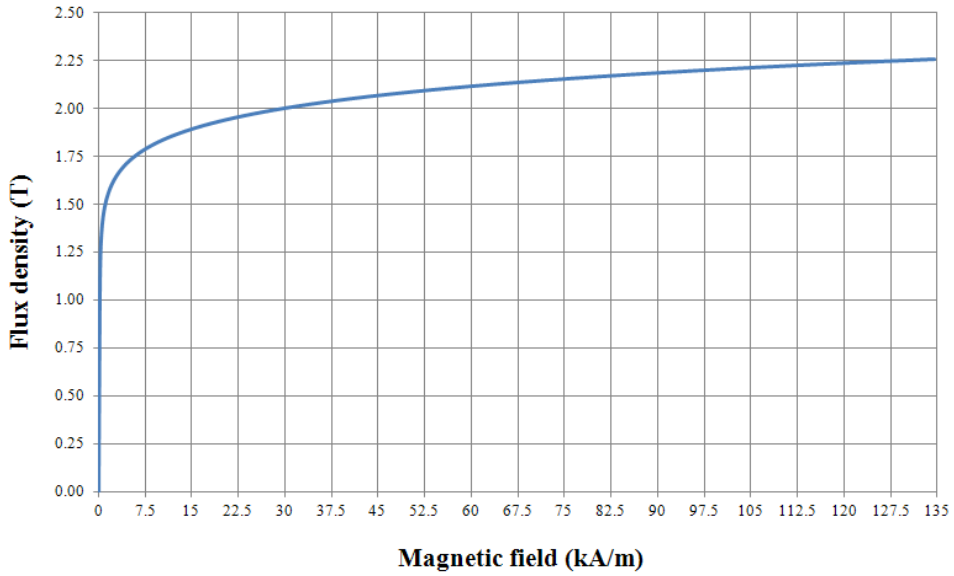

Fig. 2.6. The B-H characteristic of the material

The non-linear B-H curve of the magnetic material is shown in Fig. 2.6, the same for Machine A and for Machine B. The initial relative permeability is 4380. In Tab. I the main data of the two machines are presented.

In the following the results of the comparisons are presented in graphical form.

TABLE I. MAIN DATA OF MACHINES A E B

Param.	Description	A	B
N_{sl}	number of slots	24	30
p	pole pairs of the machine	2	1
m	number of phases	3	5
I_n	rated phase current (A_{rms})	74.78	59.82
T_n	rated torque (Nm)	42.41	30.29
g	airgap width (mm)	1	1
D_e	stator outer diameter (mm)	210	230
D_s	stator inner diameter (mm)	120	120
D_m	mean diameter of the magnet (mm)	116	116
D_{cv_ext}	diameter at the bottom of the slot (mm)	170	170
D_{cv_int}	diameter at the top of the slot (mm)	130.2	126.3
D_r	rotor outer diameter (mm)	114	114
D_{alb}	rotor inner diameter (mm)	74	60
α_{Ldg}	angle underlying the tooth surface	13.1°	10.1°
α_{sap}	semi-angle underlying the slot opening	0.95°	0.95°
α_{spm}	angle underlying the magnet gap	4°	8°
α_{cv}	slot pitch angle	15°	12°
a_{dt}	stator slot height (mm)	25	25
h_{cl}	slot opening height (mm)	1	1
L	axial length of the machine (mm)	180	180
L_m	magnet width (mm)	2	2
L_{dt}	tooth-body width (mm)	7.5	8
L_{cl}	slot opening width (mm)	2	2
L_{tc}	slot width at the top slot radius (mm)	9.6	5.23
L_{fc}	slot width at the bottom slot radius (mm)	14.8	9.7
τ_{cv}	slot pitch at the inner stator radius (mm)	15.71	12.57

2.6.1 Machine A

With reference to Machine A, Figs. 2.7, 2.8 show the results of the comparison for the same rotor position. In particular, Fig. 2.7 shows the linkage fluxes. As can be seen, the linkage fluxes of the three phases calculated using the proposed method are in very good agreement with those obtained by FEA analysis.

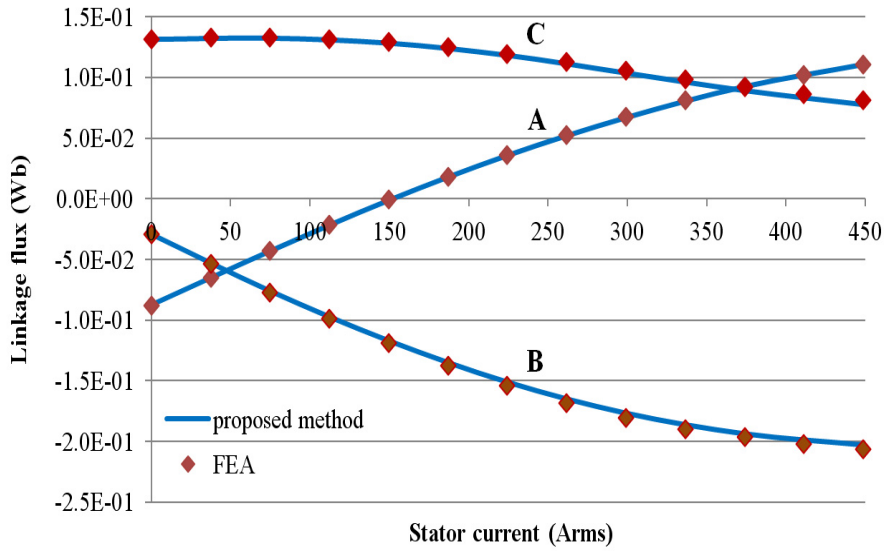

Fig. 2.7. Phase linkage fluxes vs stator RMS current (Machine A)

Small discrepancies appears only for very high values of the current (highly saturated machine). In Fig. 2.8 the torque values (p.u.) and the magnetic co-energy values, calculated using the proposed method, are compared with those obtained by FEA.

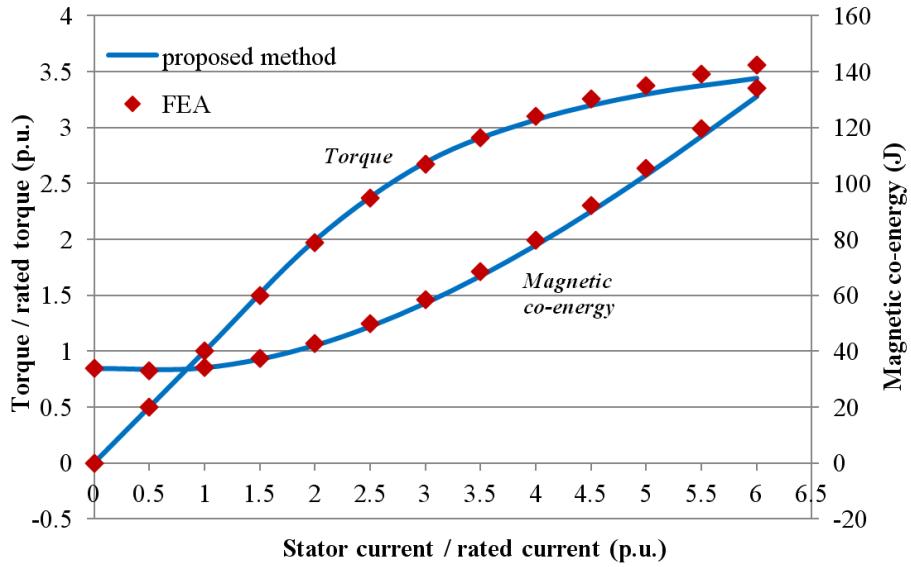

Fig. 2.8. Torque and magnetic co-energy vs stator RMS current (Machine A)

For low values of the currents the two approaches give the same results. For

higher current values (non-linear behavior) some small differences appear. However, the torque reduction with respect to the supposed linear behavior is very well represented.

2.6.2 Machine B

With reference to the 5-phase Machine B, Figs. 2.9 to 2.11 show the results of the comparison for the same rotor position.

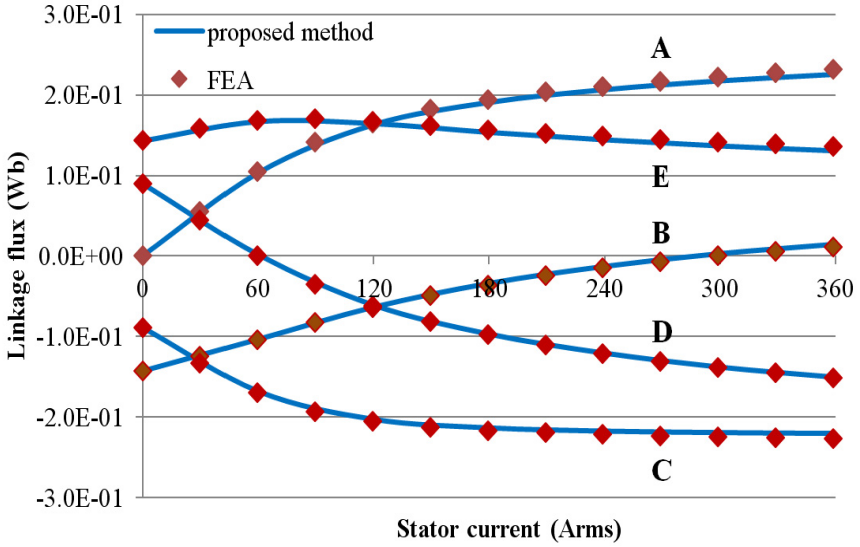

Fig. 2.9. Phase linkage fluxes vs stator RMS current (Machine B)

In particular, Fig. 2.9 shows the linkage fluxes of the five phases. Also in this case, the results obtained using the proposed method are in very good agreement with those obtained by FE analysis. Fig. 2.10 shows the torque (p.u.) and the magnetic co-energy values of the system calculated using the proposed and the FEA approach. Referring to the magnetic co-energy, a very good agreement appears, with only small differences when the machine is highly saturated; about the torque, is possible to observe a very good agreement for low and medium (rated) current values. Some small differences appear in the higly saturated behavior.

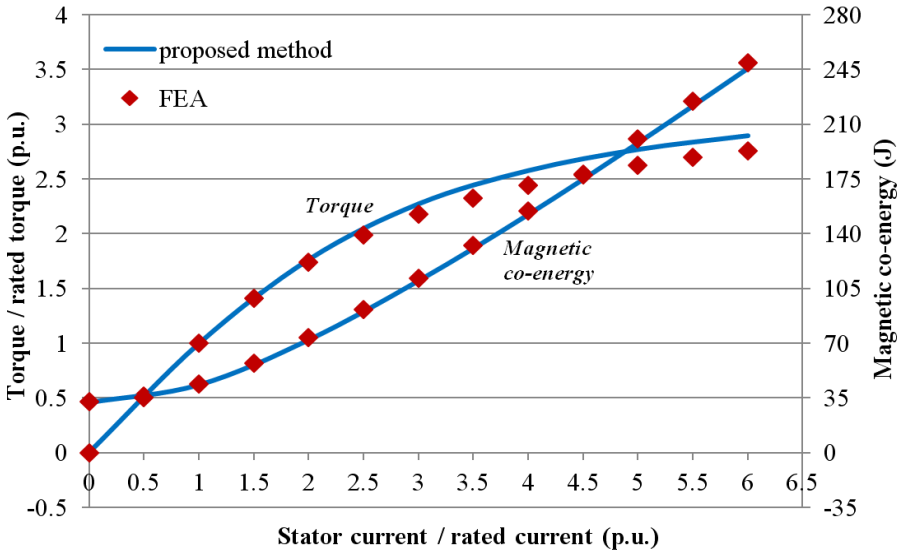

Fig. 2.10. Torque and magnetic co-energy vs stator RMS current (Machine B)

A further comparison has been made by supplying the five phases of Machine B with a balanced system of sinusoidal currents with a time-phase displacement of $4\pi/5$ (sequence 2). The considered winding arrangement produces an airgap distribution of the mmf having odd and even harmonic components.

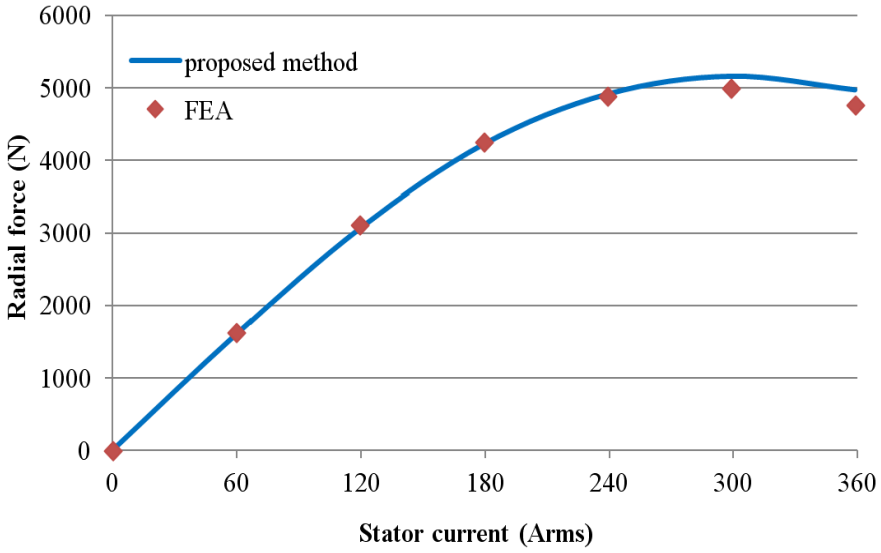

Fig. 2.11. Magnitude of the radial force vs stator RMS current (Machine B)

Taking the winding arrangement into account and the particular system of currents, it is possible to align the 4 pole harmonic component of the stator mmf with the magnet axis. In these conditions a resultant radial force exists acting on the rotor along the direction of the magnet axis [12]. Fig. 2.11 shows the calculated magnitude of the radial force compared with that obtained by FEA. As can be seen, in this case also there is a good agreement between the proposed method and the results of FEA. In Fig. 2.12 the *x*- and *y*-components of the radial force are shown. The force has been calculated for 9 values, equally spaced of π/16, of the phase angle of the second harmonic component of the stator mmf with respect to the magnet axis (*y*-axis in Fig. 2.12), and for 3 values of the stator current amplitude: the rated value, two-times and four-times the rated value.

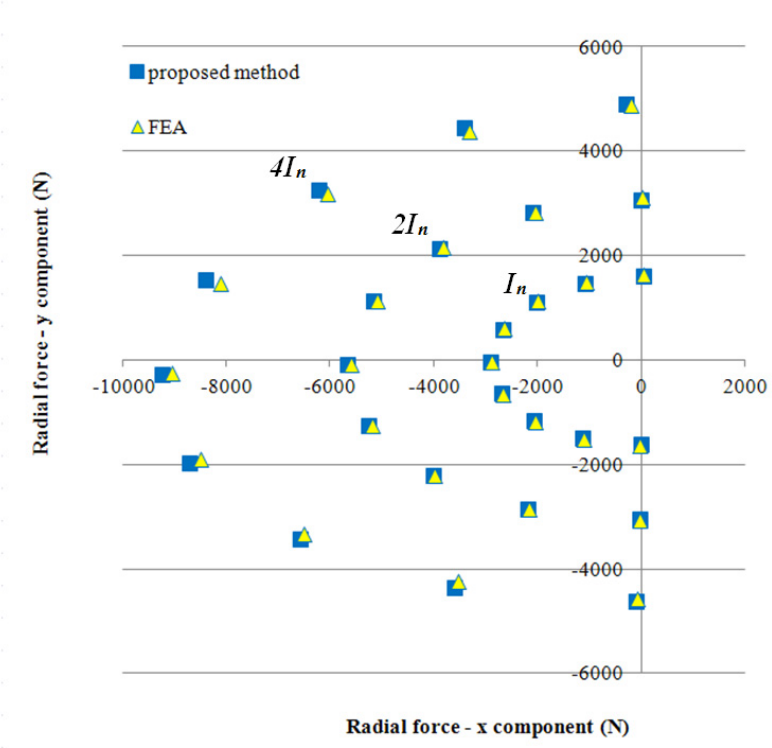

Fig. 2.12. y-component vs x-component of the radial force (Machine B)

Also in this kind of analysis, the obtained results are very similar to those obtained by FEA. It is interesting to note that, for the same currents amplitude,

the magnitude of the radial force is not constant but changes with the phase angle of the mmf. This behavior is due to the presence of higher harmonic orders in the magnet and stator mmf distribution.

2.7 Conclusion

In this chapter an algorithm for the non-linear magnetic analysis of multiphase surface-mounted PM machines with semi-closed slots has been presented.

The basic element of the geometry is duplicated allowing to build and analyze whatever typology of windings and ampere-turns distribution in a pair of poles.

The performances of the proposed method have been compared with those of a well known FEA software in terms of linkage fluxes, co-energy, torque and radial force. The obtained results for a traditional three-phase machine and for a 5-phase machine with unconventional winding distribution showed that the values of local and global quantities are practically coinciding for values of the stator currents up to rated values. Furthermore, they are very similar also in the non-linear behavior even if very large current values are injected.

When developing a new machine design the proposed method is useful not only for the reduction of computing time, but mainly for the simplicity of changing the values of the design variables, being the numerical inputs of the problem obtained by changing some critical parameters, without the need for re-designing the model in a CAD interface. It can be concluded that the proposed method provides an accurate description of electromagnetic phenomena taking magnetic saturation into account. For a given rotor position and for given stator currents, the output torque as well as the radial forces acting on the moving part of a multiphase machine can be easily and quickly calculated.

The latter feature makes the algorithm particularly suitable in order to design and analyze bearingless machines.

2.8 References

[1] D. Casadei, D. Dujic, E. Levi, G. Serra, A. Tani, and L. Zarri, "General Modulation Strategy for Seven-Phase Inverters with Independent Control of Multiple Voltage Space Vectors", *IEEE Trans. on Industrial Electronics*, Vol. 55, NO. 5, May 2008, pp. 1921-1932.

[2] Fei Yu, Xiaofeng Zhang, Huaishu Li, Zhihao Ye, "The Space Vector PWM Control Research of a Multi-Phase Permanent Magnet Synchronous Motor for Electrical Propulsion", *Electrical Machines and Systems (ICEMS)*, Vol. 2, pp. 604-607, Nov. 2003.

[3] Ruhe Shi, H.A.Toliyat, "Vector Control of Five-phase Synchronous Reluctance Motor with Space Pulse Width Modulation for Minimum Switching Losses", *Industry Applications Conference, 36th IAS Annual Meeting*. Vol. 3, pp. 2097-2103, 30 Sept.-4 Oct. 2001.

[4] M. A. Abbas, R.Christen, T.M.Jahns, "Six-phase Voltage Source Inverter Driven Induction Motor", *IEEE Trans. on IA*, Vol.IA-20, No. 5, pp. 1251-1259, 1984.

[5] E. E. Ward, H. Harer, "Preliminary Investigation of an Inverter fed 5-phase Induction Motor", *IEE Proc*, June 1969, Vol. 116(B), No. 6, pp. 980-984, 1969.

[6] Y. Zhao, T. A. Lipo, "Space Vector PWM Control of Dual Three-phase Induction Machine Using Vector Space Decompositon", *IEEE Trans. on IA*, Vol. 31, pp. 1177-1184, 1995.

[7] Xue S, Wen X.H, "Simulation Analysis of A Novel Multiphase SVPWM Strategy", *2005 IEEE International Conference on Power Electronics and Drive Systems (PEDS)*, pp. 756-760, 2005.

[8] Parsa L, H. A. Toliyat, "Multiphase Permanent Magnet Motor Drives", *Industry Applications Conference, 38th IAS Annual Meeting.* Vol. 1, pp. 401-408, 12.-16 Oct. 2003.

[9] H. Xu, H.A. Toliyat, L.J. Petersen, "Five-Phase Induction Motor Drives with DSP-based Control System", *IEEE Trans. on IA*, Vol. 17, No. 4, pp. 524-533, 2002.

[10] L. Zarri, M. Mengoni, A. Tani, G. Serra, D. Casadei: "Minimization of the Power Losses in IGBT Multiphase Inverters with Carrier-Based Pulsewidth Modulation," *IEEE Trans. on Industrial Electronics*, Vol. 57, No. 11, November 2010, pp. 3695-3706.

[11] A. Chiba, T. Deido, T. Fukao and et al., "An Analysis of Bearingless AC

Motors," *IEEE Trans. Energy Conversion*, vol. 9, no. 1, Mar. 1994, pp. 61-68.

[12] M. Kang, J. Huang, H.-b. Jiang, J.-q. Yang, "Principle and Simulation of a 5-Phase Bearingless Permanent Magnet-Type Synchronous Motor", *International Conference on Electrical Machines and Systems*, pp. 1148 – 1152, 17-20 Oct. 2008.

[13] S. W.-K. Khoo, "Bridge Configured Winding for Polyphase Self-Bearing Machines" *IEEE Trans. Magnetics*, vol. 41, no. 4, April. 2005, pp. 1289-1295.

[14] B. B. Choi, "Ultra-High-Power-Density Motor Being Developed for Future Aircraft", in NASA TM—2003-212296, *Structural Mechanics and Dynamics Branch 2002 Annual Report*, pp. 21–22, Aug. 2003.

[15] Y. Kano, T. Kosaka, N. Matsui, "Simple Nonlinear Magnetic Analysis for Permanent-Magnet Motors", *IEEE Trans. Ind. Appl.*, vol. 41, no. 5, pp. 1205–1214, Sept./Oct. 2005.

[16] B. Sheikh-Ghalavand, S. Vaez-Zadeh and A. Hassanpour Isfahani, "An Improved Magnetic Equivalent Circuit Model for Iron-Core Linear Permanent-Magnet Synchronous Motors", *IEEE Trans. on Magnetics*, vol. 46, no. 1, pp. 112–120, Jan. 2010.

[17] S. Vaez-Zadeh and A. Hassanpour Isfahani, "Enhanced Modeling of Linear Permanent-Magnet Synchronous Motors", *IEEE Trans. on Magnetics*, vol. 43, no. 1, pp. 33–39, Jan. 2007.

[18] J. M. Konernak and D. A. Torrey, "Magnetic circuit model for mutually coupled switched reluctance machine," in *Conf. Rec. IEEE-IAS Annual. Meeting*, vol. 1, 1997, pp. 302–309.

[19] R. Qu and T. A. Lipo, "Analysis and Modeling of Airgap & Zigzag Leakage Fluxes in a Surface-Mounted-PM Machine," in *Conf. Rec. IEEE-IAS Annu. Meeting*, vol. 4, pp. 2507–2513, 2002.

[20] D. C. White, H. H. Woodson, "Electromechanical Energy Conversion", MIT Press, Dec. 1959.

[21] N. Matsui, M. Nakamura, and T. Kosaka, "Instantaneous Torque Analysis of Hybrid Stepping Motor," *IEEE Trans. Ind. Appl.*, vol. 32, no. 5, pp. 1176–1182, Sep./Oct. 1996.

[22] D. C. Meeker, 'Finite Element Method Magnetics', Version 4.2 (01Oct2011Build), http://www.femm.info

Appendix A2.1

THE PROGRAMMING CODE

Part 1

In the following, the programming code of the algorithm is presented. This is the VBA version, since there is an advanced variant, implemented in Visual Basic 6.0 and not reported here. Some input files are necessary to run the program: *ordpr.txt*, *ordsc.txt*, which describe respectively the disposition in the stator slots of the first and second winding layers; *aM(pp).txt*, which describes the position of the equivalent ampere-turns distribution of the magnets. The magnetic characteristic of the material is provided through the *.xls* main file and the stator ampere-turns distribution is created by the program with the subroutine presented in Appendix A2.2.

A2.1.1 The main program

```
Const pi = 3.1415927
Const muzero As Double = 1.25664 * 10 ^ -6

Public a, aI, aI_p, aIp, aIs, aM, ASP, ainiz, noti, x, x_p, y, B, Hdt, Flux_dt, deltaBH,
normx As Variant
Public Fluxcs, mu, mu_p, mur_dt, Rildt, Rilcs, Bcs, Hcs, changer_R, changer_C As Variant
Public Fluxcvs, Hg_dt, Bg_dt, Aspcv, Bdt_r, Hdt_r, mu_dt_r As Variant
Public Blam, Hlam, Flux_tdt, Flux_dsp, dFlux_f, Flux_f, Ifs As Variant

Public piv_R, piv_C, mem, cv As Variant
Public n, m, z, fault, undteeth_1, zero_ctrl As Variant
Public pivot, a_logic, b_logic As Variant

Public xprec, Bprec, diffx, Flux_tcv, Flux_tcv_ As Variant
```

```
Public dEnM, EnM, EnM_p, deltaEnM, Vol, Ril, Sez As Variant
Public H As Variant
Public Ncv, nc, Ia0, Ib0, Ic0, Hc, mu_magr, Lm, Ldt, Lcvs, Lcl, hcl, adt, acs, acr, L,
g, havv, tollx, ta, xm, spm, dx, dx_cost, ixm_max, wm As Variant
Public Taucvs, Taucvs_Rs, Taucvs_int, Ldg, Ldg_Rs, hbd, alfa_tcv, Ltd, mu_mag, Taup,
Brm, xm2 As Double
Public ind_dt, ind_dt2 As Variant
Public ordpr, ordsc, Ifse, Ifse_p As Variant
Public npr, nsc, nfasi, w, fi_in, Irms As Variant

Public filepath As String
Public pp, kw, st As Integer
Public LdA_1, LdA_2, LdB_1, LdB_2, Ldsx_1, Ldsx_2, Lddx_1, Lddx_2, LdA_1_Rs, LdA_2_Rs,
LdB_1_Rs, LdB_2_Rs As Double
Public Fxr, Fyr, Fr_n, Fr_tsx, Fr_tdx, Fr_mod, alfa_dt, alfa_dt_deg As Variant
Public Fxr_, Fyr_, Fr As Double

Public pr01, pr02, pr03 As Double
Public Rcv_ext, Lfc, Ltc, Rcv_int, thcv, Vol_setcv, VolH_setcv, VolL_setcv, Lcvx_med,
Re, Rr, Rs, Ralb, alfa_cv, Lcs_med, Lcr_med, Vol_cs, Vol_cr As Double
Public Rcv_efz, Rcv_ifz, Rcv_mfz, LcvxH, LcvxL As Double
Public VolHcv, VolLcv As Variant

'NUOVI PARAMETRI ************************************************************************
 Public Rm, Rme, Rg, alfa_sap, alfa_Ldg, Vol_mLdg, Vol_msap, Vol_gLdg, Vol_gsap,
 alfa_spm, th_xm, th_xm2, thA_1, thA_2, thB_1, thB_2 As Double
 Public dthr_m, C_EM As Double
 Public xm_Rs, xm2_Rs, spm_Rs As Double
' ****************************************************************************************

Private Sub OptionButton2_Click()
 If OptionButton2.Value = True Then
  MsgBox "Preparare il file ASP_TOT.txt premendo" & Chr(13) & "il pulsante nel foglio
  successivo", vbOKOnly, "SATSOLVER"
 End If
End Sub

Public Sub Triang_Click()

Range("AE5:AG65492").ClearContents
Range("AH5").ClearContents
Range("AI37:IV65492").ClearContents
Range("E5:AB65492").ClearContents

ReDim Blam(1 To 452), Hlam(1 To 452), Flux_tdt(13 To 15), Flux_dsp(13 To 15), dFlux_f(1
To 3), Ifs(1 To 3) As Double

'****************************************************************************************
'INPUT

 'numero di cave per coppia polare
 Ncv = Int(Cells(4, 4))
 'conduttori in cava
 'I strato
  npr = Cells(5, 4)
 'II strato
  nsc = Cells(6, 4)
 'passo polare
 Taup = Cells(7, 4)
 Taup = Taup * 0.001
 'corrente efficace
 Irms = Cells(8, 4)
 'campo coercitivo intrinseco del magnete (A/m)
 Hc = Cells(9, 4)
 'permeabilità relativa magnete
 mu_magr = Cells(10, 4)
 'spessore magnete
 Lm = Cells(11, 4)
 Lm = Lm * 0.001
 'spessore del corpo del dente
```

```
Ldt = Cells(12, 4)
Ldt = Ldt * 0.001
'apertura di cava (reale)
Lcl = Cells(14, 4)
Lcl = Lcl * 0.001
'altezza collarino
hcl = Cells(15, 4)
hcl = hcl * 0.001
'altezza dente statore
adt = Cells(16, 4)
adt = adt * 0.001
'spessore corona statore
acs = Cells(17, 4)
acs = acs * 0.001
'spessore corona rotore
acr = Cells(18, 4)
acr = acr * 0.001
'profondità di macchina
L = Cells(19, 4)
L = L * 0.001
'spessore traferro
g = Cells(20, 4)
g = g * 0.001
'altezza dell'avvolgimento
havv = Cells(21, 4)
havv = havv * 0.001
'scarto massimo ammesso fra due soluzioni successive del sistema
tollx = Cells(22, 4)
tollx = tollx * 0.01
'parametro adimensionale che definisce il rapporto fra
'la misura della parte bassa e quella dell'intero dente
ta = Cells(23, 4)
'posizione iniziale del magnete N
xm = Cells(24, 4)
xm = xm * 0.001
'step di sospensione del movimento (<= dx)
dx_cost = Cells(25, 4)
dx_cost = dx_cost * 0.001
'step di spostamento rotore
dx = Cells(26, 4)
dx = dx * 0.001
'numero di step nel movimento
ixm_max = Cells(27, 4)
'fase iniziale
fi_in = Cells(28, 4)
'ampiezza del magnete
wm = Cells(29, 4)
wm = wm * 0.001
'numero di fasi
nfasi = Cells(30, 4)

'*********************************************************************************************
 'INPUT CARATTERISTICA DI MAGNETIZZAZIONE

  For i = 1 To 452
   Blam(i) = Cells(4 + i, 29)
   Hlam(i) = Cells(4 + i, 30)
  Next i

'*********************************************************************************************

 'frequenza elettrica
 f = 50
 kw = 1
 st = 2
 'raggio al fondo cava
 Rcv_ext = 0.085
 'coppie polari
 pp = 1
 'larghezza cava al fondo
```

```
Lfc = 0.0097
'larghezza cava in testa
Ltc = 0.00523

filepath = CStr(TextBox1.Text)

If ta <= 1 - havv / adt Then
 MsgBox ("Valore di ta troppo basso!")
 Exit Sub
End If

'angolo di cava (rad. mecc.)
alfa_cv = 2 * pi / pp / Ncv
'raggio esterno statore
Re = Rcv_ext + acs
'raggio rotore alla base del magnete
Rr = Rcv_ext - adt - g - Lm
'raggio rotore interno (raggio albero)
Ralb = Rr - acr
'raggio interno statore
Rs = Rcv_ext - adt
'raggio di cava in testa
Rcv_int = Rcv_ext - havv
'angolo corrispondente alla cava (rad.)
thcv = 2 * Atn((Lfc - Ltc) / 2 / havv)
'passo di cava statore
Taucvs = 2 * Taup / Ncv
'passo di cava al raggio interno statore
Taucvs_Rs = 2 * pi * Rs / pp / Ncv
'passo di cava al raggio di cava in testa
Taucvs_int = 2 * pi * Rcv_int / pp / Ncv
'larghezza dente al diametro di riferimento
Ldg = Taucvs - Lcl
'larghezza dente al raggio interno statore
Ldg_Rs = 2 * pi * Rs / pp / Ncv - Lcl
'larghezza cava statore in testa
Lcvs = Taucvs_int - Ldt
'spazio intermagnetico
spm = Taup - wm

'NUOVI PARAMETRI ********************************************************************

 'raggio medio magnete
 Rm = Rs - g - Lm / 2
 'raggio esterno magnete
 Rme = Rs - g
 'raggio medio traferro
 Rg = Rs - g / 2
 'angolo corrisp. alla semiapertura di cava
 alfa_sap = Lcl / 2 / Rs
 'angolo corrisp. alla testa del dente
 alfa_Ldg = alfa_cv - 2 * alfa_sap

' ************************************************************************************

'conduttori in cava
nc = npr + nsc
'pulsazione elettrica
w = 2 * pi * f
'altezza della base del dente
hbd = adt - havv - hcl
'angolo testa di cava
alfa_tcv = Atn((Lcvs - Lcl) / 2 / hbd)
'linea di sezione testa del dente
Ltd = hbd / Cos(alfa_tcv) + hcl
'permeabilità assoluta del magnete
mu_mag = mu_magr * muzero
'permeabilità relativa del magnete
Brm = mu_mag * Hc
'posizione iniziale del magnete S
```

```
 xm2 = xm + spm + wm


'*********************************************************************************************
'CONTROLLO DELLA POSIZIONE INIZIALE DEL MAGNETE
  'Alla variabile "undteeth_1" viene assegnato valore True
  'se la discontinuità N-S si trova sotto un qualsiasi dente

 undteeth_1 = 0
 For i = 1 To Ncv
  a_logic = (xm >= (Lcl / 2 + (i - 1) * Taucvs) And xm <= (Lcl / 2 + Ldg + (i - 1) *
Taucvs))
  b_logic = ((xm + spm) >= (Lcl / 2 + (i - 1) * Taucvs) And (xm + spm) <= (Lcl / 2 + Ldg
  + (i - 1) * Taucvs))
  If a_logic And b_logic = True Then
   undteeth_1 = i
   GoTo 20
  End If
 Next i

 MsgBox "ATTENZIONE: uno dei due o entrambe i magneti" & Chr(13) & "si trovano sotto
l'apertura di cava", vbCritical, "SATSOLVER"
 Exit Sub

20
  'Alla variabile "undteeth_2" viene assegnato valore True
  'se la discontinuità S-N si trova sotto un qualsiasi dente
 undteeth_2 = 0
 For i = 1 To Ncv
  c_logic = (xm2 >= (Lcl / 2 + (i - 1) * Taucvs) And xm2 <= (Lcl / 2 + Ldg + (i - 1) *
  Taucvs))
  d_logic = ((xm2 + spm) >= (Lcl / 2 + (i - 1) * Taucvs) And (xm2 + spm) <= (Lcl / 2 +
  Ldg + (i - 1) * Taucvs))
  If c_logic And d_logic = True Then
   undteeth_2 = i
   GoTo 30
  End If
 Next i

MsgBox "ATTENZIONE: uno dei due o entrambe i magneti" & Chr(13) & "si trovano sotto
l'apertura di cava", vbCritical, "SATSOLVER"
 Exit Sub

30

'*********************************************************************************************

 If undteeth_1 <> 0 And undteeth_2 <> 0 Then
  n = 18 * Ncv + 8
 Else
  n = 18 * Ncv
 End If

  m = Int(n + 1)

  ReDim a(n, m), aI(n), aI_p(n), aIp(n), aIs(n), aM(n), ASP(ixm_max * n), ainiz(n, m),
  noti(n), x(1 To n), x_p(1 To n), y(n, m), B(n), Hdt(n), Flux_dt(1 To Ncv), deltaBH(n),
  normx(199) As Double
  ReDim Fluxcs(n), mu(n), mu_p(n), mur_dt(n), Rildt(n), Rilcs(n), Bcs(n), Hcs(n),
  changer_R(m), changer_C(n) As Double
  ReDim Fluxcvs(n), Hg_dt(n), Bg_dt(n), Aspcv(n), Bdt_r(n), Hdt_r(n), mu_dt_r(n) As
  Double
  ReDim piv_R(n), piv_C(n), mem(n), cv(1 To Ncv) As Integer
  ReDim xprec(1 To n), Bprec(1 To n), diffx(1 To n), Flux_tcv(1 To Ncv), Flux_tcv_(1 To
  Ncv) As Double
  ReDim dEnM(1 To n), EnM(1 To n), EnM_p(1 To n), deltaEnM(1 To n), Vol(1 To n),
  VolHcv(1 To 2 * Ncv), VolLcv(1 To 2 * Ncv), Ril(1 To n), Sez(1 To n) As Double
  ReDim H(1 To n) As Double
  ReDim ordpr(1 To Ncv), ordsc(1 To Ncv) As Integer
  ReDim Ifse(1 To nfasi), Ifse_p(1 To nfasi), Flux_f(1 To nfasi) As Double
```

```
  ReDim Fxr(1 To Ncv), Fyr(1 To Ncv), Fr_n(1 To Ncv), Fr_tsx(1 To Ncv), Fr_tdx(1 To
  Ncv), Fr_mod(1 To Ncv), alfa_dt(1 To Ncv), alfa_dt_deg(1 To Ncv) As Double

 'PARAMETRI CIRCOLARI DI MACCHINA ************************************

 'CAVA
  'NB: i raggi "fittizi" seguono i fianchi della cava,
  '    NON convergendo al centro del motore (0,0)
  'raggio esterno fittizio
  Rcv_efz = Lfc / 2 / Tan(thcv / 2)
  'raggio interno fittizio
  Rcv_ifz = Ltc / 2 / Tan(thcv / 2)
  'raggio medio fittizio
  Rcv_mfz = Rcv_efz - (1 - ta) * adt
  'volumi nella zona alta di cava (H) e bassa (L)
  VolH_setcv = thcv * L / 2 * (Rcv_efz ^ 2 - Rcv_mfz ^ 2)
  VolL_setcv = thcv * L / 2 * (Rcv_mfz ^ 2 - Rcv_ifz ^ 2)
  'volume dell'area di cava tra il raggio TCV e FCV
  Vol_setcv = thcv * L / 2 * (Rcv_efz ^ 2 - Rcv_ifz ^ 2)
  'volume cava (escluso il collarino)
  Vol_cv = (Lcvs + Lcl) / 2 * hbd * L + Vol_setcv
  'larghezza di cava al raggio medio
  Lcvx_med = thcv * Rcv_mfz
  If Lcvx_med < 0 Then
   MsgBox ("Aumentare ta!")
   Stop
  End If
  LcvxH = thcv / 2 * (Rcv_efz + Rcv_mfz)
  LcvxL = thcv / 2 * (Rcv_mfz + Rcv_ifz)
  For i = 1 To 2 * Ncv
   VolHcv(i) = VolH_setcv / 2
   VolLcv(i) = ((Lcvs + Lcl) * (hbd - hcl) / 2 * L + VolL_setcv) / 2
  Next i

 'CORONE
  Vol_cs = alfa_cv * L / 2 * (Re ^ 2 - Rcv_ext ^ 2)
  Vol_cr = alfa_cv * L / 2 * (Rr ^ 2 - Ralb ^ 2)
  Lcs_med = alfa_cv / 2 * (Re + Rcv_ext)
  Lcr_med = alfa_cv / 2 * (Rr + Ralb)

 'NUOVI PARAMETRI ***************************************************************

    'MAGNETI
     Vol_mLdg = alfa_Ldg * L / 2 * (Rme ^ 2 - Rr ^ 2)
     Vol_msap = alfa_sap * L / 2 * (Rme ^ 2 - Rr ^ 2)
    'TRAFERRO
     Vol_gLdg = alfa_Ldg * L / 2 * (Rs ^ 2 - Rme ^ 2)
     Vol_gsap = alfa_sap * L / 2 * (Rs ^ 2 - Rme ^ 2)

' ********************************************************************************

'PARAMETRI AUSILIARI (per calcolo riluttanze) ****************************************

     pr01 = (adt - havv) * L
     pr02 = 2 * hbd * L / (Ldg - Ldt)
     pr03 = 2 * hbd * L / (Lcvx_med - Lcl)


'********************************************************************************
  'RILUTTANZE COSTANTI

   'Riluttanze MAGNETE SOTTO IL DENTE md(i)
   For i = 1 To Ncv
    Sez(i) = Rm * alfa_Ldg * L
    Vol(i) = Vol_mLdg
    Ril(i) = 1 / mu_mag * Lm / Sez(i)
   Next i

   'Riluttanze CORONA STATORICA
   For i = Ncv + 1 To 2 * Ncv
```

```
 Sez(i) = acs * L
 Vol(i) = Vol_cs
 Ril(i) = Rnd() * 3000
Next i

'Riluttanze CORONA ROTORICA
For i = 2 * Ncv + 1 To 3 * Ncv
 Sez(i) = acr * L
 Vol(i) = Vol_cr
 Ril(i) = Rnd() * 3000
Next i

'Riluttanze trasversali CAVE cvx(i)
For i = 3 * Ncv + 1 To 4 * Ncv
 Sez(i) = (Rcv_ext - Rcv_int) * L
 Vol(i) = Vol_cv
 Ril(i) = 2 / muzero * 1 / pr03 * Log((adt - hcl) / havv) + 1 / muzero * Lcl / (adt -
 hcl) / L
Next i

'Riluttanze DENTE LOW
For i = 4 * Ncv + 1 To 5 * Ncv
 Sez(i) = Ldt * L
 Vol(i) = (adt * (ta - 1) + havv) * Ldt * L
 Ril(i) = Rnd() * 3000
Next i

'Riluttanze TRAFERRO SOTTO IL DENTE gd(i)
For i = 5 * Ncv + 1 To 6 * Ncv
 Sez(i) = Rg * alfa_Ldg * L
 Vol(i) = Vol_gLdg
 Ril(i) = 1 / muzero * g / Sez(i)
Next i

'Riluttanze DENTE HIGH
For i = 6 * Ncv + 1 To 7 * Ncv
 Sez(i) = Ldt * L
 Vol(i) = adt * (1 - ta) * Ldt * L
 Ril(i) = Rnd() * 3000
Next i

'Riluttanze TRAFERRO SOTTO SEMICAVA SX gcs(i)
For i = 7 * Ncv + 1 To 8 * Ncv
 Sez(i) = Rg * alfa_sap * L
 Vol(i) = Vol_gsap + pi * hcl ^ 2 / 4 * L
 Ril(i) = pi / (2 * muzero * L * Log((2 * g + pi * hcl) / 2 / g))
Next i

'Riluttanze trasversali COLLARINO clx(i)
For i = 8 * Ncv + 1 To 9 * Ncv
 Sez(i) = hcl * L
 Vol(i) = hcl * Lcl * L
 Ril(i) = 1 / muzero * Lcl / (hcl * L)
Next i

'Riluttanze TRAFERRO SOTTO SEMICAVA DX gcd(i)
For i = 9 * Ncv + 1 To 10 * Ncv
 Sez(i) = Rg * alfa_sap * L
 Vol(i) = Vol_gsap + pi * hcl ^ 2 / 4 * L
 Ril(i) = pi / (2 * muzero * L * Log((2 * g + pi * hcl) / 2 / g))
Next i

'Riluttanze MAGNETE SOTTO SEMICAVA SX mcs(i)
For i = 10 * Ncv + 1 To 11 * Ncv
 Sez(i) = Rm * alfa_sap * L
 Vol(i) = Vol_msap
 Ril(i) = 1 / mu_mag * Lm / Sez(i)
Next i

'Riluttanze MAGNETE SOTTO SEMICAVA DX mcd(i)
```

```
   For i = 11 * Ncv + 1 To 12 * Ncv
    Sez(i) = Rm * alfa_sap * L
    Vol(i) = Vol_msap
    Ril(i) = 1 / mu_mag * Lm / Sez(i)
   Next i

   'Riluttanze nel SEMIDENTE SX e DX
   For i = 12 * Ncv + 1 To 14 * Ncv
    Sez(i) = Ldg / 2 / (Ldt / 2 / (adt - havv) / L + 1 / pr02 * Log(pr01 / (pr01 - pr02
    * (Ldg - Ldt) / 2)))
    Vol(i) = (Ldg / 2 + Ldt / 2) * hbd / 2 * L + Ldg / 2 * hcl * L
    Ril(i) = Rnd() * 3000
   Next i

   'Riluttanze longitudinali BASSE SEMICAVE Lcvys(i), Lcvyd(i)
   For i = 14 * Ncv + 1 To 16 * Ncv
    Sez(i) = LcvxL / 2 * L
    Vol(i) = VolLcv(i - 14 * Ncv)
    Ril(i) = 2 / muzero * hcl / (Lcl * L) + 2 / muzero * (hbd - hcl) / (Ltc - Lcl) / L *
    Log(Ltc / Lcl) + 2 / muzero * (ta * adt - hbd) / (Lcvx_med - Ltc) / L * Log(Lcvx_med
    / Ltc)
   Next i

   'Riluttanze longitudinali ALTE SEMICAVE Hcvys(i), Hcvyd(i)
   For i = 16 * Ncv + 1 To 18 * Ncv
    Sez(i) = LcvxH / 2 * L
    Vol(i) = VolHcv(i - 16 * Ncv)
    Ril(i) = 2 / muzero * adt * (1 - ta) / (Lfc - Lcvx_med) / L * Log(Lfc / Lcvx_med)
   Next i

'*******************************************************************************************
'ARRAY DEI TERMINI NOTI
'*******************************************************************************************

   For i = 1 To n
    aI(i) = 0
    aM(i) = 0
   Next i

   'Lettura del file relativo al I strato dell'avvolgimento statorico
   Open filepath & "\ordpr.txt" For Input As #5
    For i = 1 To Ncv
     Input #5, ordpr(i)
    Next i
   Close #5
   'Lettura del file relativo al II strato dell'avvolgimento statorico
   Open filepath & "\ordsc.txt" For Input As #6
    For i = 1 To Ncv
     Input #6, ordsc(i)
    Next i
   Close #6
  'Lettura del file contenente le amperspire equivalenti del magnete
   Open filepath & "\aM(pp).txt" For Input As #2
    For i = 1 To n
     Input #2, aM(i)
    Next i
   Close #2

  If OptionButton2.Value = True Then
  'Lettura del file contenente le amperspire con andamento SINUSOIDALE
   Open filepath & "\ASP_TOT.txt" For Input As #1
   For i = 1 To (n * ixm_max)
    Input #1, ASP(i)
   Next i
   Close #1
  Else
  'Lettura del file contenente le amperspire COSTANTI
   Open filepath & "\ASP_COST.txt" For Input As #8
   For i = 1 To n
    Input #8, aI(i)
```

```
   Next i
   Close #8
  End If

 'Creazione file di output
  Open filepath & "\PP_18Ncv_FX(1.7st).txt" For Output As #3

 Call SUBR_1

End Sub

Public Sub SUBR_1()

'Azzeramento coenergia magnetica
  EnM_tp = 0
  For i = 1 To n
   EnM_p(i) = 0
  Next i
'Inizializzazione variabile di controllo delle soluzioni nulle
  zero_ctrl = 0

'CICLO DI POSIZIONAMENTO DEL MAGNETE
'  NB: se le amperspire cambiano di posto nel vettore dei termini noti al variare
'      della posizione del magnete, è necessario inserire l'input nel ciclo "ixm"

For ixm = 1 To ixm_max
 Range("AE5:AG65492").ClearContents

 For i = 1 To Ncv
  a_logic = (xm >= (Lcl / 2 + (i - 1) * Taucvs) And xm <= (Lcl / 2 + Ldg + (i - 1) *
  Taucvs))
  b_logic = ((xm + spm) >= (Lcl / 2 + (i - 1) * Taucvs) And (xm + spm) <= (Lcl / 2 + Ldg
  + (i - 1) * Taucvs))
  If a_logic And b_logic = False Then
   MsgBox "ATTENZIONE: uno dei due o entrambe i magneti" & Chr(13) & "si trovano sotto
   l'apertura di cava", vbCritical, "SATSOLVER"
   GoTo 50
  End If
  c_logic = (xm2 >= (Lcl / 2 + (i - 1) * Taucvs) And xm2 <= (Lcl / 2 + Ldg + (i - 1) *
  Taucvs))
  d_logic = ((xm2 + spm) >= (Lcl / 2 + (i - 1) * Taucvs) And (xm2 + spm) <= (Lcl / 2 +
  Ldg + (i - 1) * Taucvs))
  If c_logic And d_logic = False Then
   MsgBox "ATTENZIONE: uno dei due o entrambe i magneti" & Chr(13) & "si trovano sotto
   l'apertura di cava", vbCritical, "SATSOLVER"
   GoTo 50
  End If
 Next i

 'INDIVIDUAZIONE POSIZIONE MAGNETE
 'Alle variabili ind_dt, ind_dt2 viene assegnato l'indice
 'numerico dei denti sotto i quali si trovano i "buchi"
 ind_dt = 0
 ind_dt2 = 0

 For i = 1 To Ncv
  If xm >= (Lcl / 2 + (i - 1) * Taucvs) And xm <= (Lcl / 2 + Ldg + (i - 1) * Taucvs)
   Then
   ind_dt = i
   GoTo 120
  End If
 Next i
120
 For i = 1 To Ncv
  If xm2 >= (Lcl / 2 + (i - 1) * Taucvs) And xm2 <= (Lcl / 2 + Ldg + (i - 1) * Taucvs)
   Then
   ind_dt2 = i
   GoTo 130
  End If
 Next i
```

```
130

 If ind_dt = ind_dt2 Then
  MsgBox "ATTENZIONE: ind_dt = ind_dt2 !" & Chr(13) & "CONDIZIONE IMPOSSIBILE !",
  vbCritical, "SATSOLVER"
  GoTo 50
 End If

'*******************************************************************************************
'PARAMETRI DIPENDENTI DALLA POSIZIONE

  'PARAMETRI GEOMETRICI f(xm,ind_dt) ***********************************

  LdA_1 = xm - Lcl / 2 - (ind_dt - 1) * Taucvs
  LdA_2 = xm2 - Lcl / 2 - (ind_dt2 - 1) * Taucvs
  LdB_1 = Taucvs - Lcl / 2 - xm - spm + (ind_dt - 1) * Taucvs
  LdB_2 = Taucvs - Lcl / 2 - xm2 - spm + (ind_dt2 - 1) * Taucvs
  Ldsx_1 = xm - Lcl / 2 + spm / 2 - (ind_dt - 1) * Taucvs
  Ldsx_2 = xm2 - Lcl / 2 + spm / 2 - (ind_dt2 - 1) * Taucvs
  Lddx_1 = Taucvs - Lcl / 2 - xm - spm / 2 + (ind_dt - 1) * Taucvs
  Lddx_2 = Taucvs - Lcl / 2 - xm2 - spm / 2 + (ind_dt2 - 1) * Taucvs

  'parametri per il calcolo della forza radiale riferiti
  'al diametro interno di statore

   xm_Rs = Rs / Rm * xm
   xm2_Rs = Rs / Rm * xm2
   spm_Rs = Rs / Rm * spm

   LdA_1_Rs = xm_Rs - Lcl / 2 - (ind_dt - 1) * Taucvs_Rs
   LdA_2_Rs = xm2_Rs - Lcl / 2 - (ind_dt2 - 1) * Taucvs_Rs
   LdB_1_Rs = Taucvs_Rs - Lcl / 2 - xm_Rs - spm_Rs + (ind_dt - 1) * Taucvs_Rs
   LdB_2_Rs = Taucvs_Rs - Lcl / 2 - xm2_Rs - spm_Rs + (ind_dt2 - 1) * Taucvs_Rs

   'NUOVI PARAMETRI ****************************************************************

    'angolo corrispondente allo spazio intermagnetico
     alfa_spm = spm / Rm
    'angoli corrisp. alle posizioni dei magneti
     th_xm = xm / Rm
     th_xm2 = xm2 / Rm
    'angoli corrisp. ai parametri variabili
     thA_1 = th_xm - alfa_sap - (ind_dt - 1) * alfa_cv
     thA_2 = th_xm2 - alfa_sap - (ind_dt2 - 1) * alfa_cv
     thB_1 = alfa_cv - alfa_sap - th_xm - alfa_spm + (ind_dt - 1) * alfa_cv
     thB_2 = alfa_cv - alfa_sap - th_xm2 - alfa_spm + (ind_dt2 - 1) * alfa_cv

   ' ********************************************************************************

 '*****************************************************************

  'RICALCOLO DI RILUTTANZE, SEZIONI E VOLUMI NELLE ZONE SOGGETTE A MODIFICHE DELLA
   GEOMETRIA

   If ind_dt <> 0 And ind_dt2 <> 0 Then

   'DISCONTINUITA' N-S

    Vol(ind_dt) = thA_1 / 2 * L * (Rme ^ 2 - Rr ^ 2)
    Sez(ind_dt) = thA_1 * (Rme + Rr) / 2 * L
    Ril(ind_dt) = 1 / mu_mag * Lm / Sez(ind_dt)

    Vol(5 * Ncv + ind_dt) = thA_1 / 2 * L * (Rs ^ 2 - Rme ^ 2)
    Sez(5 * Ncv + ind_dt) = thA_1 * (Rs + Rme) / 2 * L
    Ril(5 * Ncv + ind_dt) = 1 / muzero * g / Sez(5 * Ncv + ind_dt)

    Vol(18 * Ncv + 1) = thB_1 / 2 * L * (Rme ^ 2 - Rr ^ 2)
    Sez(18 * Ncv + 1) = thB_1 * (Rme + Rr) / 2 * L
    Ril(18 * Ncv + 1) = 1 / mu_mag * Lm / Sez(18 * Ncv + 1)
```

```
    Vol(18 * Ncv + 2) = alfa_spm / 2 * L * (Rme ^ 2 - Rr ^ 2)
    Sez(18 * Ncv + 2) = alfa_spm * (Rme + Rr) / 2 * L
    Ril(18 * Ncv + 2) = 1 / muzero * Lm / Sez(18 * Ncv + 2)

    Vol(18 * Ncv + 3) = thB_1 / 2 * L * (Rs ^ 2 - Rme ^ 2)
    Sez(18 * Ncv + 3) = thB_1 * (Rs + Rme) / 2 * L
    Ril(18 * Ncv + 3) = 1 / muzero * g / Sez(18 * Ncv + 3)

    Vol(18 * Ncv + 4) = alfa_spm / 2 * L * (Rs ^ 2 - Rme ^ 2)
    Sez(18 * Ncv + 4) = alfa_spm * (Rs + Rme) / 2 * L
    Ril(18 * Ncv + 4) = 1 / muzero * g / Sez(18 * Ncv + 4)


   'DISCONTINUITA' S-N

    Vol(ind_dt2) = thA_2 / 2 * L * (Rme ^ 2 - Rr ^ 2)
    Sez(ind_dt2) = thA_2 * (Rme + Rr) / 2 * L
    Ril(ind_dt2) = 1 / mu_mag * Lm / Sez(ind_dt2)

    Vol(5 * Ncv + ind_dt2) = thA_2 / 2 * L * (Rs ^ 2 - Rme ^ 2)
    Sez(5 * Ncv + ind_dt2) = thA_2 * (Rs + Rme) / 2 * L
    Ril(5 * Ncv + ind_dt2) = 1 / muzero * g / Sez(5 * Ncv + ind_dt2)

    Vol(18 * Ncv + 5) = thB_2 / 2 * L * (Rme ^ 2 - Rr ^ 2)
    Sez(18 * Ncv + 5) = thB_2 * (Rme + Rr) / 2 * L
    Ril(18 * Ncv + 5) = 1 / mu_mag * Lm / Sez(18 * Ncv + 5)

    Vol(18 * Ncv + 6) = alfa_spm / 2 * L * (Rme ^ 2 - Rr ^ 2)
    Sez(18 * Ncv + 6) = alfa_spm * (Rme + Rr) / 2 * L
    Ril(18 * Ncv + 6) = 1 / muzero * Lm / Sez(18 * Ncv + 6)

    Vol(18 * Ncv + 7) = thB_2 / 2 * L * (Rs ^ 2 - Rme ^ 2)
    Sez(18 * Ncv + 7) = thB_2 * (Rs + Rme) / 2 * L
    Ril(18 * Ncv + 7) = 1 / muzero * g / Sez(18 * Ncv + 7)

    Vol(18 * Ncv + 8) = alfa_spm / 2 * L * (Rs ^ 2 - Rme ^ 2)
    Sez(18 * Ncv + 8) = alfa_spm * (Rs + Rme) / 2 * L
    Ril(18 * Ncv + 8) = 1 / muzero * g / Sez(18 * Ncv + 8)

   End If

  If OptionButton2.Value = True Then
   If Int(ixm / 2) <> ixm / 2 Then
   'step di spostamento DISPARI: le correnti vengono calcolate
   'secondo l'esatto valore istantaneo correlato alla posizione
    t = pi * xm / w / Taup
    'Memorizzazione del valore delle correnti allo step precedente
    For i = 1 To nfasi
     Ifse_p(i) = Ifse(i)
    Next i
    For j = 1 To nfasi
    'Andamento cosinusoidale delle correnti
     Ifse(j) = -Sqr(2) * Irms * Cos(kw * w * t - (j - 1) * kw * st * 2 * pi / nfasi +
     fi_in)
    Next j
   Else
    For i = 1 To nfasi
     Ifse(i) = Ifse_p(i)
    Next i
   End If
  End If

'*****************************************************************************************
'COSTRUZIONE DELLA MATRICE A+B
'*****************************************************************************************

 For i = 1 To n
  For j = 1 To m
   a(i, j) = 0
  Next j
```

```
 Next i

 If OptionButton2.Value = True Then
  For i = 1 To n
   a(i, m) = ASP((ixm - 1) * n + i)
  Next i
 Else
  For i = 1 To n
   a(i, m) = aI(i) + aM(i)
  Next i
 End If

'PARTE INVARIANTE DELLA MATRICE (A)

 '5Ncv+2 to 6Ncv ***************************************************************************
 'NODO 1: CONTINUITA' DENTE H - COR.STAT.

 For i = 2 To Ncv
  a(5 * Ncv + i, Ncv + i - 1) = 1
  a(5 * Ncv + i, Ncv + i) = -1
  a(5 * Ncv + i, 6 * Ncv + i) = -1
  a(5 * Ncv + i, 16 * Ncv + i) = -1
  a(5 * Ncv + i, 17 * Ncv + i) = -1
 Next i

 '6Ncv+1 to 7Ncv ***************************************************************************
 'NODO 2: CONTINUITA' DENTE L - DENTE H

  a(6 * Ncv + 1, 4 * Ncv) = 1
  a(6 * Ncv + 1, 3 * Ncv + 1) = -1
  a(6 * Ncv + 1, 4 * Ncv + 1) = 1
  a(6 * Ncv + 1, 6 * Ncv + 1) = -1
  a(6 * Ncv + 1, 14 * Ncv + 1) = 1
  a(6 * Ncv + 1, 15 * Ncv + 1) = 1
  a(6 * Ncv + 1, 16 * Ncv + 1) = -1
  a(6 * Ncv + 1, 17 * Ncv + 1) = -1

  For i = 2 To Ncv
   a(6 * Ncv + i, 3 * Ncv + i - 1) = 1
   a(6 * Ncv + i, 3 * Ncv + i) = -1
   a(6 * Ncv + i, 4 * Ncv + i) = 1
   a(6 * Ncv + i, 6 * Ncv + i) = -1
   a(6 * Ncv + i, 14 * Ncv + i) = 1
   a(6 * Ncv + i, 15 * Ncv + i) = 1
   a(6 * Ncv + i, 16 * Ncv + i) = -1
   a(6 * Ncv + i, 17 * Ncv + i) = -1
  Next i

 '7Ncv+1 to 8Ncv ***************************************************************************
 'NODO 4

 'Equazioni standard
  For i = 1 To Ncv
   a(7 * Ncv + i, 4 * Ncv + i) = 1
   a(7 * Ncv + i, 5 * Ncv + i) = -1
   a(7 * Ncv + i, 12 * Ncv + i) = -1
   a(7 * Ncv + i, 13 * Ncv + i) = 1
  Next i

 'Variazioni
  If ind_dt <> 0 Then
   a(7 * Ncv + ind_dt, 18 * Ncv + 3) = -1
   a(7 * Ncv + ind_dt, 18 * Ncv + 4) = -1
  End If

  If ind_dt2 <> 0 Then
   a(7 * Ncv + ind_dt2, 18 * Ncv + 7) = -1
   a(7 * Ncv + ind_dt2, 18 * Ncv + 8) = -1
  End If
```

```
'8Ncv+1 to 9Ncv ************************************************************************
'NODO 7(1)

 For i = 1 To Ncv
  a(8 * Ncv + i, i) = 1
  a(8 * Ncv + i, 5 * Ncv + i) = -1
 Next i

'9Ncv+1 to 10Ncv ************************************************************************
'NODO 9: CONTINUITA' MAGNETE - COR.ROT.

 a(9 * Ncv + 1, 1) = 1
 a(9 * Ncv + 1, 2 * Ncv + 1) = 1
 a(9 * Ncv + 1, 3 * Ncv) = -1
 a(9 * Ncv + 1, 10 * Ncv + 1) = 1
 a(9 * Ncv + 1, 11 * Ncv + 1) = 1

 For i = 2 To Ncv
  a(9 * Ncv + i, i) = 1
  a(9 * Ncv + i, 2 * Ncv + i) = 1
  a(9 * Ncv + i, 2 * Ncv + i - 1) = -1
  a(9 * Ncv + i, 10 * Ncv + i) = 1
  a(9 * Ncv + i, 11 * Ncv + i) = 1
 Next i

 If ind_dt <> 0 Then
  a(9 * Ncv + ind_dt, 18 * Ncv + 1) = 1
  a(9 * Ncv + ind_dt, 18 * Ncv + 2) = 1
 End If

 If ind_dt2 <> 0 Then
  a(9 * Ncv + ind_dt2, 18 * Ncv + 5) = 1
  a(9 * Ncv + ind_dt2, 18 * Ncv + 6) = 1
 End If

'10Ncv+1 to 11Ncv ************************************************************************
'NODO 3

 a(10 * Ncv + 1, 9 * Ncv) = 1
 a(10 * Ncv + 1, 7 * Ncv + 1) = 1
 a(10 * Ncv + 1, 12 * Ncv + 1) = -1
 a(10 * Ncv + 1, 14 * Ncv + 1) = -1

 For i = 2 To Ncv
  a(10 * Ncv + i, 8 * Ncv + i - 1) = 1
  a(10 * Ncv + i, 7 * Ncv + i) = 1
  a(10 * Ncv + i, 12 * Ncv + i) = -1
  a(10 * Ncv + i, 14 * Ncv + i) = -1
 Next i

'11Ncv+1 to 12Ncv ************************************************************************
'NODO 5

 For i = 1 To Ncv
  a(11 * Ncv + i, 8 * Ncv + i) = 1
  a(11 * Ncv + i, 9 * Ncv + i) = -1
  a(11 * Ncv + i, 13 * Ncv + i) = -1
  a(11 * Ncv + i, 15 * Ncv + i) = 1
 Next i

'14Ncv+1 to 15Ncv ************************************************************************
'NODO 6

 For i = 1 To Ncv
  a(14 * Ncv + i, 7 * Ncv + i) = 1
  a(14 * Ncv + i, 10 * Ncv + i) = -1
 Next i

'15Ncv+1 to 16Ncv ************************************************************************
'NODO 8
```

```
  For i = 1 To Ncv
   a(15 * Ncv + i, 9 * Ncv + i) = 1
   a(15 * Ncv + i, 11 * Ncv + i) = -1
  Next i

'*********************************************************************************************

  If OptionButton2.Value = False Then
   For i = 1 To n
    a(i, m) = aI(i) + aM(i)
   Next i
  Else
   For i = 1 To n
    a(i, m) = ASP((ixm - 1) * n + i)
   Next i
  End If

'*********************************************************************************************
'Ai coefficienti del sistema che dipendono dalle riluttanze magnetiche vengono assegnati
'valori di primo tentativo casuali non nulli per evitare che nello step iniziale della
'soluzione vengano rilevate equazioni linearmente dipendenti

  For i = 1 To (5 * Ncv + 1)
   For j = 1 To n
    a(i, j) = Rnd() * 3000
   Next j
  Next i

  For i = (12 * Ncv + 1) To (14 * Ncv)
   For j = 1 To n
    a(i, j) = Rnd() * 3000
   Next j
  Next i

  For i = (16 * Ncv + 1) To n
   For j = 1 To n
    a(i, j) = Rnd() * 3000
   Next j
  Next i


'*********************************************************************************************
'chiamata della subroutine per la soluzione del sistema di equazioni

  Call SOLVESYS

'*********************************************************************************************

 'CALCOLO DI FLUSSI NELLE VARIE ZONE DI MACCHINA

 'flusso nel passo di cava
  For i = 1 To Ncv
   Flux_tcv_(i) = x(i + 5 * Ncv) + x(i + 7 * Ncv) + x(i + 9 * Ncv)
  Next i

 'flusso per polo al traferro
  Flux_pg = 0
  For i = 1 To Ncv
   Flux_pg = Flux_pg + Flux_tcv(i)
  Next i

 'flusso nel dente basso - alto
  Flux_pdL = 0
  Flux_pdH = 0
  For i = 1 To Ncv
   Flux_pdL = Flux_pdL + x(4 * Ncv + i)
   Flux_pdH = Flux_pdH + x(6 * Ncv + i)
  Next i
```

```
 'flusso all'altezza dei denti
  Flux_pd = ta * Flux_pdL + (1 - ta) * Flux_pdH

 'flussi nei denti
  For i = 1 To Ncv
   Flux_dt(i) = ta * x(4 * Ncv + i) + (1 - ta) * x(6 * Ncv + i)
  Next i

 'flussi nel passo di cava (inteso come semicava sx - dente - semicava dx)
  For i = 1 To Ncv
   Flux_tcv_(i) = Flux_dt(i) + x(14 * Ncv + i) + x(15 * Ncv + i)
  Next i

 'FLUSSI CONCATENATI CON LE FASI

  For i = 1 To nfasi
   Flux_f(i) = 0
  Next i

 'Flussi concatenati I strato
  For j = 1 To nfasi
   For i = 1 To Ncv
    If ordpr(i) = j Then
     Flux_f(j) = Flux_f(j) + npr * x(Ncv + i)
    ElseIf ordpr(i) = -j Then
     Flux_f(j) = Flux_f(j) - npr * x(Ncv + i)
    End If
   Next i
  Next j
 'Flussi concatenati II strato
  For j = 1 To nfasi
   For i = 1 To Ncv
    If ordsc(i) = j Then
     Flux_f(j) = Flux_f(j) + nsc * x(Ncv + i)
    ElseIf ordsc(i) = -j Then
     Flux_f(j) = Flux_f(j) - nsc * x(Ncv + i)
    End If
   Next i
  Next j

 'FORZA RADIALE
  For i = 1 To Ncv
   Fyr(i) = 0
   Fxr(i) = 0
   Fr_n(i) = 0
   Fr_tsx(i) = 0
   Fr_tdx(i) = 0
  Next i
  Fyr_ = 0
  Fxr_ = 0

 'NB: il sistema di riferimento considerato nel calcolo delle forze ha gli assi
coincidenti con il sistema di rif.
 '    x-y standard di FEMM. L'asse della fase 1, secondo l'interpretazione del segno
delle correnti in FEMM (- se
 '    ENTRANTI nello schermo, + se USCENTI), è ruotato invece di 180 gr.m. in senso
orario rispetto al sistema di
 '    riferimento in questione. Gli angoli sono valutati rispetto all'asse (x-standard).

 'angolo dell'asse del dente (gr.m.)
  For i = 1 To Ncv
   alfa_dt(i) = pi / 2 - (i - 1) * alfa_cv
   alfa_dt_deg(i) = 180 / pi * alfa_dt(i)
  Next i

 'Superfici frontali dei DENTI
  For i = 1 To Ncv
   Select Case i
    Case ind_dt
     'dente ind_dt
```

```
 If ind_dt = 1 Then
 'Componente NORMALE della forza radiale
  Fr_n(i) = 1 / 2 / muzero * L * (LdA_1_Rs * B(5 * Ncv + i) ^ 2 + spm_Rs * B(18 *
  Ncv + 4) ^ 2 + LdB_1_Rs * B(18 * Ncv + 3) ^ 2 + Lcl / 2 * B(7 * Ncv + i) ^ 2 + Lcl
  / 2 * B(9 * Ncv + i) ^ 2)
  Fr_n(i) = Fr_n(i) - 1 / 2 / muzero * Lcl / 2 * L * B(9 * Ncv) ^ 2 - 1 / 2 / muzero
  * Lcl / 2 * L * B(8 * Ncv + i) ^ 2
 'Componenti TANGENZIALI della forza radiale
  Fr_tsx(i) = 1 / muzero * Lcl / 2 * L * B(7 * Ncv + i) * B(9 * Ncv)
  Fr_tdx(i) = 1 / muzero * Lcl / 2 * L * B(9 * Ncv + i) * B(8 * Ncv + i)
 Else
 'Componente NORMALE della forza radiale
  Fr_n(i) = 1 / 2 / muzero * L * (LdA_1_Rs * B(5 * Ncv + i) ^ 2 + spm_Rs * B(18 *
  Ncv + 4) ^ 2 + LdB_1_Rs * B(18 * Ncv + 3) ^ 2 + Lcl / 2 * B(7 * Ncv + i) ^ 2 + Lcl
  / 2 * B(9 * Ncv + i) ^ 2)
  Fr_n(i) = Fr_n(i) - 1 / 2 / muzero * Lcl / 2 * L * B(8 * Ncv + i - 1) ^ 2 - 1 / 2
  / muzero * Lcl / 2 * L * B(8 * Ncv + i) ^ 2
 'Componenti TANGENZIALI della forza radiale
  Fr_tsx(i) = 1 / muzero * Lcl / 2 * L * B(7 * Ncv + i) * B(8 * Ncv + i - 1)
  Fr_tdx(i) = 1 / muzero * Lcl / 2 * L * B(9 * Ncv + i) * B(8 * Ncv + i)
 End If

Case ind_dt2
'dente ind_dt2
 If ind_dt2 = 1 Then
 'Componente NORMALE della forza radiale
  Fr_n(i) = 1 / 2 / muzero * L * (LdA_1_Rs * B(5 * Ncv + i) ^ 2 + spm_Rs * B(18 *
  Ncv + 8) ^ 2 + LdB_1_Rs * B(18 * Ncv + 7) ^ 2 + Lcl / 2 * B(7 * Ncv + i) ^ 2 + Lcl
  / 2 * B(9 * Ncv + i) ^ 2)
  Fr_n(i) = Fr_n(i) - 1 / 2 / muzero * Lcl / 2 * L * B(9 * Ncv) ^ 2 - 1 / 2 / muzero
  * Lcl / 2 * L * B(8 * Ncv + i) ^ 2
 'Componenti TANGENZIALI della forza radiale
  Fr_tsx(i) = 1 / muzero * Lcl / 2 * L * B(7 * Ncv + i) * B(9 * Ncv)
  Fr_tdx(i) = 1 / muzero * Lcl / 2 * L * B(9 * Ncv + i) * B(8 * Ncv + i)
 Else
 'Componente NORMALE della forza radiale
  Fr_n(i) = 1 / 2 / muzero * L * (LdA_1_Rs * B(5 * Ncv + i) ^ 2 + spm_Rs * B(18 *
  Ncv + 8) ^ 2 + LdB_1_Rs * B(18 * Ncv + 7) ^ 2 + Lcl / 2 * B(7 * Ncv + i) ^ 2 + Lcl
  / 2 * B(9 * Ncv + i) ^ 2)
  Fr_n(i) = Fr_n(i) - 1 / 2 / muzero * Lcl / 2 * L * B(8 * Ncv + i - 1) ^ 2 - 1 / 2
  / muzero * Lcl / 2 * L * B(8 * Ncv + i) ^ 2
 'Componenti TANGENZIALI della forza radiale
  Fr_tsx(i) = 1 / muzero * Lcl / 2 * L * B(7 * Ncv + i) * B(8 * Ncv + i - 1)
  Fr_tdx(i) = 1 / muzero * Lcl / 2 * L * B(9 * Ncv + i) * B(8 * Ncv + i)
 End If

Case Else

 If i = 1 Then
 'Componente NORMALE della forza radiale
  Fr_n(i) = 1 / 2 / muzero * L * (Ldg_Rs * B(5 * Ncv + i) ^ 2 + Lcl / 2 * B(7 * Ncv
  + i) ^ 2 + Lcl / 2 * B(9 * Ncv + i) ^ 2)
  Fr_n(i) = Fr_n(i) - 1 / 2 / muzero * Lcl / 2 * L * B(9 * Ncv) ^ 2 - 1 / 2 / muzero
  * Lcl / 2 * L * B(8 * Ncv + i) ^ 2
 'Componenti TANGENZIALI della forza radiale
  Fr_tsx(i) = 1 / muzero * Lcl / 2 * L * B(7 * Ncv + i) * B(9 * Ncv)
  Fr_tdx(i) = 1 / muzero * Lcl / 2 * L * B(9 * Ncv + i) * B(8 * Ncv + i)
 Else
 'Componente NORMALE della forza radiale
  Fr_n(i) = 1 / 2 / muzero * L * (Ldg_Rs * B(5 * Ncv + i) ^ 2 + Lcl / 2 * B(7 * Ncv
  + i) ^ 2 + Lcl / 2 * B(9 * Ncv + i) ^ 2)
  Fr_n(i) = Fr_n(i) - 1 / 2 / muzero * Lcl / 2 * L * B(8 * Ncv + i - 1) ^ 2 - 1 / 2
  / muzero * Lcl / 2 * L * B(8 * Ncv + i) ^ 2
 'Componenti TANGENZIALI della forza radiale
  Fr_tsx(i) = 1 / muzero * Lcl / 2 * L * B(7 * Ncv + i) * B(8 * Ncv + i - 1)
  Fr_tdx(i) = 1 / muzero * Lcl / 2 * L * B(9 * Ncv + i) * B(8 * Ncv + i)
 End If

End Select
```

```
  'Componenti secondo (y) della forza radiale in ogni dente
   Fyr(i) = Fr_n(i) * Sin(alfa_dt(i)) - Fr_tsx(i) * Cos(alfa_dt(i)) - Fr_tdx(i) *
   Cos(alfa_dt(i))
  'Componenti secondo (x) della forza radiale
   Fxr(i) = Fr_n(i) * Cos(alfa_dt(i)) + Fr_tsx(i) * Sin(alfa_dt(i)) + Fr_tdx(i) *
   Sin(alfa_dt(i))
  'Modulo della forza radiale in ogni dente
   Fr_mod(i) = Sqr(Fxr(i) ^ 2 + Fyr(i) ^ 2)

  Next i

 'Calcolo della risultante delle forze RADIALI
  For i = 1 To Ncv
   Fyr_ = Fyr_ + Fyr(i)
   Fxr_ = Fxr_ + Fxr(i)
  Next i
 'RISULTANTE
  Fr = Sqr(Fxr_ ^ 2 + Fyr_ ^ 2)


'*******************************************************************************************
'CICLO DI CALCOLO COENERGIA MAGNETICA DEL SISTEMA

 If OptionButton1.Value = True Then

  'Memorizzazione dei valori step precedente
  'Coenergia magnetica complessiva
   EnM_tp = EnM_t

  'Memorizzazione dei valori step precedente
  'Coenergia magnetica nel singolo volume
   For i = 1 To n
    EnM_p(i) = EnM(i)
   Next i

  EnM_t = 0
  nH = 640

 'MAGNETE (SOTTO IL DENTE)
  For i = 1 To Ncv
   dEnM(i) = 1 / 2 * B(i) ^ 2 / mu(i)
   EnM(i) = dEnM(i) * Vol(i)
   EnM_t = EnM_t + EnM(i)
  Next i

 'CORONA STAT., CORONA ROT.
  For i = Ncv + 1 To 3 * Ncv
   dEnM(i) = 0
   dH = Abs(H(i)) / nH
   For j = 1 To nH
    H1 = (j - 1) * dH
    H2 = j * dH
    B1 = Induction(n, H1, Hlam, Blam)
    B2 = Induction(n, H2, Hlam, Blam)
    dA = (B2 + B1) * dH / 2
    dEnM(i) = dEnM(i) + dA
   Next j
   EnM(i) = dEnM(i) * Vol(i)
   EnM_t = EnM_t + EnM(i)
  Next i

 'CAVE (Componenti orizzontali CVX)
  For i = 3 * Ncv + 1 To 4 * Ncv
   dEnM(i) = 1 / 2 * B(i) ^ 2 / mu(i)
   EnM(i) = dEnM(i) * Vol(i)
   EnM_t = EnM_t + EnM(i)
  Next i

 'DENTE BASSO
  For i = 4 * Ncv + 1 To 5 * Ncv
```

```
  dEnM(i) = 0
  dH = Abs(H(i)) / nH
  For j = 1 To nH
   H1 = (j - 1) * dH
   H2 = j * dH
   B1 = Induction(n, H1, Hlam, Blam)
   B2 = Induction(n, H2, Hlam, Blam)
   dA = (B2 + B1) * dH / 2
   dEnM(i) = dEnM(i) + dA
  Next j
  EnM(i) = dEnM(i) * Vol(i)
  EnM_t = EnM_t + EnM(i)
 Next i

'TRAFERRO sotto il DENTE
 For i = 5 * Ncv + 1 To 6 * Ncv
  dEnM(i) = 1 / 2 * B(i) ^ 2 / mu(i)
  EnM(i) = dEnM(i) * Vol(i)
  EnM_t = EnM_t + EnM(i)
 Next i

'DENTE ALTO
 For i = 6 * Ncv + 1 To 7 * Ncv
  dEnM(i) = 0
  dH = Abs(H(i)) / nH
  For j = 1 To nH
   H1 = (j - 1) * dH
   H2 = j * dH
   B1 = Induction(n, H1, Hlam, Blam)
   B2 = Induction(n, H2, Hlam, Blam)
   dA = (B2 + B1) * dH / 2
   dEnM(i) = dEnM(i) + dA
  Next j
  EnM(i) = dEnM(i) * Vol(i)
  EnM_t = EnM_t + EnM(i)
 Next i

'TRAFERRO sotto la SEMICAVA SX
'COLLARINO (TRASV.)
'TRAFERRO sotto la SEMICAVA DX
'MAGNETE SOTTO APERTURA CAVA SX e DX
 For i = 7 * Ncv + 1 To 12 * Ncv
  dEnM(i) = 1 / 2 * B(i) ^ 2 / mu(i)
  EnM(i) = dEnM(i) * Vol(i)
  EnM_t = EnM_t + EnM(i)
 Next i

'TESTA DENTE SX e DX
 For i = 12 * Ncv + 1 To 14 * Ncv
  dEnM(i) = 0
  dH = Abs(H(i)) / nH
  For j = 1 To nH
   H1 = (j - 1) * dH
   H2 = j * dH
   B1 = Induction(n, H1, Hlam, Blam)
   B2 = Induction(n, H2, Hlam, Blam)
   dA = (B2 + B1) * dH / 2
   dEnM(i) = dEnM(i) + dA
  Next j
  EnM(i) = dEnM(i) * Vol(i)
  EnM_t = EnM_t + EnM(i)
 Next i

'SEMICAVE SX e DX
 For i = 14 * Ncv + 1 To 16 * Ncv
  dEnM(i) = 1 / 2 * B(i) ^ 2 / mu(i)
  EnM(i) = dEnM(i) * Vol(i)
  EnM_t = EnM_t + EnM(i)
 Next i
```

```
 'CONTRIBUTI AGGIUNTIVI
  If ind_dt <> 0 And ind_dt2 <> 0 Then
   For i = 1 To 8
    dEnM(18 * Ncv + i) = 1 / 2 * B(18 * Ncv + i) ^ 2 / mu(18 * Ncv + i)
    EnM(18 * Ncv + i) = dEnM(18 * Ncv + i) * Vol(18 * Ncv + i)
    EnM_t = EnM_t + EnM(18 * Ncv + i)
   Next i
  End If

 'VARIAZIONE COENERGIA MAGNETICA TOTALE
  dEnM_t = EnM_t - EnM_tp

 'VARIAZIONE COENERGIA MAGNETICA SINGOLI VOLUMI
  If ixm = 1 Then
   For i = 1 To n
    deltaEnM(i) = 0
   Next i
  Else
   For i = 1 To n
    deltaEnM(i) = EnM(i) - EnM_p(i)
   Next i
  End If

  Cells(5 + ixm, 13 + 2 * nfasi + 1) = EnM_t * pp

 End If


'*********************************************************************************************

 If OptionButton1.Value = True And Int(ixm / 2) = ixm / 2 Then

  Fx_EM = dEnM_t / dx_cost

  'Coppia elettromagnetica
  dthr_m = pi / pp / Taup * dx_cost
  C_EM = dEnM_t / dthr_m

  Cells(5 + ixm, 13 + 2 * nfasi + 2) = C_EM * pp

 End If

'*********************************************************************************************
'OUTPUT ARRAY

   For i = 1 To Ncv
    Cells(4 + i, 5) = CStr("md")
    Cells(4 + Ncv + i, 5) = CStr("cs")
    Cells(4 + 2 * Ncv + i, 5) = CStr("cr")
    Cells(4 + 3 * Ncv + i, 5) = CStr("cvx")
    Cells(4 + 4 * Ncv + i, 5) = CStr("dL")
    Cells(4 + 5 * Ncv + i, 5) = CStr("gd")
    Cells(4 + 6 * Ncv + i, 5) = CStr("dH")
    Cells(4 + 7 * Ncv + i, 5) = CStr("gcs")
    Cells(4 + 8 * Ncv + i, 5) = CStr("clx")
    Cells(4 + 9 * Ncv + i, 5) = CStr("gcd")
    Cells(4 + 10 * Ncv + i, 5) = CStr("mcs")
    Cells(4 + 11 * Ncv + i, 5) = CStr("mcd")
    Cells(4 + 12 * Ncv + i, 5) = CStr("dsx")
    Cells(4 + 13 * Ncv + i, 5) = CStr("ddx")
    Cells(4 + 14 * Ncv + i, 5) = CStr("Lcvys")
    Cells(4 + 15 * Ncv + i, 5) = CStr("Lcvyd")
    Cells(4 + 16 * Ncv + i, 5) = CStr("Hcvys")
    Cells(4 + 17 * Ncv + i, 5) = CStr("Hcvyd")
   Next i
   Cells(5 + 18 * Ncv, 5) = CStr("mdB1")
   Cells(6 + 18 * Ncv, 5) = CStr("spm1")
   Cells(7 + 18 * Ncv, 5) = CStr("gdB1")
   Cells(8 + 18 * Ncv, 5) = CStr("gd01")
   Cells(9 + 18 * Ncv, 5) = CStr("mdB2")
```

```
  Cells(10 + 18 * Ncv, 5) = CStr("spm2")
  Cells(11 + 18 * Ncv, 5) = CStr("gdB2")
  Cells(12 + 18 * Ncv, 5) = CStr("gd02")

  For i = 1 To n
   Cells(4 + i, 6) = H(i)
   Cells(4 + i, 7) = B(i)
   Cells(4 + i, 8) = mu(i) / muzero
   Cells(4 + i, 9) = x(i)
  Next i

 Cells(5 + ixm, 12) = xm
 Cells(5 + ixm, 13) = Hc

 For i = 1 To nfasi
  Cells(5 + ixm, 13 + i) = Ifse(i)
 Next i

 For i = 1 To nfasi
  Cells(5 + ixm, 13 + nfasi + i) = Flux_f(i) * pp
 Next i

 Cells(5 + ixm, 13 + 2 * nfasi + 3) = Fxr_
 Cells(5 + ixm, 13 + 2 * nfasi + 4) = Fyr_
 Cells(5 + ixm, 13 + 2 * nfasi + 5) = Fr

If OptionButton1.Value = True Then

 Print #3, xm
 Print #3,
 Print #3, "i      VOL(m^3)      dEnM(J/m^3)   EnM(J)        H(A/m)        B(T)
 deltaEnM(J)     Ril(H-1)      x(Wb)"
 Print #3,
 For i = 1 To 18 * Ncv
  Val_00 = Format(i, "000" & "    ")
  Val_01 = Format(Vol(i), "0.00000E+" & "    ")
  Val_02 = Format(dEnM(i), "0.00000E+" & "    ")
  Val_03 = Format(EnM(i), "0.00000E+" & "    ")
  Val_04 = Format(H(i), "0000000.00" & "    ")
  Val_05 = Format(B(i), "0.000" & "    ")
  Val_06 = Format(deltaEnM(i), "0.00000E+" & "    ")
  Val_07 = Format(Ril(i), "0.00000E+" & "    ")
  Val_08 = Format(x(i), "0.000E+" & "    ")
  Print #3, Val_00 & Val_01 & Val_02 & Val_03 & Val_04 & Val_05 & Val_06 & Val_07 &
  Val_08
 Next i
'ELEMENTI AGGIUNTIVI
 For i = 18 * Ncv + 1 To n
  Val_00 = Format(i, "000" & "    ")
  Val_01 = Format(Vol(i), "0.00000E+" & "    ")
  Val_02 = Format(dEnM(i), "0.00000E+" & "    ")
  Val_03 = Format(EnM(i), "0.00000E+" & "    ")
  Val_04 = Format(H(i), "0000000.00" & "    ")
  Val_05 = Format(B(i), "0.000" & "    ")
  Val_06 = Format(deltaEnM(i), "0.00000E+" & "    ")
  Val_07 = Format(Ril(i), "0.00000E+" & "    ")
  Val_08 = Format(x(i), "0.000E+" & "    ")
  Print #3, Val_00 & Val_01 & Val_02 & Val_03 & Val_04 & Val_05 & Val_06 & Val_07 &
  Val_08
 Next i
 Print #3,
 Print #3,
 Print #3, "Fyr(N)        Fxr(N)        alfa_dt(gr.m.)  Fr_mod(N)"
 Print #3,
 For i = 1 To Ncv
  Val_09 = Format(Fyr(i), "0000000.00" & "    ")
  Val_10 = Format(Fxr(i), "0000000.00" & "    ")
  Val_11 = Format(alfa_dt_deg(i), "0000000.00" & "    ")
  Val_12 = Format(Fr_mod(i), "0000000.00" & "    ")
  Print #3, Val_09 & Val_10 & Val_11 & Val_12
```

```
  Next i
  Print #3,
  Print #3,
  Print #3,

 End If

 'aggiornamento della posizione dei magneti
 If Int(ixm / 2) <> ixm / 2 Then
  dx1 = dx_cost
 Else
  dx1 = dx
 End If

 xm = xm + dx1
 xm2 = xm + spm + wm

 Cells(5, 34) = zero_ctrl

Next ixm

50
 Close #3
 OptionButton1.Value = False
 OptionButton2.Value = False

End Sub

Public Sub SOLVESYS()

  For i = 1 To n
   For j = 1 To m
   'matrice iniziale del sistema
   ainiz(i, j) = a(i, j)
   Next j
  Next i

'*****************************************************************************************

  maxdiffx = 1000000
  z = 1

  For i = 1 To n
   mu(i) = muzero
   mu_p(i) = 0
  Next i

 Do While maxdiffx > tollx


'*****************************************************************************************
'TRASFORMAZIONE DELLA MATRICE a(i,j) IN TRIANGOLARE SUPERIORE

 pivot = False
 fault = 0

 iperm = 0
 For k = 1 To n - 1
   'lo scambio avviene con le righe successive a quella considerata (k-esima)
   r = k + 1

   Do Until a(k, k) <> 0

   'ciclo che scambia la riga k-esima con la r-esima
   'nel caso in cui un elemento diagonale sia nullo
      pivot = True
      For icol = 1 To m
       changer_R(icol) = a(k, icol)
       a(k, icol) = a(r, icol)
       a(r, icol) = changer_R(icol)
```

```
      Next icol

     For i = 1 To n
      piv_R(i) = 0
     Next i

     piv_R(k) = r
     piv_R(r) = k

     r = r + 1

     If r > n Then
      MsgBox ("Un elemento A(k,k) rimane nullo dopo aver scorso tutte le righe (r > n)")
      Stop
     End If
      iperm = iperm + 1

   Loop

     If pivot = True Then
      mem(k) = r
     Else
      mem(k) = k
     End If

  For i = k + 1 To n
   y(i, k) = -a(i, k) / a(k, k)
   a(i, k) = y(i, k)
   For j = k + 1 To m
    a(i, j) = a(i, j) + a(i, k) * a(k, j)
   Next j
  Next i

  pivot = False

 Next k

'*********************************************************************************************
'SOLUZIONE DEL SISTEMA DI EQUAZIONI CON IL METODO DIRETTO

 For i = 1 To n
  noti(i) = a(i, m)
 Next i

 x(n) = noti(n) / a(n, n)

  For i = n - 1 To 1 Step -1
   sm = 0
    For k = n To i + 1 Step -1
     sm = sm + a(i, k) * x(k)
    Next k
   x(i) = (noti(i) - sm) / a(i, i)
  Next i

'*********************************************************************************************

 'memorizzazione permeabilità allo step precedente
 For j = 1 To n
  mu_p(j) = mu(j)
 Next j

 'determinazione delle induzioni dai flussi
 For i = 1 To n
  B(i) = x(i) / Sez(i)
 Next i

 'richiama la function per il calcolo delle permeabilità magnetiche
 For j = 1 To n
  Select Case j
   Case 1 To Ncv
```

```
    mu(j) = mu_mag
    H(j) = 1 / mu_mag * B(j)
   Case Ncv + 1 To 3 * Ncv
    H(j) = Magfield(n, B(j), Hlam, Blam)
    If B(j) < 0 Then H(j) = -H(j)
    If B(j) = 0 Then
     mu(j) = (Blam(2) - Blam(1)) / (Hlam(2) - Hlam(1))
     zero_ctrl = zero_ctrl + 1
    Else
     mu(j) = B(j) / H(j)
    End If
   Case 3 * Ncv + 1 To 4 * Ncv
    mu(j) = muzero
    H(j) = 1 / muzero * B(j)
   Case 4 * Ncv + 1 To 5 * Ncv
    H(j) = Magfield(n, B(j), Hlam, Blam)
    If B(j) < 0 Then H(j) = -H(j)
    If B(j) = 0 Then
     mu(j) = (Blam(2) - Blam(1)) / (Hlam(2) - Hlam(1))
     zero_ctrl = zero_ctrl + 1
    Else
     mu(j) = B(j) / H(j)
    End If
   Case 5 * Ncv + 1 To 6 * Ncv
    mu(j) = muzero
    H(j) = 1 / muzero * B(j)
   Case 6 * Ncv + 1 To 7 * Ncv
    H(j) = Magfield(n, B(j), Hlam, Blam)
    If B(j) < 0 Then H(j) = -H(j)
    If B(j) = 0 Then
     mu(j) = (Blam(2) - Blam(1)) / (Hlam(2) - Hlam(1))
     zero_ctrl = zero_ctrl + 1
    Else
     mu(j) = B(j) / H(j)
    End If
   Case 7 * Ncv + 1 To 10 * Ncv
    mu(j) = muzero
    H(j) = 1 / muzero * B(j)
   Case 10 * Ncv + 1 To 12 * Ncv
    mu(j) = mu_mag
    H(j) = 1 / mu_mag * B(j)
   Case 12 * Ncv + 1 To 14 * Ncv
    H(j) = Magfield(n, B(j), Hlam, Blam)
    If B(j) < 0 Then H(j) = -H(j)
    If B(j) = 0 Then
     mu(j) = (Blam(2) - Blam(1)) / (Hlam(2) - Hlam(1))
     zero_ctrl = zero_ctrl + 1
    Else
     mu(j) = B(j) / H(j)
    End If
   Case 14 * Ncv + 1 To 18 * Ncv
    mu(j) = muzero
    H(j) = 1 / muzero * B(j)
  End Select
 Next j

If ind_dt <> 0 Then
 mu(18 * Ncv + 1) = mu_mag
 H(18 * Ncv + 1) = 1 / mu_mag * B(18 * Ncv + 1)
 mu(18 * Ncv + 2) = muzero
 H(18 * Ncv + 2) = 1 / muzero * B(18 * Ncv + 2)
 mu(18 * Ncv + 3) = muzero
 H(18 * Ncv + 3) = 1 / muzero * B(18 * Ncv + 3)
 mu(18 * Ncv + 4) = muzero
 H(18 * Ncv + 4) = 1 / muzero * B(18 * Ncv + 4)
End If

If ind_dt2 <> 0 Then
 mu(18 * Ncv + 5) = mu_mag
 H(18 * Ncv + 5) = 1 / mu_mag * B(18 * Ncv + 5)
```

```
  mu(18 * Ncv + 6) = muzero
  H(18 * Ncv + 6) = 1 / muzero * B(18 * Ncv + 6)
  mu(18 * Ncv + 7) = muzero
  H(18 * Ncv + 7) = 1 / muzero * B(18 * Ncv + 7)
  mu(18 * Ncv + 8) = muzero
  H(18 * Ncv + 8) = 1 / muzero * B(18 * Ncv + 8)
 End If

 'Ridefinizione delle permeabilità magnetiche
  For j = 1 To n
   mu(j) = mu(j) ^ 0.1 * mu_p(j) ^ 0.9
  Next j

  '*****************************************************************************
  '            ****               CRITERIO DI CONVERGENZA               ****

  maxdiffx = 0

  'Solo elementi NON LINEARI
   For j = Ncv + 1 To 3 * Ncv
    diffx(j) = Abs((mu(j) / muzero - mu_p(j) / muzero) / (mu_p(j) / muzero))
    If diffx(j) > maxdiffx Then
     maxdiffx = diffx(j)
    End If
   Next j
   For j = 4 * Ncv + 1 To 5 * Ncv
    diffx(j) = Abs((mu(j) / muzero - mu_p(j) / muzero) / (mu_p(j) / muzero))
    If diffx(j) > maxdiffx Then
     maxdiffx = diffx(j)
    End If
   Next j
   For j = 6 * Ncv + 1 To 7 * Ncv
    diffx(j) = Abs((mu(j) / muzero - mu_p(j) / muzero) / (mu_p(j) / muzero))
    If diffx(j) > maxdiffx Then
     maxdiffx = diffx(j)
    End If
   Next j
   For j = 12 * Ncv + 1 To 14 * Ncv
    diffx(j) = Abs((mu(j) / muzero - mu_p(j) / muzero) / (mu_p(j) / muzero))
    If diffx(j) > maxdiffx Then
     maxdiffx = diffx(j)
    End If
   Next j


'*******************************************************************************************

 'RIDEFINIZIONE MATRICE "A" DEL SISTEMA
 'vengono aggiornati i coefficienti variabili in cui compaiono i valori di permeabilità
 'magnetica delle varie parti di macchina

'*******************************************************************************************

 'azzeramento di tutti i coefficienti
 For i = 1 To n
  For j = 1 To m
  a(i, j) = 0
  Next j
 Next i

 'RIDEFINIZIONE DELLE RILUTTANZE VARIABILI f(mu)

  'corona statore
   For i = Ncv + 1 To 2 * Ncv
    Ril(i) = 1 / mu(i) * Lcs_med / Sez(i)
   Next i

  'corona rotore
   For i = 2 * Ncv + 1 To 3 * Ncv
    Ril(i) = 1 / mu(i) * Lcr_med / Sez(i)
```

```
  Next i

 'dente LOW
  For i = 4 * Ncv + 1 To 5 * Ncv
   Ril(i) = 1 / mu(i) * (adt * (ta - 1) + havv) / Sez(i)
  Next i

 'dente HIGH
  For i = 6 * Ncv + 1 To 7 * Ncv
   Ril(i) = 1 / mu(i) * (adt * (1 - ta)) / Sez(i)
  Next i

 'semidente SX e DX
  For i = 12 * Ncv + 1 To 14 * Ncv
   Ril(i) = 1 / mu(i) / pr02 * Log(2 * pr01 / (2 * pr01 - pr02 * (Ldg - Ldt))) + 1 /
   mu(i) * Ldt / 2 / (adt - havv) / L
  Next i

'le righe con coefficienti costanti della matrice del sistema vengono ricomposte come
'quelle iniziali per ripartire con la soluzione del sistema, aggiornato aggiungendo
'le permeabilità calcolate

 For i = 5 * Ncv + 2 To 12 * Ncv
  For j = 1 To n
  a(i, j) = ainiz(i, j)
  Next j
 Next i

 For i = 14 * Ncv + 1 To 16 * Ncv
  For j = 1 To n
  a(i, j) = ainiz(i, j)
  Next j
 Next i

 'l'ultima colonna della matrice (termini noti)
 'riassume i valori iniziali
 For i = 1 To n
  a(i, m) = ainiz(i, m)
 Next i

'PARTE VARIABILE DELLA MATRICE (A)
'1 to Ncv ********************************************************************************
'CIRCUITAZIONI DENTE - DENTE

 For i = 1 To Ncv - 1
  a(i, i) = Ril(i)
  a(i, i + 1) = -Ril(i + 1)
  a(i, i + Ncv) = -Ril(i + Ncv)
  a(i, i + 2 * Ncv) = -Ril(i + 2 * Ncv)
  a(i, i + 4 * Ncv) = Ril(i + 4 * Ncv)
  a(i, i + 4 * Ncv + 1) = -Ril(i + 4 * Ncv + 1)
  a(i, i + 5 * Ncv) = Ril(i + 5 * Ncv)
  a(i, i + 5 * Ncv + 1) = -Ril(i + 5 * Ncv + 1)
  a(i, i + 6 * Ncv) = Ril(i + 6 * Ncv)
  a(i, i + 6 * Ncv + 1) = -Ril(i + 6 * Ncv + 1)
 Next i

 a(Ncv, Ncv) = Ril(Ncv)
 a(Ncv, 1) = -Ril(1)
 a(Ncv, 2 * Ncv) = -Ril(2 * Ncv)
 a(Ncv, 3 * Ncv) = -Ril(3 * Ncv)
 a(Ncv, 5 * Ncv) = Ril(5 * Ncv)
 a(Ncv, 4 * Ncv + 1) = -Ril(4 * Ncv + 1)
 a(Ncv, 6 * Ncv) = Ril(6 * Ncv)
 a(Ncv, 5 * Ncv + 1) = -Ril(5 * Ncv + 1)
 a(Ncv, 7 * Ncv) = Ril(7 * Ncv)
 a(Ncv, 6 * Ncv + 1) = -Ril(6 * Ncv + 1)


Select Case ind_dt
```

```
 Case 1
 'Circuitaz. precedente
  a(Ncv, 1) = 0
  a(Ncv, 5 * Ncv + 1) = 0
  a(Ncv, 18 * Ncv + 2) = -Ril(18 * Ncv + 2)
  a(Ncv, 18 * Ncv + 4) = -Ril(18 * Ncv + 4)
 'Circuitaz. attuale
  a(1, 1) = 0
  a(1, 5 * Ncv + 1) = 0
  a(1, 18 * Ncv + 2) = Ril(18 * Ncv + 2)
  a(1, 18 * Ncv + 4) = Ril(18 * Ncv + 4)
 Case 2 To (Ncv - 1)
 'Circuitaz. precedente
  a(ind_dt - 1, ind_dt) = 0
  a(ind_dt - 1, ind_dt + 5 * Ncv) = 0
  a(ind_dt - 1, 18 * Ncv + 2) = -Ril(18 * Ncv + 2)
  a(ind_dt - 1, 18 * Ncv + 4) = -Ril(18 * Ncv + 4)
 'Circuitaz. attuale
  a(ind_dt, ind_dt) = 0
  a(ind_dt, ind_dt + 5 * Ncv) = 0
  a(ind_dt, 18 * Ncv + 2) = Ril(18 * Ncv + 2)
  a(ind_dt, 18 * Ncv + 4) = Ril(18 * Ncv + 4)
 Case Ncv
 'Circuitaz. precedente
  a(Ncv - 1, Ncv) = 0
  a(Ncv - 1, 6 * Ncv) = 0
  a(Ncv - 1, 18 * Ncv + 2) = -Ril(18 * Ncv + 2)
  a(Ncv - 1, 18 * Ncv + 4) = -Ril(18 * Ncv + 4)
 'Circuitaz. attuale
  a(Ncv, Ncv) = 0
  a(Ncv, 6 * Ncv) = 0
  a(Ncv, 18 * Ncv + 2) = Ril(18 * Ncv + 2)
  a(Ncv, 18 * Ncv + 4) = Ril(18 * Ncv + 4)
 Case Else
  Stop
End Select


Select Case ind_dt2
 Case 1
 'Circuitaz. precedente
  a(Ncv, 1) = 0
  a(Ncv, 5 * Ncv + 1) = 0
  a(Ncv, 18 * Ncv + 6) = -Ril(18 * Ncv + 6)
  a(Ncv, 18 * Ncv + 8) = -Ril(18 * Ncv + 8)
 'Circuitaz. attuale
  a(1, 1) = 0
  a(1, 5 * Ncv + 1) = 0
  a(1, 18 * Ncv + 6) = Ril(18 * Ncv + 6)
  a(1, 18 * Ncv + 8) = Ril(18 * Ncv + 8)
 Case 2 To (Ncv - 1)
 'Circuitaz. precedente
  a(ind_dt2 - 1, ind_dt2) = 0
  a(ind_dt2 - 1, ind_dt2 + 5 * Ncv) = 0
  a(ind_dt2 - 1, 18 * Ncv + 6) = -Ril(18 * Ncv + 6)
  a(ind_dt2 - 1, 18 * Ncv + 8) = -Ril(18 * Ncv + 8)
 'Circuitaz. attuale
  a(ind_dt2, ind_dt2) = 0
  a(ind_dt2, ind_dt2 + 5 * Ncv) = 0
  a(ind_dt2, 18 * Ncv + 6) = Ril(18 * Ncv + 6)
  a(ind_dt2, 18 * Ncv + 8) = Ril(18 * Ncv + 8)
 Case Ncv
 'Circuitaz. precedente
  a(Ncv - 1, Ncv) = 0
  a(Ncv - 1, 6 * Ncv) = 0
  a(Ncv - 1, 18 * Ncv + 6) = -Ril(18 * Ncv + 6)
  a(Ncv - 1, 18 * Ncv + 8) = -Ril(18 * Ncv + 8)
 'Circuitaz. attuale
  a(Ncv, Ncv) = 0
  a(Ncv, 6 * Ncv) = 0
```

```
   a(Ncv, 18 * Ncv + 6) = Ril(18 * Ncv + 6)
   a(Ncv, 18 * Ncv + 8) = Ril(18 * Ncv + 8)
  Case Else
   Stop
 End Select

'Ncv+1 to 2Ncv ********************************************************************
'CIRCUITAZIONI DENTE H

 For i = 1 To Ncv - 1
  a(Ncv + i, Ncv + i) = -Ril(Ncv + i)
  a(Ncv + i, 3 * Ncv + i) = -Ril(3 * Ncv + i)
  a(Ncv + i, 6 * Ncv + i) = Ril(6 * Ncv + i)
  a(Ncv + i, 6 * Ncv + 1 + i) = -Ril(6 * Ncv + 1 + i)
 Next i

 a(2 * Ncv, 2 * Ncv) = -Ril(2 * Ncv)
 a(2 * Ncv, 4 * Ncv) = -Ril(4 * Ncv)
 a(2 * Ncv, 7 * Ncv) = Ril(7 * Ncv)
 a(2 * Ncv, 6 * Ncv + 1) = -Ril(6 * Ncv + 1)

'2Ncv+1 to 3Ncv ********************************************************************
'CIRCUITAZIONI DENTE - DENTE (without AIRGAP)

 For i = 1 To Ncv - 1
  a(2 * Ncv + i, Ncv + i) = -Ril(Ncv + i)
  a(2 * Ncv + i, 4 * Ncv + i) = Ril(4 * Ncv + i)
  a(2 * Ncv + i, 4 * Ncv + 1 + i) = -Ril(4 * Ncv + 1 + i)
  a(2 * Ncv + i, 6 * Ncv + i) = Ril(6 * Ncv + i)
  a(2 * Ncv + i, 6 * Ncv + 1 + i) = -Ril(6 * Ncv + 1 + i)
  a(2 * Ncv + i, 8 * Ncv + i) = -Ril(8 * Ncv + i)
  a(2 * Ncv + i, 12 * Ncv + 1 + i) = -Ril(12 * Ncv + 1 + i)
  a(2 * Ncv + i, 13 * Ncv + i) = -Ril(13 * Ncv + i)
 Next i

 a(3 * Ncv, 2 * Ncv) = -Ril(2 * Ncv)
 a(3 * Ncv, 5 * Ncv) = Ril(5 * Ncv)
 a(3 * Ncv, 4 * Ncv + 1) = -Ril(4 * Ncv + 1)
 a(3 * Ncv, 7 * Ncv) = Ril(7 * Ncv)
 a(3 * Ncv, 6 * Ncv + 1) = -Ril(6 * Ncv + 1)
 a(3 * Ncv, 9 * Ncv) = -Ril(9 * Ncv)
 a(3 * Ncv, 12 * Ncv + 1) = -Ril(12 * Ncv + 1)
 a(3 * Ncv, 14 * Ncv) = -Ril(14 * Ncv)

'3Ncv+1 to 4Ncv ********************************************************************
'CIRCUITAZIONI BASE DENTE - TRAFERRO - MAGNETE DX

 For i = 1 To Ncv
  a(3 * Ncv + i, i) = Ril(i)
  a(3 * Ncv + i, 11 * Ncv + i) = -Ril(11 * Ncv + i)
  a(3 * Ncv + i, 5 * Ncv + i) = Ril(5 * Ncv + i)
  a(3 * Ncv + i, 9 * Ncv + i) = -Ril(9 * Ncv + i)
  a(3 * Ncv + i, 13 * Ncv + i) = Ril(13 * Ncv + i)
 Next i

 If ind_dt <> 0 Then
  a(3 * Ncv + ind_dt, ind_dt) = 0
  a(3 * Ncv + ind_dt, 5 * Ncv + ind_dt) = 0
  a(3 * Ncv + ind_dt, 18 * Ncv + 1) = Ril(18 * Ncv + 1)
  a(3 * Ncv + ind_dt, 18 * Ncv + 3) = Ril(18 * Ncv + 3)
 End If

 If ind_dt2 <> 0 Then
  a(3 * Ncv + ind_dt2, ind_dt2) = 0
  a(3 * Ncv + ind_dt2, 5 * Ncv + ind_dt2) = 0
  a(3 * Ncv + ind_dt2, 18 * Ncv + 5) = Ril(18 * Ncv + 5)
  a(3 * Ncv + ind_dt2, 18 * Ncv + 7) = Ril(18 * Ncv + 7)
 End If

'4Ncv+1 to 5Ncv ********************************************************************
```

```
'CIRCUITAZIONI BASE DENTE - TRAFERRO - MAGNETE SX

 For i = 1 To Ncv
  a(4 * Ncv + i, i) = -Ril(i)
  a(4 * Ncv + i, 10 * Ncv + i) = Ril(10 * Ncv + i)
  a(4 * Ncv + i, 5 * Ncv + i) = -Ril(5 * Ncv + i)
  a(4 * Ncv + i, 7 * Ncv + i) = Ril(7 * Ncv + i)
  a(4 * Ncv + i, 12 * Ncv + i) = Ril(12 * Ncv + i)
 Next i

'5Ncv+1 ********************************************************************************
'CIRCUITAZIONE HcS
 For i = 1 To Ncv
  a(5 * Ncv + 1, Ncv + i) = Ril(Ncv + i)
 Next i

'12Ncv+1 to 13Ncv ***************************************************************************
'CIRCUITAZIONI DENTE - SEMIDENTE - SEMICAVA DX

 For i = 1 To Ncv
  a(12 * Ncv + i, 4 * Ncv + i) = Ril(4 * Ncv + i)
  a(12 * Ncv + i, 6 * Ncv + i) = Ril(6 * Ncv + i)
  a(12 * Ncv + i, 13 * Ncv + i) = -Ril(13 * Ncv + i)
  a(12 * Ncv + i, 15 * Ncv + i) = -Ril(15 * Ncv + i)
  a(12 * Ncv + i, 17 * Ncv + i) = -Ril(17 * Ncv + i)
 Next i

'13Ncv+1 to 14Ncv ***************************************************************************
'CIRCUITAZIONI SEMICAVA SX LOW

 For i = 1 To Ncv
  'a(13 * Ncv + i, 4 * Ncv + i) = -Ril(4 * Ncv + i)
  a(13 * Ncv + i, 12 * Ncv + i) = -Ril(12 * Ncv + i)
  a(13 * Ncv + i, 13 * Ncv + i) = -Ril(13 * Ncv + i)
  a(13 * Ncv + i, 14 * Ncv + i) = Ril(14 * Ncv + i)
  a(13 * Ncv + i, 15 * Ncv + i) = -Ril(15 * Ncv + i)
 Next i

 '16Ncv+1 to 17Ncv ***************************************************************************
 'CIRCUITAZIONI ALTA SEMICAVA - ALTO SEMIDENTE SX

  For i = 1 To Ncv
   a(16 * Ncv + i, 16 * Ncv + i) = Ril(16 * Ncv + i)
   a(16 * Ncv + i, 6 * Ncv + i) = -Ril(6 * Ncv + i)
  Next i

 '17Ncv+1 to 18Ncv ***************************************************************************
 'CIRCUITAZIONI ALTA SEMICAVA - ALTO SEMIDENTE DX

  For i = 1 To Ncv
   a(17 * Ncv + i, 6 * Ncv + i) = Ril(6 * Ncv + i)
   a(17 * Ncv + i, 17 * Ncv + i) = -Ril(17 * Ncv + i)
  Next i

 '18Ncv+1 to 18Ncv+8 *************************************************************************
 'EQUAZIONI AGGIUNTIVE

 If ind_dt <> 0 Then
 'Circuitazione PRIMA discontinuità del magnete
  a(18 * Ncv + 1, ind_dt) = Ril(ind_dt)
  a(18 * Ncv + 1, 5 * Ncv + ind_dt) = Ril(5 * Ncv + ind_dt)
  a(18 * Ncv + 1, 18 * Ncv + 4) = -Ril(18 * Ncv + 4)
  a(18 * Ncv + 1, 18 * Ncv + 2) = -Ril(18 * Ncv + 2)

 'Circuitazione SECONDA discontinuità del magnete
  a(18 * Ncv + 2, 18 * Ncv + 2) = Ril(18 * Ncv + 2)
  a(18 * Ncv + 2, 18 * Ncv + 1) = -Ril(18 * Ncv + 1)
  a(18 * Ncv + 2, 18 * Ncv + 4) = Ril(18 * Ncv + 4)
  a(18 * Ncv + 2, 18 * Ncv + 3) = -Ril(18 * Ncv + 3)
```

```
 'NODI 7(2)
  a(18 * Ncv + 3, 18 * Ncv + 2) = -1
  a(18 * Ncv + 3, 18 * Ncv + 4) = 1

 'NODI 7(3)
  a(18 * Ncv + 4, 18 * Ncv + 1) = -1
  a(18 * Ncv + 4, 18 * Ncv + 3) = 1

 End If

 If ind_dt2 <> 0 Then
 'Circuitazione PRIMA discontinuità del magnete
  a(18 * Ncv + 5, ind_dt2) = Ril(ind_dt2)
  a(18 * Ncv + 5, 5 * Ncv + ind_dt2) = Ril(5 * Ncv + ind_dt2)
  a(18 * Ncv + 5, 18 * Ncv + 8) = -Ril(18 * Ncv + 8)
  a(18 * Ncv + 5, 18 * Ncv + 6) = -Ril(18 * Ncv + 6)

 'Circuitazione SECONDA discontinuità del magnete
  a(18 * Ncv + 6, 18 * Ncv + 6) = Ril(18 * Ncv + 6)
  a(18 * Ncv + 6, 18 * Ncv + 5) = -Ril(18 * Ncv + 5)
  a(18 * Ncv + 6, 18 * Ncv + 8) = Ril(18 * Ncv + 8)
  a(18 * Ncv + 6, 18 * Ncv + 7) = -Ril(18 * Ncv + 7)

 'NODI 7(2)
  a(18 * Ncv + 7, 18 * Ncv + 6) = -1
  a(18 * Ncv + 7, 18 * Ncv + 8) = 1

 'NODI 7(3)
  a(18 * Ncv + 8, 18 * Ncv + 5) = -1
  a(18 * Ncv + 8, 18 * Ncv + 7) = 1

 End If

 Cells(4 + z, 31) = z
 Cells(4 + z, 32) = maxdiffx * 100

 z = z + 1

Loop

End Sub


Public Function Induction(n, x_, Hlam, Blam)

 'NON LINEARE
  For i = 1 To 451
   If Abs(x_) >= Hlam(i) And Abs(x_) <= Hlam(i + 1) Then
    deltaBH = (Blam(i + 1) - Blam(i)) / (Hlam(i + 1) - Hlam(i))
    Induction = deltaBH * (Abs(x_) - Hlam(i)) + Blam(i)
   End If
  Next i

  If Abs(x_) >= Hlam(452) Then
   deltaBH = (Blam(452) - Blam(451)) / (Hlam(452) - Hlam(451))
   Induction = deltaBH * (Abs(x_) - Hlam(452)) + Blam(452)
  End If

End Function


Public Function Magfield(n, x_, Hlam, Blam)

 'NON LINEARE
  For i = 1 To 451
   If Abs(x_) >= Blam(i) And Abs(x_) <= Blam(i + 1) Then
   deltaHB = (Hlam(i + 1) - Hlam(i)) / (Blam(i + 1) - Blam(i))
    Magfield = deltaHB * (Abs(x_) - Blam(i)) + Hlam(i)
   End If
  Next i
```

```
  If Abs(x_) >= Blam(452) Then
   deltaHB = (Hlam(452) - Hlam(451)) / (Blam(452) - Blam(451))
   Magfield = deltaHB * (Abs(x_) - Blam(452)) + Hlam(452)
  End If

End Function
```

Appendix A2.2

THE PROGRAMMING CODE

Part 2

In the following, the programming code of the subroutine to determine the array of the stator ampere-turns distribution, to save in the file *ASP_TOT.txt* combined with the magnets distribution. Two versions are presented, a simpler one and a more elaborate one.

A2.2.1 The MMF array (simplified version)

```
Const pi = 3.1415927

Private Sub CommandButton1_Click()

'INPUT

 Ncv = Foglio2.Cells(4, 4)
 npr = Foglio2.Cells(5, 4)
 nsc = Foglio2.Cells(6, 4)
 Taup = Foglio2.Cells(7, 4)
 Taup = Taup * 0.001
 Irms = Foglio2.Cells(8, 4)
 adt = Foglio2.Cells(16, 4)
 adt = adt * 0.001
 havv = Foglio2.Cells(21, 4)
 havv = havv * 0.001
 ta = Foglio2.Cells(23, 4)
 xm = Foglio2.Cells(24, 4)
 xm = xm * 0.001
 dx_cost = Foglio2.Cells(25, 4)
 dx_cost = dx_cost * 0.001
 dx = Foglio2.Cells(26, 4)
 dx = dx * 0.001
 ixm_max = Foglio2.Cells(27, 4)
 fi_in = Foglio2.Cells(28, 4)
 nfasi = Foglio2.Cells(30, 4)
```

```
 filepath = CStr(Foglio2.TextBox1.Text)

 If ta <= 1 - havv / adt Then
  MsgBox ("Valore di ta troppo basso!")
  Stop
 End If

 f = 50
 kw = 1
 st = 2

'Grandezze derivate
 w = 2 * pi * f
 n = 18 * Ncv + 8
 kcir = adt * (1 - ta) / havv

ReDim ordpr(1 To Ncv), ordsc(1 To Ncv) As Integer
ReDim aI(1 To n), aIp(1 To n), aIs(1 To n), aI_p(1 To n), aM(1 To n), ASP(1 To n) As
Double
ReDim Ifse(1 To nfasi), Ifse_p(1 To nfasi) As Double

 'Lettura del file relativo al I strato dell'avvolgimento statorico
 Open filepath & "\ordpr.txt" For Input As #1
  For i = 1 To Ncv
   Input #1, ordpr(i)
  Next i
 Close #1
 'Lettura del file relativo al II strato dell'avvolgimento statorico
 Open filepath & "\ordsc.txt" For Input As #2
  For i = 1 To Ncv
   Input #2, ordsc(i)
  Next i
 Close #2
 'Lettura del file contenente le amperspire equivalenti del magnete
 Open filepath & "\aM(pp).txt" For Input As #3
  For i = 1 To n
   Input #3, aM(i)
  Next i
 Close #3

 Open filepath & "\ASP_TOT.txt" For Output As #4

For ixm = 1 To ixm_max

 If Int(ixm / 2) <> ixm / 2 Then
  'step di spostamento DISPARI: le correnti vengono calcolate
  'secondo l'esatto valore istantaneo correlato alla posizione

  'inizializzazione dell'array
   For i = 1 To n
    aI(i) = 0
   Next i

   'Andamento sinusoidale delle correnti
    t = pi * xm / w / Taup

   'Memorizzazione del valore delle correnti allo step precedente
    For i = 1 To nfasi
     Ifse_p(i) = Ifse(i)
    Next i
    For j = 1 To nfasi
     Ifse(j) = -Sqr(2) * Irms * Cos(kw * w * t - (j - 1) * kw * st * 2 * pi / nfasi +
     fi_in)
    Next j

  'ARRAY AMPERSPIRE STATORICHE

    For i = 1 To Ncv
     aIp(i) = npr * Sgn(ordpr(i)) * Ifse(Abs(ordpr(i)))
```

```
    aIs(i) = nsc * Sgn(ordsc(i)) * Ifse(Abs(ordsc(i)))
   Next i

   For i = 1 To Ncv
    aIp(Ncv + i) = 0
    aIs(Ncv + i) = nsc * Sgn(ordsc(i)) * Ifse(Abs(ordsc(i)))
   Next i

   For i = 1 To Ncv
    aIp(2 * Ncv + i) = npr * Sgn(ordpr(i)) * Ifse(Abs(ordpr(i)))
    aIs(2 * Ncv + i) = nsc * Sgn(ordsc(i)) * Ifse(Abs(ordsc(i)))
   Next i

   For i = 1 To Ncv
    aIp(12 * Ncv + i) = npr / 2 * Sgn(ordpr(i)) * Ifse(Abs(ordpr(i)))
    aIs(12 * Ncv + i) = nsc / 2 * Sgn(ordsc(i)) * Ifse(Abs(ordsc(i)))
   Next i

    aIp(13 * Ncv + 1) = npr / 2 * Sgn(ordpr(Ncv)) * Ifse(Abs(ordpr(Ncv))) + npr / 2 *
    Sgn(ordpr(1)) * Ifse(Abs(ordpr(1)))
    aIs(13 * Ncv + 1) = 0
   For i = 2 To Ncv
    aIp(13 * Ncv + i) = npr / 2 * Sgn(ordpr(i - 1)) * Ifse(Abs(ordpr(i - 1))) + npr / 2
    * Sgn(ordpr(i)) * Ifse(Abs(ordpr(i)))
    aIs(13 * Ncv + i) = 0
   Next i

    aIp(16 * Ncv + 1) = 0
    aIs(16 * Ncv + 1) = nsc / 2 * Sgn(ordsc(Ncv)) * Ifse(Abs(ordsc(Ncv)))
   For i = 2 To Ncv
    aIp(16 * Ncv + i) = 0
    aIs(16 * Ncv + i) = nsc / 2 * Sgn(ordsc(i - 1)) * Ifse(Abs(ordsc(i - 1)))
   Next i

   For i = 1 To Ncv
    aIp(17 * Ncv + i) = 0
    aIs(17 * Ncv + i) = nsc / 2 * Sgn(ordsc(i)) * Ifse(Abs(ordsc(i)))
   Next i

  'composizione dei vettori dei due strati in un unico (ASP TOTALI STATORICHE)

   For i = 1 To 3 * Ncv
    aI(i) = aIp(i) + aIs(i)
   Next i
   For i = 12 * Ncv + 1 To 14 * Ncv
    aI(i) = aIp(i) + aIs(i)
   Next i
   For i = 16 * Ncv + 1 To 18 * Ncv
    aI(i) = aIp(i) + aIs(i)
   Next i

  'memorizzazione per lo step successivo
  '(nel quale le correnti restano invariate)
   For i = 1 To n
    aI_p(i) = aI(i)
   Next i

   dx1 = dx_cost

Else
 'step di spostamento PARI: le correnti vengono
 'mantenute costanti per il calcolo della Fx

   For i = 1 To n
    aI(i) = aI_p(i)
   Next i

   dx1 = dx

End If
```

```
 'composizione vettore amperspire totali
  For i = 1 To n
   ASP(i) = aI(i) + aM(i)
  Next i

 'scrittura su file
  For i = 1 To n
   Print #4, ASP(i)
  Next i

  xm = xm + dx1

Next ixm

Close #4

End Sub
```

A2.2.2 The MMF array (original version)

```
Const pi = 3.1415927

Private Sub CommandButton1_Click()

'INPUT

 Ncv = Foglio2.Cells(4, 4)
 npr = Foglio2.Cells(5, 4)
 nsc = Foglio2.Cells(6, 4)
 Taup = Foglio2.Cells(7, 4)
 Taup = Taup * 0.001
 Irms = Foglio2.Cells(8, 4)
 adt = Foglio2.Cells(16, 4)
 adt = adt * 0.001
 havv = Foglio2.Cells(21, 4)
 havv = havv * 0.001
 ta = Foglio2.Cells(23, 4)
 xm = Foglio2.Cells(24, 4)
 xm = xm * 0.001
 dx_cost = Foglio2.Cells(25, 4)
 dx_cost = dx_cost * 0.001
 dx = Foglio2.Cells(26, 4)
 dx = dx * 0.001
 ixm_max = Foglio2.Cells(27, 4)
 fi_in = Foglio2.Cells(28, 4)
 nfasi = Foglio2.Cells(30, 4)

 filepath = CStr(Foglio2.TextBox1.Text)

 If ta <= 1 - havv / adt Then
  MsgBox ("Valore di ta troppo basso!")
  Stop
 End If

 f = 50
 kw = 1
 st = 2
```

```
'Grandezze derivate
 w = 2 * pi * f
 n = 18 * Ncv + 8
 kcir = adt * (1 - ta) / havv

ReDim ordpr(1 To Ncv), ordsc(1 To Ncv) As Integer
ReDim aI(1 To n), aIp(1 To n), aIs(1 To n), aI_p(1 To n), aM(1 To n), ASP(1 To n) As
Double
ReDim Ifse(1 To nfasi), Ifse_p(1 To nfasi) As Double

 'Lettura del file relativo al I strato dell'avvolgimento statorico
 Open filepath & "\ordpr.txt" For Input As #1
  For i = 1 To Ncv
   Input #1, ordpr(i)
  Next i
 Close #1
 'Lettura del file relativo al II strato dell'avvolgimento statorico
 Open filepath & "\ordsc.txt" For Input As #2
  For i = 1 To Ncv
   Input #2, ordsc(i)
  Next i
 Close #2
 'Lettura del file contenente le amperspire equivalenti del magnete
 Open filepath & "\aM(pp).txt" For Input As #3
  For i = 1 To n
   Input #3, aM(i)
  Next i
 Close #3

 Open filepath & "\ASP_TOT.txt" For Output As #4

For ixm = 1 To ixm_max


 If Int(ixm / 2) <> ixm / 2 Then
  'step di spostamento DISPARI: le correnti vengono calcolate
  'secondo l'esatto valore istantaneo correlato alla posizione

  'inizializzazione dell'array
   For i = 1 To n
    aI(i) = 0
   Next i

   'Andamento sinusoidale delle correnti
    t = pi * xm / w / Taup
   'Memorizzazione del valore delle correnti allo step precedente
    For i = 1 To nfasi
     Ifse_p(i) = Ifse(i)
    Next i
    For j = 1 To nfasi
     Ifse(j) = -Sqr(2) * Irms * Cos(kw * w * t - (j - 1) * kw * st * 2 * pi / nfasi +
     fi_in)
    Next j

  'ARRAY AMPERSPIRE STATORICHE

    For i = 1 To Ncv
     aIp(i) = npr * Sgn(ordpr(i)) * Ifse(Abs(ordpr(i)))
     aIs(i) = nsc * Sgn(ordsc(i)) * Ifse(Abs(ordsc(i)))
    Next i

    For i = 1 To Ncv
     If (0 <= kcir) And (kcir <= 0.5) Then
      aIp(Ncv + i) = 0
      aIs(Ncv + i) = 2 * nsc * kcir * Sgn(ordsc(i)) * Ifse(Abs(ordsc(i)))
     ElseIf (0.5 < kcir) And (kcir < 1) Then
      aIp(Ncv + i) = (2 * npr * kcir - npr) * Sgn(ordpr(i)) * Ifse(Abs(ordpr(i)))
      aIs(Ncv + i) = nsc * Sgn(ordsc(i)) * Ifse(Abs(ordsc(i)))
     Else
      aIp(Ncv + i) = npr * Sgn(ordpr(i)) * Ifse(Abs(ordpr(i)))
```

```
  aIs(Ncv + i) = nsc * Sgn(ordsc(i)) * Ifse(Abs(ordsc(i)))
 End If
Next i

For i = 1 To Ncv
 aIp(2 * Ncv + i) = npr * Sgn(ordpr(i)) * Ifse(Abs(ordpr(i)))
 aIs(2 * Ncv + i) = nsc * Sgn(ordsc(i)) * Ifse(Abs(ordsc(i)))
Next i

For i = 1 To Ncv
 aIp(12 * Ncv + i) = npr / 2 * Sgn(ordpr(i)) * Ifse(Abs(ordpr(i)))
 aIs(12 * Ncv + i) = nsc / 2 * Sgn(ordsc(i)) * Ifse(Abs(ordsc(i)))
Next i

If (0 <= kcir) And (kcir <= 0.5) Then
'concatena in ogni caso sempre tutto il (I)
 aIp(13 * Ncv + 1) = npr / 2 * Sgn(ordpr(Ncv)) * Ifse(Abs(ordpr(Ncv))) + npr / 2 *
 Sgn(ordpr(1)) * Ifse(Abs(ordpr(1)))
'concatena una parte del (II), a seconda del valore di ta
 aIs(13 * Ncv + 1) = (nsc - 2 * nsc * kcir) / 2 * Sgn(ordsc(Ncv)) *
 Ifse(Abs(ordsc(Ncv))) + (nsc - 2 * nsc * kcir) / 2 * Sgn(ordsc(1)) *
 Ifse(Abs(ordsc(1)))
ElseIf (0.5 < kcir) And (kcir < 1) Then
 aIp(13 * Ncv + 1) = 2 * npr * (1 - kcir) / 2 * Sgn(ordpr(Ncv)) *
 Ifse(Abs(ordpr(Ncv))) + 2 * npr * (1 - kcir) / 2 * Sgn(ordpr(1)) *
 Ifse(Abs(ordpr(1)))
 aIs(13 * Ncv + 1) = 0
Else
 aIp(13 * Ncv + 1) = 0
 aIs(13 * Ncv + 1) = 0
End If
For i = 2 To Ncv
 If (0 <= kcir) And (kcir <= 0.5) Then
 'concatena in ogni caso sempre tutto il (I)
  aIp(13 * Ncv + i) = npr / 2 * Sgn(ordpr(i - 1)) * Ifse(Abs(ordpr(i - 1))) + npr /
  2 * Sgn(ordpr(i)) * Ifse(Abs(ordpr(i)))
 'concatena una parte del (II), a seconda del valore di ta
  aIs(13 * Ncv + i) = (nsc - 2 * nsc * kcir) / 2 * Sgn(ordsc(i - 1)) *
  Ifse(Abs(ordsc(i - 1))) + (nsc - 2 * nsc * kcir) / 2 * Sgn(ordsc(i)) *
  Ifse(Abs(ordsc(i)))
 ElseIf (0.5 < kcir) And (kcir < 1) Then
  aIp(13 * Ncv + i) = 2 * npr * (1 - kcir) / 2 * Sgn(ordpr(i - 1)) *
  Ifse(Abs(ordpr(i - 1))) + 2 * npr * (1 - kcir) / 2 * Sgn(ordpr(i)) *
  Ifse(Abs(ordpr(i)))
  aIs(13 * Ncv + i) = 0
 Else
  aIp(13 * Ncv + i) = 0
  aIs(13 * Ncv + i) = 0
 End If
Next i

If (0 <= kcir) And (kcir <= 0.5) Then
 aIp(16 * Ncv + 1) = 0
 aIs(16 * Ncv + 1) = 2 * nsc * kcir / 2 * Sgn(ordsc(Ncv)) * Ifse(Abs(ordsc(Ncv)))
ElseIf (0.5 < kcir) And (kcir < 1) Then
 aIp(16 * Ncv + 1) = (2 * npr * kcir - npr) / 2 * Sgn(ordpr(Ncv)) *
 Ifse(Abs(ordpr(Ncv)))
 aIs(16 * Ncv + 1) = nsc / 2 * Sgn(ordsc(Ncv)) * Ifse(Abs(ordsc(Ncv)))
Else
 aIp(16 * Ncv + 1) = npr / 2 * Sgn(ordpr(Ncv)) * Ifse(Abs(ordpr(Ncv)))
 aIs(16 * Ncv + 1) = nsc / 2 * Sgn(ordsc(Ncv)) * Ifse(Abs(ordsc(Ncv)))
End If
For i = 2 To Ncv
 If (0 <= kcir) And (kcir <= 0.5) Then
  aIp(16 * Ncv + i) = 0
  aIs(16 * Ncv + i) = 2 * nsc * kcir / 2 * Sgn(ordsc(i)) * Ifse(Abs(ordsc(i)))
 ElseIf (0.5 < kcir) And (kcir < 1) Then
  aIp(16 * Ncv + i) = (2 * npr * kcir - npr) / 2 * Sgn(ordpr(i)) *
  Ifse(Abs(ordpr(i)))
  aIs(16 * Ncv + i) = nsc / 2 * Sgn(ordsc(i)) * Ifse(Abs(ordsc(i)))
```

```
     Else
      aIp(16 * Ncv + i) = npr / 2 * Sgn(ordpr(i)) * Ifse(Abs(ordpr(i)))
      aIs(16 * Ncv + i) = nsc / 2 * Sgn(ordsc(i)) * Ifse(Abs(ordsc(i)))
     End If
    Next i

    For i = 1 To Ncv
     If (0 <= kcir) And (kcir <= 0.5) Then
      aIp(17 * Ncv + i) = 0
      aIs(17 * Ncv + i) = 2 * nsc * kcir / 2 * Sgn(ordsc(i)) * Ifse(Abs(ordsc(i)))
     ElseIf (0.5 < kcir) And (kcir < 1) Then
      aIp(17 * Ncv + i) = (2 * npr * kcir - npr) / 2 * Sgn(ordpr(i)) *
      Ifse(Abs(ordpr(i)))
      aIs(17 * Ncv + i) = nsc / 2 * Sgn(ordsc(i)) * Ifse(Abs(ordsc(i)))
     Else
      aIp(17 * Ncv + i) = npr / 2 * Sgn(ordpr(i)) * Ifse(Abs(ordpr(i)))
      aIs(17 * Ncv + i) = nsc / 2 * Sgn(ordsc(i)) * Ifse(Abs(ordsc(i)))
     End If
    Next i

   'composizione dei vettori dei due strati in un unico (ASP TOTALI STATORICHE)

    For i = 1 To 3 * Ncv
     aI(i) = aIp(i) + aIs(i)
    Next i
    For i = 12 * Ncv + 1 To 14 * Ncv
     aI(i) = aIp(i) + aIs(i)
    Next i
    For i = 16 * Ncv + 1 To 18 * Ncv
     aI(i) = aIp(i) + aIs(i)
    Next i

   'memorizzazione per lo step successivo
   '(nel quale le correnti restano invariate)
    For i = 1 To n
     aI_p(i) = aI(i)
    Next i

    dx1 = dx_cost

 Else
  'step di spostamento PARI: le correnti vengono
  'mantenute costanti per il calcolo della Fx
    For i = 1 To n
     aI(i) = aI_p(i)
    Next i

    dx1 = dx

 End If
 'composizione vettore amperspire totali
  For i = 1 To n
   ASP(i) = aI(i) + aM(i)
  Next i
 'scrittura su file
  For i = 1 To n
   Print #4, ASP(i)
  Next i

  xm = xm + dx1

Next ixm

Close #4

End Sub
```

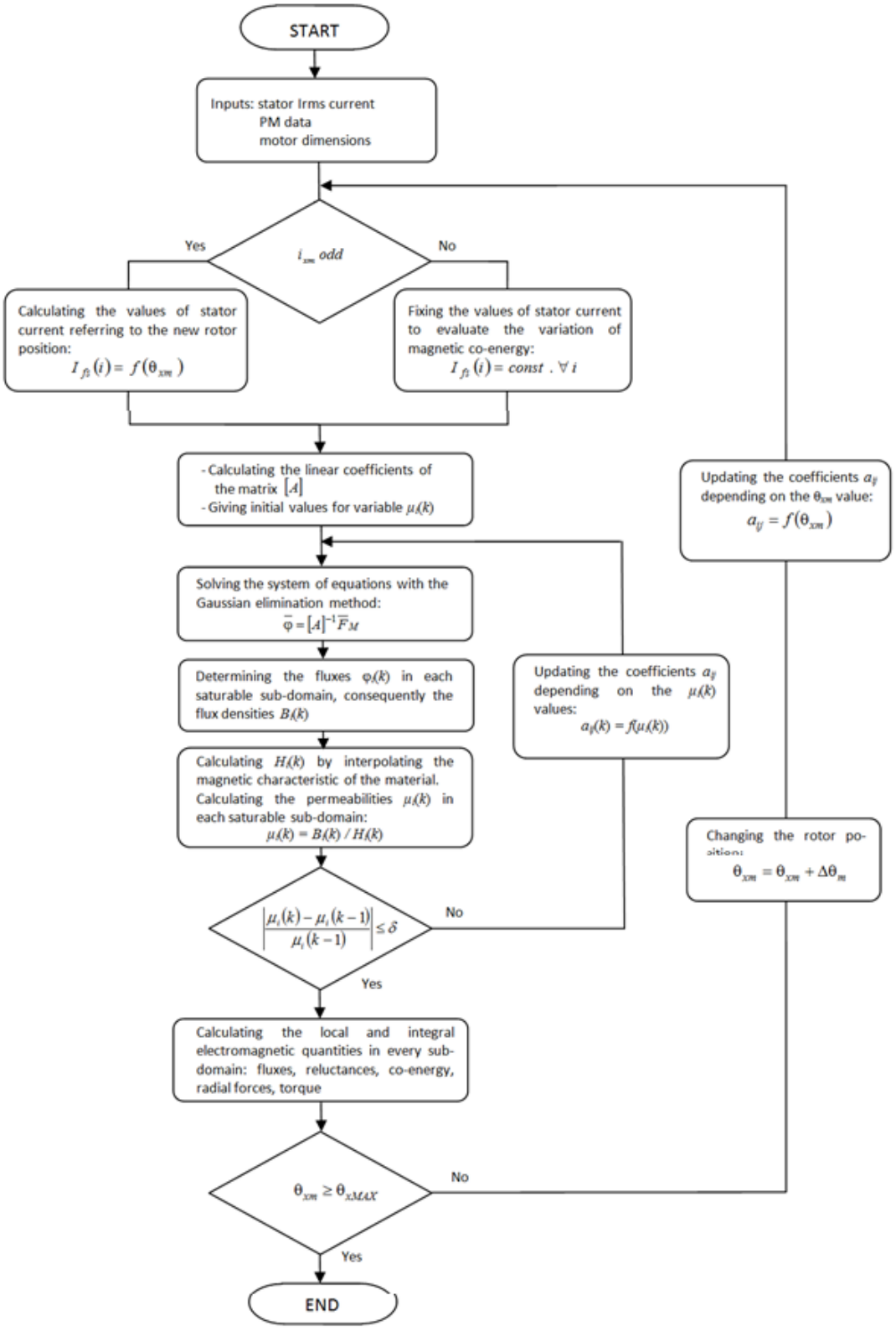

Fig. A2.2-1. The flow-chart of the algorithm

Chapter 3

PRINCIPLES OF BEARINGLESS MACHINES

3.1 Introduction

A bearingless motor is an electrical machine where the suspension and the centering of the rotor is provided by radial forces generated by the interactions between the magnetic fields acting in the airgap, avoiding the use of mechanical bearings and achieving in this way much higher maximum speed [1], as in [2] where is proposed a 60000 rpm motor for compressors and special pumps. In this way, the rotor is suspended and centered by a radial force distribution, suitably created by the interactions between different harmonic orders of the magnetic fields produced by the stator and rotor sources, whatever they are: in fact, the

principle can be applied to the permanent magnet surface-mounted synchronous machine [3], [4], [5], internal PM motors, induction motors. An interesting general method for a comparison of bearingless machines is presented in literature [6]: PM synchronous motors have the advantage that the control of rotation and levitation are independent, while the levitation force is weak. Conversely, induction motors produce a strong levitation force, but their efficiency is poor and the control of rotation and levitation are coupled. The internal permanent magnet (IPM) type bearingless motor represents a compromise, being characterized by strong levitation force and relatively easy control properties.

The radial force are generated by creating an unbalanced flux density distribution in the airgap, which results in a magnetic force acting on the rotor. In fact, in this situation by summing the force vectors related to every pole, they give a not null resultant. On the contrary, in the electrical machines of conventional typology, the magnetic poles have equal flux density and hence equal magnitudes of the attractive forces, with a null vector sum of the radial forces. An unbalanced magnetic field distribution in a bearingless machine can be obtained by two different winding distributions:

1) 'Dual set of windings', characterized by two systems of three-phase windings physically separated, one dedicated to the generation of tangential forces which produce torque, the other to the generation of the radial forces of levitation; a bearingless motor previously proposed in literature, presents a 2-pole radial force windings wounded in the stator of a 4-pole motor [1], could be applied to super high speed motors as well as induction and synchronous reluctance machines, as theorized in [7], [8]. An analysis and classification of 3-phase separated and concentrated windings bearingless machines is proposed by [9], which constitutes a relief in the design of this typology of motors.

2) 'Single set of multiphase windings', in which the two typologies of force are obtained from a single winding, exploiting the potential of multiphase motors to produce spatial harmonics of odd and even orders, by injecting different current space vectors: in this way two stator magnetic fields of different harmonic order, by acting with the rotor magnetic field, ensure one the suspension of the rotor, the other the generation of torque. In [10] is proposed a 6-phase induction machine with one set of windings instead of two sets of 3-phase windings, taking advantage of the multiple control degrees of freedom given by multiphase machines; [11] presents a 5-phase bearingless motor, explicating the principle of generating the torque and suspension forces by feeding two groups of currents projected into 2 orthogonal d-q planes. In the same paper is also presented a control system which estimates the parameters of the current levitation system by means of PID controllers, acquiring the position error of the rotor and estimates the parameters of the current motor system by means of a PI controller, acquiring the angular speed error.

3.2 General Principles of Magnetic Force Generation

Fig. 3.1 shows the cross section of a general bearingless motor under different operative conditions [1], [12]. In Fig. 3.1(a), the flux distribution is a symmetrical 4-pole, the flux paths around the conductors **4a** being shown: the four pole flux wave ψ_{4a} produces alternating magnetic poles in the airgap. Since the flux distribution is symmetrical, the flux density distribution is identical, apart from the sign, in the airgap sections 1, 2, 3 and 4. There are attractive magnetic forces between the rotor poles and stator iron, which have identical amplitudes, but with equally distributed directions, so that the sum of radial force

acting on the rotor is zero. Fig. 3.1(b) shows the principle of radial force generation: a 2-pole winding, represented by conductors **2a**, produces a magnetic flux ψ_{2a} having the same direction than the one generated from the 4-pole winding in the section 1, but having the opposite direction in section 3. In this way, the flux density will increase in section 1, while will be reduced in section 3, generating a radial force F according to the x-axis direction. It follows that the amplitude of the radial force increases as the current value in conductors **2a** increases. Fig. 3.1(c) shows how a negative radial force in the x-axis direction is generated. The current in conductors **2a** is reversed so that the flux density in airgap section 1 now decreases while that in airgap section 3 increases. Hence the magnetic force in airgap section 3 is larger than that in airgap section 1, producing a radial force in the negative x-axis direction.

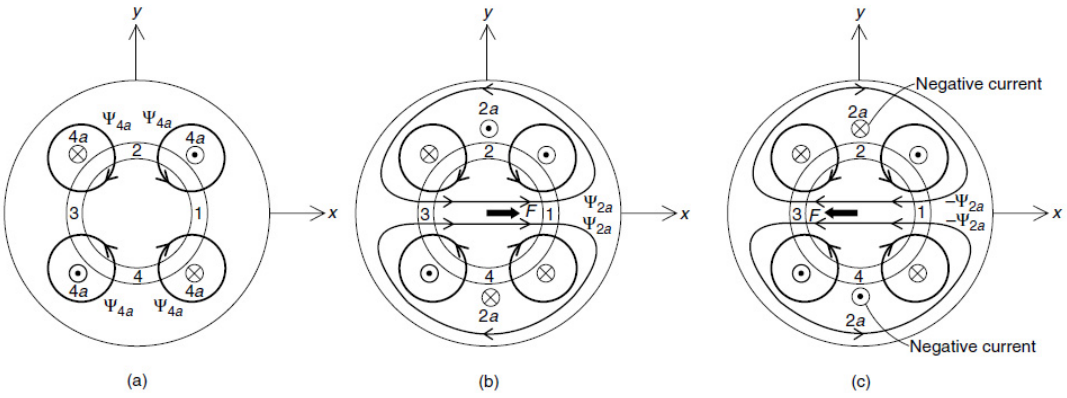

Fig. 3.1

Fig. 3.2 shows the radial force generation in the y-axis direction. The conductors **2b**, which have an MMF direction along the y-axis, produce a flux through the airgap sections 2 and 4, thus resulting in a force along the y-axis. The polarity of the current will dictate the direction of the force. These are the principles of the radial force generation, being its value almost proportional to the current in the

windings **2a** and **2b** (assuming a constant 4-pole current). The vector sum of these two perpendicular radial forces can produce a radial force in whatever direction, with any amplitude. As an essential condition to generate radial forces, the difference of pole pair numbers of the motoring and levitation fields has to be ± 1.

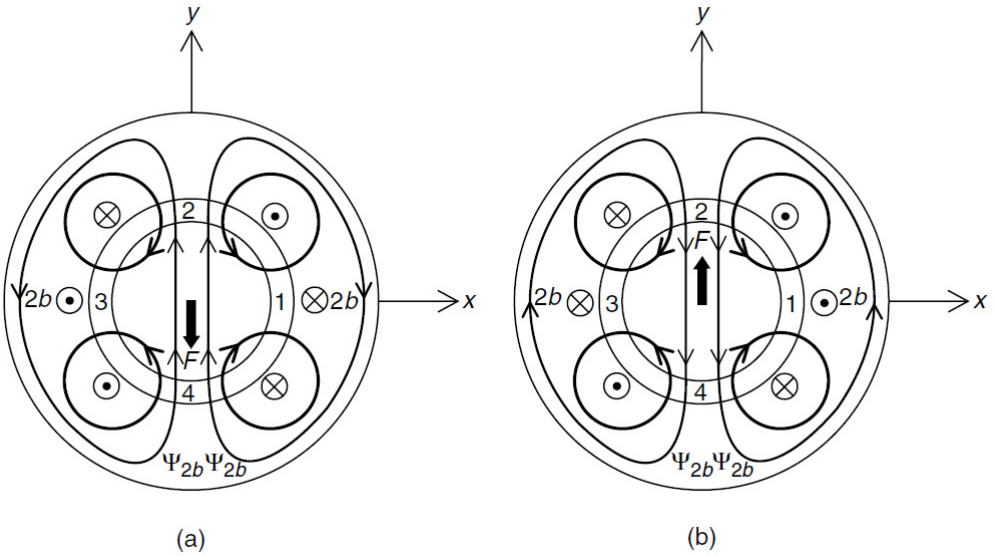

Fig. 3.2

3.3 Bearingless Machines with a Dual Set of Windings

In [13] is presented an interesting analysis of a bearingless permanent magnet motor with a dual set of windings, reported in the following. The 4-pole magnetic field (produced by the torque current system) and the 2-pole magnetic field (produced by the levitation current system) are generated by separated, physically distinct, windings. This method allows to design the two windings independently, but has the disadvantage of reserving part of the copper surface in the slot to the levitation winding (Fig. 3.3), used to produce radial forces, causing in this way higher Joule losses to give the same torque output with respect to the

conventional electrical machines.

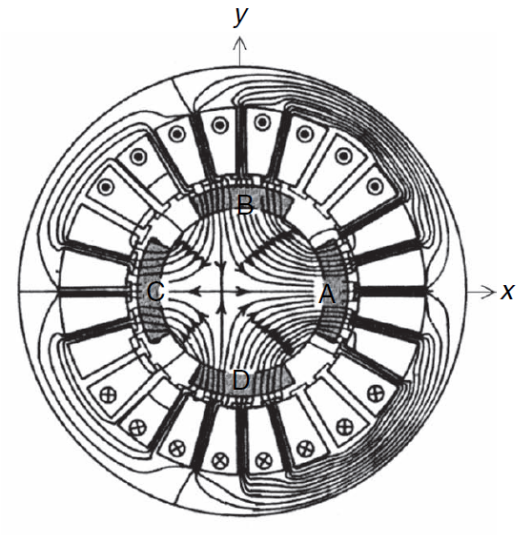

Fig. 3.3

With reference to Fig. 3.4, the additional 2-pole windings N_α and N_β are wound in the stator slots with the conventional 4-pole windings. The radial force is caused by the unbalanced distribution of the flux density in the airgap, caused by the existing interaction between the excitation flux ψ_P, which flows in the 4 poles and in the permanent magnets, and the flux generated by the 2-pole windings currents i_α and i_β.

The current i_α, with a direction and orientation as in Fig. 3.4, generates the flux ψ_α. The flux density increases in the airgap section 2 and decreases in the airgap section 1, the radial force F is generated in the negative direction of the α axis. For simplicity, it will analyzed a model of two-phase machine. The current able to generate a magneto-motive force equal to that of the permanent magnets is represented as an equivalent current in the motor windings. The currents i_{ap} and i_{bp}, in the motor windings N_a and N_b, are the sum of the actual components of the motor current with amplitude I_q and of the equivalent current

of permanent magnets with amplitude I_p.

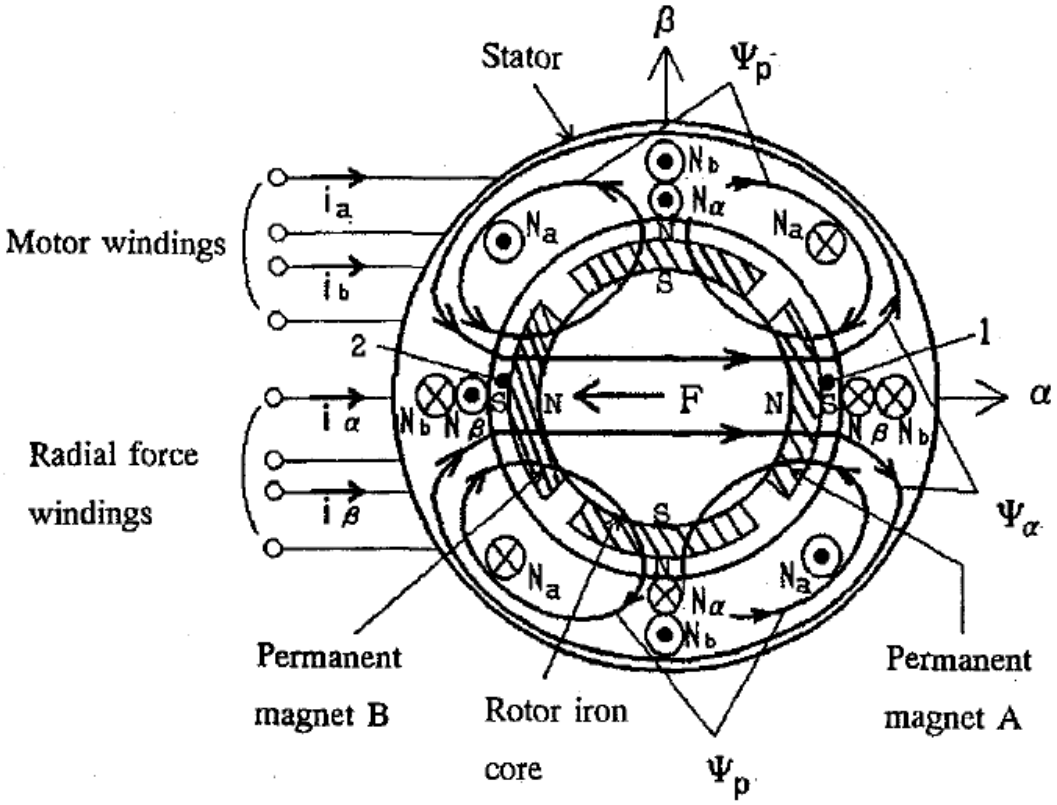

Fig. 3.4. PM bearingless motor with a dual set of windings

The currents can be written as:

$$i_{ap} = -I_q \sin 2\omega t + I_p \cos 2\omega t \tag{3.1}$$

$$i_{bp} = I_q \cos 2\omega t + I_p \sin 2\omega t \tag{3.2}$$

Where ω represents the angular frequency If the bearingless motor is in open-circuit operating condition I_q is about zero and can be neglected:

$$i_{ap} \cong I_p \cos 2\omega t \tag{3.3}$$

$$i_{bp} \cong I_p \sin 2\omega t \tag{3.4}$$

By defining ψ_{ap}, ψ_{bp}, ψ_α, ψ_β respectively as the 4-pole fluxes related to

windings N_a, N_b and the 2-pole fluxes related to windings N_α, N_β, the relationships between them and the currents that flow in the motor and levitation windings can be written as:

$$\begin{bmatrix} \psi_{ap} \\ \psi_{bp} \\ \psi_\alpha \\ \psi_\beta \end{bmatrix} = \begin{bmatrix} L_4 & 0 & -M'\alpha & M'\beta \\ 0 & L_4 & M'\beta & M'\alpha \\ -M'\alpha & M'\beta & L_2 & 0 \\ M'\beta & M'\alpha & 0 & L_2 \end{bmatrix} \begin{bmatrix} i_{ap} \\ i_{bp} \\ i_\alpha \\ i_\beta \end{bmatrix} \tag{3.5}$$

Being L_4 and L_2 respectively the self-induction coefficients of motor and levitation windings, α e β the rotor displacements along the x and y axes, M' the derivative of the mutual-induction coefficient, related to the coupling between motor and levitation windings with respect to rotor displacements.
L_4, L_2 and M are functions of the airgap lenght, number of turns and rotor dimension. By assuming a magnetic linear system, M' can be written as:

$$M' = \frac{\mu_0 \pi n_2 n_4 l}{8} \frac{r - (l_m + l_g)}{(l_m + l_g)^2} \tag{3.6}$$

where n_2 and n_4 are the real number of turns of the windings, l is the axial length of the machine, r is the internal stator radius, l_m the magnet thickness, l_g the airgap length. Consequently, $(l_m + l_g)$ represents the distance between the internal stator surface and external rotor surface. The stored magnetic energy W_m can be expressed as:

$$W_m = \frac{1}{2} \begin{bmatrix} i_{ap} & i_{bp} & i_\alpha & i_\beta \end{bmatrix} \begin{bmatrix} L_4 & 0 & -M'\alpha & M'\beta \\ 0 & L_4 & M'\beta & M'\alpha \\ -M'\alpha & M'\beta & L_2 & 0 \\ M'\beta & M'\alpha & 0 & L_2 \end{bmatrix} \begin{bmatrix} i_{ap} \\ i_{bp} \\ i_\alpha \\ i_\beta \end{bmatrix} \tag{3.7}$$

The radial force produced by the interactions between the two windings and the

rotor magnetic field can be calculated in terms of its components F_α and F_β along the axes direction α e β:

$$F_\alpha = \frac{\partial W_m}{\partial \alpha} \tag{3.8}$$

$$F_\beta = \frac{\partial W_m}{\partial \beta} \tag{3.9}$$

By executing the calculations is obtained:

$$\begin{bmatrix} F_\alpha \\ F_\beta \end{bmatrix} = M' I_p \begin{bmatrix} -cos\,2\omega t & sin\,2\omega t \\ sin\,2\omega t & cos\,2\omega t \end{bmatrix} \begin{bmatrix} i_\alpha \\ i_\beta \end{bmatrix} \tag{3.10}$$

It can be seen that the radial force is proportional to M' and to the equivalent current of the permanent magnets I_p; thus, if the factor $M' I_p$ has an high value, the levitation windings current can be reduced. In order to do this, I_p and the magnet thickness are increased but, consequently, the total gap between rotor and stator grows causing a decreasing of M'.

So, it results very important to choose the right compromise between the optimum thickness of the permanent magnets and the motor performances.

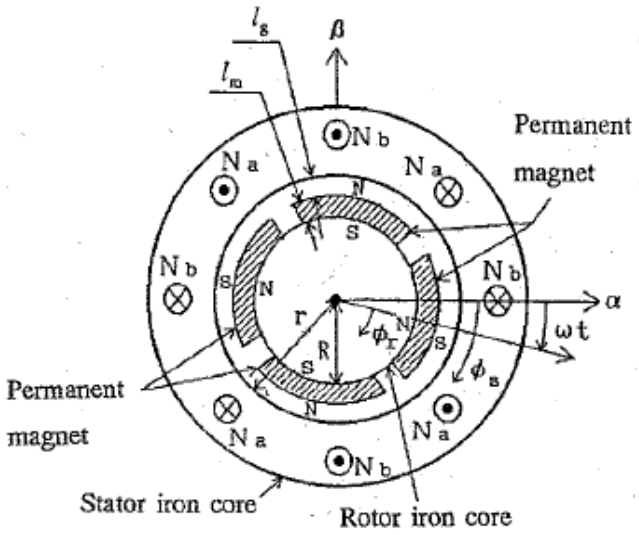

Fig. 3.5(a).

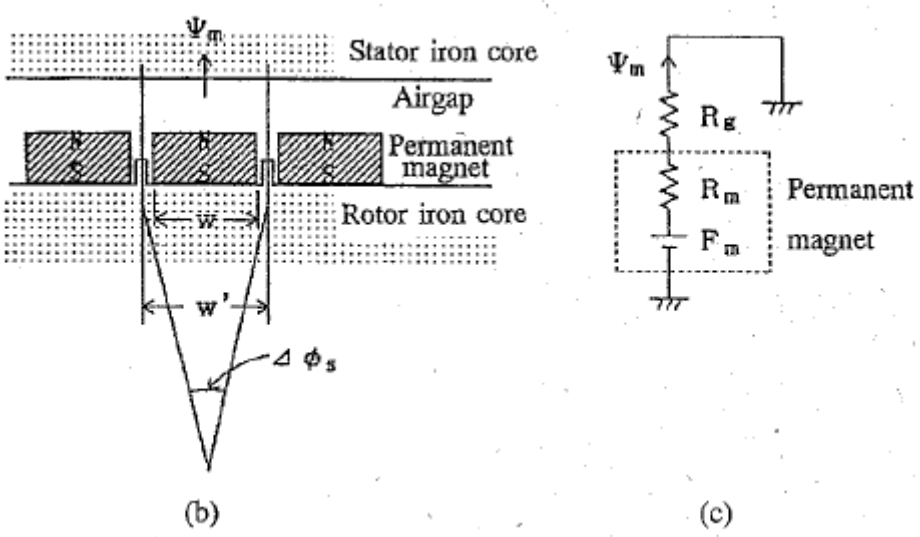

Fig. 3.5(b)-(c).

In order to do this, was defined a performance index which correlates the radial force-versus-current ratio to the flux density in the airgap. In Fig. 3.5 is shown the cross-section of the examined permanent magnet bearingless motor, being R the rotor radius, ϕ_s and ϕ_r the angular positions along the stator and rotor periphery with respect to the α axis, ωt the rotor angular displacement.

The rotor iron core is made from the laminated silicon steels with the small projections. Permanent magnets are mounted on the surface of the rotor core as shown in Fig. 3.5(b). w is the width of permanent magnets. w' is the width between the small projections. Then, an area S' between small projections and an area S of a permanent magnet can be represented as $w'l$ and wl, respectively. Fig. 3.5(c) shows a magnetic equivalent circuit of the permanent magnet having width w. The magneto-motive force F_m of permanent magnet is given as

$$F_m = \frac{l_m}{\mu_0} B_r \tag{3.11}$$

where B_r is the remanent flux density of the permanent magnet, μ_0 is the air

permeability, R_g and R_m, in Fig. 3.5(c) are the reluctances of mechanical airgap clearance and permanent magnet, respectively:

$$R_g = \frac{l_g}{\mu_0 S} \tag{3.12}$$

$$R_m = \frac{l_m}{\mu_0 S} \tag{3.13}$$

Neglecting magnetic saturation, slot ripples and permeance in the small projections, the flux linkage ψ_m, caused by permanent magnets can be written as

$$\psi_m = \frac{F_m}{R_g + R_m} = \frac{\frac{l_m}{\mu_0} B_r}{\frac{l_g}{\mu_0 S} + \frac{l_m}{\mu_0 S}} = \frac{S l_m}{l_m + l_g} B_r \tag{3.14}$$

Therefore, peak values of the flux density B,, in the airgap can be written as

$$B_{gp} = \frac{\psi_m}{S'} = \frac{l_m}{l_m + l_g} \frac{S}{S'} B_r \tag{3.15}$$

Let us define the terms l_{mn}, and l_{gn}, as l_m / r and l_g / r,respectively. These normalized lengths with respect to the stator inner radius can be used to derive the general expression of the peak air-gap flux density. Thus, B_{gp} can be rewritten as

$$B_{gp} = \frac{\frac{l_m}{r}}{\frac{l_m}{r} + \frac{l_g}{r}} \frac{S}{S'} B_r = \frac{l_{mn}}{l_{mn} + l_{gn}} \frac{S}{S'} B_r \tag{3.16}$$

Fig. 3.6 shows the relationships between l_{mn}, and B_{gp}, with parameters of l_{gn}. The term SB_r / S' in the vertical axis is a constant determined by the remanent

flux density of permanent magnets and the area density of mounted permanent magnet. In the case of Sm-Co magnets, B_r = 1 T. The ratio S/S' is equal to 1 if a cylindrical magnet is used, but it is slightly smaller than 1 if small permanent magnets are mounted on the surface of rotor iron core as shown in Fig. 3.5(b).

The decrease in l_{gn}, i.e. a reduction of the ratio of mechanical air-gap width l_g to radius r of stator inner surface, and the increase in l_{mn}, i.e. the ratio of permanent magnet thickness l_m to r results in an increase in airgap flux density. The desired value of the peak airgap flux density is generally determined at a rated rotational speed and heat dissipation.

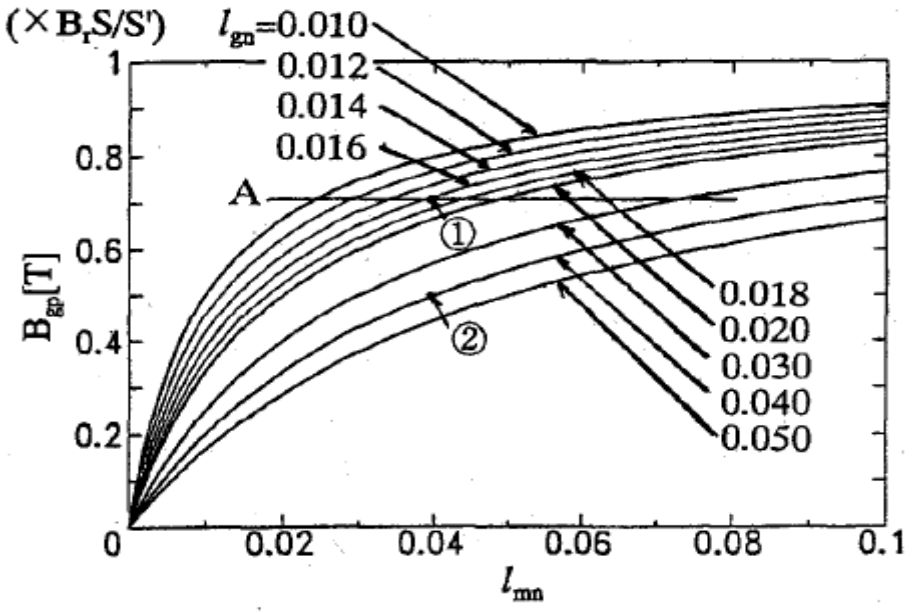

Fig. 3.6.

An important result achieved in [13], is given by analyzing the quantity radial force for unit current F_α / I_α as a function of the machine parameters:

$$\frac{F_\alpha}{I_\alpha} = \frac{n_2 l B_r S}{S'} \frac{\sqrt{2} l_{mn}\left(1 - l_{mn} - l_{gn}\right)}{\left(l_{mn} + l_{gn}\right)^2} \tag{3.17}$$

The first term of (3.17) depends on the number of turns of levitation windings,

the rotor stack length, the remanent flux density of permanent magnets, and the area density of mounted permanent magnet. Thus, is not possible to increase it without an increase in dimension or an improvement in materials. The second term is determined by ratios of permanent magnet thickness and mechanical airgap width to the radius of the stator inner surface. Radial force can be produced most efficiently when the second term has its maximum value. The question is if the airgap flux density value is to determine at rated motor speed and rated heat dissipation or for the optimal condition to produce radial forces. However, by differentiating (3.17) with respect to l_{mn}, it can be found that F_α / I_α is maximum when $l_{mn} = l_{gn}$, i.e. radial forces can be produced most efficiently when permanent magnet thickness is equal to mechanical airgap width (Fig. 3.7).

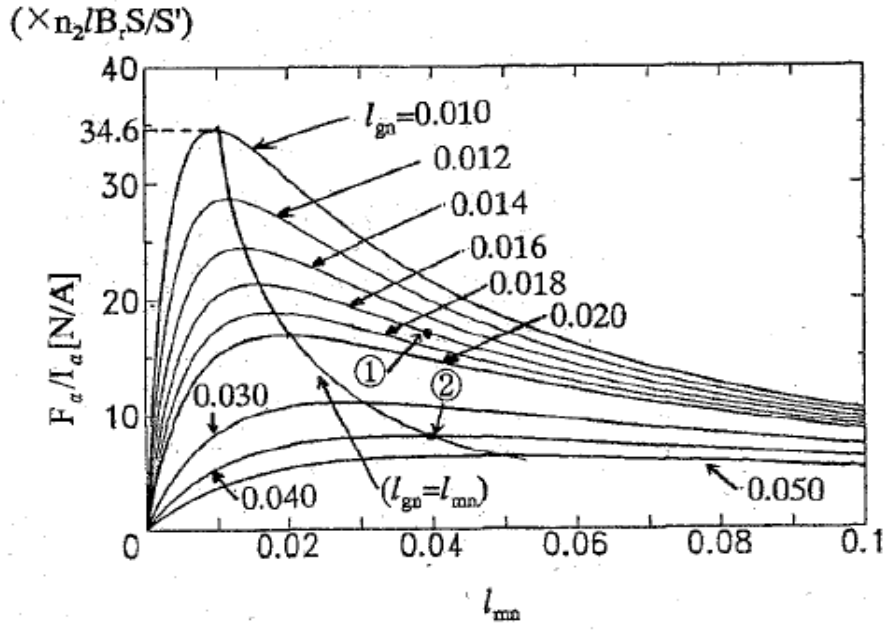

Fig. 3.7.

3.4 Bearingless Machines with a Single Set of Windings

It is known that a multiphase system of currents can be represented by using temporal sequences (if in sinusoidal alternating regime) or, more generally, by using space vectors of different orders (if in non-periodic regime).

By controlling separately and in an appropriate manner various orders of the current space vectors it is possible, for example, to generate and control the torque produced by the motor with a certain order and to produce and control the suspension radial forces with other orders.

The advantage of the single set of winding consists in the possibility of implementing both the above functions using a single winding, with a simpler construction process, without designing another one which subtracts a useful section of copper, with a reduction of power losses. In this type of machines is however necessary to provide asymmetric shortened pitch windings, in order to generate even harmonic orders in the magnetic fields that permit to create a radial forces distribution.

This typology of windings has the disadvantage of reducing the available torque, so the designer must then find a compromise between the intensity of the radial force and the motor performances.

In [11] is presented an interesting analysis of a bearingless permanent magnet motor with a single set of 5-phase windings, reported in the following. The two needed magnetic fields are produced by feeding two groups of currents which are projected into 2 orthogonal d-q planes respectively.

The radial force acting on the rotor can be obtained from Maxwell stress tensor:

$$\sigma = \frac{1}{2\mu_o}\left(b_n^2 - b_t^2\right) \tag{3.18}$$

where the contribution of b_t^2 can be neglected with respect to b_n^2. By supposing that there are two revolving magnetic fields in the airgap B_1 and B_2:

$$b_n = B_1 + B_2 \tag{3.19}$$

$$B_1 = B_{1m}\, cos(\omega_1 t - p_1\theta + \varphi_1) \tag{3.20}$$

$$B_2 = B_{2m}\, cos(\omega_2 t - p_2\theta + \varphi_2) \tag{3.21}$$

where p_1 and p_2 are their corresponding numbers of pole pair, ω_1 and ω_2 are their corresponding angular frequencies, and θ is an arbitrary angle in stator surface. The horizontal and vertical force components are given by:

$$F_\alpha = \int \sigma\, cos(\theta) lrd\theta \tag{3.22}$$

$$F_\beta = \int \sigma\, sin(\theta) lrd\theta \tag{3.23}$$

where l is the length of the stack, and r is the radius of airgap. By combining the equations (3.19)-(3.21), then substituting in (3.18) and integrating by means of (3.22), (3.23), the projections of the force on the horizontal α axis and vertical β axis are obtained.

$$F_\alpha = \begin{cases} \dfrac{lr\pi}{2\mu_0} B_{1m} B_{2m}\, cos(\omega_1 t - \omega_2 t + \varphi_1 - \varphi_2), & p_1 - p_2 = \pm 1 \\ 0, & p_1 - p_2 \neq \pm 1 \end{cases} \tag{3.24}$$

$$F_\beta = \begin{cases} \dfrac{lr\pi}{2\mu_0} B_{1m} B_{2m}\, sin(\omega_2 t - \omega_1 t + \varphi_2 - \varphi_1), & p_1 - p_2 = -1 \\ 0, & p_1 - p_2 \neq \pm 1 \\ \dfrac{lr\pi}{2\mu_0} B_{1m} B_{2m}\, sin(\omega_1 t - \omega_2 t + \varphi_1 - \varphi_2), & p_1 - p_2 = +1 \end{cases} \tag{3.25}$$

So, it result that a radial force can be obtained when $p_1 = p_2 \pm 1$, and the force is

stable when $\omega_1 = \omega_2$.

The Modified Winding Function Method is applied in order to analyze the magneto-motive force. In an *n*-phase symmetric system, the winding functions of each phase can be written as:

$$\begin{aligned}
N_a &= N_1 \cos\theta + N_2 \cos 2\theta + N_3 \cos 3\theta + .. \\
N_b &= N_1 \cos(\theta - \xi) + N_2 \cos(2(\theta - \xi)) + N_3 \cos(3(\theta - \xi)) + .. \\
N_c &= N_1 \cos(\theta - 2\xi) + N_2 \cos(2(\theta - 2\xi)) + N_3 \cos(3(\theta - 2\xi)) + .. \\
&\vdots \\
N_n &= N_1 \cos(\theta - (n-1)\xi) + N_2 \cos(2(\theta - (n-1)\xi)) + \\
&\quad + N_3 \cos(3(\theta - (n-1)\xi)) + ..
\end{aligned} \tag{3.26}$$

where $\xi = 2\pi/n$ and $N_1,\ N_2,\ N_3$ are coefficients of the winding function. The group of currents is defined as I_k:

$$\boldsymbol{I}_k = \begin{bmatrix} i_{ak} \\ i_{bk} \\ i_{ck} \\ \vdots \\ i_{nk} \end{bmatrix} = I_{km} \begin{bmatrix} \cos(\omega t + \phi_k) \\ \cos(\omega t + \phi_k - k\xi) \\ \cos(\omega t + \phi_k - 2k\xi) \\ \vdots \\ \cos(\omega t + \phi_k - (n-1)k\xi) \end{bmatrix} \tag{3.27}$$

where I_{km} is the amplitude of $\boldsymbol{I}_k$ and ϕ_k is the initial phase of i_{ak}. The MMF wave of an *n*-phase symmetric system fed by $\boldsymbol{I}_k$ can be expressed as

$$\begin{aligned}
F &= \sum_{i=1}^{n} \left\{ I_{km} \cos[\omega t + \phi_k - k(i-1)\xi] \sum_{v} N_v \cos v[\theta - (i-1)\xi] \right\} = \\
&= \frac{I_{km}}{2} \sum_{i=1}^{n} \sum_{v} N_v \{ \cos[\omega t + \phi_k + v\theta - (k+v)(i-1)\xi] + \\
&\qquad + \cos[\omega t + \phi_k - v\theta - (k-v)(i-1)\xi] \}
\end{aligned} \tag{3.28}$$

Thus, the v-th harmonic mmf wave results:

$$F_v = \begin{cases} \dfrac{nN_vI_{km}}{2}\cos(\omega t + \phi_k + v\theta) & ,k+v=\mu n \quad ,\mu = 0,\pm 1,... \\ 0 & ,k \pm v \neq \mu n \quad ,\mu = 0,\pm 1,... \\ \dfrac{nN_vI_{km}}{2}\cos(\omega t + \phi_k - v\theta) & ,k-v=\mu n \quad ,\mu = 0,\pm 1,... \end{cases} \tag{3.29}$$

From (3.29), the resultant MMF of 5-phase symmetrical windings can be shown in Tab. I. “F” and “B” indicate the harmonic orders of MMF rotating forward and backward respectively,“±” denotes a pulsating MMF.

TABLE I. SPACE HARMONICS OF A 5-PHASE MOTOR

v= / k=	Space harmonics of resultant MMF					
	1	2	3	4	5	6
$\boldsymbol{I}_1$	$\frac{5N_1I_{1m}}{2}$ (F)			$\frac{5N_4I_{1m}}{2}$ (B)		$\frac{5N_6I_{1m}}{2}$ (F)
$\boldsymbol{I}_2$		$\frac{5N_2I_{2m}}{2}$ (F)	$\frac{5N_3I_{2m}}{2}$ (B)			
$\boldsymbol{I}_3$		$\frac{5N_2I_{3m}}{2}$ (B)	$\frac{5N_3I_{3m}}{2}$ (F)			
$\boldsymbol{I}_4$	$\frac{5N_1I_{4m}}{2}$ (B)			$\frac{5N_4I_{4m}}{2}$ (F)		$\frac{5N_6I_{4m}}{2}$ (B)
$\boldsymbol{I}_5$					±	

In a 5-phase winding motor, $\boldsymbol{I}_1$ generates 1 pole-pair revolving magnetic field in the airgap, $\boldsymbol{I}_2$ generates 2 pole-pair revolving magnetic field when $N_2 \neq 0$.So the suspension force can be produced by the interaction of $\boldsymbol{I}_1$ and $\boldsymbol{I}_2$.

In the analyzed machine, the 5-phase windings are identical and each of them is 72° displaced in angular space around the stator. Fig. 3.8 shows the windings configuration and the slots where a phase goes in, in capital letter, where goes out, in lowercase letter. The phases are star-connected, as can be seen in the same Fig. 3.8.

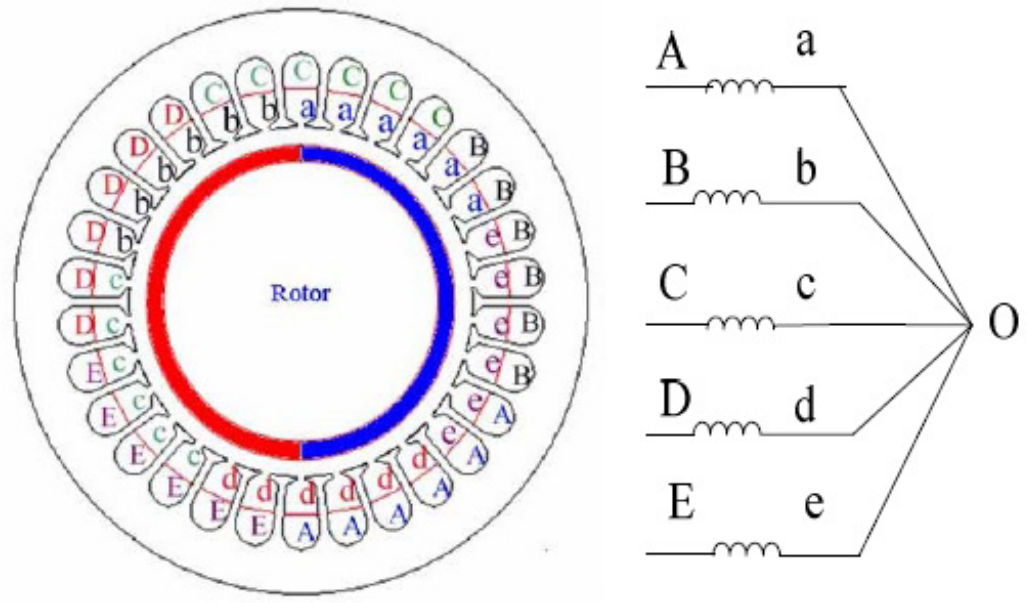

Fig. 3.8.

Voltage equations in stationary reference frame are given by

$$\boldsymbol{U}_s = \boldsymbol{R}_s \boldsymbol{I}_s + p\left(\boldsymbol{L}_s \boldsymbol{I}_s + \boldsymbol{\Psi}_r\right) \tag{3.30}$$

where $\boldsymbol{U}$, $\boldsymbol{I}$, $\boldsymbol{R}$, $\boldsymbol{L}$ and $\boldsymbol{\Psi}$ are matrices of voltage, current, resistance, inductance and flux linkage respectively, subscript *s* and *r* represent stator and rotor respectively, and *p* is the differential operator.

A transformation has to be applied to equation (3.30) in order to express the voltages and currents of stator to synchronous reference frame, given by a matrix $\boldsymbol{C}$ not reported here. The form of the voltage equations in the new reference frame results:

$$\boldsymbol{U}_{st} = \boldsymbol{R}_{st} \boldsymbol{I}_{st} + \boldsymbol{L}_{st} p \boldsymbol{I}_{st} + \boldsymbol{W}_s \boldsymbol{L}_{st} \boldsymbol{I}_{st} + \omega_1 \begin{bmatrix} \psi_{d1r} \\ -\psi_{q1r} \\ 0 \\ 0 \end{bmatrix} \tag{3.31}$$

where ψ_{q1r}, ψ_{d1r} are the q- and d-axis flux linkages of rotor respectively. The

radial force acting on rotor can be calculated with Virtual Displacement Method:

$$F_\alpha = \frac{1}{2}\begin{bmatrix} i_{q1s}+i_{q1r} \\ i_{d1s}+i_{d1r} \\ i_{q2s} \\ i_{d2s} \end{bmatrix}^T \frac{d\boldsymbol{L}_{st}}{d\alpha}\begin{bmatrix} i_{q1s}+i_{q1r} \\ i_{d1s}+i_{d1r} \\ i_{q2s} \\ i_{d2s} \end{bmatrix} \tag{3.32}$$

$$F_\beta = \frac{1}{2}\begin{bmatrix} i_{q1s}+i_{q1r} \\ i_{d1s}+i_{d1r} \\ i_{q2s} \\ i_{d2s} \end{bmatrix}^T \frac{d\boldsymbol{L}_{st}}{d\beta}\begin{bmatrix} i_{q1s}+i_{q1r} \\ i_{d1s}+i_{d1r} \\ i_{q2s} \\ i_{d2s} \end{bmatrix} \tag{3.33}$$

being $i_{d1r} = \psi_{d1r}/L_{1m}$, $i_{q1r} = \psi_{q1r}/L_{1m}$, equivalent rotor currents and L_{1m}, L_{2m} leakage winding inductances related to 1 pole pair and 2 pole pair fields. By developing (3.32), (3.33), the radial force can be seen as composed of two parts. One part is related to eccentricity:

$$F_\alpha = \frac{\alpha L_{1m}}{4{g_0}^2}\left[(i_{q1s}+i_{q1r})^2+(i_{d1s}+i_{d1r})^2\right]+\frac{\alpha L_{2m}}{2{g_0}^2}(i_{q2s}+i_{d2s})^2 \tag{3.34}$$

$$F_\beta = \frac{\beta L_{1m}}{4{g_0}^2}\left[(i_{q1s}+i_{q1r})^2+(i_{d1s}+i_{d1r})^2\right]+\frac{\beta L_{2m}}{2{g_0}^2}(i_{q2s}+i_{d2s})^2 \tag{3.35}$$

while the other results independent of eccentricity, used to control the rotor suspension:

$$F_\alpha = \frac{1}{2g_0\sqrt{L_{1m}L_{2m}}}(\psi_{d2m}\psi_{d1m}+\psi_{q2m}\psi_{q1m}) \tag{3.36}$$

$$F_\beta = \frac{1}{2g_0\sqrt{L_{1m}L_{2m}}}(\psi_{d2m}\psi_{d1m}-\psi_{q2m}\psi_{q1m}) \tag{3.37}$$

where g_0 is the equivalent radial length of a uniform air gap, α and β are the displacement of rotor center. The fluxes which appear in (3.36), (3.37) are

defined as:

$$\begin{aligned}\psi_{d1m} &= L_{1m} i_{d1s} + \psi_{d1r} \\ \psi_{q1m} &= L_{1m} i_{q1s} + \psi_{q1r}\end{aligned} \tag{3.38}$$

$$\begin{aligned}\psi_{d2m} &= L_{2m} i_{d2s} \\ \psi_{q2m} &= L_{2m} i_{q2s}\end{aligned} \tag{3.39}$$

The rotor displacements in stationary reference frame are given by:

$$\begin{bmatrix}\ddot{\alpha} \\ \ddot{\beta}\end{bmatrix} = \frac{1}{m}\begin{bmatrix}F_\alpha \\ F_\beta - G_r\end{bmatrix} \tag{3.40}$$

where m and G_r are the mass and weight of rotor respectively. The "motor currents" command i_{q1s}^* is generated from speed controller. Suspension force command F_α^*, F_β^* are generated by rotor displacement controller, after that,"levitation currents" commands i_{q2s}^* i_{d2s}^* are given by (3.41), (3.42), which are derived by (3.36), (3.37). Phase currents are given by the inverse transformation of i_{q1s}^* i_{d1s}^* and i_{q2s}^* i_{d2s}^*.

$$i_{q2s} = \frac{2g_0\sqrt{L_{1m}/L_{2m}}}{\psi_{q1m}^2 + \psi_{d1m}^2}\left(\psi_{q1m}F_\alpha + \psi_{d1m}F_\beta\right) \tag{3.41}$$

$$i_{d2s} = \frac{2g_0\sqrt{L_{1m}/L_{2m}}}{\psi_{q1m}^2 + \psi_{d1m}^2}\left(\psi_{d1m}F_\alpha - \psi_{q1m}F_\beta\right) \tag{3.42}$$

In the following, the main data of the proposed motor: L_{1m} = 36 mH, L_{2m} = 6.3 mH, L_{0s1} = 1.3 mH, L_{0s2} = 1 mH, r_s = 1.1 Ω, ψ_f =1.05 Wb, J=0.012 kgm^2, airgap thickness: 2 mm , magnet thickness 3mm , g_0 = 5mm. The airgap length between the rotor shaft and the touchdown bearing is 0.6 mm. In Fig. 3.9 is shown the control diagram of the 5-phase PM bearingless motor.

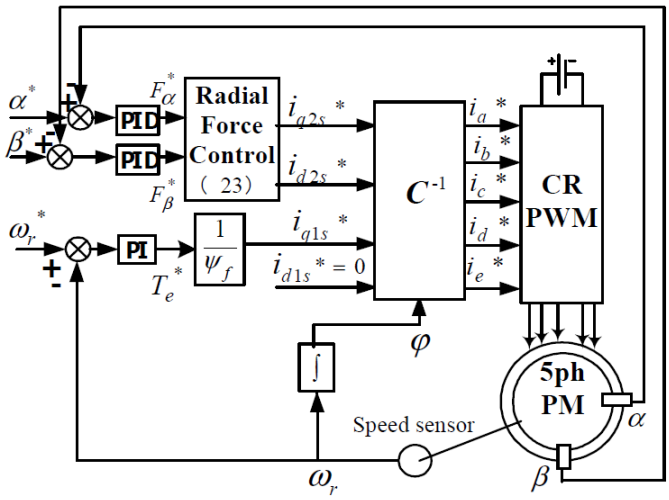

Fig. 3.9.

Fig. 3.10 shows angular speed, torque and rotor displacement during the start up operation. The shaft results successfully suspended and the dynamic of rotor suspension is stable with radial displacement variations less than 50 μm . It is also obvious that the system has good speed-regulation performance.

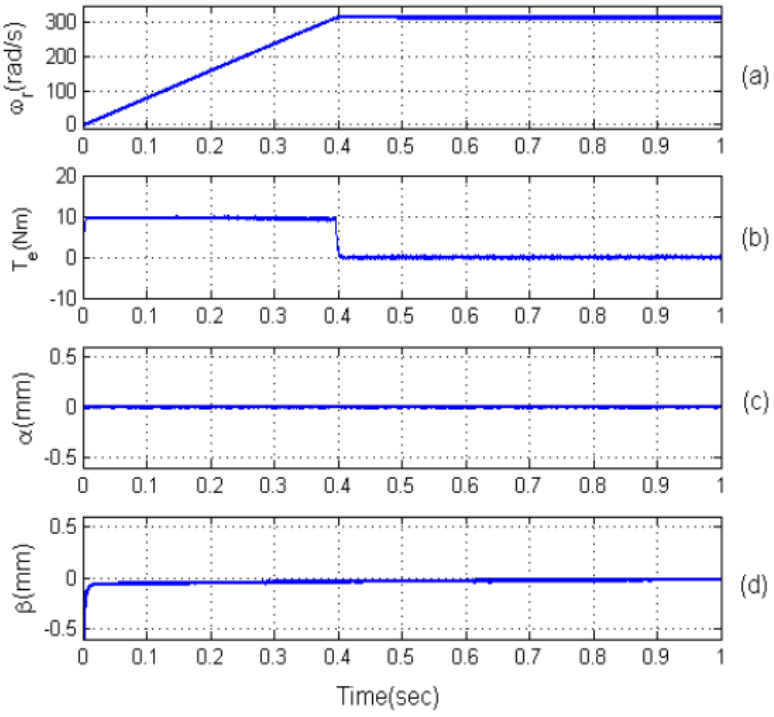

Fig. 3.10.

3.5 Rotor eccentricity

In bearingless machines, due to the fact that the rotor is not sustained by mechanical bearings, a rotor eccentricity is determined while the motor is operating and has to be compensated by the control system. This phenomenon leads to a variation in the values of the airgap flux density, as these resulting decrease in the areas where the airgap widens, and increase in the areas where the airgap is reduced, causing a similar behavior in the radial force distribution.

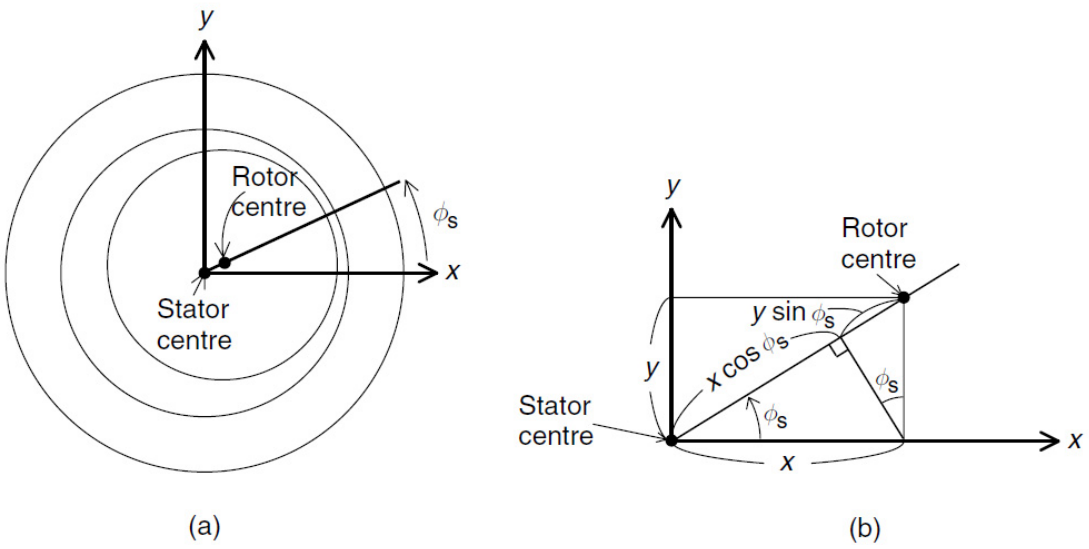

Fig. 3.11

In Fig. 3.11 is shown the reference system in which a simplified calculation [12] permits to take into account the eccentricity by writing the airgap width g as a function of the angle ϕ_s, that the line joining the effective rotor centre with the origin, describes with the x-axis:

$$g(\phi_s) = g_0 - x\cos\phi_s - y\sin\phi_s \tag{3.43}$$

being x and y the actual coordinates of the rotor centre. With the assumption of small displacements compared to the nominal airgap length g_0, is possible to

write:

$$\frac{1}{g(\phi_s)} = \frac{1}{g_0}\left(1 + \frac{x}{g_0}cos\,\phi_s + \frac{y}{g_0}sin\,\phi_s\right) \tag{3.44}$$

and, consequently, to calculate the permeance P_0 in the generic angular position ϕ_s:

$$P_0(\phi_s) = \frac{\mu_0 Rl}{g_0}\left(1 + \frac{x}{g_0}cos\,\phi_s + \frac{y}{g_0}sin\,\phi_s\right) \tag{3.45}$$

being R the rotor radius and l the axial length. By using properly (3.45) in the equations of the machine, is possible to take into account the force variation with respect to rotor position. Two typologies of eccentricity can be defined in bearingless machines:

- **Static eccentricity**: it occurs when the rotor is not centred in the stator bore;
- **Dynamic eccentricity**: it occurs when the rotor is not rotating on the rotor axis but is rotating on the centre axis.

Various authors developed models able to interpret and calculate the effects of eccentricity on the radial forces and on the rotor position. In [14] is presented, by using the nonlinear FEM and a theoretical analysis, an analytical model for calculating the levitation force under airgap eccentricity by means of the interaction between harmonic field components and a simplified modeling for levitation force control in bearingless induction machines; [15] describes a method for modeling a bearingless IPM motor, for calculating the forces on the rotor by using complex winding analysis and rotating field theory and comparing the results to FEA analysis; the model allows the introduction of levitation and main windings and rotor eccentricity. In [16] an analytical expression of the levitation force for an induction-type bearingless motor is proposed, taking into

account the rotor eccentricity, being its computation accuracy verified by ANSOFT. A real-time observation of magnetic levitation force can be realized, is then implemented a closed-loop control of levitation force on the basis of airgap-flux-oriented decoupling control system of the bearingless motor.

A very interesting work about the analysis of static and dynamic eccentricity is presented in [17], which refers to an analytical modeling technique for calculating the radial force on the rotor of a bearingless consequent-pole permanent magnet motor. The flexibility of the method permits to identify vibration components and calculate the force in various situations when the rotor is not centred in the bore, in case of either dynamic eccentricity, static eccentricity or when the rotor is vibrating. It also allows a calculations of the force in presence of a varying load or with load imbalance. The paper also studies the effects of winding design and gives a validation of the results using 2D finite element analysis.

Another particular work which could be applied also to the force calculation in bearingless machines is [18], where a general analytical model, formulated in 2-D polar coordinates, is developed to predict the unbalanced magnetic force, which results in permanent-magnet brushless ac and dc machines having a diametrically asymmetric disposition of slots and phase windings. The unbalanced magnetic force can be significant in machines having a fractional ratio of slot number to pole number, particularly when the electric loading is high. The developed model is validated by FE calculations on 9-slot/8-pole and 3-slot/2-pole machines. Finally, [19] proposes a novel approach to control the rotor radial displacement in bearingless permanent-magnet-type synchronous motors, based on the relationship between radial displacement and radial suspension force. The rotor flux orientation is adopted to decouple the electromagnetic torque and the radial suspension force. This approach, which directly controls the rotor radial displacement, was applied by designing a

suitable control system.

3.6 Conclusion

The main features and issues of bearingless machines were presented in this chapter, highlighting the potential of the multiphase single set of windings type, which surely represents the most effective design methodology to adopt in the future. In fact, it permits valid control strategies for suspending the rotor, for controlling the motor and, at the same time, for generating torque by using the properties of multiphase current systems, without the need of altering the physical structure of the machine by designing other groups of windings in addition to the main one.

Thus, the focus of the activity in the next chapters will be on the analysis of this typology of bearingless machines.

3.7 References

[1] A. Chiba, T. Deido, T. Fukao, M.A. Rahman, "An Analysis of Bearingless AC Motors," *IEEE Trans. Energy Conversion*, vol. 9, no. 1, Mar. 1994, pp. 61-68.

[2] T. Schneider and A. Binder, "Design and evaluation of a 60000 RPM permanent magnet bearingless high speed motor," *Proc. Conf. on Power Electronics and Drive Systems,* Bangkok, Thailand, Nov. 27–30, 2007, pp. 1-8.

[3] M. Oshima. S. Mivazawa. T. Deido, A. Chiba. F. Nakamura, and T. Fukao, "Characteristics of a permanent magnet type bearingless motor," *in IEEE IAS Annu. Meet.,* 1994, pp. 196-202.

[4] K. Dejima, T. Ohishi, and Y. Okada, "Analysis and control of a permanent magnet type levitated rotating motor," in *ZEEJ Proc. Symp. Dynamics of Electro Magn. Force,* June 1992, pp. 251-256.

[5] M. A. Rahman, T. Fukao, and A. Chiba, "Principles and development of bearingless AC motors," in *Proc. IPEC-95,* Yokohama, 1995, pp. 1334-1339.

[6] Y. Okada, S. Miyamoto and T. Ohishi, "Levitation and-torque control of internal permanent magnet type hearingless motor," *IEEE Transactions on Control Systems Technology*, Vol. 4, NOS, 1996, pp. 565-571.

[7] A. Chiba, K. Chida, and T. Fukao, "Principles and characteristics of a reluctance motor with windings of magnetic bearing," in *Proc. IPEC-Tokyo,*1990, pp. 919-926.

[8] A. Chiba, D. T. Power, and M. A. Rahman, "No load characteristics of a bearingless induction motor," in *IEEE IAS Annu. Meet.,* 1991, pp. 126-132.

[9] W.-R. Canders, D. Hulsmann, "Analysis and classification of bearingless machines with symmetric 3-phase concentrated windings" *XIX International Conference on Electrical Machines (ICEM), 2010*, pp 1–6.

[10] M. Kang, J. Huang, J.-q. Yang and H.-b. Jiang "Analysis and Experiment of a 6-phase Bearingless Induction Motor," *Int. Conf. on Electrical Machines and Systems ICEMS 2008,* Oct. 2008, pp. 990–994.

[11] M. Kang, J. Huang, H.-b. Jiang, J.-q. Yang, "Principle and simulation of a 5-phase bearingless permanent magnet-type synchronous motor" *International Conference on Electrical Machines and Systems (ICEM) 2008*., 2008 , Page(s): 1148–1152.

[12] A. Chiba, T. Fukao, O. Ichikawa, M. Oshima, M. Takemoto and D. G. Dorrell "Magnetic Bearings and Bearingless Drives", Elsevier, Mar. 2005.

[13] M. Ooshima, A. Chiba, T. Fukao, M.A. Rahman, "Design and Analysis of Permanent Magnet-Type Bearingless Motors," *IEEE Trans. On Industrial Electronics*, vol. 43, no. 2, Apr. 1996, pp. 292-299.

[14] W. Baoguo, W. Fengxiang, "Modeling and Analysis of Levitation Force Considering Air-gap Eccentricity in a Bearingless Induction Motor," *Proc. of the fifth International Conference on Electrical Machine and Systems*, 2001, pp. 934-937.

[15] D. G. Dorrell, M. Oshima, A. Chiba, "Force Analysis of a Buried Permanent Magnet Bearingless Motor" *IEEE IEMDC, Proc.*, June 1-4 2003, Madison Wisconsin USA, pp. 1091-1097.

[16] H. Yikang and N. Heng, "Analytical model and feedback control of the levitation force for an induction type bearingless motor," in *IEEE Proc. PEDS*, Nov. 2003, vol. 1, pp. 242–246.

[17] D. G. Dorrell, J. Amemiya, A. Chiba, and T. Takenaga, "Analytical Modeling of a Consequent-Pole Bearingless Permanent Magnet Motor," in *Proc. IEEE Power Electronics and Electric Drives Conf.*, Singapore, Nov. 1–5, 2003, pp. 247-252.

[18] Z. Q. Zhu, D. Ishak, D. Howe, and J. Chen, "Unbalanced magnetic forces in permanent-magnet brushless machines with diametrically asymmetric phase windings," *IEEE Trans. Magn.*, vol. 43, no. 6, Nov./Dec. 2007, pp. 1544-1553.

[19] Shaoru Zhang and Fang Lin Luo, "Direct Control of Radial Displacement for Bearingless Permanent-Magnet-Type Synchronous Motors," *IEEE Transactions on Industrial Electronics*, vol. 56, no. 2, Feb. 2009, pp. 542-552.

Chapter 4

AN ANALYTICAL METHOD FOR CALCULATING THE DISTRIBUTION OF FORCES IN A BEARINGLESS MULTIPHASE SURFACE-MOUNTED PM SYNCHRONOUS MACHINE

4.1 Introduction

Bearingless motors have the capability to achieve much higher maximum speed in comparison to conventional electrical machines [1],[2]. The typology "dual set windings", has a main one which carries the 'torque currents' for driving the rotor and producing torque, while the other carries the 'levitation

currents', to suspend the rotor [3],[4]. Its advantages consist of a simpler construction process, higher flexibility in control strategy and relatively low power losses [5].

The typology "single set windings" produces torque and radial forces by means of injecting different current space vectors within the same winding to give odd and even harmonic orders of magnetic field, using the properties of multiphase current systems with multiple orthogonal d-q planes. One of them can be used to control the torque, as in [6]. The additional degrees of freedom can be used to produce levitation forces [7],[8].

An important development of this technology is expected to be in the design of electromechanical devices for More Electric Aircraft (MEA), mainly for the possibility of achieving higher speed in comparison to conventional electrical machines [9]. Also, it would be applicable in the aerospace field, where the lubricants of mechanical bearings evaporate in the presence of vacuum [10].

The multiphase motors with respect to conventional three-phase motors gives a series of advantages [11], in particular in the cases of high power, high reliability, low dc bus voltage and reduction of power losses in IGBT inverters [12] as it happens in ship propulsion, electrical vehicles and MEA applications.

In the control system of multiphase bearingless motors is necessary to calculate the levitation current able to compensate the actual error in the rotor shaft position, thus the analytical function which correlates the applied currents to the resulting suspension force on the rotor. In order to do this and to simplify the problem, some authors consider only the interactions between the main harmonic orders of the stator and rotor magnetic fields, in the particular case of steady-state AC conditions, with sinusoidal systems of currents, as done in [7]; nevertheless, by proceeding in this way, a relevant error in the prediction of the force vector can be committed, because the interactions between higher harmonic orders of the magnetic fields acting on the rotor and the effect of the torque

current on the radial force are neglected.

The aim of this chapter is to present a model allowing to predict amplitude and direction of the force for given values of the torque current, of the levitation current and of the rotor position [13], based on the space vectors method, being able to include in this way also the analysis of transients.

For this purpose, a generalized analytical model for the calculation of radial forces in multiphase bearingless Surface-Mounted Permanent Magnet Synchronous Motors (SPMSM) is presented. The stator magnetic field is represented as the sum of separated contributions given by the different current space vectors. In this way it is possible to analyze the interactions between the torque current system, the levitation current system and the rotor magnetic field. In fact, in multiphase machines the combined effect of two stator current space vectors leads to a resulting levitation force which is sensibly different from that, foreseeable, produced by the currents in the separated windings of traditional bearingless machines. In Tab. I are shown all the possible interactions between the harmonic orders of the magnetic fields The results are compared with those of FE analysis to demonstrate their accuracy.

4.2 Definition of variables

In the following, is presented a list of the variables used in the equations and relationships of this chapter:

θ_s Angular abscissa in the stator reference system
p_s Number of stator pole pairs
p_r Number of rotor pole pairs
$k_{1(2)}$ Spatial harmonic order of the space vector 1 (2) stator field distribution
h Spatial harmonic order of the rotor field distribution
$\varphi_{1(2)}$ Phase of the current space vector 1 (2)
n Half of the number of conductors in a slot
δ Total airgap height
g Airgap height
L_m Magnet height
q Number of slots per pole per phase
$k_{dk1(2)}$ k-th harmonic component of the winding distribution factor related to the space vector 1 (2)
γ Half of the coil pitch angle
$s_{v1(2)}$ Order of the space vector 1 (2)
$\Delta\theta$ Angular displacement between phase-1 axis and magnet axis
B_{rem} Remanent flux density of the magnets
K_c Karter factor
μ_0 Magnetic permeability of the air
μ_{mr} Relative magnetic permeability of the magnets
α_m Angle underlying the magnet pitch
$i_{sv1(2)}$ Amplitude of the current space vector 1 (2)
r Mean airgap radius
L Axial length of the machine
$B_{Sk1(2)}$ peak value of the k-th harmonic order of flux density distribution produced by current space vector 1 (2)
B_{Rh} peak value of the h-th harmonic order of flux density distribution produced by rotor magnets
n_{ac} Number of slots forming the coil pitch
N_0 Set of natural numbers including zero
N_{odd} Set of odd natural numbers

4.3 Analysis of flux density distribution in the airgap

Considering 5 real variables $x_1,..,\ x_l,..,\ x_5$, an associated set of complex variables $\bar{x}_0, \bar{x}_1, \bar{x}_2$ can be obtained by means of the following symmetrical linear transformations:

$$\bar{x}_\rho = \frac{2}{5}\sum_{l=1}^{5} x_l \bar{\alpha}^{\rho(l-1)}, \qquad (\rho = 0,1,2) \qquad (4.1)$$

where $\bar{\alpha} = exp(j2\pi/5)$. The inverse transformations of (4.1) are as follows:

$$x_l = \frac{1}{2}x_0 + \sum_{\rho=1,2} \bar{x}_\rho \cdot \bar{\alpha}^{\rho(l-1)}, \qquad (l = 1,2,..,5) \qquad (4.2)$$

where the symbol " · " represents the scalar product, defined as the real part of the product between the first operand and the complex conjugate of the second.

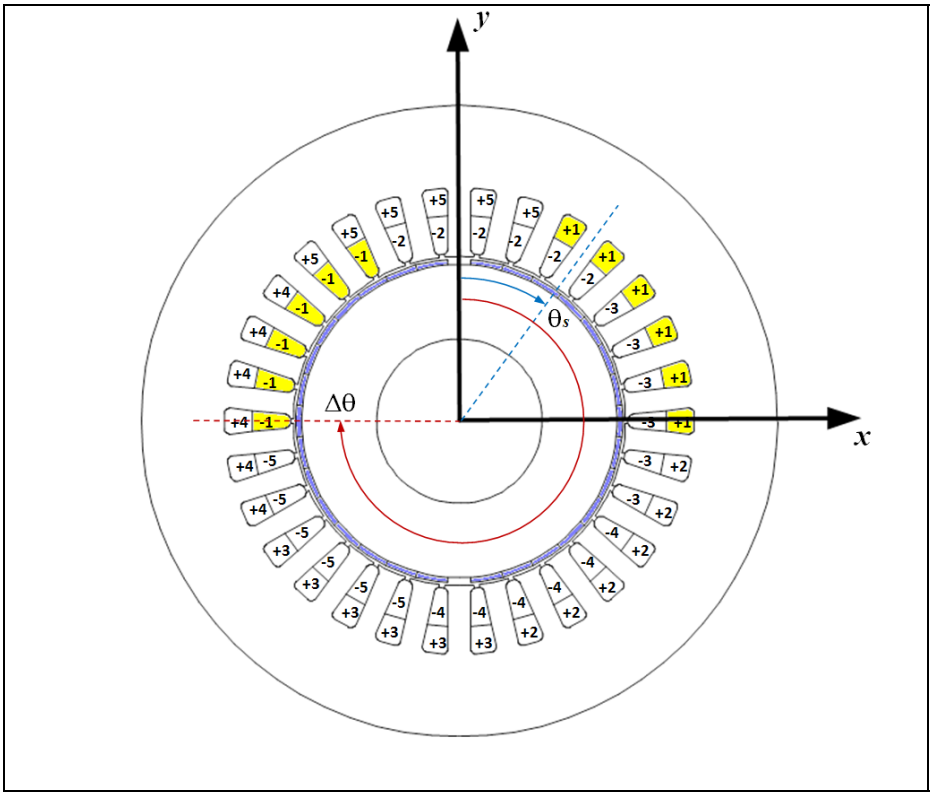

Fig. 4.1

The considered reference system is a cartesian one, whose axes *x*- (horizontal) and *y*- (vertical) have the origin in the motor shaft center, the *y*-axis coinciding with phase "1" axis (Fig. 4.1). The assumptions taken into account are: infinite iron permeability, current distribution concentrated at the slot opening, almost unitary relative permeability of the magnets.

The method will be applied to SPMSM machine with 5 star-connected stator phase windings, symmetrically distributed within the stator slots: the windings are supposed to be shifted by 2π/5 electrical radians, with a single neutral point. According to (4.1) and (4.2), it is possible in this case to represent the currents system using 2 space vectors in different α - β planes, being the zero-sequence component null because of the star-connection of the phases:

$$\bar{i}_{sv1} = i_{sv1}(t)e^{j\varphi_1(t)}, \quad \bar{i}_{sv2} = i_{sv2}(t)e^{j\varphi_2(t)} \tag{4.3}$$

By applying (4.3) to (4.2) and by explicating some variables, the *l*-th phase current can be written as:

$$i_l = \sum_{\rho=1,2} \bar{i}_{sv\rho} \cdot \bar{\alpha}^{\rho(l-1)} = \bar{i}_{sv1} \cdot e^{j\frac{2\pi}{5}(l-1)} + \bar{i}_{sv2} \cdot e^{j\frac{4\pi}{5}(l-1)}, \quad (l = 1,2,..,5) \tag{4.4}$$

By developing (4.4), it gives:

$$i_l(t) = i_{sv1}\, cos\left[\varphi_1(t) - (l-1)\frac{2\pi}{5}\right] + i_{sv2}\, cos\left[\varphi_2(t) - (l-1)\frac{4\pi}{5}\right], \quad (l = 1,2,..,5) \tag{4.5}$$

When the *sv*-th space vector current is flowing in the coils, the *l*-th phase of the motor produces a magnetic field distribution whose the radial component is given by (4.6):

$$H_l(\theta_s, t) = \sum_{k=1,2,3..}^{\infty} H_{Mk}\, cos\left[kp_s\theta_s - k(l-1)\frac{2\pi}{5}\right] cos\left[\varphi(t) - s_v(l-1)\frac{2\pi}{5}\right] \tag{4.6}$$

with H_{Mk} defined as follows:

$$H_{Mk} = \frac{4}{k\pi}\frac{ni_{sv}}{2\delta} qk_{dk}\, sin(k\gamma) \tag{4.7}$$

Note that the expanded Fourier harmonic series (4.6) contains odd and even orders, differently from the representations of the magnetic field distributions in the usual electrical machines, because of the particular location of the coils in the stator slots; (4.6) is also a function of the angular abscissa θ_s whose origin coincides with the *y*-axis, as shown in Fig. 4.1.

By combining the relationship (4.6) considering all the phase currents, the *k*-th harmonic order H_{sk} of the 5-phase stator magnetic field, related to the current space vector s_v, can be expressed as:

$$H_{sk}(\theta_s, t) = \begin{cases} \frac{5}{2} H_{Mk}\, cos[kp_s\theta_s \mp \varphi(t)] & \text{if } \frac{k \mp s_v}{5} \in N_0 \\ 0 & \text{if } \frac{k \mp s_v}{5} \notin N_0 \end{cases} \tag{4.8}$$

The total stator magnetic field is the summation of all the existing terms given by (4.8), depending on the value of *k*. The rotor magnetic field generated by the magnets can be written as:

$$H_r(\theta_s, t) = \sum_{h=1,3,5..}^{\infty} H_{Rh}\, cos[hp_r\theta_s - hp_r\Delta\theta] \tag{4.9}$$

where H_{Rh}, B_{RM} are defined as follows:

$$H_{Rh} = \frac{4}{h\pi}\frac{B_{RM}}{\mu_0} sin\left(h\frac{\alpha_m}{2}\right), \qquad B_{RM} = \frac{L_m}{L_m + \mu_{mr}K_c g} B_{rem} \tag{4.10}$$

Two different current space vectors, one for torque production and the other for levitation (4.5), are injected: respectively s_{v1} and s_{v2}, so that the resulting radial component of flux density in the airgap can be written by means of the principle

of superposition:

$$B_n(\theta_s,t)=\sum_{k_1,k_2,h}\left[B_{sk1}(\theta_s,t)+B_{sk2}(\theta_s,t)+B_{rh}(\theta_s,t)\right]=\sum_{k_1}B_{Sk1}\cos\left[k_1 p_s\theta_s\mp\varphi_1(t)\right]+$$
$$+\sum_{k_2}B_{Sk2}\cos\left[k_2 p_s\theta_s\mp\varphi_2(t)\right]+\sum_{h}B_{Rh}\cos\left[hp_r\theta_s-hp_r\Delta\theta\right] \tag{4.11}$$

where the values of k_1 and k_2 follow the conditions explained in (4.8), and the amplitudes of the three distributions are defined as follows:

$$B_{Sk1}=\mu_0\frac{5}{2}H_{Mk1}=\mu_0\frac{5}{2}\frac{4}{k_1\pi}\frac{ni_{sv1}}{2\delta}qk_{dk1}\sin(k_1\gamma) \tag{4.12}$$

$$B_{Sk2}=\mu_0\frac{5}{2}H_{Mk2}=\mu_0\frac{5}{2}\frac{4}{k_2\pi}\frac{ni_{sv2}}{2\delta}qk_{dk2}\sin(k_2\gamma) \tag{4.13}$$

$$B_{Rh}=\frac{4}{h\pi}B_{RM}\sin\left(h\frac{\alpha_m}{2}\right) \tag{4.14}$$

4.4 Calculation of the force acting on the rotor

The resulting force acting on the rotor can be determined by applying the Maxwell Stress Tensor method on a closed surface enveloping the frontal cross sections of the teeth in the stator:

$$\overline{T} = \frac{1}{2}\left(H_n B_n - H_t B_t\right)\hat{n} + H_t B_n \hat{t} \cong \frac{B_n^2}{2\mu_0}\hat{n} + \frac{B_t B_n}{\mu_0}\hat{t} \tag{4.15}$$

Taking the normal and tangential components of flux density and of magnetic field into account and neglecting the term related to the product of tangential components, the expression of the elementary force $d\overline{F}$, acting at the angular abscissa θ_s on the elementary surface $dS = Lrd\theta_s$, results:

$$d\overline{F}\left(\theta_s,t\right) = \overline{T}\left(\theta_s,t\right)dS = \frac{B_n^2\left(\theta_s,t\right)}{2\mu_0}dS\hat{n} + \frac{B_t\left(\theta_s,t\right)B_n\left(\theta_s,t\right)}{\mu_0}dS\hat{t} \tag{4.16}$$

By substituting the expression of dS in (4.16), it gives:

$$d\overline{F}\left(\theta_s,t\right) = \underbrace{\frac{LrB_n^2}{2\mu_0}d\theta_s}_{dF_n}\hat{n} + \underbrace{\frac{LrB_tB_n}{\mu_0}d\theta_s}_{dF_t}\hat{t} \tag{4.17}$$

where can be recognized the elementary normal component dF_n and the tangential component dF_t.

4.4.1 Normal Components of the Force

With the previous assumptions the resulting force acting on the rotor can be expressed as:

$$F_{xn} = \int_0^{2\pi} dF_n \sin\theta_s = \frac{Lr}{2\mu_0}\int_0^{2\pi} B_n^2\left(\theta_s,t\right)\sin\theta_s d\theta_s \tag{4.18}$$

$$F_{yn} = \int_0^{2\pi} dF_n \cos\theta_s = \frac{Lr}{2\mu_0} \int_0^{2\pi} B_n^2(\theta_s, t) \cos\theta_s d\theta_s \tag{4.19}$$

Remember that the reference axis for the angle θ_s is the *y*-axis. Considering the integer values of k_1, k_2 and h that makes non-zero the related harmonic components of the flux densities in (4.11), we obtain six terms representing the square of B_n:

$$B_n^2(\theta_s, t) = B_{sk1}^2 + B_{sk2}^2 + B_{rh}^2 + 2B_{sk1}B_{sk2} + 2B_{sk1}B_{rh} + 2B_{sk2}B_{rh} \tag{4.20}$$

When integrating all the terms in (4.20), taking (4.18)-(4.19) into account, it is important to consider that the components of forces have to be added in summation only for the existing harmonic orders of k_1, k_2 (k_2'), which are related to the stator magnetic fields respectively given by the current space vectors s_{v1} and s_{v2}, and the existing harmonic orders of h, which are related to the rotor magnetic field. This fact is expressed by means of the pre-conditions (4.21)-(4.23):

$$\frac{k_1 \mp s_{v1}}{5} \in N_0 \tag{4.21}$$

$$\frac{k_2 \mp s_{v2}}{5} \in N_0, \quad \frac{k_2' \mp s_{v2}}{5} \in N_0 \tag{4.22}$$

$$h \in N_{odd} \tag{4.23}$$

In (4.22) it is highlighted the interaction between different harmonic orders of the same current space vector s_{v2}: in fact, as will be clear later, some components of the force depend on this phenomenon.

In Tab. I are presented all the possible interactions, in this case until the 18-th order for reasons of brevity, determined by using the equations (4.21), (4.22), (4.23). By performing the calculations (4.19) and considering term by term of (4.20):

TABLE I. INTERACTIONS BETWEEN HARMONIC ORDERS

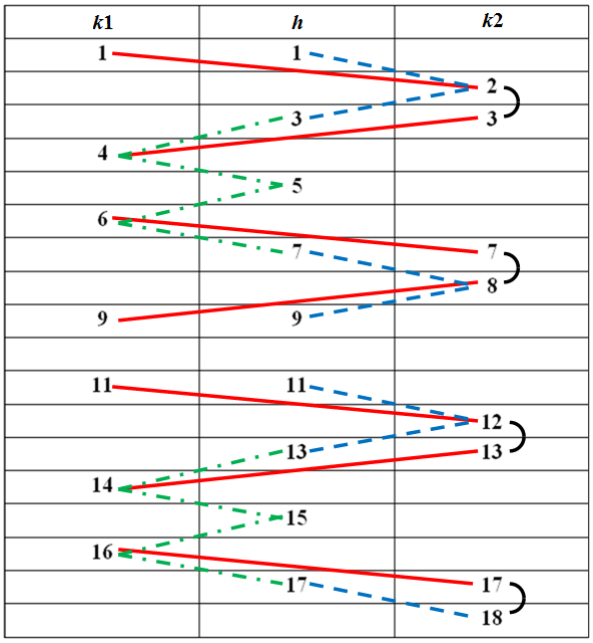

$$F_{yn}^{(a)} = \frac{Lr}{2\mu_0}\int_0^{2\pi} B_{sk}^2(\theta_s,t)\cos\theta_s d\theta_s = \frac{Lr}{2\mu_0}\int_0^{2\pi} B_{Sk}^2\cos^2\left[kp_s\theta_s \mp \varphi(t)\right]\cos\theta_s d\theta_s \tag{4.24}$$

By considering that:

$$\cos^2(\alpha) = \frac{1+\cos(2\alpha)}{2} \tag{4.25}$$

Applying (4.25) to (4.24), it gives:

$$F_{yn}^{(a)} = \frac{LrB_{Sk}^2}{4\mu_0}\int_0^{2\pi}\cos\theta_s d\theta_s + \frac{LrB_{Sk}^2}{4\mu_0}\int_0^{2\pi}\cos\left[2kp_s\theta_s \mp 2\varphi(t)\right]\cos\theta_s d\theta_s \tag{4.26}$$

By considering that:

$$\cos(\alpha)\cos(\beta) = \frac{\cos(\alpha+\beta)+\cos(\alpha-\beta)}{2} \tag{4.27}$$

Applying (4.27) to (4.26), it gives:

$$F_{yn}^{(a)} = \frac{LrB_{Sk}^2}{8\mu_0}\int_0^{2\pi} cos\left[(2kp_s+1)\theta_s \mp 2\varphi(t)\right]d\theta_s + \frac{LrB_{Sk}^2}{8\mu_0}\int_0^{2\pi} cos\left[(2kp_s-1)\theta_s \mp 2\varphi(t)\right]d\theta_s \tag{4.28}$$

$$F_{yn}^{(a)} = \frac{LrB_{Sk}^2}{8\mu_0}\left\{\frac{1}{2kp_s+1}\left[sin\left[(2kp_s+1)\theta_s \mp 2\varphi\right]\right]_0^{2\pi} + \right. \\ \left. + \frac{1}{2kp_s-1}\left[sin\left[(2kp_s-1)\theta_s \mp 2\varphi\right]\right]_0^{2\pi}\right\} \tag{4.29}$$

$$F_{yn}^{(a)} = \frac{LrB_{Sk}^2}{8\mu_0}\left\{\frac{1}{2kp_s+1}\left[sin\left[2\pi(2kp_s+1)\mp 2\varphi\right] - sin\left[\mp 2\varphi\right]\right] + \right. \\ \left. + \frac{1}{2kp_s-1}\left[sin\left[2\pi(2kp_s-1)\mp 2\varphi\right] - sin\left[\mp 2\varphi\right]\right]\right\} = 0 \tag{4.30}$$

Note that, being both $2kp_s+1$ and $2kp_s-1$ integer numbers, the angular arguments in (4.30) differ by integer multiples of 2π, thus the sinusoidal functions assume the same value and their difference is equal to zero.

Hence, the contribution of the terms in the form (4.24) to the *y*-component of the force is zero:

$$F_{yn}^{(a)} = \frac{Lr}{2\mu_0}\int_0^{2\pi} B_{sk1}^2(\theta_s,t)cos\,\theta_s d\theta_s = \frac{Lr}{2\mu_0}\int_0^{2\pi} B_{Sk1}^2\, cos^2\left[k_1 p_s\theta_s \mp \varphi_1\right]cos\,\theta_s d\theta_s = 0 \tag{4.31}$$

For the same reason, the similar quadratic term related to the space vector s_{v2} and the one related to the rotor magnetic field give a null result (4.32), (4.33):

$$F_{yn}^{(b)} = \frac{Lr}{2\mu_0}\int_0^{2\pi} B_{sk2}^2(\theta_s,t)cos\,\theta_s d\theta_s = \frac{Lr}{2\mu_0}\int_0^{2\pi} B_{Sk2}^2\, cos^2\left[k_2 p_s\theta_s \mp \varphi_2\right]cos\,\theta_s d\theta_s = 0 \tag{4.32}$$

$$F_{yn}^{(c)} = \frac{Lr}{2\mu_0}\int_0^{2\pi} B_{rh}^2(\theta_s,t)cos\,\theta_s d\theta_s = \frac{Lr}{2\mu_0}\int_0^{2\pi} B_{Rh}^2\, cos^2\left[hp_r(\theta_s-\Delta\theta)\right]cos\,\theta_s d\theta_s = 0 \tag{4.33}$$

Now, examine the fourth term of (4.20):

$$F_{yn}^{(d)} = \frac{Lr}{2\mu_0}\int_0^{2\pi} 2B_{sk1}(\theta_s,t)B_{sk2}(\theta_s,t)\cos\theta_s d\theta_s = \\ = \frac{Lr}{\mu_0}B_{Sk1}B_{Sk2}\int_0^{2\pi}\cos[k_1 p_s\theta_s \mp \varphi_1]\cos[k_2 p_s\theta_s \mp \varphi_2]\cos\theta_s d\theta_s \tag{4.34}$$

By applying (4.27):

$$F_{yn}^{(d)} = \frac{Lr}{\mu_0}B_{Sk1}B_{Sk2}\left\{\int_0^{2\pi}\frac{1}{2}\cos[(k_1 p_s + k_2 p_s)\theta_s \mp \varphi_1 \mp \varphi_2]\cos\theta_s d\theta_s + \right. \\ \left. + \int_0^{2\pi}\frac{1}{2}\cos[(k_1 p_s - k_2 p_s)\theta_s \mp \varphi_1 \pm \varphi_2]\cos\theta_s d\theta_s\right\} \tag{4.35}$$

Repeating the same process (4.27) in both the integrals of (4.35):

$$F_{yn}^{(d)} = \frac{Lr}{2\mu_0}B_{Sk1}B_{Sk2}\left\{\int_0^{2\pi}\frac{1}{2}\cos[(k_1 p_s + k_2 p_s + 1)\theta_s \mp \varphi_1 \mp \varphi_2]d\theta_s + \right. \\ + \int_0^{2\pi}\frac{1}{2}\cos[(k_1 p_s + k_2 p_s - 1)\theta_s \mp \varphi_1 \mp \varphi_2]d\theta_s + \\ + \int_0^{2\pi}\frac{1}{2}\cos[(k_1 p_s - k_2 p_s + 1)\theta_s \mp \varphi_1 \pm \varphi_2]d\theta_s + \\ \left. + \int_0^{2\pi}\frac{1}{2}\cos[(k_1 p_s - k_2 p_s - 1)\theta_s \mp \varphi_1 \pm \varphi_2]d\theta_s\right\} \tag{4.36}$$

We make the assumption (4.37), that according to (4.36) gives the relationship (4.38) and consequently (4.39):

$$k_1 p_s - k_2 p_s + 1 = 0 \quad \Rightarrow \quad k_2 p_s = 1 + k_1 p_s \tag{4.37}$$

$$F_{yn}^{(d)} = \frac{Lr}{2\mu_0}B_{Sk1}B_{Sk2}\left\{\int_0^{2\pi}\frac{1}{2}\cos[2(k_1 p_s + 1)\theta_s \mp \varphi_1 \mp \varphi_2]d\theta_s + \right. \\ + \int_0^{2\pi}\frac{1}{2}\cos[2k_1 p_s\theta_s \mp \varphi_1 \mp \varphi_2]d\theta_s + \\ \left. + \int_0^{2\pi}\frac{1}{2}\cos[\mp\varphi_1 \pm \varphi_2]d\theta_s + \int_0^{2\pi}\frac{1}{2}\cos[-2\theta_s \mp \varphi_1 \pm \varphi_2]d\theta_s\right\} \tag{4.38}$$

$$F_{yn}^{(d)} = \frac{Lr}{4\mu_0} B_{Sk1} B_{Sk2} \left\{ \frac{1}{2(k_1 p_s + 1)} \left[sin\left[2(k_1 p_s + 1)\theta_s \mp \varphi_1 \mp \varphi_2 \right] \right]_0^{2\pi} + \right.$$
$$\left. + \frac{1}{2k_1 p_s} \left[sin\left[2k_1 p_s \theta_s \mp \varphi_1 \mp \varphi_2 \right] \right]_0^{2\pi} + 2\pi cos(\mp \varphi_1 \pm \varphi_2) - \frac{1}{2} sin\left[-2\theta_s \mp \varphi_1 \pm \varphi_2 \right]_0^{2\pi} \right\} \tag{4.39}$$

As observed above, the first, second and fourth terms in (4.39) have a null result, being the difference of sine functions with multiples arguments of 2π. The only term different from zero is the third, not depending on the integration variable θ_s. Finally, the result of the integral (4.34), under the hypothesis (4.37) is:

$$F_{yn}^{(d)} = \frac{\pi Lr}{2\mu_0} B_{Sk1} B_{Sk2} \, cos(\mp \varphi_1 \pm \varphi_2) \qquad \text{if} \quad k_1 p_s - k_2 p_s = -1 \tag{4.40}$$

We make the assumption (4.41), that according to (4.36) gives the relationship (4.42):

$$k_1 p_s - k_2 p_s - 1 = 0 \quad \Rightarrow \quad k_2 p_s = -1 + k_1 p_s \tag{4.41}$$

$$F_{yn}^{(d)} = \frac{Lr}{2\mu_0} B_{Sk1} B_{Sk2} \left\{ \int_0^{2\pi} \frac{1}{2} cos\left[2k_1 p_s \theta_s \mp \varphi_1 \mp \varphi_2 \right] d\theta_s \right.$$
$$+ \int_0^{2\pi} \frac{1}{2} cos\left[2(k_1 p_s - 1)\theta_s \mp \varphi_1 \mp \varphi_2 \right] d\theta_s \tag{4.42}$$
$$\left. + \int_0^{2\pi} \frac{1}{2} cos\left[2\theta_s \mp \varphi_1 \pm \varphi_2 \right] d\theta_s + \int_0^{2\pi} \frac{1}{2} cos\left[\mp \varphi_1 \pm \varphi_2 \right] d\theta_s \right\}$$

$$F_{yn}^{(d)} = \frac{Lr}{4\mu_0} B_{Sk1} B_{Sk2} \left\{ \frac{1}{2k_1 p_s} \left[sin(2k_1 p_s \theta_s \mp \varphi_1 \mp \varphi_2) \right]_0^{2\pi} + \right.$$
$$+ \frac{1}{2(k_1 p_s - 1)} \left[sin\left[2(k_1 p_s - 1)\theta_s \mp \varphi_1 \mp \varphi_2 \right] \right]_0^{2\pi} + \tag{4.43}$$
$$\left. + \left[\frac{1}{2} sin(2\theta_s \mp \varphi_1 \pm \varphi_2) \right]_0^{2\pi} + 2\pi cos(\mp \varphi_1 \pm \varphi_2) \right\}$$

With very similar conclusions of the other assumption, the result of the integral (4.34), under the hypothesis (4.41) is:

$$F_{yn}^{(d)} = \frac{\pi L r}{2\mu_0} B_{Sk1} B_{Sk2} \cos\left(\mp\varphi_1 \pm \varphi_2\right) \qquad \text{if} \quad k_1 p_s - k_2 p_s = 1 \tag{4.44}$$

Note that the assumptions regarding the sum of the numbers of pole pairs, shown in (4.45), (4.46) are not examined because they don't correspond to real cases, being impossible to occur.

$$k_1 p_s + k_2 p_s - 1 = 0 \quad \Rightarrow \quad k_1 p_s + k_2 p_s = 1 \tag{4.45}$$

$$k_1 p_s + k_2 p_s + 1 = 0 \quad \Rightarrow \quad k_1 p_s + k_2 p_s = -1 \tag{4.46}$$

So, the final form of the *y*-projection of the normal component of the force, related to the *d* factor of (4.20), is given by:

$$F_{yn}^{(d)} = \frac{\pi L r}{2\mu_0} B_{Sk1} B_{Sk2} \cos\left(\mp\varphi_1 \pm \varphi_2\right) \qquad \begin{cases} \text{if} \quad k_1 p_s - k_2 p_s = -1 \\ \text{if} \quad k_1 p_s - k_2 p_s = 1 \end{cases} \tag{4.47}$$

$$\text{with :} \quad \frac{k_1 \mp s_{v1}}{m} \in N_0 \quad \wedge \quad \frac{k_2 \mp s_{v2}}{m} \in N_0$$

It is very important to observe that the signs of the conditions of existence have to be accorded to signs of the angular phases in the same order that appears in (4.47). Performing similar calculations, by integrating the *e* and *f* factors in (4.20) which refer to the interactions between every single stator current space vector and the rotor field produced by the magnets, the following relationships can be found:

$$F_{yn}^{(e)} = \frac{\pi L r}{2\mu_0} B_{Sk1} B_{Rh} \cos\left(h p_r \Delta\theta \mp \varphi_1\right) \qquad \begin{cases} \text{if} \quad k_1 p_s - h p_r = -1 \\ \text{if} \quad k_1 p_s - h p_r = 1 \end{cases} \tag{4.48}$$

$$\text{with :} \quad \frac{k_1 \mp s_{v1}}{m} \in N_0 \quad \wedge \quad h \in N_{odd}$$

$$F_{yn}^{(f)} = \frac{\pi Lr}{2\mu_0} B_{Sk2} B_{Rh} \cos\left(hp_r \Delta\theta \mp \varphi_2\right) \qquad \begin{cases} \text{if} & k_2 p_s - hp_r = -1 \\ \text{if} & k_2 p_s - hp_r = 1 \end{cases} \tag{4.49}$$

$$\text{with :} \quad \frac{k_2 \mp s_{v2}}{m} \in N_0 \quad \wedge \quad h \in N_{odd}$$

By adding up all the non-zero terms of the *y*-projection of the normal component of the force, is obtained:

$$F_{yn}^{(k_1,k_2)} = \sum_{k_1} \frac{\pi Lr}{2\mu_0} B_{Sk1} B_{Sk2} \cos\left(\mp\varphi_1 \pm \varphi_2\right) \qquad \forall \begin{cases} k_2 = \dfrac{1 + k_1 p_s}{p_s} \in N_0 \\ k_2 = \dfrac{-1 + k_1 p_s}{p_s} \in N_0 \end{cases} \tag{4.50}$$

$$\text{with :} \quad \frac{k_1 \mp s_{v1}}{m} \in N_0 \quad \wedge \quad \frac{k_2 \mp s_{v2}}{m} \in N_0$$

$$F_{yn}^{(k_1,h)} = \sum_{k_1} \frac{\pi Lr}{2\mu_0} B_{Sk1} B_{Rh} \cos\left[hp_r \Delta\theta \mp \varphi_1\right] \quad \forall \begin{cases} h = \dfrac{1 + k_1 p_s}{p_r} \in N_{odd} \\ h = \dfrac{-1 + k_1 p_s}{p_r} \in N_{odd} \end{cases} \tag{4.51}$$

$$\text{with :} \quad \frac{k_1 \mp s_{v1}}{m} \in N_0$$

$$F_{yn}^{(k_2,h)} = \sum_{k_2} \frac{\pi Lr}{2\mu_0} B_{Sk2} B_{Rh} \cos\left[hp_r \Delta\theta \mp \varphi_2\right] \quad \forall \begin{cases} h = \dfrac{1 + k_2 p_s}{p_r} \in N_{odd} \\ h = \dfrac{-1 + k_2 p_s}{p_r} \in N_{odd} \end{cases} \tag{4.52}$$

$$\text{with :} \quad \frac{k_2 \mp s_{v2}}{m} \in N_0$$

$$F_{yn}^{(k_2,k_{2'})} = \sum_{k_2} \frac{\pi Lr}{2\mu_0} B_{Sk_2} B_{Sk_{2'}} \cos\left[\mp\varphi_2 \pm \varphi_{2'}\right] \quad \forall \begin{cases} k_2' = \dfrac{1 + k_2 p_s}{p_s} \in N_0 \\ k_2' = \dfrac{-1 + k_2 p_s}{p_s} \in N_0 \end{cases} \tag{4.53}$$

$$\text{with :} \quad \frac{k_2 \mp s_{v2}}{m} \in N_0 \quad \wedge \quad \frac{k_2' \mp s_{v2}}{m} \in N_0$$

The equations (4.53) represent a typology of interaction not explicated in (4.20): it is the influence between different harmonic orders belonging to the same current space vector s_{v2}, denoted with k_2 and $k_2^{'}$. In fact, it happens in the analyzed bearingless machine that some harmonic orders of s_{v2} exist, whose number of pole pairs differ of ± 1: in this case, they also give a contribution to the resultant force. Is important to note that the phase angle $\varphi_{2'}$ in (4.53) represents exactly the same phase angle φ_2, being only a formal distinction which indicates that the sign of $\varphi_{2'}$ depends on the existing harmonic order $k_2^{'}$, while the sign of φ_2 is obviously related to k_2: in this way the argument of the function cosine in (4.53) has to be understood as the algebraic sum of the same variable φ_2, resulting in a 0, $2\varphi_2$ or $-2\varphi_2$. Finally, the resultant *y*-projection of the normal component of the force transmitted to the rotor is the sum of the equations (4.50), (4.51), (4.52), (4.53):

$$F_{yn} = F_{yn}^{(k_1,k_2)} + F_{yn}^{(k_1,h)} + F_{yn}^{(k_2,h)} + F_{yn}^{(k_2,k_{2'})} \tag{4.54}$$

A similar calculation can be performed to determine the resultant *x*-projection, by considering term by term of (4.20) integrating with (4.18):

$$F_{xn}^{(a)} = \frac{Lr}{2\mu_0}\int_0^{2\pi} B_{sk}^2(\theta_s,t)\sin\theta_s d\theta_s = \frac{Lr}{2\mu_0}\int_0^{2\pi} B_{Sk}^2 \cos^2\left[kp_s\theta_s \mp \varphi(t)\right]\sin\theta_s d\theta_s \tag{4.55}$$

By applying (4.25) to (4.55), it gives:

$$F_{xn}^{(a)} = \frac{LrB_{Sk}^2}{4\mu_0}\int_0^{2\pi}\sin\theta_s d\theta_s + \frac{LrB_{Sk}^2}{4\mu_0}\int_0^{2\pi}\cos\left[2kp_s\theta_s \mp 2\varphi(t)\right]\sin\theta_s d\theta_s \tag{4.56}$$

By considering that:

$$\cos(\alpha)\sin(\beta) = \frac{\sin(\alpha+\beta)-\sin(\alpha-\beta)}{2} \tag{4.57}$$

By applying (4.57) to (4.56), it gives:

$$F_{xn}^{(a)} = \frac{LrB_{Sk}^2}{8\mu_0}\int_0^{2\pi} sin\left[\left(2kp_s+1\right)\theta_s \mp 2\varphi(t)\right]d\theta_s - \frac{LrB_{Sk}^2}{8\mu_0}\int_0^{2\pi} sin\left[\left(2kp_s-1\right)\theta_s \mp 2\varphi(t)\right]d\theta_s \tag{4.58}$$

$$F_{xn}^{(a)} = \frac{LrB_{Sk}^2}{8\mu_0}\left\{\frac{1}{2kp_s+1}\left[-cos\left[\left(2kp_s+1\right)\theta_s \mp 2\varphi\right]\right]_0^{2\pi} + \right. \\ \left. -\frac{1}{2kp_s-1}\left[-cos\left[\left(2kp_s-1\right)\theta_s \mp 2\varphi\right]\right]_0^{2\pi}\right\} \tag{4.59}$$

$$F_{xn}^{(a)} = \frac{LrB_{Sk}^2}{8\mu_0}\left\{\frac{1}{2kp_s+1}\left[-cos\left[2\pi\left(2kp_s+1\right)\mp 2\varphi\right]+cos\left[\mp 2\varphi\right]\right]+ \right. \\ \left. -\frac{1}{2kp_s-1}\left[-cos\left[2\pi\left(2kp_s-1\right)\mp 2\varphi\right]+cos\left[\mp 2\varphi\right]\right]\right\} = 0 \tag{4.60}$$

In a very similar way to the equation (4.30), being both $2kp_s+1$ and $2kp_s-1$ integer numbers, the arguments of the cosines in (4.60) differ by integer multiples of 2π, thus they assume the same value and their difference is equal to zero. Hence, the contribution of the terms in the form (4.55) to the *x*-component of the force is zero:

$$F_{xn}^{(a)} = \frac{Lr}{2\mu_0}\int_0^{2\pi} B_{sk1}^2\left(\theta_s,t\right)sin\,\theta_s d\theta_s = \frac{Lr}{2\mu_0}\int_0^{2\pi} B_{Sk1}^2\,cos^2\left[k_1 p_s\theta_s \mp \varphi_1\right]sin\,\theta_s d\theta_s = 0 \tag{4.61}$$

For the same reason, the similar quadratic term related to the space vector s_{v2} and the one related to the rotor magnetic field give a null result (4.62), (4.63):

$$F_{xn}^{(b)} = \frac{Lr}{2\mu_0}\int_0^{2\pi} B_{sk2}^2\left(\theta_s,t\right)sin\,\theta_s d\theta_s = \frac{Lr}{2\mu_0}\int_0^{2\pi} B_{Sk2}^2\,cos^2\left[k_2 p_s\theta_s \mp \varphi_2\right]sin\,\theta_s d\theta_s = 0 \tag{4.62}$$

$$F_{xn}^{(c)} = \frac{Lr}{2\mu_0}\int_0^{2\pi} B_{rh}^2\left(\theta_s,t\right)sin\,\theta_s d\theta_s = \frac{Lr}{2\mu_0}\int_0^{2\pi} B_{Rh}^2\,cos^2\left[hp_r\left(\theta_s-\Delta\theta\right)\right]sin\,\theta_s d\theta_s = 0 \tag{4.63}$$

By integrating the fourth term of (4.20):

$$F_{xn}^{(d)} = \frac{Lr}{2\mu_0}\int_0^{2\pi} 2B_{sk1}(\theta_s,t)B_{sk2}(\theta_s,t)\sin\theta_s d\theta_s = \\ = \frac{Lr}{\mu_0}B_{Sk1}B_{Sk2}\int_0^{2\pi}\cos[k_1 p_s\theta_s \mp \varphi_1]\cos[k_2 p_s\theta_s \mp \varphi_2]\sin\theta_s d\theta_s \tag{4.64}$$

By applying (4.27) to (4.64):

$$F_{xn}^{(d)} = \frac{Lr}{\mu_0}B_{Sk1}B_{Sk2}\left\{\int_0^{2\pi}\frac{1}{2}\cos[(k_1 p_s + k_2 p_s)\theta_s \mp \varphi_1 \mp \varphi_2]\sin\theta_s d\theta_s + \right. \\ \left. + \int_0^{2\pi}\frac{1}{2}\cos[(k_1 p_s - k_2 p_s)\theta_s \mp \varphi_1 \pm \varphi_2]\sin\theta_s d\theta_s\right\} \tag{4.65}$$

By applying (4.57) to both the integrals of (4.65):

$$F_{xn}^{(d)} = \frac{Lr}{2\mu_0}B_{Sk1}B_{Sk2}\left\{\int_0^{2\pi}\frac{1}{2}\sin[(k_1 p_s + k_2 p_s + 1)\theta_s \mp \varphi_1 \mp \varphi_2]d\theta_s + \right. \\ - \int_0^{2\pi}\frac{1}{2}\sin[(k_1 p_s + k_2 p_s - 1)\theta_s \mp \varphi_1 \mp \varphi_2]d\theta_s + \\ + \int_0^{2\pi}\frac{1}{2}\sin[(k_1 p_s - k_2 p_s + 1)\theta_s \mp \varphi_1 \pm \varphi_2]d\theta_s + \\ \left. - \int_0^{2\pi}\frac{1}{2}\sin[(k_1 p_s - k_2 p_s - 1)\theta_s \mp \varphi_1 \pm \varphi_2]d\theta_s\right\} \tag{4.66}$$

We make the assumption (4.67), that according to (4.66) gives the relationship (4.68) and, consequently, (4.69):

$$k_1 p_s - k_2 p_s + 1 = 0 \quad \Rightarrow \quad k_2 p_s = 1 + k_1 p_s \tag{4.67}$$

$$F_{xn}^{(d)} = \frac{Lr}{2\mu_0}B_{Sk1}B_{Sk2}\left\{\int_0^{2\pi}\frac{1}{2}\sin[2(k_1 p_s + 1)\theta_s \mp \varphi_1 \mp \varphi_2]d\theta_s + \right. \\ - \int_0^{2\pi}\frac{1}{2}\sin[2k_1 p_s\theta_s \mp \varphi_1 \mp \varphi_2]d\theta_s + \\ \left. + \int_0^{2\pi}\frac{1}{2}\sin[\mp \varphi_1 \pm \varphi_2]d\theta_s - \int_0^{2\pi}\frac{1}{2}\sin[-2\theta_s \mp \varphi_1 \pm \varphi_2]d\theta_s\right\} \tag{4.68}$$

$$F_{xn}^{(d)} = \frac{Lr}{4\mu_0} B_{Sk1} B_{Sk2} \left\{ \frac{1}{2(k_1 p_s + 1)} \left[-\cos\left[2(k_1 p_s + 1)\theta_s \mp \varphi_1 \mp \varphi_2\right]\right]_0^{2\pi} + \right.$$
$$+ \frac{1}{2k_1 p_s} \left[\cos\left[2k_1 p_s \theta_s \mp \varphi_1 \mp \varphi_2\right]\right]_0^{2\pi} + \qquad (4.69)$$
$$\left. + 2\pi \sin(\mp\varphi_1 \pm \varphi_2) + \frac{1}{2}\cos\left[-2\theta_s \mp \varphi_1 \pm \varphi_2\right]_0^{2\pi} \right\}$$

The first, second and fourth terms in (4.69) have a null result, being differences between cosines with arguments multiples of 2π. The only term different from zero is the third, not depending on the integration variable θ_s. Finally, the result of the integral (4.64), under the hypothesis (4.67) is:

$$F_{xn}^{(d)} = \frac{\pi Lr}{2\mu_0} B_{Sk1} B_{Sk2} \sin(\mp\varphi_1 \pm \varphi_2) \qquad \text{if} \quad k_1 p_s - k_2 p_s = -1 \qquad (4.70)$$

We make the assumption (4.71), that according to (4.66) gives the relationship (4.72) and, consequently, (4.73):

$$k_1 p_s - k_2 p_s - 1 = 0 \quad \Rightarrow \quad k_2 p_s = -1 + k_1 p_s \qquad (4.71)$$

$$F_{xn}^{(d)} = \frac{Lr}{2\mu_0} B_{Sk1} B_{Sk2} \left\{ \int_0^{2\pi} \frac{1}{2} \sin\left[2k_1 p_s \theta_s \mp \varphi_1 \mp \varphi_2\right] d\theta_s + \right.$$
$$- \int_0^{2\pi} \frac{1}{2} \sin\left[2(k_1 p_s - 1)\theta_s \mp \varphi_1 \mp \varphi_2\right] d\theta_s \qquad (4.72)$$
$$\left. + \int_0^{2\pi} \frac{1}{2} \sin\left[2\theta_s \mp \varphi_1 \pm \varphi_2\right] d\theta_s - \int_0^{2\pi} \frac{1}{2} \sin\left[\mp \varphi_1 \pm \varphi_2\right] d\theta_s \right\}$$

$$F_{xn}^{(d)} = \frac{Lr}{4\mu_0} B_{Sk1} B_{Sk2} \left\{ \frac{1}{2k_1 p_s} \left[-\cos\left(2k_1 p_s \theta_s \mp \varphi_1 \mp \varphi_2\right)\right]_0^{2\pi} \right.$$
$$+ \frac{1}{2(k_1 p_s - 1)} \left[\cos\left[2(k_1 p_s - 1)\theta_s \mp \varphi_1 \mp \varphi_2\right]\right]_0^{2\pi} \qquad (4.73)$$
$$\left. - \left[\frac{1}{2}\cos\left(2\theta_s \mp \varphi_1 \pm \varphi_2\right)\right]_0^{2\pi} - 2\pi \sin\left(\mp\varphi_1 \pm \varphi_2\right) \right\}$$

With very similar conclusions of the other assumption, the result of the integral

(4.64), under the hypothesis (4.71) is:

$$F_{xn}^{(d)} = -\frac{\pi L r}{2\mu_0} B_{Sk1} B_{Sk2}\, sin\left(\mp\varphi_1 \pm \varphi_2\right) \qquad \text{if} \quad k_1 p_s - k_2 p_s = 1 \tag{4.74}$$

As done before, the assumptions regarding the sum of the numbers of pole pairs, replicated in (4.75), (4.76) are not examined because they don't correspond to real cases.

$$k_1 p_s + k_2 p_s - 1 = 0 \quad \Rightarrow \quad k_1 p_s + k_2 p_s = 1 \tag{4.75}$$

$$k_1 p_s + k_2 p_s + 1 = 0 \quad \Rightarrow \quad k_1 p_s + k_2 p_s = -1 \tag{4.76}$$

So, the final form of the *x*-projection of the normal component of the force, related to the *d* factor of (4.20), is given by:

$$F_{xn}^{(d)} = \begin{cases} \dfrac{\pi L r}{2\mu_0} B_{Sk1} B_{Sk2}\, sin\left(\mp\varphi_1 \pm \varphi_2\right) & \text{if} \quad k_1 p_s - k_2 p_s = -1 \\ -\dfrac{\pi L r}{2\mu_0} B_{Sk1} B_{Sk2}\, sin\left(\mp\varphi_1 \pm \varphi_2\right) & \text{if} \quad k_1 p_s - k_2 p_s = 1 \end{cases} \tag{4.77}$$

$$\text{with}: \quad \frac{k_1 \mp s_{v1}}{m} \in N_0 \quad \wedge \quad \frac{k_2 \mp s_{v2}}{m} \in N_0$$

As said before, the signs of the conditions of existence have to be accorded to signs of the angular phases in the same order that appears in (4.77). Note that the sign of the *x*-component changes depending on the condition to be verified (4.67) or (4.71), differently from the *y*-component (4.47).

By integrating the *e* and *f* factors of (4.20) in a very similar way to what has been done for *d*, the interactions between every single stator current space vector and the rotor field produced by the magnets can be expressed as:

$$F_{xn}^{(e)} = \begin{cases} \frac{\pi Lr}{2\mu_0} B_{Sk1} B_{Rh} \, sin\left[hp_r \Delta\theta \mp \varphi_1\right] & \text{if } k_1 p_s - hp_r = -1 \\ -\frac{\pi Lr}{2\mu_0} B_{Sk1} B_{Rh} \, sin\left[hp_r \Delta\theta \mp \varphi_1\right] & \text{if } k_1 p_s - hp_r = 1 \end{cases} \tag{4.78}$$

$$\text{with: } \quad \frac{k_1 \mp s_{v1}}{m} \in N_0 \quad \wedge \quad h \in N_{odd}$$

$$F_{xn}^{(f)} = \begin{cases} \frac{\pi Lr}{2\mu_0} B_{Sk2} B_{Rh} \, sin\left[hp_r \Delta\theta \mp \varphi_2\right] & \text{if } k_2 p_s - hp_r = -1 \\ -\frac{\pi Lr}{2\mu_0} B_{Sk2} B_{Rh} \, sin\left[hp_r \Delta\theta \mp \varphi_2\right] & \text{if } k_2 p_s - hp_r = 1 \end{cases} \tag{4.79}$$

$$\text{with: } \quad \frac{k_2 \mp s_{v2}}{m} \in N_0 \quad \wedge \quad h \in N_{odd}$$

By adding up all the non-zero terms of the *x*-projections of the normal component of the force, is obtained:

$$F_{xn}^{(k_1,k_2)} = \begin{cases} \sum_{k_1} \frac{\pi Lr}{2\mu_0} B_{Sk_1} B_{Sk_2} \, sin\left[\mp \varphi_1 \pm \varphi_2\right] & \forall \, k_2 = \frac{1 + k_1 p_s}{p_s} \in N \\ \sum_{k_1} -\frac{\pi Lr}{2\mu_0} B_{Sk_1} B_{Sk_2} \, sin\left[\mp \varphi_1 \pm \varphi_2\right] & \forall \, k_2 = \frac{-1 + k_1 p_s}{p_s} \in N \end{cases} \tag{4.80}$$

$$\text{with: } \quad \frac{k_1 \mp s_{v1}}{m} \in N_0 \quad \wedge \quad \frac{k_2 \mp s_{v2}}{m} \in N_0$$

$$F_{xn}^{(k_1,h)} = \begin{cases} \sum_{k_1} \frac{\pi Lr}{2\mu_0} B_{Sk1} B_{Rh} \, sin\left[hp_r \Delta\theta \mp \varphi_1\right] & \forall \, h = \frac{1 + k_1 p_s}{p_r} \in N_{odd} \\ \sum_{k_1} -\frac{\pi Lr}{2\mu_0} B_{Sk1} B_{Rh} \, sin\left[hp_r \Delta\theta \mp \varphi_1\right] & \forall \, h = \frac{-1 + k_1 p_s}{p_r} \in N_{odd} \end{cases} \tag{4.81}$$

$$\text{with: } \quad \frac{k_1 \mp s_{v1}}{m} \in N_0 \quad \wedge \quad h \in N_{odd}$$

$$F_{xn}^{(k_2,h)} = \begin{cases} \sum_{k_2} \frac{\pi L r}{2\mu_0} B_{Sk2} B_{Rh} \; sin\left[hp_r \Delta\theta \mp \varphi_2\right] & \forall\; h = \frac{1 + k_2 p_s}{p_r} \in N_{odd} \\ \sum_{k_2} -\frac{\pi L r}{2\mu_0} B_{Sk2} B_{Rh} \; sin\left[hp_r \Delta\theta \mp \varphi_2\right] & \forall\; h = \frac{-1 + k_2 p_s}{p_r} \in N_{odd} \end{cases}$$

$$\text{with :} \quad \frac{k_2 \mp s_{v2}}{m} \in N_0 \quad \wedge \quad h \in N_{odd} \tag{4.82}$$

$$F_{xn}^{(k_2,k_{2'})} = \begin{cases} \sum_{k_2} \frac{\pi L r}{2\mu_0} B_{Sk_2} B_{Sk_{2'}} \; sin\left[\mp \varphi_2 \pm \varphi_{2'}\right] & \forall\; k_2^{'} = \frac{1 + k_2 p_s}{p_s} \in N \\ \sum_{k_2} -\frac{\pi L r}{2\mu_0} B_{Sk_2} B_{Sk_{2'}} \; sin\left[\mp \varphi_2 \pm \varphi_{2'}\right] & \forall\; k_2^{'} = \frac{-1 + k_2 p_s}{p_s} \in N \end{cases}$$

$$\text{with :} \quad \frac{k_2 \mp s_{v2}}{m} \in N_0 \quad \wedge \quad \frac{k_2^{'} \mp s_{v2}}{m} \in N_0 \tag{4.83}$$

The same considerations done for the equation (4.53), related to the meaning of k_2 and $k_2^{'}$, are valid for (4.83). So, the resultant *x*-projection of the normal component of the force transmitted to the rotor is the sum of the equations (4.80), (4.81), (4.82), (4.83), taking into account all the presented assumptions:

$$F_{xn} = F_{xn}^{(k_1,k_2)} + F_{xn}^{(k_1,h)} + F_{xn}^{(k_2,h)} + F_{xn}^{(k_2,k_{2'})} \tag{4.84}$$

4.4.2 Tangential components of the force

An analysis to determine the contribution of the tangential components of the magnetic field to the radial forces is presented, with reference to the equivalent surface current density $G(x_s,t)$, responsible for the normal component distribution of the magnetic field:

$$G(x_s,t)=\frac{\partial H_n}{\partial x_s} \tag{4.85}$$

Note that x_s is the linear abscissa corresponding to the angular one θ_s. By considering the simplified assumption that gives the tangential component of magnetic field H_t equal to the linear current density J, it is possible to find a correlation between H_t and H_n:

$$H_t(x_s,t)\cong J(x_s,t)=G\delta=\frac{\partial H_n}{\partial x_s}\delta \quad \Rightarrow \quad H_t\cong\frac{\partial H_n}{\partial x_s}\delta \tag{4.86}$$

In order to determine the expression of (4.86), based on (4.11), it is possible to write:

$$H_n(\theta_s,t)=\sum_{k_1}H_{sk1}(k_1p_s\theta_s,t)+\sum_{k_2}H_{sk2}(k_2p_s\theta_s,t)+\sum_{h}H_{rh}(hp_r\theta_s,t) \tag{4.87}$$

where

$$p_s\theta_s=p_r\theta_s=\frac{\pi}{\tau}x_s \tag{4.88}$$

Note that as specified in (4.88), p_s and p_r have the same value, being the pole pair number of stator and rotor fields for the motoring torque. The derivative of H_n by using (4.87), (4.88) can be expressed as:

$$\frac{\partial H_n}{\partial x_s}=\sum_{k_1}\frac{k_1\pi}{\tau}\frac{\partial H_{sk1}(k_1p_s\theta_s,t)}{\partial(k_1p_s\theta_s)}+\sum_{k_2}\frac{k_2\pi}{\tau}\frac{\partial H_{sk2}(k_2p_s\theta_s,t)}{\partial(k_2p_s\theta_s)}+\sum_{h}\frac{h\pi}{\tau}\frac{\partial H_{rh}(hp_r\theta_s,t)}{\partial(hp_r\theta_s)} \tag{4.89}$$

By substituting (4.89) in (4.86), calculating the derivatives and explicating the values of the flux densities, H_t can be finally expressed as:

$$H_t(\theta_s,t) = -\sum_{k_1}\frac{\delta}{\mu_0}\frac{k_1\pi}{\tau}B_{Sk1}\,sin\left[k_1 p_s\theta_s \mp \varphi_1(t)\right] + \\ -\sum_{k_2}\frac{\delta}{\mu_0}\frac{k_2\pi}{\tau}B_{Sk2}\,sin\left[k_2 p_s\theta_s \mp \varphi_2(t)\right] - \sum_{h}\frac{\delta}{\mu_0}\frac{h\pi}{\tau}B_{Rh}\,sin\left[hp_r\theta_s - hp_r\Delta\theta\right] \tag{4.90}$$

According to the Maxwell stress tensor expression (4.15), the tangential component of $\overline{T}$ is given by $H_t B_n$, calculated by multiplying (4.11) and (4.90), resulting in the sum of the following nine terms:

$$\sum_{k_1} -\frac{k_1\delta\pi}{\mu_0\tau}B_{Sk1}^2\,sin\left[k_1 p_s\theta_s \mp \varphi_1(t)\right]cos\left[k_1 p_s\theta_s \mp \varphi_1(t)\right] \tag{4.91}$$

$$\sum_{k_1,k_2} -\frac{k_1\delta\pi}{\mu_0\tau}B_{Sk1}B_{Sk2}\,sin\left[k_1 p_s\theta_s \mp \varphi_1(t)\right]cos\left[k_2 p_s\theta_s \mp \varphi_2(t)\right] \tag{4.92}$$

$$\sum_{k_1,h} -\frac{k_1\delta\pi}{\mu_0\tau}B_{Sk1}B_{Rh}\,sin\left[k_1 p_s\theta_s \mp \varphi_1(t)\right]cos\left[hp_r\theta_s - hp_r\Delta\theta\right] \tag{4.93}$$

$$\sum_{k_1,k_2} -\frac{k_2\delta\pi}{\mu_0\tau}B_{Sk1}B_{Sk2}\,cos\left[k_1 p_s\theta_s \mp \varphi_1(t)\right]sin\left[k_2 p_s\theta_s \mp \varphi_2(t)\right] \tag{4.94}$$

$$\sum_{k_2} -\frac{k_2\delta\pi}{\mu_0\tau}B_{Sk2}^2\,sin\left[k_2 p_s\theta_s \mp \varphi_2(t)\right]cos\left[k_2 p_s\theta_s \mp \varphi_2(t)\right] \tag{4.95}$$

$$\sum_{k_2,h} -\frac{k_2\delta\pi}{\mu_0\tau}B_{Sk2}B_{Rh}\,sin\left[k_2 p_s\theta_s \mp \varphi_2(t)\right]cos\left[hp_r\theta_s - hp_r\Delta\theta\right] \tag{4.96}$$

$$\sum_{h,k_1} -\frac{h\delta\pi}{\mu_0\tau}B_{Sk1}B_{Rh}\,cos\left[k_1 p_s\theta_s \mp \varphi_1(t)\right]sin\left[hp_r\theta_s - hp_r\Delta\theta\right] \tag{4.97}$$

$$\sum_{h,k_2} -\frac{h\delta\pi}{\mu_0\tau} B_{Sk2} B_{Rh} \cos\left[k_2 p_s \theta_s \mp \varphi_2(t)\right] \sin\left[hp_r\theta_s - hp_r\Delta\theta\right] \tag{4.98}$$

$$\sum_{h} -\frac{h\delta\pi}{\mu_0\tau} B_{Rh}^2 \sin\left[hp_r\theta_s - hp_r\Delta\theta\right] \cos\left[hp_r\theta_s - hp_r\Delta\theta\right] \tag{4.99}$$

As done in section 4.4.1, every summation described in (4.91)-(4.99) has to be projected along the axes directions and integrated between 0 and 2π in order to determine the *x*- and *y*-components of the resulting tangential force in the cartesian reference system (4.100), (4.101):

$$F_{xt} = \int_0^{2\pi} dF_t \cos\theta_s = Lr \int_0^{2\pi} H_t(\theta_s, t) B_n(\theta_s, t) \cos\theta_s d\theta_s \tag{4.100}$$

$$F_{yt} = \int_0^{2\pi} dF_t(-\sin\theta_s) = -Lr \int_0^{2\pi} H_t(\theta_s, t) B_n(\theta_s, t) \sin\theta_s d\theta_s \tag{4.101}$$

As seen in the previous, the result of the integrals is non-zero when the difference between the pole pairs numbers of two fields in exam is equal to ± 1. Furthermore, the terms in summation are considered for the existing harmonic orders of k_1, k_2, h. Let us perform the calculations (4.101), considering the terms (4.91), (4.95):

$$F_{yt}^{(a,e)} = -Lr \int_0^{2\pi} -\frac{k\delta\pi}{\mu_0\tau} B_{Sk}^2 \sin\left[kp_s\theta_s \mp \varphi(t)\right] \cos\left[kp_s\theta_s \mp \varphi(t)\right] \sin\theta_s d\theta_s \tag{4.102}$$

By considering that:

$$\sin(\alpha)\cos(\alpha) = \frac{1}{2}\sin(2\alpha) \tag{4.103}$$

Applying (4.103) to (4.102), it gives:

$$F_{yt}^{(a,e)} = \frac{1}{2}\frac{\delta\pi}{\mu_0\tau} k B_{Sk}^2 Lr \int_0^{2\pi} \sin\left[2kp_s\theta_s \mp 2\varphi(t)\right] \sin\theta_s d\theta_s \tag{4.104}$$

By assuming that:

$$sin(\alpha)sin(\beta)=\frac{cos(\alpha-\beta)-cos(\alpha+\beta)}{2} \tag{4.105}$$

Applying (4.105) to (4.104), it gives:

$$F_{yt}^{(a,e)}=\frac{1}{4}\frac{\delta\pi}{\mu_0\tau}kB_{Sk}^2Lr\left\{\int_0^{2\pi}cos\left[(2kp_s-1)\theta_s\mp2\varphi\right]d\theta_s-\int_0^{2\pi}cos\left[(2kp_s+1)\theta_s\mp2\varphi\right]d\theta_s\right\} \tag{4.106}$$

$$F_{yt}^{(a,e)}=\frac{1}{4}\frac{\delta\pi}{\mu_0\tau}kB_{Sk}^2Lr\left\{\frac{1}{2kp_s-1}\left[sin\left[(2kp_s-1)\theta_s\mp2\varphi\right]\right]_0^{2\pi}+-\frac{1}{2kp_s+1}\left[sin\left[(2kp_s+1)\theta_s\mp2\varphi\right]\right]_0^{2\pi}\right\}=0 \tag{4.107}$$

Proceeding by analogy, it can be assumed that:

$$F_{yt}^{(i)}=\frac{1}{4}\frac{\delta\pi}{\mu_0\tau}hB_{Rh}^2Lr\left\{\frac{1}{2hp_r-1}\left[sin\left[(2hp_r-1)\theta_s-2hp_r\Delta\theta\right]\right]_0^{2\pi}+-\frac{1}{2hp_r+1}\left[sin\left[(2hp_r+1)\theta_s-2hp_r\Delta\theta\right]\right]_0^{2\pi}\right\}=0 \tag{4.108}$$

Thus, the integrals related to the terms of the typologies a, e, i, are zero. Let us calculate the terms of the typology c, f, corresponding to equations (4.93), (4.96):

$$F_{yt}^{(c,f)}=-Lr\int_0^{2\pi}-\frac{k\delta\pi}{\mu_0\tau}B_{Sk}B_{Rh}\,sin\left[kp_s\theta_s\mp\varphi(t)\right]cos\left[hp_r(\theta_s-\Delta\theta)\right]sin\,\theta_s d\theta_s \tag{4.109}$$

By considering (4.110) and applying it to (4.109), it gives (4.111):

$$sin(\alpha)cos(\beta)=\frac{sin(\alpha+\beta)+sin(\alpha-\beta)}{2} \tag{4.110}$$

$$F_{yt}^{(c,f)}=\frac{1}{2}\frac{\delta\pi}{\mu_0\tau}kB_{Sk}B_{Rh}Lr\left\{\int_0^{2\pi}sin\left[(kp_s+hp_r)\theta_s\mp\varphi-hp_r\Delta\theta\right]sin\,\theta_s d\theta_s+\int_0^{2\pi}sin\left[(kp_s-hp_r)\theta_s\mp\varphi+hp_r\Delta\theta\right]sin\,\theta_s d\theta_s\right\} \tag{4.111}$$

By using (4.105) in (4.111):

$$F_{yt}^{(c,f)} = \frac{1}{4}\frac{\delta\pi}{\mu_0\tau} kB_{Sk}B_{Rh}Lr\left\{\int_0^{2\pi} cos\left[(kp_s + hp_r - 1)\theta_s \mp \varphi - hp_r\Delta\theta\right]d\theta_s + \right.$$
$$- \int_0^{2\pi} cos\left[(kp_s + hp_r + 1)\theta_s \mp \varphi - hp_r\Delta\theta\right]d\theta_s +$$
$$+ \int_0^{2\pi} cos\left[(kp_s - hp_r - 1)\theta_s \mp \varphi + hp_r\Delta\theta\right]d\theta_s + \qquad (4.112)$$
$$\left. - \int_0^{2\pi} cos\left[(kp_s - hp_r + 1)\theta_s \mp \varphi + hp_r\Delta\theta\right]d\theta_s \right\}$$

Consider, as done above, that the sum of the pole pairs of the stator and rotor fields cannot be equal to ± 1, conditions impossible to verify, thus the hypothesis (4.113), (4.114) aren't admitted:

$$kp_s + hp_r - 1 = 0 \qquad \Rightarrow \qquad kp_s + hp_r = 1 \qquad (4.113)$$

$$kp_s + hp_r + 1 = 0 \qquad \Rightarrow \qquad kp_s + hp_r = -1 \qquad (4.114)$$

Let us suppose that (4.115):

$$kp_s - hp_r - 1 = 0 \qquad \Rightarrow \qquad kp_s - hp_r = 1 \qquad (4.115)$$

By using (4.115) in (4.112), it gives (4.116) and consequently (4.117):

$$F_{yt}^{(c,f)} = \frac{1}{4}\frac{\delta\pi}{\mu_0\tau} kB_{Sk}B_{Rh}Lr\left\{\int_0^{2\pi} cos\left[2(kp_s - 1)\theta_s \mp \varphi - hp_r\Delta\theta\right]d\theta_s + \right.$$
$$- \int_0^{2\pi} cos\left(2kp_s\theta_s \mp \varphi - hp_r\Delta\theta\right)d\theta_s + \int_0^{2\pi} cos\left(\mp\varphi + hp_r\Delta\theta\right)d\theta_s + \qquad (4.116)$$
$$\left. - \int_0^{2\pi} cos\left(2\theta_s \mp \varphi + hp_r\Delta\theta\right)d\theta_s \right\}$$

$$F_{yt}^{(c,f)} = \frac{1}{4}\frac{\delta\pi}{\mu_0\tau} kB_{Sk}B_{Rh}Lr\left\{\frac{1}{2(kp_s - 1)}\left[sin\left[2(kp_s - 1)\theta_s \mp \varphi - hp_r\Delta\theta\right]\right]_0^{2\pi} + \right.$$
$$- \frac{1}{2kp_s}\left[sin\left(2kp_s\theta_s \mp \varphi - hp_r\Delta\theta\right)\right]_0^{2\pi} + 2\pi cos\left(\mp\varphi + hp_r\Delta\theta\right) + \qquad (4.117)$$
$$\left. - \frac{1}{2}\left[sin\left(2\theta_s \mp \varphi + hp_r\Delta\theta\right)\right]_0^{2\pi} \right\}$$

For the reasons already mentioned several times, all the integrals dependent on θ_s calculated on the interval $[0, 2\pi]$ are zero; so, the third term is the only contribution to the force:

$$F_{yt}^{(c,f)} = k\frac{\pi^2}{2}\frac{\delta Lr}{\mu_0\tau}B_{Sk}B_{Rh}\cos\left[hp_r\Delta\theta \mp \varphi(t)\right] \qquad \text{if} \quad kp_s - hp_r = 1 \tag{4.118}$$

Let us suppose that (4.119) is verified:

$$kp_s - hp_r + 1 = 0 \qquad \Rightarrow \qquad kp_s - hp_r = -1 \tag{4.119}$$

By using (4.119) in (4.112), it gives:

$$\begin{aligned} F_{yt}^{(c,f)} = \frac{1}{4}\frac{\delta\pi}{\mu_0\tau}kB_{Sk}B_{Rh}Lr\Bigg\{&\int_0^{2\pi}\cos\left(2kp_s\theta_s \mp \varphi - hp_r\Delta\theta\right)d\theta_s + \\ -&\int_0^{2\pi}\cos\left[(2kp_s+1)\theta_s \mp \varphi - hp_r\Delta\theta\right]d\theta_s + \int_0^{2\pi}\cos\left(-2\theta_s \mp \varphi + hp_r\Delta\theta\right)d\theta_s + \\ &-\int_0^{2\pi}\cos\left(\mp\varphi + hp_r\Delta\theta\right)d\theta_s\Bigg\} \end{aligned} \tag{4.120}$$

By executing the integrals in (4.120):

$$\begin{aligned} F_{yt}^{(c,f)} = \frac{1}{4}\frac{\delta\pi}{\mu_0\tau}kB_{Sk}B_{Rh}Lr\Bigg\{&\frac{1}{2kp_s}\left[\sin\left(2kp_s\theta_s \mp \varphi - hp_r\Delta\theta\right)\right]_0^{2\pi} + \\ &-\frac{1}{2(kp_s+1)}\left[\sin\left[2(kp_s+1)\theta_s \mp \varphi - hp_r\Delta\theta\right]\right]_0^{2\pi} + \\ &-\frac{1}{2}\left[\sin\left(-2\theta_s \mp \varphi + hp_r\Delta\theta\right)\right]_0^{2\pi} - 2\pi\cos\left(\mp\varphi + hp_r\Delta\theta\right)\Bigg\} \end{aligned} \tag{4.121}$$

The only not null contribution to the force is the fourth term of (4.121):

$$F_{yt}^{(c,f)} = -k\frac{\pi^2}{2}\frac{\delta Lr}{\mu_0\tau}B_{Sk}B_{Rh}\cos\left[hp_r\Delta\theta \mp \varphi(t)\right] \qquad \text{if} \quad kp_s - hp_r = -1 \tag{4.122}$$

So, it can be concluded that the contribution of the terms of the typologies c and f to the y-component of the tangential force acting on the rotor is given as:

$$F_{yt}^{(c,f)} = \begin{cases} k\frac{\pi^2}{2}\frac{\delta Lr}{\mu_0 \tau} B_{Sk} B_{Rh} \cos\left[hp_r \Delta\theta \mp \varphi(t)\right] & \text{if} \quad kp_s - hp_r = 1 \\ -k\frac{\pi^2}{2}\frac{\delta Lr}{\mu_0 \tau} B_{Sk} B_{Rh} \cos\left[hp_r \Delta\theta \mp \varphi(t)\right] & \text{if} \quad kp_s - hp_r = -1 \end{cases} \tag{4.123}$$

Obviously, this contribution has to be considered in the interaction between everyone of the current space vector s_{v1}, s_{v2}, and the rotor magnetic field produced by the magnets:

$$F_{yt}^{(c)} = \begin{cases} k_1\frac{\pi^2}{2}\frac{\delta Lr}{\mu_0 \tau} B_{Sk1} B_{Rh} \cos\left[hp_r \Delta\theta \mp \varphi_1(t)\right] & \text{if} \quad k_1 p_s - hp_r = 1 \\ -k_1\frac{\pi^2}{2}\frac{\delta Lr}{\mu_0 \tau} B_{Sk1} B_{Rh} \cos\left[hp_r \Delta\theta \mp \varphi_1(t)\right] & \text{if} \quad k_1 p_s - hp_r = -1 \end{cases} \tag{4.124}$$

$$F_{yt}^{(f)} = \begin{cases} k_2\frac{\pi^2}{2}\frac{\delta Lr}{\mu_0 \tau} B_{Sk2} B_{Rh} \cos\left[hp_r \Delta\theta \mp \varphi_2(t)\right] & \text{if} \quad k_2 p_s - hp_r = 1 \\ -k_2\frac{\pi^2}{2}\frac{\delta Lr}{\mu_0 \tau} B_{Sk2} B_{Rh} \cos\left[hp_r \Delta\theta \mp \varphi_2(t)\right] & \text{if} \quad k_2 p_s - hp_r = -1 \end{cases} \tag{4.125}$$

Let us calculate the terms of the typology g, h, corresponding to equations (4.97), (4.98):

$$F_{yt}^{(g,h)} = -Lr\int_0^{2\pi} -\frac{h\delta\pi}{\mu_0 \tau} B_{Sk} B_{Rh} \cos\left[kp_s \theta_s \mp \varphi(t)\right] \sin\left[hp_r(\theta_s - \Delta\theta)\right] \sin\theta_s d\theta_s \tag{4.126}$$

By considering (4.127) and applying it to (4.126), it gives (4.128):

$$\cos(\alpha)\sin(\beta) = \frac{\sin(\alpha+\beta) - \sin(\alpha-\beta)}{2} \tag{4.127}$$

$$\begin{aligned} F_{yt}^{(g,h)} = \frac{1}{2}\frac{\delta\pi}{\mu_0 \tau} hB_{Sk} B_{Rh} Lr \Bigg\{ & \int_0^{2\pi} \sin\left[(kp_s + hp_r)\theta_s \mp \varphi - hp_r \Delta\theta\right] \sin\theta_s d\theta_s + \\ & - \int_0^{2\pi} \sin\left[(kp_s - hp_r)\theta_s \mp \varphi + hp_r \Delta\theta\right] \sin\theta_s d\theta_s \Bigg\} \end{aligned} \tag{4.128}$$

By using (4.105) in (4.128):

$$F_{yt}^{(g,h)} = \frac{1}{4}\frac{\delta\pi}{\mu_0\tau} hB_{Sk}B_{Rh}Lr\left\{\int_0^{2\pi} cos\left[\left(kp_s + hp_r - 1\right)\theta_s \mp \varphi - hp_r\Delta\theta\right]d\theta_s + \right.$$
$$- \int_0^{2\pi} cos\left[\left(kp_s + hp_r + 1\right)\theta_s \mp \varphi - hp_r\Delta\theta\right]d\theta_s +$$
$$- \int_0^{2\pi} cos\left[\left(kp_s - hp_r - 1\right)\theta_s \mp \varphi + hp_r\Delta\theta\right]d\theta_s + \qquad (4.129)$$
$$\left. + \int_0^{2\pi} cos\left[\left(kp_s - hp_r + 1\right)\theta_s \mp \varphi + hp_r\Delta\theta\right]d\theta_s \right\}$$

As done in the previous, the hypothesis (4.113), (4.114) are to be considered not valid, so suppose that:

$$kp_s - hp_r - 1 = 0 \qquad \Rightarrow \qquad kp_s - hp_r = 1 \qquad (4.130)$$

By using (4.130) in (4.129), it gives:

$$F_{yt}^{(g,h)} = \frac{1}{4}\frac{\delta\pi}{\mu_0\tau} hB_{Sk}B_{Rh}Lr\left\{\int_0^{2\pi} cos\left[2\left(kp_s - 1\right)\theta_s \mp \varphi - hp_r\Delta\theta\right]d\theta_s + \right.$$
$$- \int_0^{2\pi} cos\left(2kp_s\theta_s \mp \varphi - hp_r\Delta\theta\right)d\theta_s - \int_0^{2\pi} cos\left(\mp\varphi + hp_r\Delta\theta\right)d\theta_s + \qquad (4.131)$$
$$\left. + \int_0^{2\pi} cos\left(2\theta_s \mp \varphi + hp_r\Delta\theta\right)d\theta_s \right\}$$

By executing the integrals in (4.131):

$$F_{yt}^{(g,h)} = \frac{1}{4}\frac{\delta\pi}{\mu_0\tau} hB_{Sk}B_{Rh}Lr\left\{\frac{1}{2\left(kp_s - 1\right)}\left[sin\left[2\left(kp_s - 1\right)\theta_s \mp \varphi - hp_r\Delta\theta\right]\right]_0^{2\pi} + \right.$$
$$- \frac{1}{2kp_s}\left[sin\left(2kp_s\theta_s \mp \varphi - hp_r\Delta\theta\right)\right]_0^{2\pi} - 2\pi cos\left(\mp\varphi + hp_r\Delta\theta\right) + \qquad (4.132)$$
$$\left. + \frac{1}{2}\left[sin\left(2\theta_s \mp \varphi + hp_r\Delta\theta\right)\right]_0^{2\pi} \right\}$$

The third term of (4.132) is the only contribution to the force:

$$F_{yt}^{(g,h)} = -h\frac{\pi^2}{2}\frac{\delta Lr}{\mu_0\tau}B_{Sk}B_{Rh}\cos\left[hp_r\Delta\theta \mp \varphi(t)\right] \qquad \text{if} \quad kp_s - hp_r = 1 \tag{4.133}$$

Let us suppose that (4.134) is verified:

$$kp_s - hp_r + 1 = 0 \qquad \Rightarrow \qquad kp_s - hp_r = -1 \tag{4.134}$$

By using (4.134) in (4.129), it gives:

$$\begin{aligned} F_{yt}^{(g,h)} = \frac{1}{4}\frac{\delta\pi}{\mu_0\tau}hB_{Sk}B_{Rh}Lr\Bigg\{&\int_0^{2\pi}\cos\left(2kp_s\theta_s \mp \varphi - hp_r\Delta\theta\right)d\theta_s + \\ -\int_0^{2\pi}\cos\left[2\left(kp_s+1\right)\theta_s \mp \varphi - hp_r\Delta\theta\right]d\theta_s &- \int_0^{2\pi}\cos\left(-2\theta_s \mp \varphi + hp_r\Delta\theta\right)d\theta_s + \\ &+\int_0^{2\pi}\cos\left(\mp\varphi + hp_r\Delta\theta\right)d\theta_s\Bigg\} \end{aligned} \tag{4.135}$$

By executing the integrals in (4.135):

$$\begin{aligned} F_{yt}^{(g,h)} = \frac{1}{4}\frac{\delta\pi}{\mu_0\tau}hB_{Sk}B_{Rh}Lr\Bigg\{&\frac{1}{2kp_s}\left[\sin\left(2kp_s\theta_s \mp \varphi - hp_r\Delta\theta\right)\right]_0^{2\pi} + \\ &-\frac{1}{2\left(kp_s+1\right)}\left[\sin\left[2\left(kp_s+1\right)\theta_s \mp \varphi - hp_r\Delta\theta\right]\right]_0^{2\pi} + \\ &+\frac{1}{2}\left[\sin\left(-2\theta_s \mp \varphi + hp_r\Delta\theta\right)\right]_0^{2\pi} + 2\pi\cos\left(\mp\varphi + hp_r\Delta\theta\right)\Bigg\} \end{aligned} \tag{4.136}$$

The only not null contribution to the force is the fourth term of (4.136):

$$F_{yt}^{(g,h)} = h\frac{\pi^2}{2}\frac{\delta Lr}{\mu_0\tau}B_{Sk}B_{Rh}\cos\left[hp_r\Delta\theta \mp \varphi(t)\right] \qquad \text{if} \quad kp_s - hp_r = -1 \tag{4.137}$$

So, it can be concluded that the contribution of the terms of the typologies g and h to the y-component of the tangential force acting on the rotor is given as:

$$F_{yt}^{(g,h)} = \begin{cases} -h\dfrac{\pi^2}{2}\dfrac{\delta Lr}{\mu_0\tau}B_{Sk}B_{Rh}\cos\left[hp_r\Delta\theta \mp \varphi(t)\right] & \text{if} \quad kp_s - hp_r = 1 \\ h\dfrac{\pi^2}{2}\dfrac{\delta Lr}{\mu_0\tau}B_{Sk}B_{Rh}\cos\left[hp_r\Delta\theta \mp \varphi(t)\right] & \text{if} \quad kp_s - hp_r = -1 \end{cases} \tag{4.138}$$

As in the previous, this contribution has to be considered in the interaction between everyone of the current space vector s_{v1}, s_{v2}, and the rotor magnetic field produced by the magnets (4.139), (4.140):

$$F_{yt}^{(g)} = \begin{cases} -h\frac{\pi^2}{2}\frac{\delta Lr}{\mu_0\tau}B_{Sk1}B_{Rh}\cos\left[hp_r\Delta\theta \mp \varphi_1(t)\right] & \text{if} \quad k_1p_s - hp_r = 1 \\ h\frac{\pi^2}{2}\frac{\delta Lr}{\mu_0\tau}B_{Sk1}B_{Rh}\cos\left[hp_r\Delta\theta \mp \varphi_1(t)\right] & \text{if} \quad k_1p_s - hp_r = -1 \end{cases} \tag{4.139}$$

$$F_{yt}^{(h)} = \begin{cases} -h\frac{\pi^2}{2}\frac{\delta Lr}{\mu_0\tau}B_{Sk2}B_{Rh}\cos\left[hp_r\Delta\theta \mp \varphi_2(t)\right] & \text{if} \quad k_2p_s - hp_r = 1 \\ h\frac{\pi^2}{2}\frac{\delta Lr}{\mu_0\tau}B_{Sk2}B_{Rh}\cos\left[hp_r\Delta\theta \mp \varphi_2(t)\right] & \text{if} \quad k_2p_s - hp_r = -1 \end{cases} \tag{4.140}$$

The last typologies to analyze are b and d, related to the equations (4.92), (4.94):

$$F_{yt}^{(b)} = -Lr\int_0^{2\pi} -\frac{k_1\delta\pi}{\mu_0\tau}B_{Sk1}B_{Sk2}\sin\left[k_1p_s\theta_s \mp \varphi_1\right]\cos\left[k_2p_s\theta_s \mp \varphi_2\right]\sin\theta_s d\theta_s \tag{4.141}$$

By applying (4.110) to (4.141), it gives (4.142):

$$F_{yt}^{(b)} = \frac{1}{2}\frac{\delta\pi}{\mu_0\tau}k_1B_{Sk1}B_{Sk2}Lr\left\{\int_0^{2\pi}\sin\left[(k_1p_s + k_2p_s)\theta_s \mp \varphi_1 \mp \varphi_2\right]\sin\theta_s d\theta_s + \right. \\ \left. + \int_0^{2\pi}\sin\left[(k_1p_s - k_2p_s)\theta_s \mp \varphi_1 \pm \varphi_2\right]\sin\theta_s d\theta_s\right\} \tag{4.142}$$

By using (4.105) in (4.142):

$$F_{yt}^{(b)} = \frac{1}{4}\frac{\delta\pi}{\mu_0\tau}k_1B_{Sk1}B_{Sk2}Lr\left\{\int_0^{2\pi}\cos\left[(k_1p_s + k_2p_s - 1)\theta_s \mp \varphi_1 \mp \varphi_2\right]d\theta_s + \right.$$
$$- \int_0^{2\pi}\cos\left[(k_1p_s + k_2p_s + 1)\theta_s \mp \varphi_1 \mp \varphi_2\right]d\theta_s + \int_0^{2\pi}\cos\left[(k_1p_s - k_2p_s - 1)\theta_s \mp \varphi_1 \pm \varphi_2\right]d\theta_s +$$
$$\left. - \int_0^{2\pi}\cos\left[(k_1p_s - k_2p_s + 1)\theta_s \mp \varphi_1 \pm \varphi_2\right]d\theta_s\right\} \tag{4.143}$$

As done in the previous, the assumptions (4.144), (4.145) are to be considered not valid:

$$k_1 p_s + k_2 p_s - 1 = 0 \qquad \Rightarrow \qquad k_1 p_s + k_2 p_s = 1 \tag{4.144}$$

$$k_1 p_s + k_2 p_s + 1 = 0 \qquad \Rightarrow \qquad k_1 p_s + k_2 p_s = -1 \tag{4.145}$$

So, let us to examine the hypothesis (4.146):

$$k_1 p_s - k_2 p_s - 1 = 0 \qquad \Rightarrow \qquad k_1 p_s - k_2 p_s = 1 \tag{4.146}$$

By using (4.146) in (4.143), it gives:

$$F_{yt}^{(b)} = \frac{1}{4}\frac{\delta\pi}{\mu_0\tau} k_1 B_{Sk1} B_{Sk2} Lr \left\{ \int_0^{2\pi} cos\left[2(k_1 p_s - 1)\theta_s \mp \varphi_1 \mp \varphi_2\right] d\theta_s + \right.$$
$$\left. - \int_0^{2\pi} cos\left[2k_1 p_s \theta_s \mp \varphi_1 \mp \varphi_2\right] d\theta_s + \int_0^{2\pi} cos\left[\mp \varphi_1 \pm \varphi_2\right] d\theta_s - \int_0^{2\pi} cos\left[2\theta_s \mp \varphi_1 \pm \varphi_2\right] d\theta_s \right\} \tag{4.147}$$

By executing the integrals in (4.147):

$$F_{yt}^{(b)} = \frac{1}{4}\frac{\delta\pi}{\mu_0\tau} k_1 B_{Sk1} B_{Sk2} Lr \left\{ \frac{1}{2(k_1 p_s - 1)} \left[sin\left[2(k_1 p_s - 1)\theta_s \mp \varphi_1 \mp \varphi_2\right] \right]_0^{2\pi} + \right.$$
$$- \frac{1}{2k_1 p_s} \left[sin\left(2k_1 p_s \theta_s \mp \varphi_1 \mp \varphi_2\right) \right]_0^{2\pi} + 2\pi\, cos\left(\mp \varphi_1 \pm \varphi_2\right) + \tag{4.148}$$
$$\left. - \frac{1}{2} \left[sin\left(2\theta_s \mp \varphi_1 \pm \varphi_2\right) \right]_0^{2\pi} \right\}$$

The third term of (4.148) is the only not null contribution to the force:

$$F_{yt}^{(b)} = k_1 \frac{\pi^2}{2} \frac{\delta Lr}{\mu_0\tau} B_{Sk1} B_{Sk2}\, cos\left[\mp \varphi_1(t) \pm \varphi_2(t)\right] \qquad \text{if} \quad k_1 p_s - k_2 p_s = 1 \tag{4.149}$$

Let us suppose that (4.150) is verified:

$$k_1 p_s - k_2 p_s + 1 = 0 \qquad \Rightarrow \qquad k_1 p_s - k_2 p_s = -1 \tag{4.150}$$

By using (4.150) in (4.143), it gives:

$$F_{yt}^{(b)} = \frac{1}{4}\frac{\delta\pi}{\mu_0\tau}k_1 B_{Sk1}B_{Sk2}Lr\left\{\int_0^{2\pi} cos\left[2k_1 p_s\theta_s \mp \varphi_1 \mp \varphi_2\right]d\theta_s + \right.$$
$$-\int_0^{2\pi} cos\left[2(k_1 p_s+1)\theta_s \mp \varphi_1 \mp \varphi_2\right]d\theta_s + \int_0^{2\pi} cos\left[-2\theta_s \mp \varphi_1 \pm \varphi_2\right]d\theta_s + \quad (4.151)$$
$$\left.-\int_0^{2\pi} cos\left[\mp \varphi_1 \pm \varphi_2\right]d\theta_s\right\}$$

By executing the integrals in (4.151):

$$F_{yt}^{(b)} = \frac{1}{4}\frac{\delta\pi}{\mu_0\tau}k_1 B_{Sk1}B_{Sk2}Lr\left\{\frac{1}{2k_1 p_s}\left[sin\left[2k_1 p_s\theta_s \mp \varphi_1 \mp \varphi_2\right]\right]_0^{2\pi} + \right.$$
$$-\frac{1}{2(k_1 p_s+1)}\left[sin\left[2(k_1 p_s+1)\theta_s \mp \varphi_1 \mp \varphi_2\right]\right]_0^{2\pi} - \frac{1}{2}\left[sin(-2\theta_s \mp \varphi_1 \pm \varphi_2)\right]_0^{2\pi} + \quad (4.152)$$
$$\left.-2\pi\, cos(\mp \varphi_1 \pm \varphi_2)\right\}$$

The only not null contribution to the force is the fourth term of (4.152):

$$F_{yt}^{(b)} = -k_1\frac{\pi^2}{2}\frac{\delta Lr}{\mu_0\tau}B_{Sk1}B_{Sk2}\,cos\left[\mp\varphi_1(t)\pm\varphi_2(t)\right] \qquad \text{if} \quad k_1 p_s - k_2 p_s = -1 \quad (4.153)$$

So, it can be concluded that the contribution of the term of the typology b to the y-component of the tangential force acting on the rotor is given as:

$$F_{yt}^{(b)} = \begin{cases} k_1\dfrac{\pi^2}{2}\dfrac{\delta Lr}{\mu_0\tau}B_{Sk1}B_{Sk2}\,cos\left[\mp\varphi_1(t)\pm\varphi_2(t)\right] & \text{if} \quad k_1 p_s - k_2 p_s = 1 \\ -k_1\dfrac{\pi^2}{2}\dfrac{\delta Lr}{\mu_0\tau}B_{Sk1}B_{Sk2}\,cos\left[\mp\varphi_1(t)\pm\varphi_2(t)\right] & \text{if} \quad k_1 p_s - k_2 p_s = -1 \end{cases} \quad (4.154)$$

Without the need to execute the whole calculation, the contribution of the term of the typology d can be determined by analogy with respect to (4.154):

$$F_{yt}^{(d)} = \begin{cases} -k_2\dfrac{\pi^2}{2}\dfrac{\delta Lr}{\mu_0\tau}B_{Sk1}B_{Sk2}\,cos\left[\pm\varphi_1(t)\mp\varphi_2(t)\right] & \text{if} \quad k_1 p_s - k_2 p_s = 1 \\ k_2\dfrac{\pi^2}{2}\dfrac{\delta Lr}{\mu_0\tau}B_{Sk1}B_{Sk2}\,cos\left[\pm\varphi_1(t)\mp\varphi_2(t)\right] & \text{if} \quad k_1 p_s - k_2 p_s = -1 \end{cases} \quad (4.155)$$

4.4.3 Projections of the tangential force

The components related to the x-projection were calculated in a very similar way to that shown in the case of y-projection; only the final results being reported here. In the following are listed all the contributions to the *y*-projection (4.156)-(4.161) and *x*-projection (4.162)-(4.167) of the tangential component of the force. Note that the equations (4.160), (4.161) and (4.166), (4.167) related to the interactions between different harmonic orders of the same current space vector s_{v2}, were determined by analogy. The resultant tangential force is given by adding all the terms, respectively along the x and y axis.

$$F_{yt}^{(k_1,k_2)} = \begin{cases} \sum_{k_1} k_1 \frac{\pi^2}{2} \frac{\delta Lr}{\mu_0 \tau} B_{Sk_1} B_{Sk_2} \cos\left[\mp \varphi_1 \pm \varphi_2\right] & \forall\, k_2 = \frac{-1 + k_1 p_s}{p_s} \in N \\ \sum_{k_1} -k_1 \frac{\pi^2}{2} \frac{\delta Lr}{\mu_0 \tau} B_{Sk_1} B_{Sk_2} \cos\left[\mp \varphi_1 \pm \varphi_2\right] & \forall\, k_2 = \frac{1 + k_1 p_s}{p_s} \in N \end{cases}$$

$$\text{with :} \quad \frac{k_1 \mp s_{v1}}{m} \in N_0 \quad \wedge \quad \frac{k_2 \mp s_{v2}}{m} \in N_0$$

(4.156)

$$F_{yt}^{(k_2,k_1)} = \begin{cases} \sum_{k_1} -k_2 \frac{\pi^2}{2} \frac{\delta Lr}{\mu_0 \tau} B_{Sk_1} B_{Sk_2} \cos\left[\pm \varphi_1 \mp \varphi_2\right] & \forall\, k_2 = \frac{-1 + k_1 p_s}{p_s} \in N \\ \sum_{k_1} k_2 \frac{\pi^2}{2} \frac{\delta Lr}{\mu_0 \tau} B_{Sk_1} B_{Sk_2} \cos\left[\pm \varphi_1 \mp \varphi_2\right] & \forall\, k_2 = \frac{1 + k_1 p_s}{p_s} \in N \end{cases}$$

$$\text{with :} \quad \frac{k_1 \mp s_{v1}}{m} \in N_0 \quad \wedge \quad \frac{k_2 \mp s_{v2}}{m} \in N_0$$

(4.157)

$$F_{yt}^{(k_1,h)} = \begin{cases} \sum_{k_1} (k_1 - h)\frac{\pi^2}{2}\frac{\delta L r}{\mu_0 \tau} B_{Sk1} B_{Rh} \cos\left[h p_r \Delta\theta \mp \varphi_1\right] & \forall\ h = \frac{-1 + k_1 p_s}{p_r} \in N_{odd} \\ \sum_{k_1} (h - k_1)\frac{\pi^2}{2}\frac{\delta L r}{\mu_0 \tau} B_{Sk1} B_{Rh} \cos\left[h p_r \Delta\theta \mp \varphi_1\right] & \forall\ h = \frac{1 + k_1 p_s}{p_r} \in N_{odd} \end{cases}$$

$$\text{with}: \quad \frac{k_1 \mp s_{v1}}{m} \in N_0 \quad \wedge \quad h \in N_{odd}$$

(4.158)

$$F_{yt}^{(k_2,h)} = \begin{cases} \sum_{k_2} (k_2 - h)\frac{\pi^2}{2}\frac{\delta L r}{\mu_0 \tau} B_{Sk2} B_{Rh} \cos\left[h p_r \Delta\theta \mp \varphi_2\right] & \forall\ h = \frac{-1 + k_2 p_s}{p_r} \in N_{odd} \\ \sum_{k_2} (h - k_2)\frac{\pi^2}{2}\frac{\delta L r}{\mu_0 \tau} B_{Sk2} B_{Rh} \cos\left[h p_r \Delta\theta \mp \varphi_2\right] & \forall\ h = \frac{1 + k_2 p_s}{p_r} \in N_{odd} \end{cases}$$

$$\text{with}: \quad \frac{k_2 \mp s_{v2}}{m} \in N_0 \quad \wedge \quad h \in N_{odd}$$

(4.159)

$$F_{yt}^{(k_2,k_{2'})} = \begin{cases} \sum_{k_2} k_2 \frac{\pi^2}{2}\frac{\delta L r}{\mu_0 \tau} B_{Sk_2} B_{Sk_{2'}} \cos\left[\mp \varphi_2 \pm \varphi_{2'}\right] & \forall\ k_2' = \frac{-1 + k_2 p_s}{p_s} \in N \\ \sum_{k_2} -k_2 \frac{\pi^2}{2}\frac{\delta L r}{\mu_0 \tau} B_{Sk_2} B_{Sk_{2'}} \cos\left[\mp \varphi_2 \pm \varphi_{2'}\right] & \forall\ k_2' = \frac{1 + k_2 p_s}{p_s} \in N \end{cases}$$

$$\text{with}: \quad \frac{k_2 \mp s_{v2}}{m} \in N_0 \quad \wedge \quad \frac{k_2' \mp s_{v2}}{m} \in N_0$$

(4.160)

$$F_{yt}^{(k_{2'},k_2)} = \begin{cases} \sum_{k_2} -k_2' \frac{\pi^2}{2} \frac{\delta Lr}{\mu_0 \tau} B_{Sk_2} B_{Sk_{2'}} cos\left[\pm \varphi_2 \mp \varphi_{2'}\right] & \forall\ k_2' = \frac{-1 + k_2 p_s}{p_s} \in N \\ \sum_{k_2} k_2' \frac{\pi^2}{2} \frac{\delta Lr}{\mu_0 \tau} B_{Sk_2} B_{Sk_{2'}} cos\left[\pm \varphi_2 \mp \varphi_{2'}\right] & \forall\ k_2' = \frac{1 + k_2 p_s}{p_s} \in N \end{cases}$$

$$\text{with :} \quad \frac{k_2 \mp s_{v2}}{m} \in N_0 \quad \wedge \quad \frac{k_2' \mp s_{v2}}{m} \in N_0$$

(4.161)

$$F_{xt}^{(k_1,k_2)} = \sum_{k_1} -k_1 \frac{\pi^2}{2} \frac{\delta Lr}{\mu_0 \tau} B_{Sk_1} B_{Sk_2} sin\left[\mp \varphi_1 \pm \varphi_2\right] \quad \begin{cases} \forall\ k_2 = \frac{-1 + k_1 p_s}{p_s} \in N \\ \forall\ k_2 = \frac{1 + k_1 p_s}{p_s} \in N \end{cases}$$

$$\text{with :} \quad \frac{k_1 \mp s_{v1}}{m} \in N_0 \quad \wedge \quad \frac{k_2 \mp s_{v2}}{m} \in N_0$$

(4.162)

$$F_{xt}^{(k_2,k_1)} = \sum_{k_1} -k_2 \frac{\pi^2}{2} \frac{\delta Lr}{\mu_0 \tau} B_{Sk_1} B_{Sk_2} sin\left[\pm \varphi_1 \mp \varphi_2\right] \quad \begin{cases} \forall\ k_2 = \frac{-1 + k_1 p_s}{p_s} \in N \\ \forall\ k_2 = \frac{1 + k_1 p_s}{p_s} \in N \end{cases}$$

$$\text{with :} \quad \frac{k_1 \mp s_{v1}}{m} \in N_0 \quad \wedge \quad \frac{k_2 \mp s_{v2}}{m} \in N_0$$

(4.163)

$$F_{xt}^{(k_1,h)} = \sum_{k_1} (h - k_1) \frac{\pi^2}{2} \frac{\delta L r}{\mu_0 \tau} B_{Sk1} B_{Rh} \, sin\left[h p_r \Delta\theta \mp \varphi_1\right] \quad \begin{cases} \forall\ h = \dfrac{-1 + k_1 p_s}{p_r} \in N_{odd} \\ \forall\ h = \dfrac{1 + k_1 p_s}{p_r} \in N_{odd} \end{cases}$$

$$\text{with :} \quad \frac{k_1 \mp s_{v1}}{m} \in N_0 \quad \wedge \quad h \in N_{odd}$$

(4.164)

$$F_{xt}^{(k_2,h)} = \sum_{k_2} (h - k_2) \frac{\pi^2}{2} \frac{\delta L r}{\mu_0 \tau} B_{Sk2} B_{Rh} \, sin\left[h p_r \Delta\theta \mp \varphi_2\right] \quad \begin{cases} \forall\ h = \dfrac{-1 + k_2 p_s}{p_r} \in N_{odd} \\ \forall\ h = \dfrac{1 + k_2 p_s}{p_r} \in N_{odd} \end{cases}$$

$$\text{with :} \quad \frac{k_2 \mp s_{v2}}{m} \in N_0 \quad \wedge \quad h \in N_{odd}$$

(4.165)

$$F_{xt}^{(k_2,k_{2'})} = \sum_{k_2} -k_2 \frac{\pi^2}{2} \frac{\delta L r}{\mu_0 \tau} B_{Sk_2} B_{Sk_{2'}} \, sin\left[\mp \varphi_2 \pm \varphi_{2'}\right] \quad \begin{cases} \forall\ k_2' = \dfrac{-1 + k_2 p_s}{p_s} \in N \\ \forall\ k_2' = \dfrac{1 + k_2 p_s}{p_s} \in N \end{cases}$$

$$\text{with :} \quad \frac{k_2 \mp s_{v2}}{m} \in N_0 \quad \wedge \quad \frac{k_2' \mp s_{v2}}{m} \in N_0$$

(4.166)

$$F_{xt}^{(k_{2'},k_2)} = \sum_{k_2} -k_2' \frac{\pi^2}{2} \frac{\delta L r}{\mu_0 \tau} B_{Sk_2} B_{Sk_{2'}} \, sin\left[\pm \varphi_2 \mp \varphi_{2'}\right] \quad \begin{cases} \forall\ k_2' = \dfrac{-1 + k_2 p_s}{p_s} \in N \\ \forall\ k_2' = \dfrac{1 + k_2 p_s}{p_s} \in N \end{cases}$$

$$\text{with :} \quad \frac{k_2 \mp s_{v2}}{m} \in N_0 \quad \wedge \quad \frac{k_2' \mp s_{v2}}{m} \in N_0$$

(4.167)

The same considerations done for the equation (4.53), related to the meaning of k_2 and $k_2^{'}$, are valid for equations (4.160), (4.161), (4.166), (4.167).

4.5 Simulations and results

An electrical machine suitable for bearingless application (Tab. II) was analyzed in order to validate the relationships presented in the previous chapters, making a comparison with the results of the 2D FEA software "FEMM 4.2" [14].

TABLE II. DATA OF THE MACHINE

Param.	Description	Value
N_{sl}	number of slots	30
p	pole pairs of the machine	1
m	number of phases	5
I_n	rated phase current (A_{rms})	64.68
T_n	rated torque (Nm)	30.29
g	airgap width (mm)	1
D_e	stator outer diameter (mm)	230
D_s	stator inner diameter (mm)	120
D_m	mean diameter of the magnet (mm)	116
D_{cv_ext}	diameter at the bottom of the slot (mm)	170
D_{cv_int}	diameter at the top of the slot (mm)	126.3
D_r	rotor outer diameter (mm)	114
D_{alb}	rotor inner diameter (mm)	60
α_{Ldg}	angle underlying the tooth surface	10.1°
α_{sap}	semi-angle underlying the slot opening	0.95°
α_m	angle underlying the magnet	172°
α_{cv}	slot pitch angle	12°
a_{dt}	stator slot height (mm)	25
h_{cl}	slot opening height (mm)	1
L	axial length of the machine (mm)	180
L_m	magnet width (mm)	2
L_{dt}	tooth-body width (mm)	8
L_{cl}	slot opening width (mm)	2
L_{tc}	slot width at the top slot radius (mm)	5.23
L_{fc}	slot width at the bottom slot radius (mm)	9.7
τ_{cv}	slot pitch at the inner stator radius (mm)	12.57

The analysis was carried out considering only the normal components of the force, after having verified that the contributions of tangential components are negligible, by applying phase currents given by the sum of the two space vectors $s_{v1} = 1$ and $s_{v2} = 2$. As a general criterion, the torque current space vector is maintained in leading by 90 electrical degrees with respect to the rotor position in order to reach the maximum torque per ampere behavior of the motor. In the following, the force is calculated by varying the phase angle φ_2 related to the levitation current space vector. From (4.52), (4.82) it is possible to determine the relationship between the direction of the force φ_{Fr}, measured with respect to y-axis and positive when clockwise-oriented, the phase φ_2 and the angular position of the rotor $\Delta\theta$, obtaining:

$$\varphi_{Fr}^{(k_2,h)} = atn\left(\frac{F_{xn}^{(k_2,h)}}{F_{yn}^{(k_2,h)}}\right) = hp_r\Delta\theta \mp \varphi_2, \quad \forall\, h = \frac{1 + k_2 p_s}{p_r} \in N_{odd} \tag{4.168}$$

$$\varphi_{Fr}^{(k_2,h)} = atn\left(\frac{F_{xn}^{(k_2,h)}}{F_{yn}^{(k_2,h)}}\right) = -\left(hp_r\Delta\theta \mp \varphi_2\right), \quad \forall\, h = \frac{-1 + k_2 p_s}{p_r} \in N_{odd} \tag{4.169}$$

Considering the effects of the second spatial harmonic component of the stator magneto-motive force ($k_2 = 2$) which interacts with the first spatial harmonic component of the PM ($h = 1$), (4.169) allows to calculate the direction of the force φ_{Fr} by means of the following relationship:

$$\varphi_{Fr}^{(2,1)} = \varphi_2 - \Delta\theta \tag{4.170}$$

In the equation is considered only the interaction between the main harmonic orders of the levitation current space vector and the rotor magnetic field: this is the usual approach when designing a control system for bearingless machines, following the relationship (4.170). In multiphase machines this can produce mistakes in determining both the module and the spatial phase of the radial force,

due to the interactions between the higher harmonic orders. The relationships (4.50)-(4.53) and (4.80)-(4.83), taking into account all the possible interactions, allows to calculate these errors in terms of differences, in module and phase of the radial forces, between the simplified prediction (4.170) and the actual function, representing the locus of radial force vector and allowing the appropriate corrections.

Figs. 4.2-4.3 show a comparison between the simplified equation "main harmonic orders" (4.170) and the actual radial force vector determined by using both the "proposed method", both the FEA software. The analysis was conducted by varying the phase angle of levitation current φ_2 by multiple values of 22.5 electrical degrees. Particularly, in the Figs. 4.2-4.3 are shown the x- and y-components of the calculated radial force and the good agreement with the FE software results, represented by the red dots.

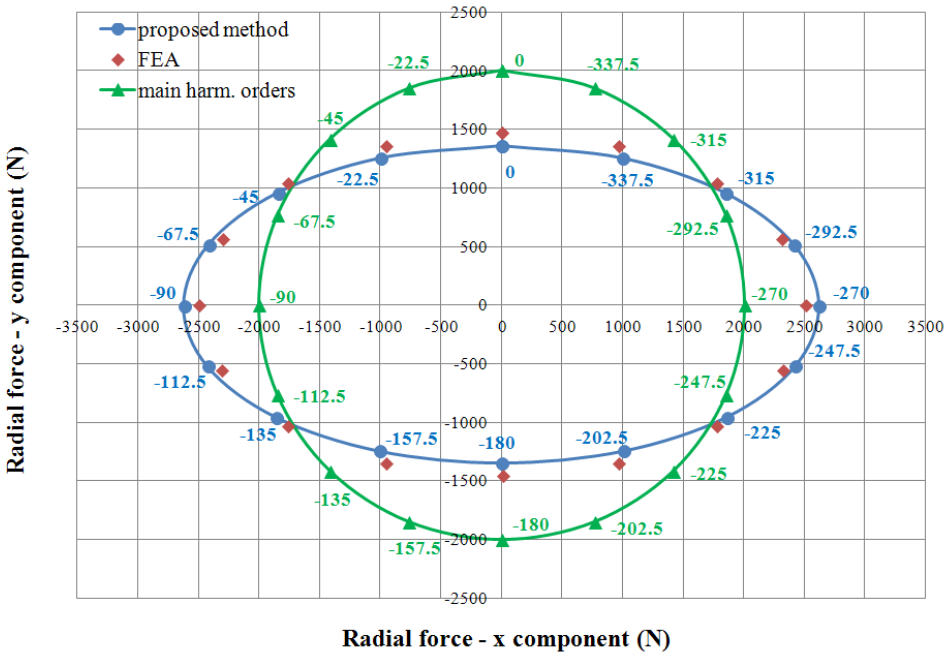

Fig. 4.2. y-component vs x-component of the radial force:
i_{sv1} = 0 A_{rms}, i_{sv2} = 45.74 A_{rms}, $\Delta\theta$ = 0 mech. degrees, n_{ac} = 10 (/15)

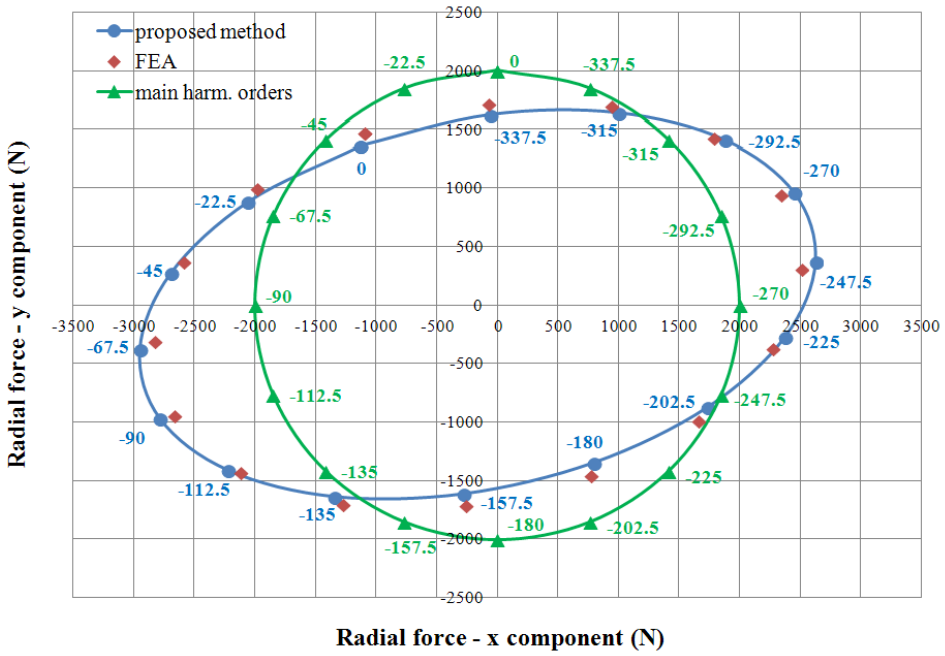

Fig. 4.3. *y*-component vs *x*-component of the radial force:
i_{sv1} = 45.74 A_{rms}, i_{sv2} = 45.74 A_{rms}, $\Delta\theta$ = 0 mech. degrees, n_{ac} = 10 (/15)

In this case, the magnet axis is aligned to the phase "1" axis, consequently $\Delta\theta$ = 0 and the phase φ_1 of the torque current space vector is 90 electrical degrees. By comparing Fig. 4.2 to Fig. 4.3, the value of $\bar{i}_{sv1}$ was changed from 0 to the rated value of 45.74 A_{rms}. As it is possible to see, the effect of the torque current space vector s_{v1} determines a counterclockwise rotation of the locus that describes the position of the resultant radial force vector. In fact, for a null value of the torque current space vector, the actual direction of the radial force is practically coinciding with that of the phase angle φ_2 related to the space vector s_{v2} given by (4.170), as shown in Fig. 4.2; the influence of $\bar{i}_{sv1}$ determines a significant change with respect to the actual value of φ_2 and the predicted one. The pitch winding is another important factor which influences the locus of radial force vector, that is represented by a nearly ellipsoidal shape only in the particular case of a shortened pitch winding, able to eliminate the third harmonic order

(corresponding to a n_{ac} value of 10).

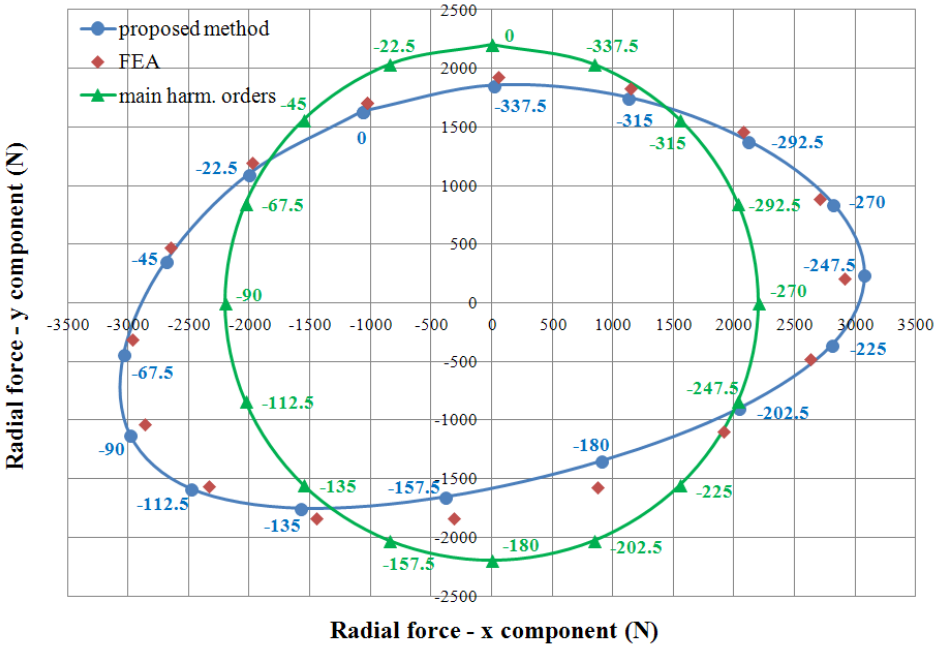

Fig. 4.4. y-component vs x-component of the radial force:
i_{sv1} = 45.74 A_{rms}, i_{sv2} = 45.74 A_{rms}, $\Delta\theta$ = 0 mech. degrees, n_{ac} = 9 (/15)

In general, by changing this value, the locus seems to be warped with respect to this ideal shape, as can be seen in Fig. 4.4 for a n_{ac} value of 9. In the Figs. 4.5-4.6, modulus and phase of the radial force are presented in terms of differences with respect to the values of the "main harmonic orders" locus: in this way, they give the corrections to be made in order to obtain the actual radial force vector.

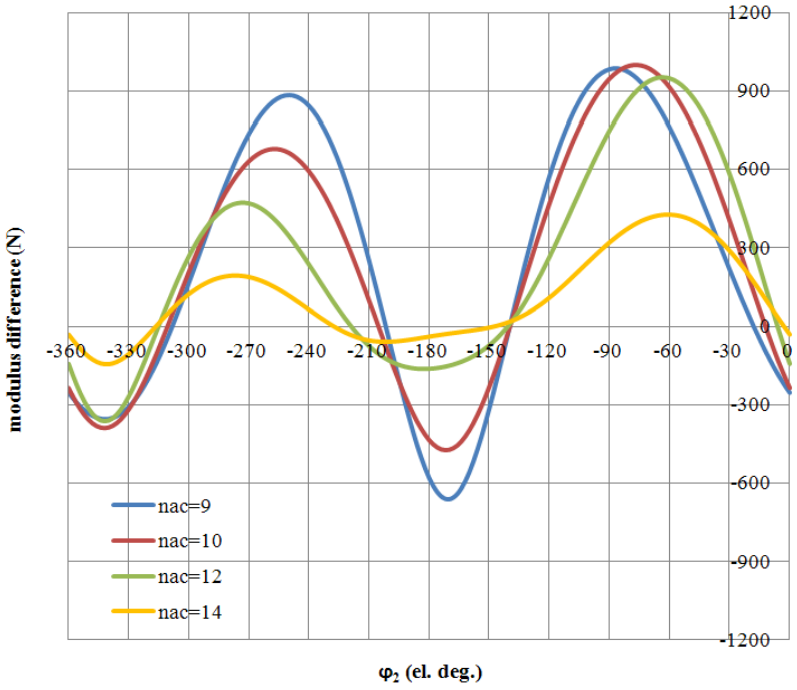

Fig. 4.5. Modulus of the difference of the radial force:
i_{sv1} = 45.74 A_{rms}, i_{sv2} = 45.74 A_{rms}, Δθ = 0 mech. Degrees

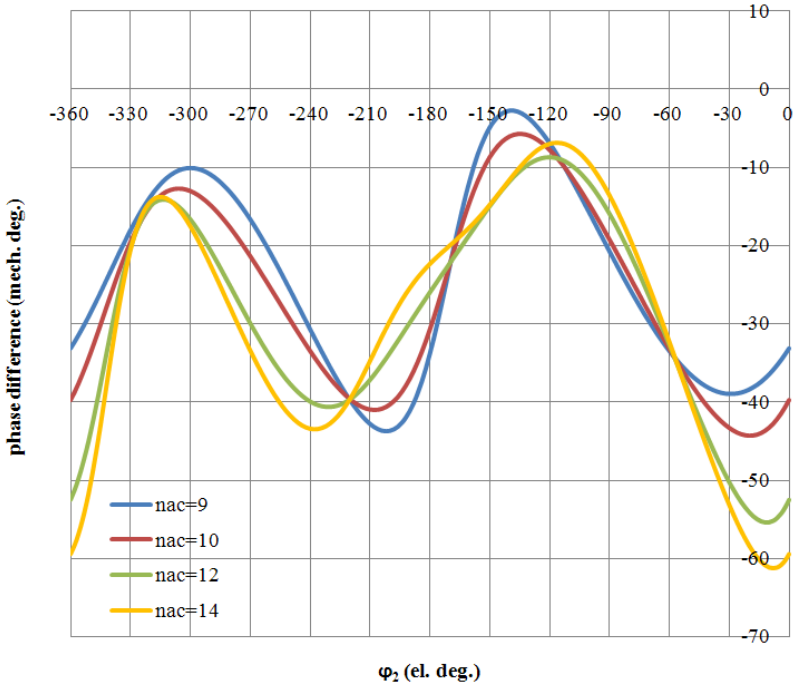

Fig. 4.6. Phase difference of the radial force:
i_{sv1} = 45.74 A_{rms}, i_{sv2} = 45.74 A_{rms}, Δθ = 0 mech. Degrees

The influence of the rotor position, for a fixed space vector $\bar{i}_{sv1}$, represents another analysis tool, shown in Figs. 4.7-4.8. In Fig. 4.7 the rms torque current is null, while in Fig. 4.8 is equal to the rated value of 45.74 A_{rms}. In every picture the magnet axis is rotated in three different positions with respect to phase "1" axis: 0, 45 and 90 mechanical degrees. The analysis shows a clockwise rotation of the locus by the same mechanical angle than the magnet axis, but is important to note that the position of the corresponding points, characterized by a same value of the phase φ_2, changes by the same amount but in a counterclockwise rotation.

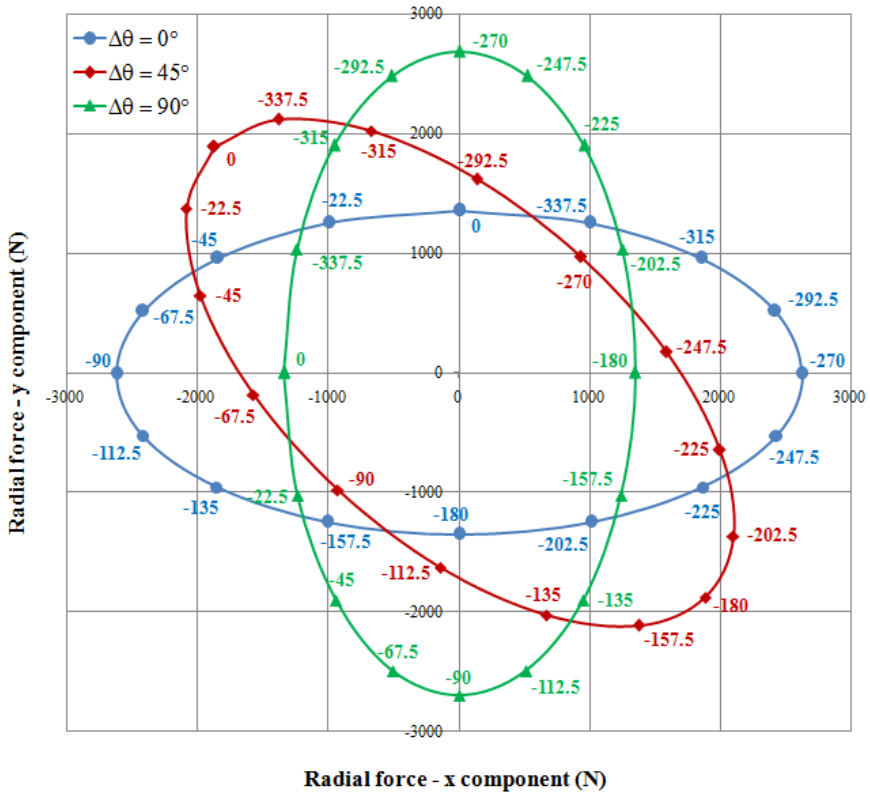

Fig. 4.7. *y*-component vs *x*-component of the radial force:
i_{sv1} = 0 A_{rms}, i_{sv2} = 45.74 A_{rms}, Δθ = 0, 45, 90 mech. degrees, n_{ac} = 10 (/15)

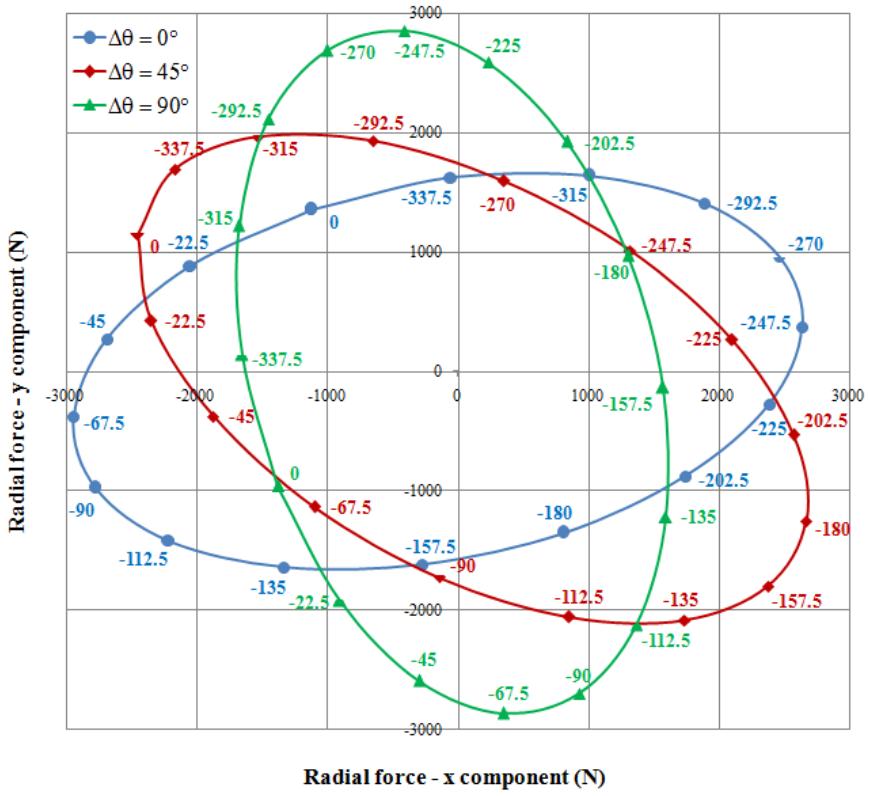

Fig. 4.8. *y*-component vs *x*-component of the radial force:
i_{sv1} = 45.74 A_{rms}, i_{sv2} = 45.74 A_{rms}, Δθ = 0, 45, 90 mech. degrees, n_{ac} = 10 (/15)

In the next will be shown an in-depth analysis, conducted with the presented algorithm by varying the main parameters in a large number of possible combinations, to highlight the influence of the magnet pitch, the rotor position and the coil pitch (α_m, $\Delta\theta$, n_{ac}); the rms values of the modulus of current space vectors i_{sv1}, i_{sv2} are fixed to their maximum value. The results are presented in terms of modulus and phase differences, showing in this way the corrections which can be applied to the simplified function "main harmonic orders" to obtain the absolute values of the modulus and difference of the force. All the quantities are determined as functions of the levitation current space vector phase angle φ_2.

$\alpha_m = 172°^{mech.}, i_{sv1} = 45.74\ A_{rms}, i_{sv2} = 45.74\ A_{rms}, \Delta\theta = 0°^{mech.}, n_{ac}$ varies

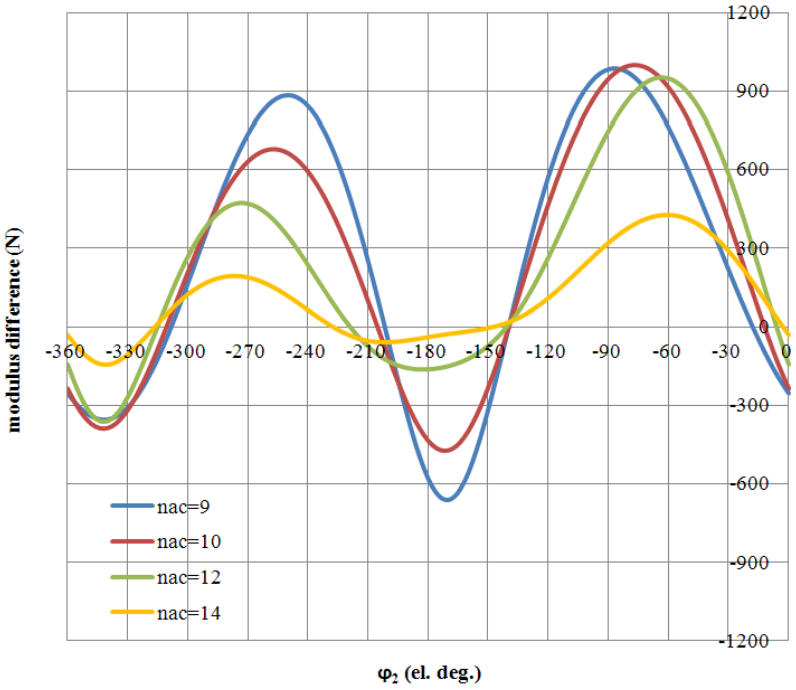

Fig. 4.9.

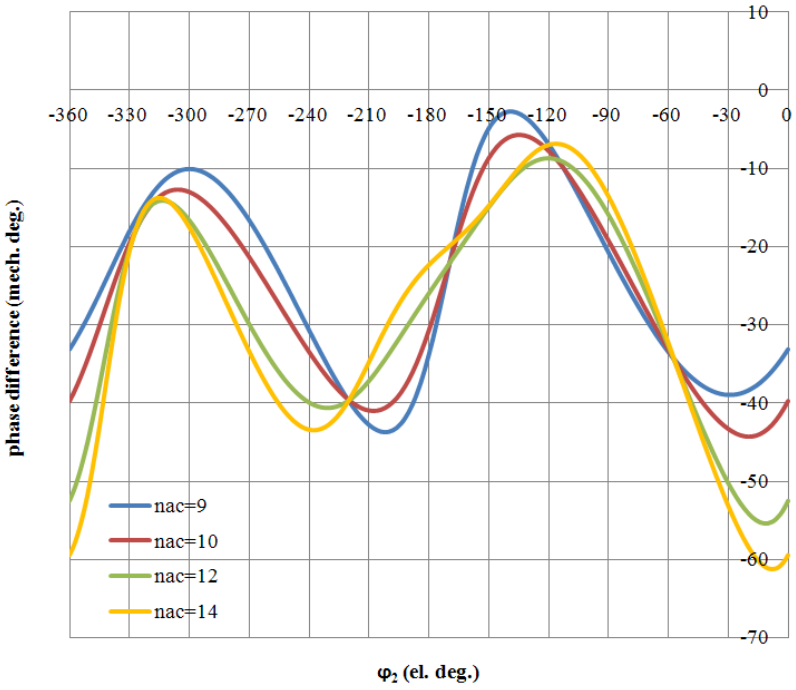

Fig. 4.10.

$\alpha_m = 172°^{mech.}, i_{sv1} = 45.74\ A_{rms}, i_{sv2} = 45.74\ A_{rms}, \Delta\theta = 45°^{mech.}, n_{ac}$ varies

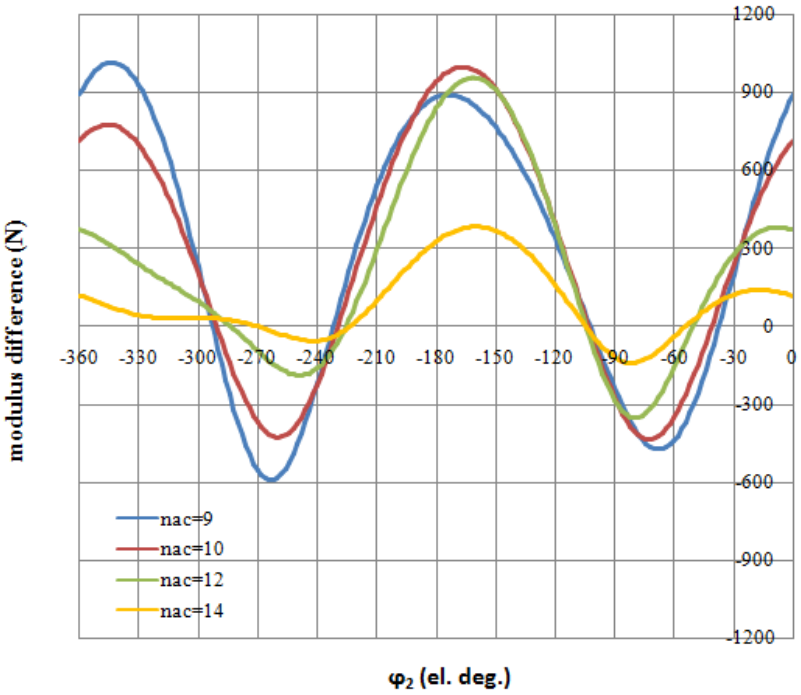

Fig. 4.11.

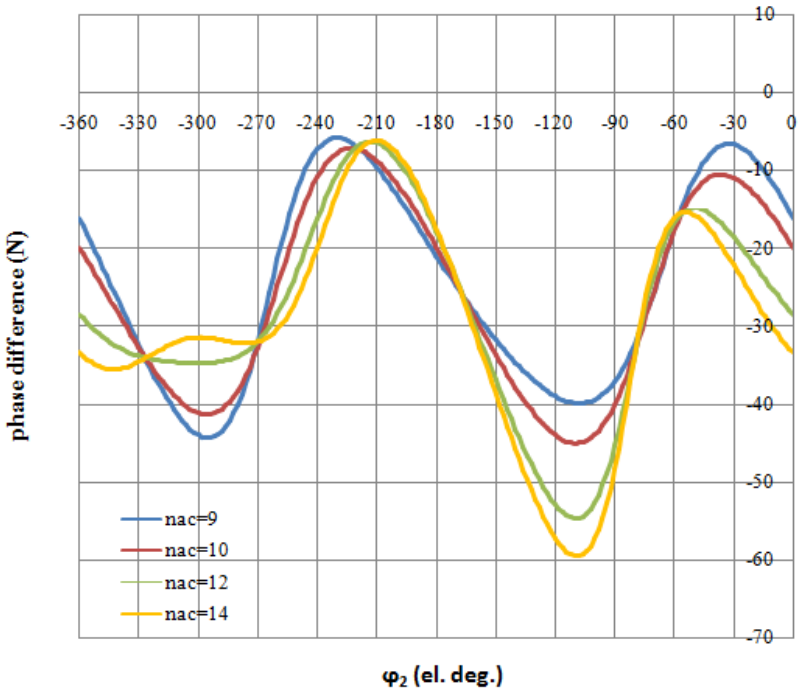

Fig. 4.12.

$\alpha_m = 120°^{mech.}, i_{sv1} = 45.74\ A_{rms}, i_{sv2} = 45.74\ A_{rms}, \Delta\theta = 0°^{mech.}, n_{ac}$ varies

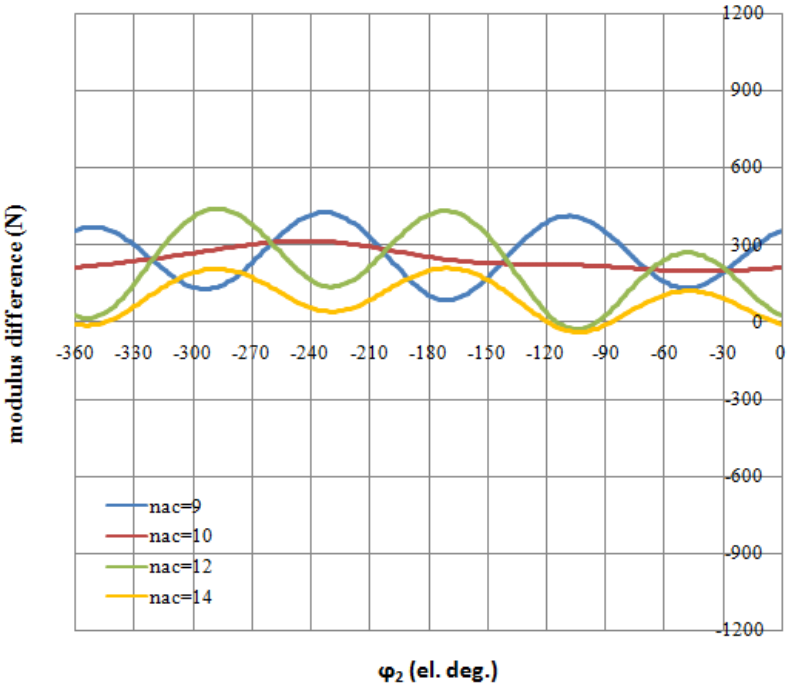

Fig. 4.13.

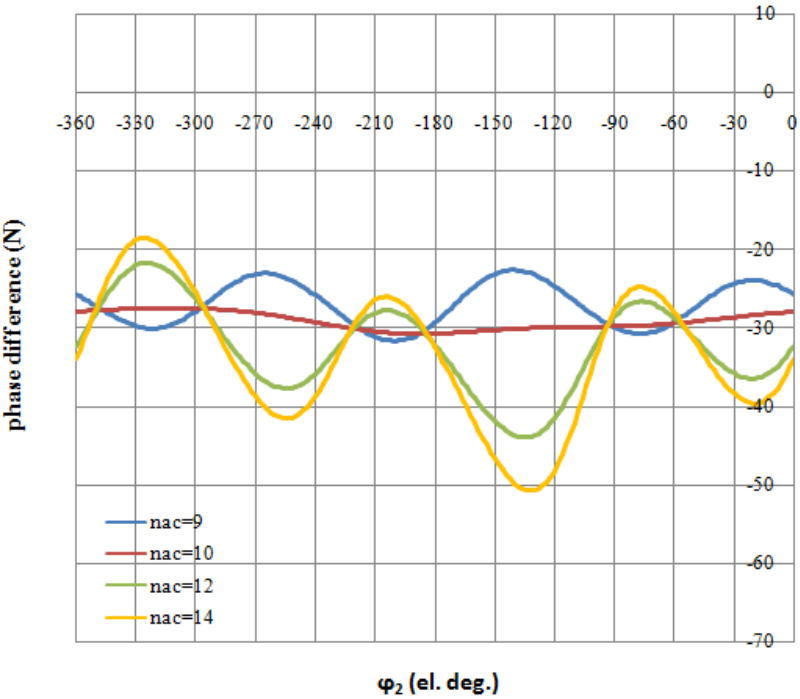

Fig. 4.14.

$\alpha_m = 90°^{mech.}, i_{sv1} = 45.74\ A_{rms}, i_{sv2} = 45.74\ A_{rms}, \Delta\theta = 0°^{mech.}, n_{ac}$ varies

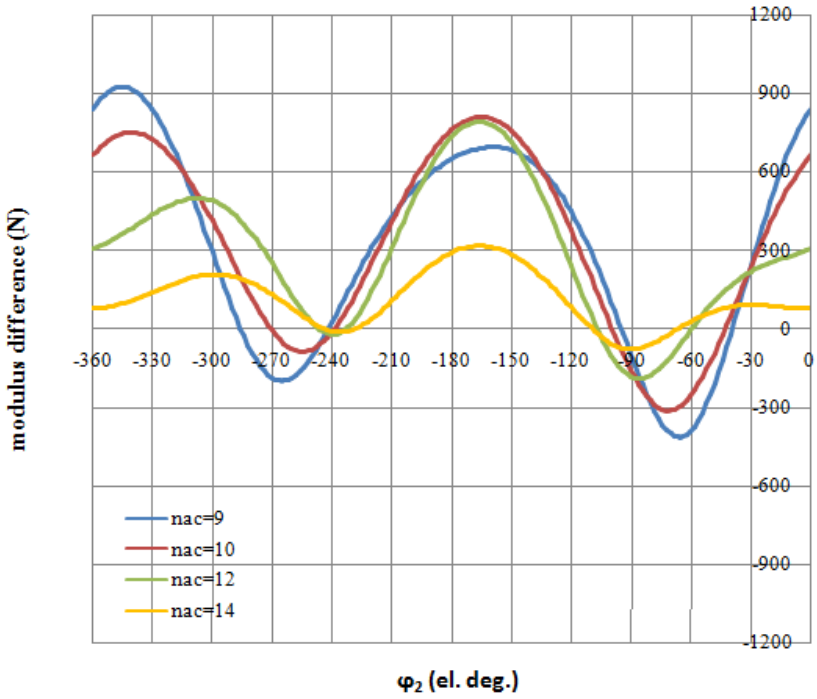

Fig. 4.15.

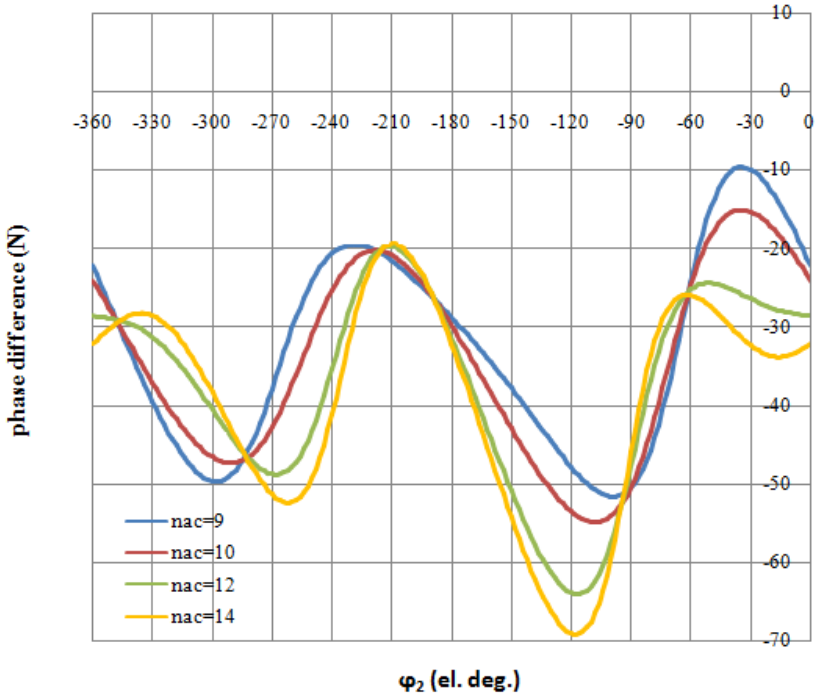

Fig. 4.16.

$\alpha_m = 90°^{mech.}, i_{sv1} = 45.74\ A_{rms}, i_{sv2} = 45.74\ A_{rms}, \Delta\theta = 90°^{mech.}, n_{ac}$ varies

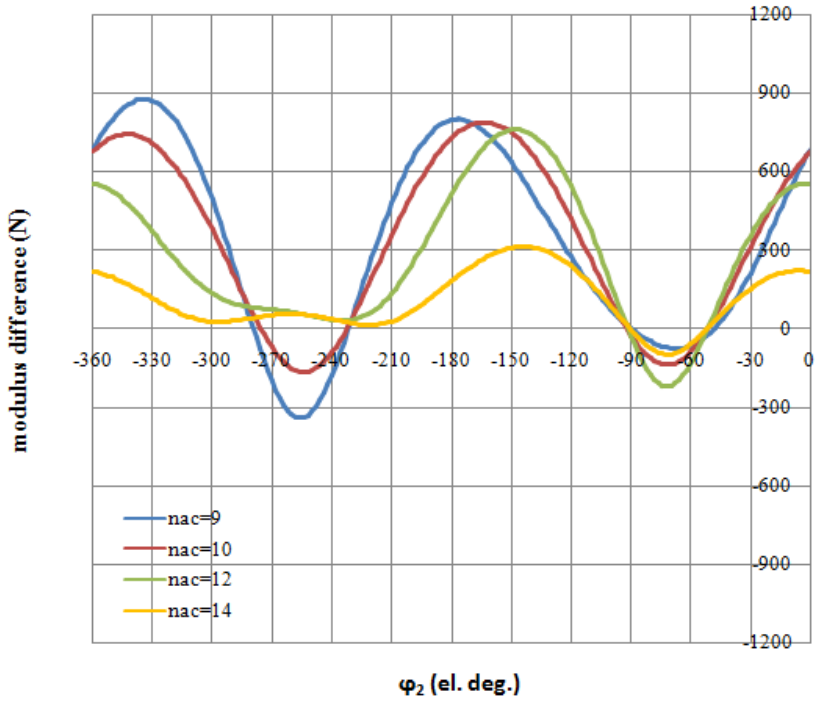

Fig. 4.17.

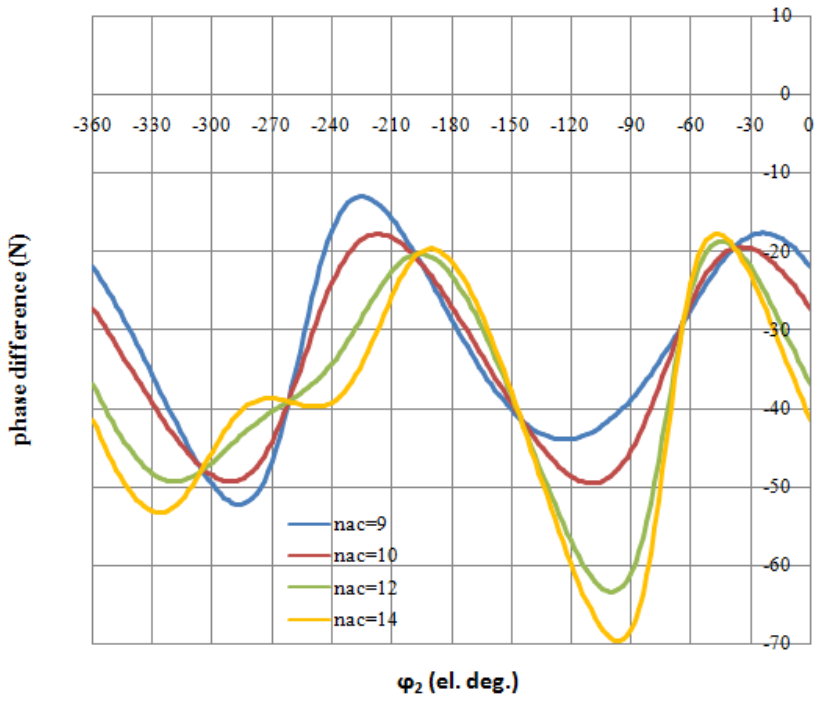

Fig. 4.18.

4.6 Conclusion

In this chapter an analytical model for radial forces calculation in multiphase bearingless Surface-Mounted Permanent Magnet Synchronous Motors (SPMSM) is presented. It allows to predict amplitude and direction of the force, depending on the values of the torque current, of the levitation current and of the rotor position. It is based on the space vectors method, letting the analysis of the machine not only in steady-state conditions but also during transients.

When designing a control system for bearingless machines, it is usual to consider only the interaction between the main harmonic orders of the stator and rotor magnetic fields: in multiphase machines this can produce mistakes in determining both the module and the spatial phase of the radial force, due to the interactions between the higher harmonic orders. The presented algorithm allows to calculate these errors, taking into account all the possible interactions; by representing the locus of radial force vector, it allows the appropriate corrections.

In addition, the algorithm permits to study whatever configuration of SPMSM machine, being parameterized as a function of the electrical and geometrical quantities, as the coil pitch, the width and length of the magnets, the rotor position, the amplitude and phase of current space vector, etc.

Finally, the results of the proposed method have been compared with those of a most used FEA software, obtaining very similar values of the analyzed quantities.

4.7 References

[1] T. Schneider and A. Binder, “Design and evaluation of a 60000 RPM permanent magnet bearingless high speed motor,” *Proc. Conf. on Power Electronics and Drive Systems*, Bangkok, Thailand, Nov. 27–30, 2007, pp. 1-8.

[2] A. Salazar, A. Chiba, T. Fukao, "A Review of Development in Bearingless Motors", *7th Int. Symp. on Magn. Bearings*, Zurich, Switzerland, Aug. 23-25, 2000, pp. 335-340.

[3] A. Chiba, T. Deido, T. Fukao, M.A. Rahman, "An Analysis of Bearingless AC Motors," *IEEE Trans. Energy Conversion*, vol. 9, no. 1, Mar. 1994, pp. 61-68.

[4] M. Ooshima, A. Chiba, T. Fukao, M. A. Rahman, “Design and Analysis of Permanent Magnet-Type Bearingless Motors” *IEEE Trans. on Industrial Electronics*, vol. 43, no. 2, Apr. 1996, pp. 292-299.

[5] S. W.-K. Khoo, "Bridge Configured Winding for Polyphase Self-Bearing Machines" *IEEE Trans. Magnetics*, vol. 41, no. 4, April. 2005, pp. 1289-1295.

[6] H. Xu, H. A. Toliyat, L. J. Petersen, "Rotor Field Oriented Control of a Five-Phase Induction Motor with the Combined Fundamental and Third Harmonic Currents", *Proc. APEC '01 Conf.*, Vol. 1, 2001, pp. 392-398.

[7] M. Kang, J. Huang, H.-b. Jiang, J.-q. Yang, “Principle and Simulation of a 5-Phase Bearingless Permanent Magnet-Type Synchronous Motor”, *International Conference on Electrical Machines and Systems*, pp. 1148-1152, 17-20 Oct. 2008.

[8] Y. Okada, S. Miyamoto, T. Ohishi, “Levitation and Torque Control of Internal Permanent Magnet Type Bearingless Motor”, *IEEE Transactions on Control Systems Technology*, Vol. 4, No. 5, September 1996, pp. 565-571.

[9] B. B. Choi, “Ultra-High-Power-Density Motor Being Developed for Future Aircraft”, in *NASA TM—2003-212296, Structural Mechanics and Dynamics Branch 2002 Annual Report*, pp. 21–22, Aug. 2003.

[10] Y. Chisti and M. Moo-Young, “Clean-in-place Systems for Industrial Bioreactors: Design, Validation and Operation”, *Journal of Industrial Microbiology and Biotechnology*, Vol. 13, pp. 201-207, July 1994.

[11] D. Casadei, D. Dujic, E. Levi, G. Serra, A. Tani, and L. Zarri, “General Modulation Strategy for Seven-Phase Inverters with Independent Control

of Multiple Voltage Space Vectors", *IEEE Trans. on Industrial Electronics*, Vol. 55, NO. 5, May 2008, pp. 1921-1932.

[12] L. Zarri, M. Mengoni, A. Tani, G. Serra, D. Casadei: "Minimization of the Power Losses in IGBT Multiphase Inverters with Carrier-Based Pulsewidth Modulation," *IEEE Trans. on Industrial Electronics*, Vol. 57, No. 11, November 2010, pp. 3695-3706.

[13] S. Serri, A. Tani, G. Serra, "A Method for Non-linear Analysis and Calculation of Torque and Radial Forces in Permanent Magnet Multiphase Bearingless Motors", *Int. Symp. on Power Electronics, Electrical Drives, Automation and Motion SPEEDAM 2012*, Sorrento, Italy, June 20-22, 2012, pp. 75-82.

[14] D. C. Meeker, 'Finite Element Method Magnetics', Version 4.2 (01Oct2011Build), http://www.femm.info

Appendix A4.1

MAGNETIC FIELD DISTRIBUTION IN THE AIRGAP OF MULTIPHASE ELECTRICAL MACHINES

A4.1.1 Introduction

In recent years, more and more advanced technologies and an impressive rise in the use of electronics, both in civil as in the industrial sector, given a contribution to reduce the cost of the components, allowing the use of complex technologies which in the past had high costs and therefore of little industrial interest. In the field of electrical machines this evolution led not only to the realization of power drives controlled by an inverter, capable of ensuring performance significantly better than those obtained with the previous control systems, but also the advent of a new type of machines with a different number of phases from the traditional three-phase, usually employed in generation and distribution of electric energy. This has reawakened the interest in the study of multi-phase electrical machines.

The field of study of polyphase machines is relatively new and in rapid evolution, but it is already possible to say that these machines are able to provide better performances of the classical ones, and precisely for this reason, are currently a matter of great interest. Indeed, the multiphase machines have several advantages compared to the traditional three-phase machines, such as the amplitude reduction and the increase of the frequency of pulsating torque, the reduction of stator phase current, the increase of the fault tolerance. In addition, the multiphase machines offer a larger number of degrees of freedom with respect to the three-phase machines, which can be used to improve the performances.

Furthermore, the creation of software for analyzing the behavior of magnetic fields in electromechanical devices, based on numerical methods as the FEA, has greatly contributed to the improvement in the design of electrical machines by introducing, in addition to an excellent accuracy of the results, also a considerable saving of time and money.

A4.1.2 The multiphase rotating magnetic field

For an in-depth understanding on the topic of multi-phase machines, making a brief reference to the theory of the rotating magnetic field, in steady state conditions, to better understand the equations that will be proposed in the following sections.

By supposing to operate in linear regime, with an iron magnetic permeability of infinite value, it can be concluded that there are no appreciable drops of magneto-motive force (mmf) in the iron, considering in this region a null value for the magnetic field.

Thus the study is conducted only in the airgap, considering the hypothesis of the representation along a straight line, as in Fig. A4.1-1, the distribution of

the current density $\bar{J}(x,y,z)$ being only by means of z-component (A4.1-6); the current sources are located in the slots and considered as concentrated in a point. With reference to the Maxwell's equations, develop the first of (A4.1-1):

$$\begin{cases} rot\bar{H} = \bar{J} \\ div\bar{B} = 0 \end{cases} \tag{A4.1-1}$$

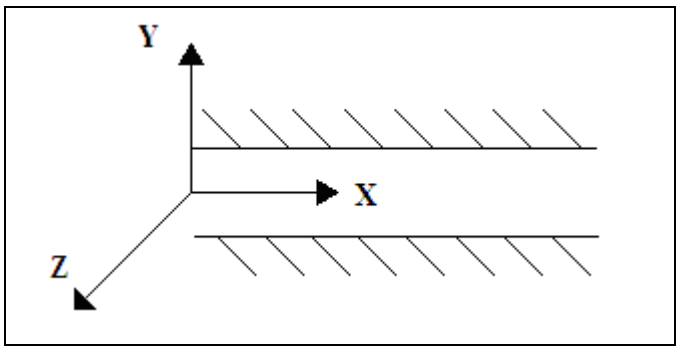

Fig. A4.1-1. Reference system in the airgap

$$rot\bar{H} = \begin{vmatrix} \hat{i} & \hat{j} & \hat{k} \\ \dfrac{\partial}{\partial x} & \dfrac{\partial}{\partial y} & \dfrac{\partial}{\partial z} \\ H_x & H_y & H_z \end{vmatrix} \tag{A4.1-2}$$

By executing the calculations, the first equation of (A4.1-1) gives three scalar components:

$$\frac{\partial H_z}{\partial y} - \frac{\partial H_y}{\partial z} = J_x = 0 \tag{A4.1-3}$$

$$\frac{\partial H_x}{\partial z} - \frac{\partial H_z}{\partial x} = J_y = 0 \tag{A4.1-4}$$

$$\frac{\partial H_y}{\partial x} - \frac{\partial H_x}{\partial y} = J_z \tag{A4.1-5}$$

$$\bar{J} = 0\hat{i} + 0\hat{j} + J_z(x)\hat{k} \tag{A4.1-6}$$

Another very important hypothesis about the magnetic field distribution, gives

the only component in the y direction, being $\overline{H} = H_y \hat{j}$: by applying this to (A4.1-3)-(A4.1-5), it is obtained:

$$\begin{cases} -\dfrac{\partial H_y}{\partial z} = 0 \\ 0 = 0 \\ \dfrac{\partial H_y}{\partial x} = J_z \end{cases} \qquad \text{(A4.1-7)}$$

From the first equation of (A4.1-7) it results that H_y does not depend on z, varying only as a function of the x coordinate.

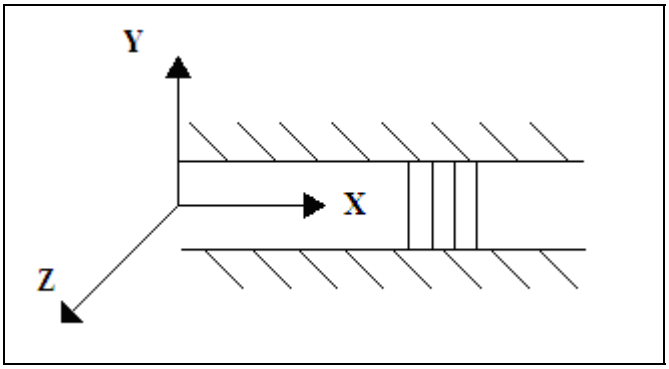

Fig. A4.1-2. Representation of magnetic field distribution in the airgap

$$\frac{\partial H_y}{\partial x} = J_z(x) \qquad \text{(A4.1-8)}$$

In the Figs. A4.1-3 and A4.1-4 are shown the most known typologies of current density and the related magnetic field distributions, by following the relationship A4.1-8.

The presented analysis of magnetic field distribution is based on the following assumptions:

I) The permeability of iron is infinite;

II) The slots of the machine are semi-closed, having an infinitesimal slot opening width and height;

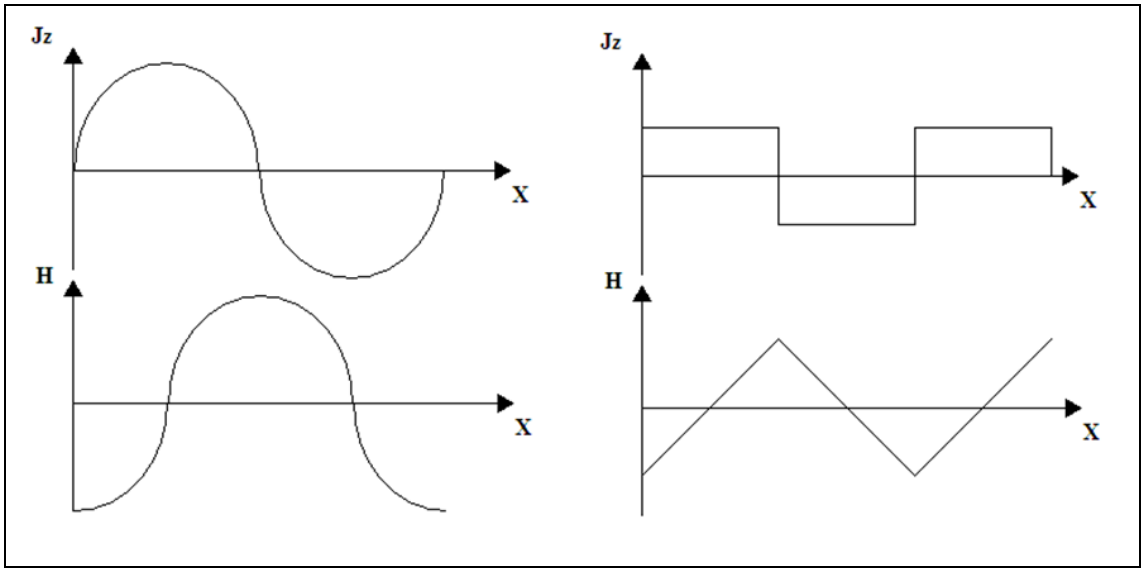

Fig. A4.1-3. Sinusoidal (left) and square wave (right) distributions

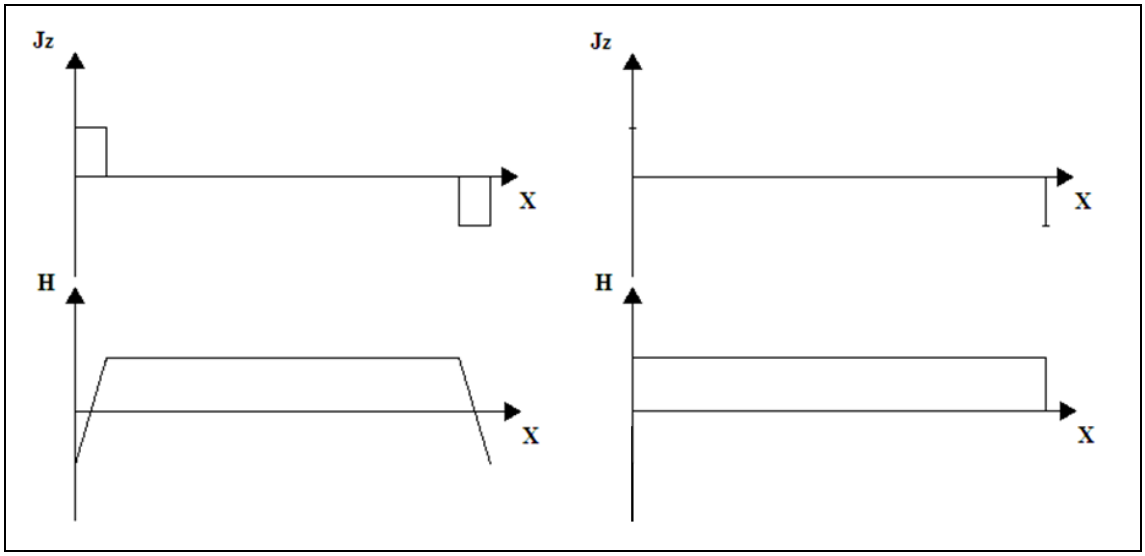

Fig. A4.1-4. Rectangular (left) and impulsive (right) distributions

III) The magnetic field lines are radial and perpendicular to the rotor and stator boundary surfaces;

IV) The mean airgap radius of curvature is infinite, so that the airgap path can be considered as a straight line;

V) Extremity effects are neglected.

VI) The effects of the leakage fluxes are neglected.

The analysis will be conducted starting from the magnetic field distribution produced by a one slot-per-pole winding (Fig. A4.1-5). Considering, with no lack of generality, a 2-pole machine and by applying the second equation of (A4.1-1):

$$\begin{aligned} div\overline{B} = 0 \quad &\Rightarrow \quad \int_{S_c} \overline{B} \cdot \hat{n} dS = B_1 \tau_p L + B_2 \tau_p L = 0 \\ &\Rightarrow \quad \mu_0 H_1 \tau_p L + \mu_0 H_2 \tau_p L = 0 \quad \Rightarrow \quad H_1 = -H_2 \left(= H\right) \end{aligned} \tag{A4.1-9}$$

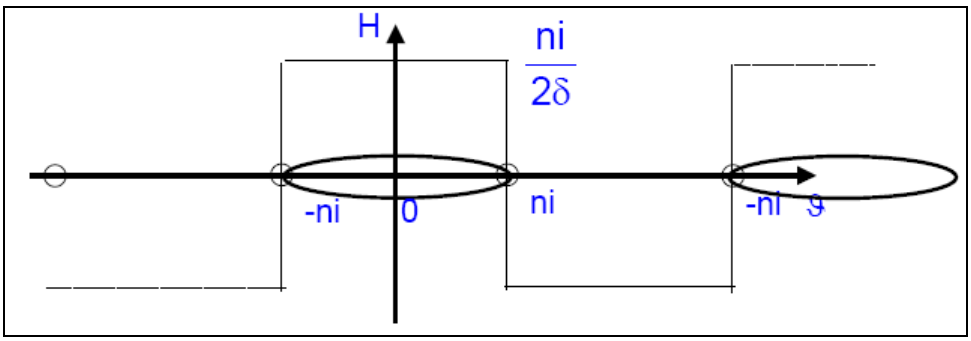

Fig. A4.1-5. Magnetic field distribution (1 slot-per-pole winding)

By applying Ampere's law on a path crossing the airgap which includes a group of n conductors, neglecting the x-components of $\overline{H}$ and taking into account (A4.1-9) it gives:

$$\oint \overline{H} \cdot d\bar{l} = ni \quad \Rightarrow \quad H_1 \delta - H_2 \delta = ni \quad \Rightarrow \quad 2H\delta = ni \tag{A4.1-10}$$

where it is understood that H stays for H_y. After a simple step:

$$H = \frac{ni}{2\delta} \tag{A4.1-11}$$

As shown in Fig. A4.1-5, the considered reference system has the origin in the middle of the coil. So, the spatial distribution of the magnetic field is a periodic function of θ and can be developed in Fourier harmonic series:

$$H_s(\theta) = \sum_{k=1,3,\ldots}^{\infty} H_k \cos(k\theta) \tag{A4.1-12}$$

where:

$$H_k = \frac{1}{\pi}\int_{-\pi}^{\pi} H(\theta)cos(k\theta)d\theta \qquad \text{(A4.1-13)}$$

Having all the coils the same pitch, equal to π electrical radians, it can be easily prove that the Fourier series has only odd harmonic orders. Furthermore, it presents only cosine terms due to the choice of the reference system.
The calculation of (A4.1-13) gives:

$$H_k = \frac{1}{\pi}\int_{-\pi}^{\pi} H(\theta)cos(k\theta)d\theta = \frac{2}{\pi}\left\{\int_{0}^{\pi/2} \frac{ni}{2\delta}cos(k\theta)d\theta + \int_{\pi/2}^{\pi} -\frac{ni}{2\delta}cos(k\theta)d\theta\right\} =$$

$$= \frac{2}{\pi k}\left[\frac{ni}{2\delta}sin(k\theta)\right]_0^{\pi/2} - \frac{2}{\pi k}\left[\frac{ni}{2\delta}sin(k\theta)\right]_{\pi/2}^{\pi} = \frac{4}{\pi}\frac{ni}{2\delta}\frac{1}{k}sin\left(k\frac{\pi}{2}\right) \qquad \text{(A4.1-14)}$$

To obtain:

$$H_k = \frac{4}{\pi}\frac{ni}{2\delta}\frac{1}{k}sin\left(k\frac{\pi}{2}\right) \qquad \text{(A4.1-15)}$$

By substituting (A4.1-15) in (A4.1-12):

$$H_s(\theta) = \sum_{k=1,3,\ldots}^{\infty} \frac{4}{\pi}\frac{ni}{2\delta}\frac{1}{k}sin\left(k\frac{\pi}{2}\right)cos(k\theta) \qquad \text{(A4.1-16)}$$

By assumption the slot opening width and height are considered to be infinitesimal, without creating leakage fluxes; the coils of one phase are series-connected with the same current flowing in. The equation (A4.1-16) contains the following terms: $\frac{4}{\pi}\frac{ni}{2\delta}$ represents the amplitude of fundamental harmonic order, $1/k\,sin(k\pi/2)$ is the harmonic factor whose value is $\pm 1/k$, the dependence on the function $cos(k\theta)$ represents the spatial harmonic distribution.

The spatial distribution of the magnetic field is constituted by the superposition of sinusoidal distributions of decreasing amplitude with the harmonic order $1/k$. For each harmonic the maximum value of the field occurs at the center of the coil. The amplitude of each harmonic is proportional to the value of the current flowing in the coil.

Consider a magnetic field distribution generated by a q slots-per-pole winding, as shown in Fig. A4.1-6:

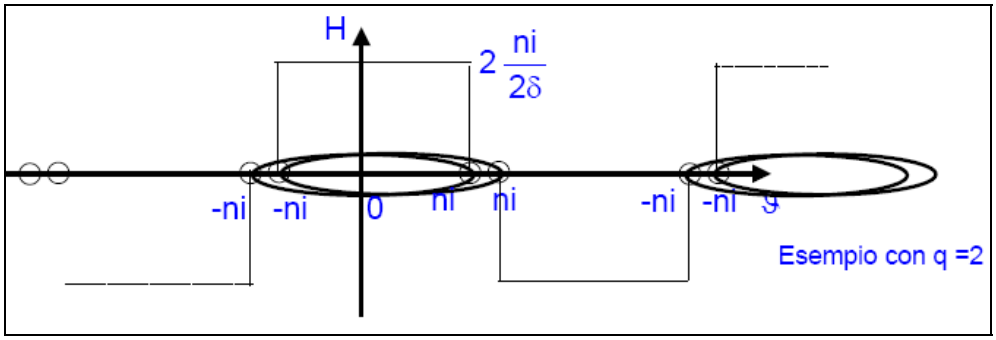

Fig. A4.1-6. Magnetic field distribution generated by a q slots-per-pole winding.

The field distribution is formed by the superposition of q contributions, relatively displaced by an electrical angle α (the angle between two adjacent slots): the related representation, by means of the Fourier harmonic series, becomes:

$$H^q(\theta)=\sum_{j=1}^{q}\sum_{k=1,3,\ldots}^{\infty}\frac{4}{\pi}\frac{ni}{2\delta}\frac{1}{k}sin\left(k\frac{\pi}{2}\right)cos\left(k\left[\theta-(j-1)\alpha\right]\right) \qquad \text{(A4.1-17)}$$

By varying the index j from 1 to q it is obtained a summation of cosine functions which can be calculated as:

$$cos(k\theta)+cos\left(k\left[\theta-\alpha\right]\right)+cos\left(k\left[\theta-2\alpha\right]\right)+\ldots+cos\left(k\left[\theta-(q-1)\alpha\right]\right)=$$
$$=\frac{sin\frac{kq\alpha}{2}}{sin\frac{k\alpha}{2}}cos\left(k\left[\theta-\frac{q-1}{2}\alpha\right]\right)=qK_{dk}\,cos\left(k\left[\theta-\frac{q-1}{2}\alpha\right]\right) \qquad \text{(A4.1-18)}$$

where the terms K_{dk} is defined distribution factor of Blondel (A4.1-19):

$$K_{dk} = \frac{sin\frac{kq\alpha}{2}}{q\,sin\frac{k\alpha}{2}} \qquad \text{(A4.1-19)}$$

By adopting a suitable winding distribution in the slots, K_{dk} allows to reduce, even remarkably, some harmonic orders. By substituting the relation (A4.1-18) in the expression (A4.1-17), it gives:

$$H^q(\theta) = \sum_{k=1,3,\ldots}^{\infty} \frac{4}{\pi}\frac{ni}{2\delta} qK_{dk} \frac{1}{k} sin\left(k\frac{\pi}{2}\right) cos\left(k\left[\theta - \frac{q-1}{2}\alpha\right]\right) \qquad \text{(A4.1-20)}$$

Note that the diagram of the magnetic field distribution $H^q(\theta)$ moved in the original reference system with respect to (A4.1-16) due to the modification of the distribution, that now is related to q slots-per-pole-per-phase: thus, is necessary to shift the reference system by an angle $(q-1)\alpha/2$, corresponding with the new peak value of the $H^q(\theta)$ distribution as the centre of the phase.

$$H^q(\theta) = \sum_{k=1,3,\ldots}^{\infty} \frac{4}{\pi}\frac{ni}{2\delta} qK_{dk} \frac{1}{k} sin\left(k\frac{\pi}{2}\right) cos(k\theta) \qquad \text{(A4.1-21)}$$

In the comparison between (A4.1-21) and (A4.1-16) the contribution of the q slots-per-pole-per-phase can be recognized in the term qK_{dk}.

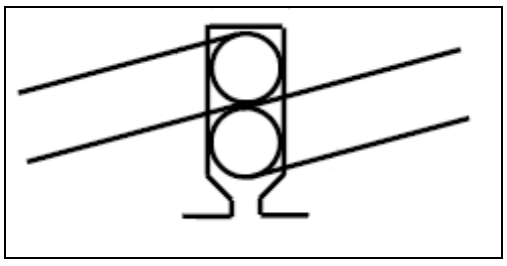

Fig. A4.1-7. A slot with double layer winding

Consider now the distribution of magnetic field produced by a winding of q slots-per-pole-per-phase in double-layer. It is shown in Fig. A4.1-7 the representation of a slot in double layer, while in Fig. A4.1-8 the representation of a double layer winding.

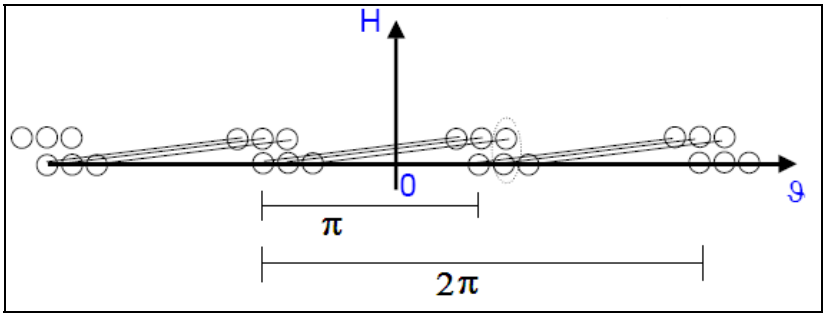

Fig. A4.1-8. Double layer winding representation

As can be seen, in a double layer winding it could happen to find, in the same slot, groups of conductors belonging to different coils. The magnetic field distributions produced by different layers of the same phase, can be seen as identical to (A4.1-21) but shifted by a β electrical angle. Also, is important to note that in (A4.1-22) the number of conductors-per-slot n is divided by 2 due to the presence of the layers. Thus, the resultant distribution can be written as:

$$H^q(\theta) = \sum_{k=1,3,\ldots}^{\infty} \frac{4}{\pi}\frac{n}{2}\frac{i}{2\delta} qK_{dk}\frac{1}{k} sin\left(k\frac{\pi}{2}\right) cos(k\theta) + \\ + \sum_{k=1,3,\ldots}^{\infty} \frac{4}{\pi}\frac{n}{2}\frac{i}{2\delta} qK_{dk}\frac{1}{k} sin\left(k\frac{\pi}{2}\right) cos(k[\theta-\beta]) \qquad \text{(A4.1-22)}$$

The even harmonic orders cancel each other for the two layers. Both the bottom layer than the top one, produces a field of q slots-per-pole: being a phase shift between them, it is necessary to add the two sinusoidal functions taking into account of it. The result, by applying again an angular shift to the reference system on the new center of the phase, is equivalent to multiplying by 2 and by the shortened pitch factor (A4.1-23):

$$K_{rk} = cos\left(\frac{k\beta}{2}\right) \tag{A4.1-23}$$

The relationship (A4.1-24) represents the magnetic field distribution produced by a double layer winding of one phase, having q slots-per-pole-per-phase:

$$H(\theta) = \sum_{k=1,3,\ldots}^{\infty} \frac{4}{\pi}\frac{ni}{2\delta} qK_{dk}K_{rk}\frac{1}{k} sin\left(k\frac{\pi}{2}\right) cos(k\theta) \tag{A4.1-24}$$

The product of the Blondel's factor K_{dk} and the shortened pitch factor K_{rk} gives the winding factor K_{ak} related to k -th harmonic order:

$$K_{ak} = K_{dk}K_{rk} = \frac{sin\left(\frac{kq\alpha}{2}\right)}{q\, sin\left(\frac{k\alpha}{2}\right)} cos\left(\frac{k\beta}{2}\right) \tag{A4.1-25}$$

Consider an instantaneous phase current $i(t)$ which varies following a sinusoidal law (A4.1-26), being I the rms value and ω the angular frequency:

$$i(t) = \sqrt{2} I\, cos(\omega t) \tag{A4.1-26}$$

By substituting it in (A4.1-24) it gives:

$$H(\theta,t) = \sum_{k=1,3,\ldots}^{\infty} \frac{4}{\pi}\frac{\sqrt{2}nI}{2\delta} qK_{ak}\frac{1}{k} sin\left(k\frac{\pi}{2}\right) cos(k\theta) cos(\omega t) \tag{A4.1-27}$$

The equation (A4.1-27) can be written as:

$$H(\theta,t) = \sum_{k=1,3,\ldots}^{\infty} H_{Mk}\, cos(k\theta) cos(\omega t) \tag{A4.1-28}$$

where:

$$H_{Mk} = \frac{4}{\pi}\frac{\sqrt{2}nI}{2\delta} qK_{ak}\frac{1}{k} sin\left(k\frac{\pi}{2}\right) \tag{A4.1-29}$$

The distribution given by (A4.1-28) represents, for each value of k , a stationary

wave with kp pole pairs, shown in Fig. A4.1-9 in a succession of time instants.

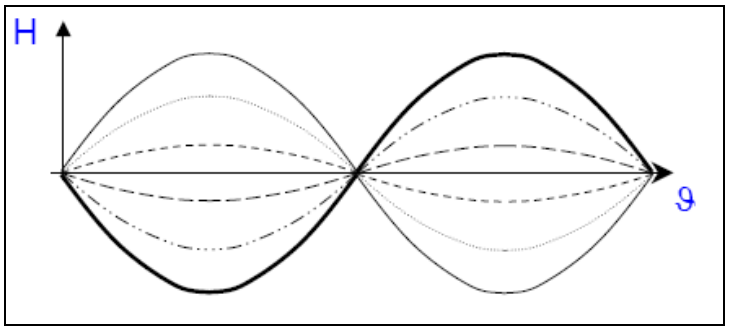

Fig. A4.1-9. The stationary wave shown in different time instants

The equation (A4.1-28) can be seen also as the sum of two counter-rotating fields depending on a space-time variable $f(k\theta \mp \omega t)$, each one moving in or opposite to the θ axis direction without warping, as shown in Fig. A4.1-10 and in the relationship (A4.1-31).

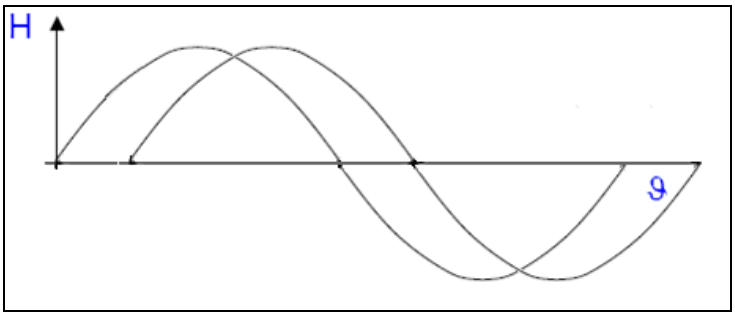

Fig. A4.1-10. A traslating wave

$$H(\theta,t)=\sum_{k=1,3,\ldots}^{\infty} H_{Mk}\frac{1}{2}\left[cos(k\theta-\omega t)+cos(k\theta+\omega t)\right] \qquad \text{(A4.1-30)}$$

$$H(\theta,t)=\sum_{k=1,3,\ldots}^{\infty}\frac{1}{2}H_{Mk}\,cos(k\theta-\omega t)+\sum_{k=1,3,\ldots}^{\infty}\frac{1}{2}H_{Mk}\,cos(k\theta+\omega t) \qquad \text{(A4.1-31)}$$

Each distribution in (A4.1-31) represents, for each value of k, a rotating wave with kp pole pairs: in particular, the first summation is a wave which rotates in

the same direction of θ, while the second one is a wave which rotates in the opposite direction of θ. In Fig. A4.1-11 is shown the dual interpretation of this phenomenon: the concepts of the stationary wave and the counter-rotating fields.

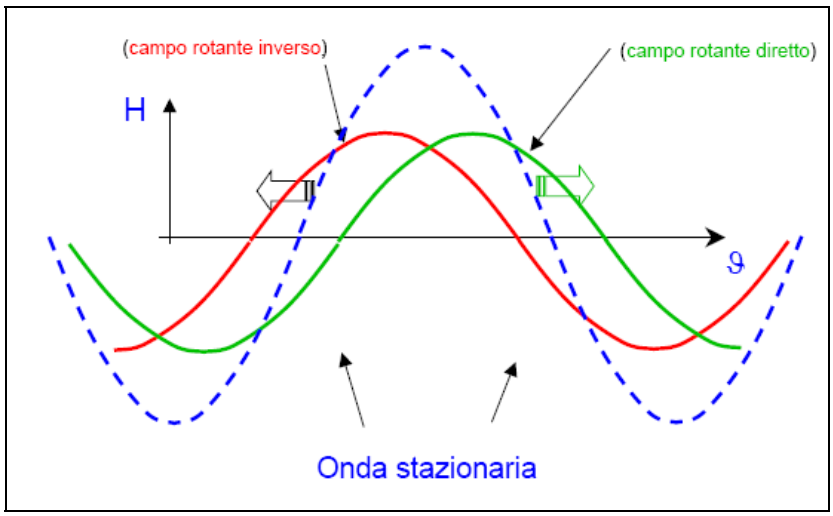

Fig. A4.1-11. The stationary and the counter-rotating distributions

The space-time distribution produced by one of the two rotating fields is repeated identical in the following situations: in a position θ_1 at the instant of time t_1 and in the position θ_2 at the instant of time t_2, such that:

$$\theta_1 \pm \frac{\omega}{k} t_1 = \theta_2 \pm \frac{\omega}{k} t_2 \qquad \text{(A4.1-32)}$$

After some simple calculations:

$$\theta_2 - \theta_1 = \mp \frac{\omega}{k} t_2 \pm \frac{\omega}{k} t_1 = \pm \frac{\omega}{k} (-t_2 + t_1) = \mp \frac{\omega}{k} (t_2 - t_1) \qquad \text{(A4.1-33)}$$

The electrical angular velocity ω_{ckE} of the distribution, measured in radians per sec., is given by:

$$\omega_{ckE} = \frac{\theta_2 - \theta_1}{t_2 - t_1} = \mp \frac{\omega}{k} \qquad \text{(A4.1-34)}$$

The mechanical angular velocity ω_{ck} of the rotating field, measured in radians

per sec., is given by:

$$\omega_{ck} = \pm\frac{\omega}{kp} \qquad \text{(A4.1-35)}$$

From which follows the rpm speed of the k -th order of the magnetic field:

$$n_k = \pm\frac{60f}{kp} \qquad \text{(A4.1-36)}$$

Consider a system of currents characterized by a phase difference $S_t(2\pi/m)$: S_t is defined as "sequence of time". Some examples are presented in the Figs. A4.1-12 - A4.1-14 (in the following, k_m will be assumed equal to 1):

$$i_j(t) = \sqrt{2}I\cos\left[k_m\omega\left(t - S_t(j-1)\frac{T}{m}\right)\right] \qquad \text{(A4.1-37)}$$

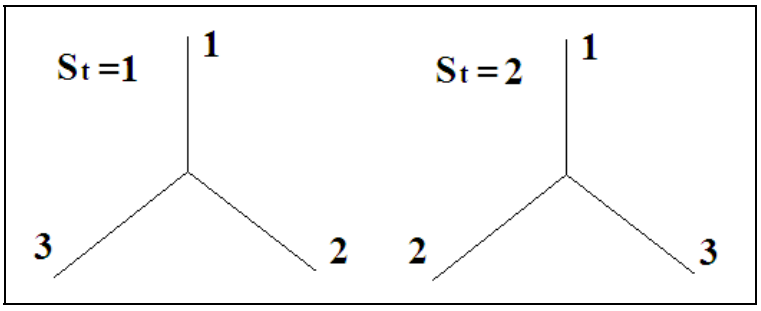

Fig. A4.1-12. Sequences of time with m = 3

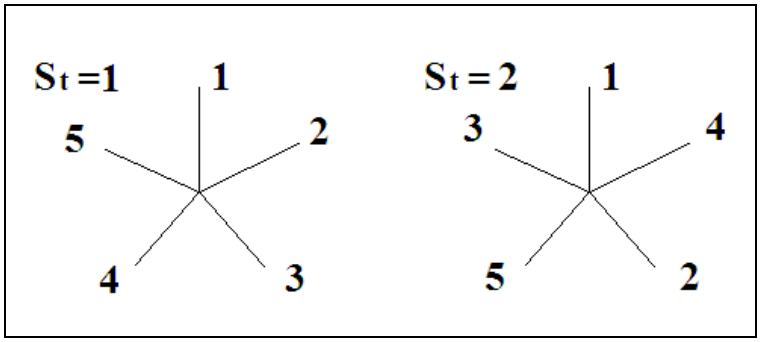

Fig. A4.1-13. Sequences of time with m = 5

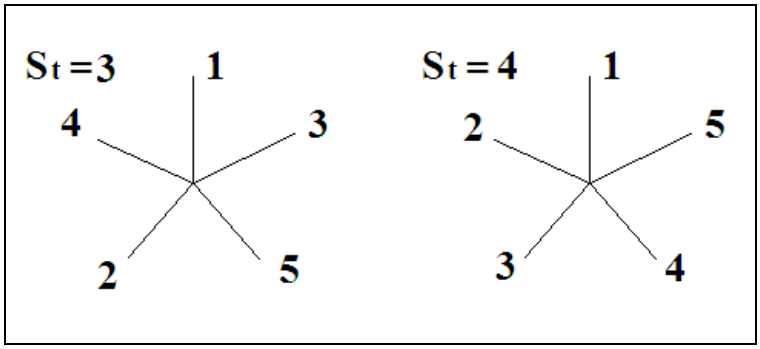

Fig. A4.1-14. Sequences of time with m = 5

The sequence of time must comply with the following constraint:

$$0 \le S_t \le m-1 \qquad \text{(A4.1-38)}$$

If the phases are disposed by following different spatial configurations, in this case one speaks of sequence of space S_s. Consider a machine with p pole pairs, m phases shifted in space by an angle equal to $S_s(2\pi/m)$, in which flows a balanced system of currents.

In the reference system centered in the phase 1, the magnetic field distribution produced by the j-th phase is given by:

$$H_j(\theta,t) = \sum_{k=1,3,\ldots}^{\infty} H_{Mk}\, cos\left(k\left(\theta - S_s(j-1)\frac{2\pi}{m} \right)\right) cos\left(\omega t - S_t(j-1)\frac{2\pi}{m} \right) \qquad \text{(A4.1-39)}$$

The resulting magnetic field produced by all the phases of the machine can be expressed as:

$$H(\theta,t) = \sum_{j=1}^{m}\sum_{k=1,3,\ldots}^{\infty} H_{Mk}\, cos\left(k\left(\theta - S_s(j-1)\frac{2\pi}{m} \right)\right) cos\left(\omega t - S_t(j-1)\frac{2\pi}{m} \right) =$$

$$= \sum_{j=1}^{m}\sum_{k=1,3,\ldots}^{\infty} \frac{1}{2} H_{Mk}\left\{ cos\left(k\theta \mp \omega t - (j-1)(kS_s \mp S_t)\frac{2\pi}{m} \right)\right\} \qquad \text{(A4.1-40)}$$

Finally is obtained:

$$H(\theta,t)=\sum_{j=1}^{m}\sum_{k=1,3,\ldots}^{\infty}\frac{1}{2}H_{Mk}\left\{cos\left(k\theta\mp\omega t-(j-1)(kS_s\mp S_t)\frac{2\pi}{m}\right)\right\} \qquad \text{(A4.1-41)}$$

The resulting magnetic field is given by adding m sinusoidal contributions with a phase difference equal to $(kS_s\mp S_t)2\pi/m$.

There are two possible cases: if all the contributions have the same phase, the result is m times the contribution; if the contributions are shifted by the same angle, their resultant is null. This result is explained in (A4.1-42):

$$H(\theta,t)=\begin{cases}\displaystyle\sum_{k=1}^{\infty}\frac{m}{2}H_{Mk}\,cos(k\theta\mp\omega t) & \Rightarrow \quad \text{if } \dfrac{kS_s\mp S_t}{m}=\text{integer}\\ 0 & \Rightarrow \quad \text{if } \dfrac{kS_s\mp S_t}{m}\neq\text{integer}\end{cases} \qquad \text{(A4.1-42)}$$

For a fixed value of k, the magnetic field distribution has a direction of rotation:

direct, if $\dfrac{kS_s-S_t}{m}=\text{integer}$

reverse, if $\dfrac{kS_s+S_t}{m}=\text{integer}$

A symmetrical polyphase winding in which flows a balanced system of currents, produces a distribution of magnetic field in the airgap described by the following relation:

$$H(\theta,t)=\sum_{k=1,\ldots}^{\infty}\frac{m}{2}\frac{4}{\pi}\frac{n\sqrt{2}I}{2\delta}qK_{ak}\,\frac{1}{k}\,sin\left(k\frac{\pi}{2}\right)cos(k\theta\mp\omega t) \qquad \text{(A4.1-43)}$$

The terms in summation (A4.1-43) have to be considered not null only for the values of k such that $\dfrac{kS_s\mp S_t}{m}$ is integer. This distribution can therefore be considered formed by the overlap of direct and inverse harmonic rotating magnetic fields.

Chapter 5

DESIGN AND DEVELOPMENT OF A CONTROL SYSTEM FOR MULTIPHASE SYNCHRONOUS PERMANENT MAGNET BEARINGLESS MACHINES

5.1 Introduction

In this chapter a control system for bearingless multiphase synchronous PM machines is presented, integrating the electromagnetic model seen in Chapter 4 with a three-dimensional mechanical model developed based on the Euler's equations. One end of the motor shaft is constrained, to simulate the presence of a mechanical bearing, while the other is free, only supported by the radial forces developed in the interactions between magnetic fields, to simulate a bearingless

system with three degrees of freedom.

The body in Fig. 5.1 represents the rotor and the shaft of the machine, rotating around an axis with a fixed point. The interactions between the levitation current space vector $\bar{i}_{sv2}$ and the other sources of magnetic fields, i.e. rotor magnets and torque current space vector $\bar{i}_{sv1}$, provide to generate the levitation forces, as seen in the previous chapter by means of the analytical formulation. The system was implemented on a SIMULINK® model, representing the conceptual design of the experimental device and related control system that could be realized in a test bench application.

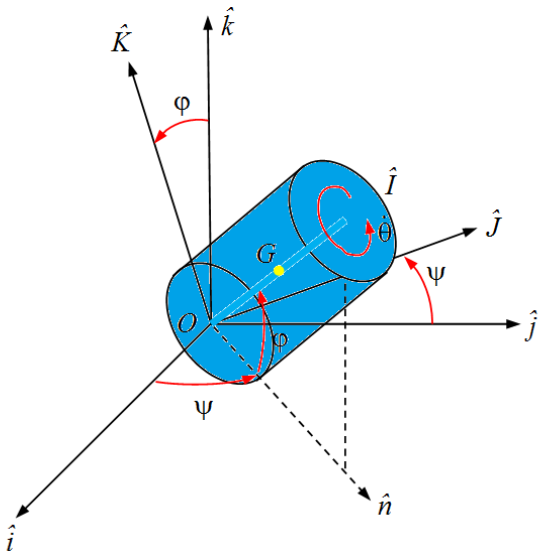

Fig. 5.1

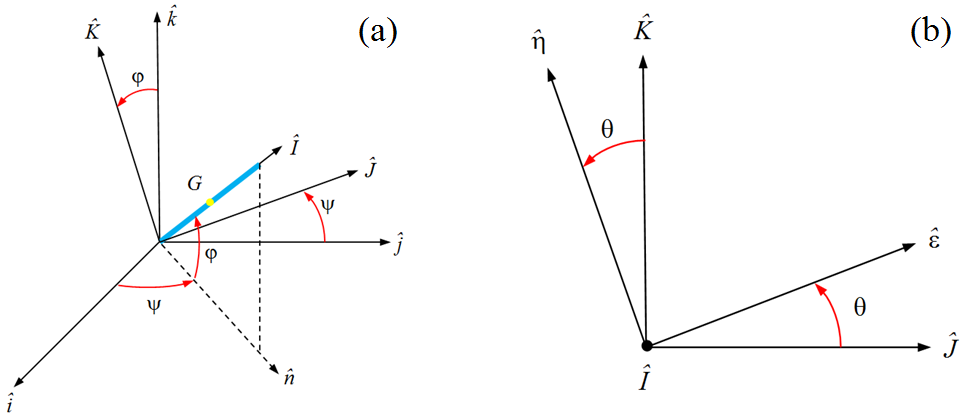

Fig. 5.2

Consider three reference systems in the space:

- **Absolute (*abs*)**, characterized by the unit vectors $\left(\hat{i}, \hat{j}, \hat{k}\right)$, Fig. 5.1;
- **Relative (*rel*)**, characterized by the unit vectors $\left(\hat{I}, \hat{J}, \hat{K}\right)$, Fig. 5.2(a);
- **Fixed-to-rotor (*ftr*)**, characterized by the unit vectors $\left(\hat{I}, \hat{\varepsilon}, \hat{\eta}\right)$, Fig. 5.2(b).

The last two systems have a common unit vector because their first axes coincide.

5.2 Mechanical equations

The rotor angular speed in the absolute reference system is calculated by applying the "principle of composition of angular speed":

$$\overline{\omega} = \overline{\Omega} + \overline{\omega}_{rel} \tag{5.1}$$

where $\overline{\Omega}$ is the angular speed of the relative reference system with respect to the absolute and $\overline{\omega}_{rel}$ is the angular speed of the rotor with respect to the relative reference system. They can be expressed as:

$$\overline{\Omega} = \dot{\psi}\hat{k} - \dot{\varphi}\hat{J} \tag{5.2}$$

$$\overline{\omega}_{rel} = \dot{\theta}\hat{I} \tag{5.3}$$

By substituting (5.2), (5.3) in (5.1), it gives the rotor angular speed vector:

$$\overline{\omega} = \dot{\psi}\hat{k} - \dot{\varphi}\hat{J} + \dot{\theta}\hat{I} \tag{5.4}$$

The equations of the motion are given by:

$$\frac{d\overline{\Gamma}_o}{dt} = \overline{M}_o \tag{5.5}$$

Being $\overline{\Gamma}_o$, $\overline{M}_o$ respectively the moment of momentum and the moment of the external forces evaluated with respect to the point *O*. $\overline{\Gamma}_o$ is given by:

$$\overline{\Gamma}_o = \overline{\overline{\Im}}_o \cdot \overline{\omega} \tag{5.6}$$

The fixed-to-rotor reference system is obtained by rotation of an angle θ around the *X*-axis, and the relationships between its unit vectors and the ones of the relative system are (note that the unit vector $\hat{I}$ is the same because the *X*-axis is in common):

$$\hat{J} = cos\,\theta\hat{\varepsilon} - sin\,\theta\hat{\eta} \tag{5.7}$$

$$\hat{K} = sin\,\theta\hat{\varepsilon} + cos\,\theta\hat{\eta} \tag{5.8}$$

In order to write the angular speed vector with respect to the fixed-to-rotor reference system, is necessary firstly to write it in explicit way, with respect to the relative system:

$$\hat{k} = sin\,\varphi\hat{I} + cos\,\varphi\hat{K} \tag{5.9}$$

By substituting (5.9) in (5.4):

$$\overline{\omega} = \left(\dot{\psi}\,sin\,\varphi + \dot{\theta}\right)\hat{I} - \dot{\varphi}\hat{J} + \dot{\psi}\,cos\,\varphi\hat{K} \tag{5.10}$$

By substituting (5.7) and (5.8) in (5.10):

$$\overline{\omega} = \left(\dot{\psi}\,sin\,\varphi + \dot{\theta}\right)\hat{I} + \left(\dot{\psi}\,cos\,\varphi\,sin\,\theta - \dot{\varphi}\,cos\,\theta\right)\hat{\varepsilon} + \left(\dot{\varphi}\,sin\,\theta + \dot{\psi}\,cos\,\varphi\,cos\,\theta\right)\hat{\eta} \tag{5.11}$$

which can be expressed in matrix form in the following:

$$\begin{bmatrix} \omega_I \\ \omega_\varepsilon \\ \omega_\eta \end{bmatrix} = \begin{bmatrix} sin\,\varphi & 0 & 1 \\ cos\,\varphi\,sin\,\theta & -cos\,\theta & 0 \\ cos\,\varphi\,cos\,\theta & sin\,\theta & 0 \end{bmatrix} \begin{bmatrix} \dot{\psi} \\ \dot{\varphi} \\ \dot{\theta} \end{bmatrix} \tag{5.12}$$

As the system chosen is principal of inertia, the $\overline{\overline{\Im}}_o$ is a diagonal matrix thus,

with reference to (5.6), is possible to write:

$$\overline{\Gamma}_o = \overline{\overline{\Im}}_o \cdot \overline{\omega} = \begin{bmatrix} I_{oI} & 0 & 0 \\ 0 & I_{o\varepsilon} & 0 \\ 0 & 0 & I_{o\eta} \end{bmatrix} \begin{bmatrix} \omega_I \\ \omega_\varepsilon \\ \omega_\eta \end{bmatrix} = I_{oI}\omega_I \hat{I} + I_{o\varepsilon}\omega_\varepsilon \hat{\varepsilon} + I_{o\eta}\omega_\eta \hat{\eta} \tag{5.13}$$

Reminding that $\overline{\omega}$ is defined with respect to a stationary observer, the derivative $\frac{d\overline{\Gamma}_o}{dt}$ has to be determined with respect to the same observer. It is possible to write:

$$\left(\frac{d\overline{\Gamma}_o}{dt}\right)_{(abs)} = \left(\frac{d\overline{\Gamma}_o}{dt}\right)_{(ftr)} + \overline{\omega} \times \overline{\Gamma}_o \tag{5.14}$$

By considering the equation (5.6) and that the matrix of inertia $\overline{\overline{\Im}}_o$ doesn't change, it can be calculated:

$$\left(\frac{d\overline{\Gamma}_o}{dt}\right)_{(ftr)} = \overline{\overline{\Im}}_o \cdot \dot{\overline{\omega}} \tag{5.15}$$

By substituting (5.6) and (5.15) in (5.14):

$$\left(\frac{d\overline{\Gamma}_o}{dt}\right)_{(abs)} = \overline{\overline{\Im}}_o \cdot \dot{\overline{\omega}} + \overline{\omega} \times \overline{\overline{\Im}}_o \cdot \overline{\omega} \tag{5.16}$$

$$\left(\frac{d\overline{\Gamma}_o}{dt}\right)_{(abs)} = I_{oI}\dot{\omega}_I \hat{I} + I_{o\varepsilon}\dot{\omega}_\varepsilon \hat{\varepsilon} + I_{o\eta}\dot{\omega}_\eta \hat{\eta} + \begin{vmatrix} \hat{I} & \hat{\varepsilon} & \hat{\eta} \\ \omega_I & \omega_\varepsilon & \omega_\eta \\ I_{oI}\omega_I & I_{o\varepsilon}\omega_\varepsilon & I_{o\eta}\omega_\eta \end{vmatrix} \tag{5.17}$$

By executing the calculations:

$$\left(\frac{d\overline{\Gamma}_o}{dt}\right)_{(abs)} = \left[I_{oI}\dot{\omega}_I + \left(I_{o\eta} - I_{o\varepsilon}\right)\omega_\varepsilon\omega_\eta\right]\hat{I} + \left[I_{o\varepsilon}\dot{\omega}_\varepsilon + \left(I_{oI} - I_{o\eta}\right)\omega_I\omega_\eta\right]\hat{\varepsilon} + \left[I_{o\eta}\dot{\omega}_\eta + \left(I_{o\varepsilon} - I_{oI}\right)\omega_I\omega_\varepsilon\right]\hat{\eta} \tag{5.18}$$

Writing the moment of the external forces vector $\overline{M}_o$ with respect to the point O in the ***ftr*** reference system:

$$\overline{M}_o = M_{oI}\hat{I} + M_{o\varepsilon}\hat{\varepsilon} + M_{o\eta}\hat{\eta} \tag{5.19}$$

By substituting (5.18) and (5.19) in (5.5) is possible to determine the equations of the motion, also called "Euler equations":

$$\begin{cases} I_{oI}\dot{\omega}_I + \left(I_{o\eta} - I_{o\varepsilon}\right)\omega_\varepsilon\omega_\eta = M_{oI} \\ I_{o\varepsilon}\dot{\omega}_\varepsilon + \left(I_{oI} - I_{o\eta}\right)\omega_I\omega_\eta = M_{o\varepsilon} \\ I_{o\eta}\dot{\omega}_\eta + \left(I_{o\varepsilon} - I_{oI}\right)\omega_I\omega_\varepsilon = M_{o\eta} \end{cases} \tag{5.20}$$

It is now useful to define the relationship between the moment of the external forces vector evaluated in the ***ftr*** reference system and the one evaluated in the ***abs*** reference system. Thus, is necessary to write the unit vectors $\left(\hat{i}, \hat{j}, \hat{k}\right)$ with respect the unit vectors $\left(\hat{I}, \hat{\varepsilon}, \hat{\eta}\right)$. Firstly, the equations (5.7), (5.8) are presented in matrix form:

$$\begin{bmatrix} \hat{I} \\ \hat{J} \\ \hat{K} \end{bmatrix} = \begin{bmatrix} 1 & 0 & 0 \\ 0 & cos\,\theta & -sin\,\theta \\ 0 & sin\,\theta & cos\,\theta \end{bmatrix} \begin{bmatrix} \hat{I} \\ \hat{\varepsilon} \\ \hat{\eta} \end{bmatrix} \tag{5.21}$$

The unit vector $\hat{n}$ is defined as the projection of the unit vector $\hat{I}$ on the xy plane:

$$\hat{n} = cos\,\varphi\hat{I} - sin\,\varphi\hat{K} \tag{5.22}$$

By substituting (5.22) in (5.23), (5.24), the relationships between the unit vectors $\left(\hat{i}, \hat{j}, \hat{k}\right)$ and the unit vectors $\left(\hat{I}, \hat{J}, \hat{K}\right)$ are found:

$$\hat{i} = cos\,\psi\hat{n} - sin\,\psi\hat{J} = cos\,\psi\,cos\,\varphi\hat{I} - sin\,\psi\hat{J} - cos\,\psi\,sin\,\varphi\hat{K} \tag{5.23}$$

$$\hat{j} = sin\,\psi\hat{n} + cos\,\psi\hat{J} = sin\,\psi\,cos\,\varphi\hat{I} + cos\,\psi\hat{J} - sin\,\psi\,sin\,\varphi\hat{K} \tag{5.24}$$

$$\hat{k} = sin\,\varphi\hat{I} + cos\,\varphi\hat{K} \tag{5.25}$$

By expressing (5.23)-(5.25) in the matrix form:

$$\begin{bmatrix} \hat{i} \\ \hat{j} \\ \hat{k} \end{bmatrix} = \begin{bmatrix} cos\,\psi\,cos\,\varphi & -sin\,\psi & -cos\,\psi\,sin\,\varphi \\ sin\,\psi\,cos\,\varphi & cos\,\psi & -sin\,\psi\,sin\,\varphi \\ sin\,\varphi & 0 & cos\,\varphi \end{bmatrix} \begin{bmatrix} \hat{I} \\ \hat{J} \\ \hat{K} \end{bmatrix} \tag{5.26}$$

By combining (5.21) and (5.26), are presented the relationships between the unit vectors $(\hat{i},\hat{j},\hat{k})$ related to absolute reference system and the unit vectors $(\hat{I},\hat{\varepsilon},\hat{\eta})$ related to fixed-to-rotor reference system:

$$\begin{bmatrix} \hat{i} \\ \hat{j} \\ \hat{k} \end{bmatrix} = \begin{bmatrix} cos\,\psi\,cos\,\varphi & -sin\,\psi & -cos\,\psi\,sin\,\varphi \\ sin\,\psi\,cos\,\varphi & cos\,\psi & -sin\,\psi\,sin\,\varphi \\ sin\,\varphi & 0 & cos\,\varphi \end{bmatrix} \begin{bmatrix} 1 & 0 & 0 \\ 0 & cos\,\theta & -sin\,\theta \\ 0 & sin\,\theta & cos\,\theta \end{bmatrix} \begin{bmatrix} \hat{I} \\ \hat{\varepsilon} \\ \hat{\eta} \end{bmatrix} \tag{5.27}$$

By multiplying the matrices in (5.27) it gives:

$$\underbrace{\begin{bmatrix} cos\,\psi\,cos\,\varphi & -sin\,\psi\,cos\,\theta - cos\,\psi\,sin\,\varphi\,sin\,\theta & sin\,\psi\,sin\,\theta - cos\,\psi\,sin\,\varphi\,cos\,\theta \\ sin\,\psi\,cos\,\varphi & cos\,\psi\,cos\,\theta - sin\,\psi\,sin\,\varphi\,sin\,\theta & -cos\,\psi\,sin\,\theta - sin\,\psi\,sin\,\varphi\,cos\,\theta \\ sin\,\varphi & cos\,\varphi\,sin\,\theta & cos\,\varphi\,cos\,\theta \end{bmatrix}}_{\overline{\overline{B}}^{-1}(\theta,\varphi,\psi)} \tag{5.28}$$

The matrix obtained in (5.28), called $\overline{\overline{B}}^{-1}(\theta,\varphi,\psi)$, permits to directly convert the ***abs*** unit vectors in the ***ftr*** unit vectors. It is mentioned as an inverse matrix because the main matrix $\overline{\overline{B}}(\theta,\varphi,\psi)$ is that one which defines the moment of external forces vector $\overline{M}_o$ in the ***ftr*** reference system, being the most used.

In fact, the latter can be immediately substituted in the Euler's equations (5.20). By combining (5.29) and (5.30), is obtained (5.31):

$$\begin{bmatrix} M_{oX} \\ M_{oY} \\ M_{oZ} \end{bmatrix} = \begin{bmatrix} cos\,\psi\, cos\,\varphi & sin\,\psi\, cos\,\varphi & sin\,\varphi \\ -sin\,\psi & cos\,\psi & 0 \\ -cos\,\psi\, sin\,\varphi & -sin\,\psi\, sin\,\varphi & cos\,\varphi \end{bmatrix} \begin{bmatrix} M_{ox} \\ M_{oy} \\ M_{oz} \end{bmatrix} \tag{5.29}$$

$$\begin{bmatrix} M_{oI} \\ M_{o\varepsilon} \\ M_{o\eta} \end{bmatrix} = \underbrace{\begin{bmatrix} 1 & 0 & 0 \\ 0 & cos\,\theta & sin\,\theta \\ 0 & -sin\,\theta & cos\,\theta \end{bmatrix}}_{\Theta(\theta)} \begin{bmatrix} M_{oX} \\ M_{oY} \\ M_{oZ} \end{bmatrix} \tag{5.30}$$

In (5.31), (5.32) is shown the $\overline{\overline{B}}(\theta,\varphi,\psi)$ matrix, which permits to calculate the moment of the external forces vector $\overline{M}_o$ in the fixed-to-rotor reference system:

$$\underbrace{\begin{bmatrix} cos\,\psi\, cos\,\varphi & sin\,\psi\, cos\,\varphi & sin\,\varphi \\ -sin\,\psi\, cos\,\theta - cos\,\psi\, sin\,\varphi\, sin\,\theta & cos\,\psi\, cos\,\theta - sin\,\varphi\, sin\,\psi\, sin\,\theta & cos\,\varphi\, sin\,\theta \\ sin\,\psi\, sin\,\theta - cos\,\psi\, sin\,\varphi\, cos\,\theta & -cos\,\psi\, sin\,\theta - sin\,\varphi\, sin\,\psi\, cos\,\theta & cos\,\varphi\, cos\,\theta \end{bmatrix}}_{\overline{\overline{B}}(\theta,\varphi,\psi)} \tag{5.31}$$

$$\begin{bmatrix} M_{oI} \\ M_{o\varepsilon} \\ M_{o\eta} \end{bmatrix} = \begin{bmatrix} \\ \overline{\overline{B}}(\theta,\varphi,\psi) \\ \\ \end{bmatrix} \begin{bmatrix} M_{ox} \\ M_{oy} \\ M_{oz} \end{bmatrix} \tag{5.32}$$

The relationship (5.32) is really important because the moments of external forces are given in the absolute reference system, but is necessary to express them in the fixed-to-rotor reference system in order to apply equations (5.20).

5.3 General structure of the control system

The external structure of the control system, realized with SIMULINK®, is composed by four main blocks, the other being "scope blocks" and "integrators": **Levitation forces block**, **Euler equations block**, **Lagrangian variables block**,

Axis coordinates block.

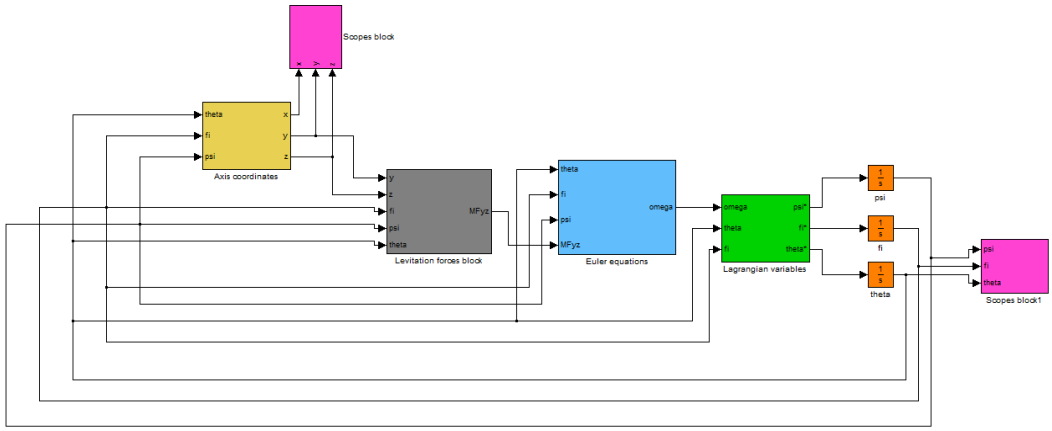

Fig. 5.3. General structure of the control system

1) **Levitation forces block**: the action of PID controllers is based on the position error along the y and z axes, by calculating the force, of modulus F_r and spatial phase fi_Fr, requested to maintain the rotor in the centre of the stator bore. Together with the angular position of the magnets theta, the **Force Controller** block determines the modulus and the phase of the $\bar{i}_{sv2}$ current space vector, called as variables Irms_ and fi_In_, to produce the requested force. This couple of values is necessarily provisional, being the analytic relationship that gives the $\bar{i}_{sv2}$ parameters univocal only considering the main harmonic orders of stator and rotor magnetic fields.

   The next block, **Electromagnetic Model**, determines the real value of the force to suspend the rotor, by taking into account all the possible interactions between harmonic orders of the magnetic fields. Also, this model consider the effects of both current space vectors $\bar{i}_{sv1}$, $\bar{i}_{sv2}$, respectively torque and

levitation. It gives in this way an exact prediction of the radial force and electromagnetic torque produced by the motor.

The drive maintains constantly the current space vector $\bar{i}_{sv1}$ in leading by 90 electrical degrees with respect to magnet axis, in order to give the requested torque in whatever operating condition. The output gives in particular the components of the force (variables F_y, F_z) which are used to calculate the moments with respect to the absolute reference system, by means of the **"Forces to Moments matrix"** block.

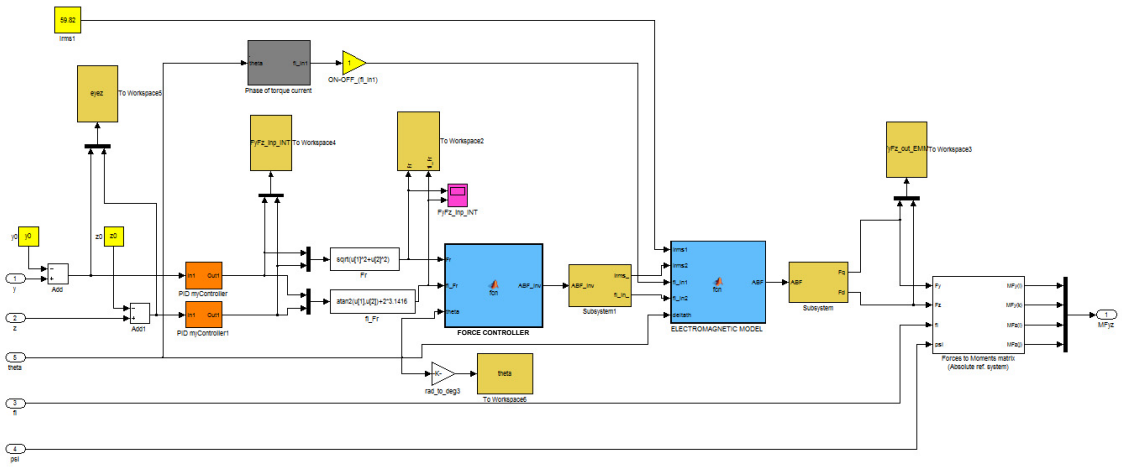

Fig. 5.4. Diagram of the Levitation Forces block

2) **Euler equations block**: the sub-block **"Applied Moments"** calculates the moments of external forces with respect to the fixed-to-rotor reference system and applies them to the Euler's equations (5.20) in the form (5.33), achievable after some simple calculations. The output is constituted by the components of angular speed vector, evaluated in the fixed-to-rotor reference system and determined by integrating (5.33), as can be seen in the SIMULINK® diagram of Fig. 5.5.

$$\begin{cases} \dot{\omega}_I = \dfrac{M_{oI}}{I_{oI}} - \dfrac{I_{o\eta} - I_{o\varepsilon}}{I_{oI}} \omega_\varepsilon \omega_\eta \\ \dot{\omega}_\varepsilon = \dfrac{M_{o\varepsilon}}{I_{o\varepsilon}} - \dfrac{I_{oI} - I_{o\eta}}{I_{o\varepsilon}} \omega_I \omega_\eta \\ \dot{\omega}_\eta = \dfrac{M_{o\eta}}{I_{o\eta}} - \dfrac{I_{o\varepsilon} - I_{oI}}{I_{o\eta}} \omega_I \omega_\varepsilon \end{cases} \tag{5.33}$$

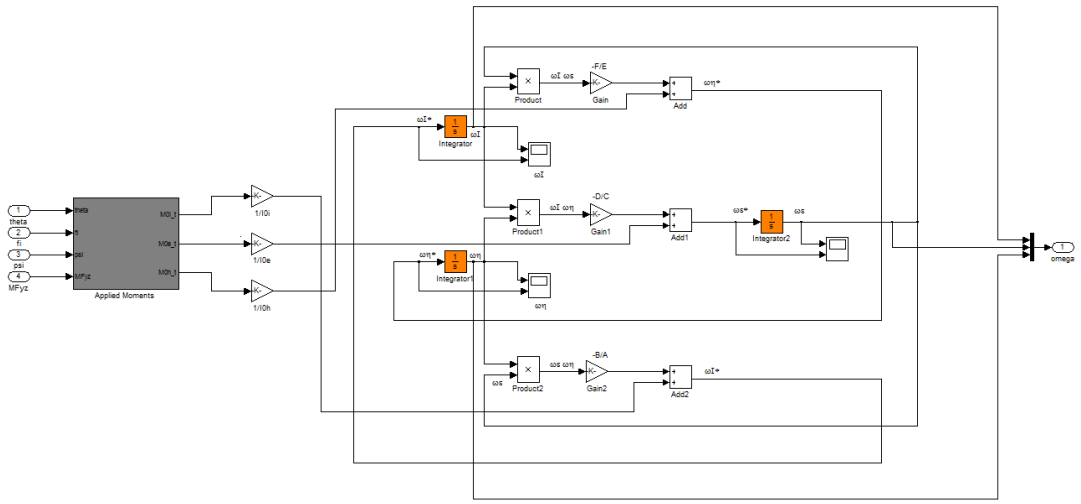

Fig. 5.5. Diagram of the Euler equations block

3) **Lagrangian variables block:** applies the inverse matrix of (5.12), described in the equation (5.34), to the angular speed vector $\overline{\omega}$ in order to determine the derivatives with respect to time $[\dot{\psi}, \dot{\varphi}, \dot{\theta}]$ of the lagrangian variables $[\psi, \varphi, \theta]$, which are obtained by means of integration: they constitute the components of the angular speed vector $\overline{\omega}$ evaluated in the absolute reference system.

$$\begin{bmatrix} \dot{\psi} \\ \dot{\varphi} \\ \dot{\theta} \end{bmatrix} = \begin{bmatrix} 0 & sin\,\theta/cos\,\varphi & cos\,\theta/cos\,\varphi \\ 0 & -cos\,\theta & sin\,\theta \\ 1 & -tan\,\varphi\, sin\,\theta & -tan\,\varphi\, cos\,\theta \end{bmatrix} \begin{bmatrix} \omega_I \\ \omega_\varepsilon \\ \omega_\eta \end{bmatrix} \tag{5.34}$$

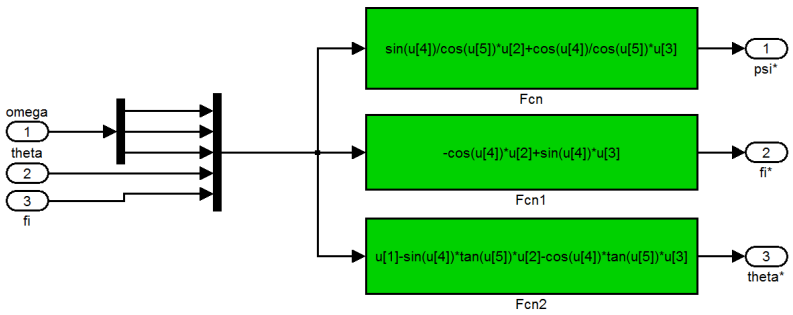

Fig. 5.6. Diagram of the Lagrangian variables block

4) **Axis coordinates block:** it converts the lagrangian variables $[\psi, \varphi, \theta]$, constituted by angular coordinates, in the linear coordinates $[x, y, z]$ which describe the position of the motor shaft end point. These are then used in a closed loop feedback to return as an input in the "Levitation forces block", closing in this way the loop of the bearingless machine control system.

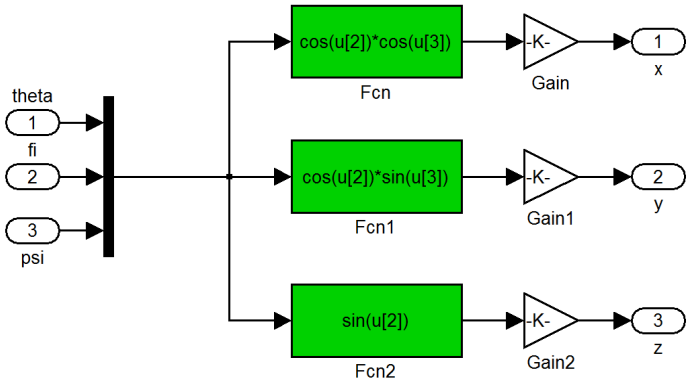

Fig. 5.7. Diagram of the "Axis coordinates block"

5.4 Detailed analysis of the control system

5.4.1 Levitation Forces Block

A) Position Errors

These blocks determines the errors along the *y* and *z* axes, calculating the difference between the actual position, on the *y*-*z* plane, of the end shaft point and the reference values y0 and z0, which obviously have to be set to zero requiring a centered rotor (Fig. 5.8).

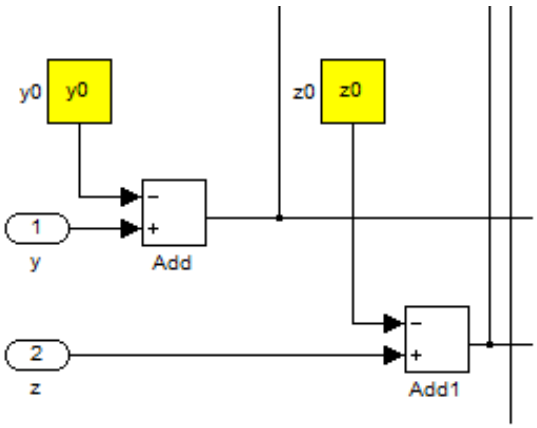

Fig. 5.8. Position errors

B) Pid Controllers

In Fig. 5.9 is represented the general structure of the PID controller, where is possible to distinguish the three actions: proportional, integrator, derivative.

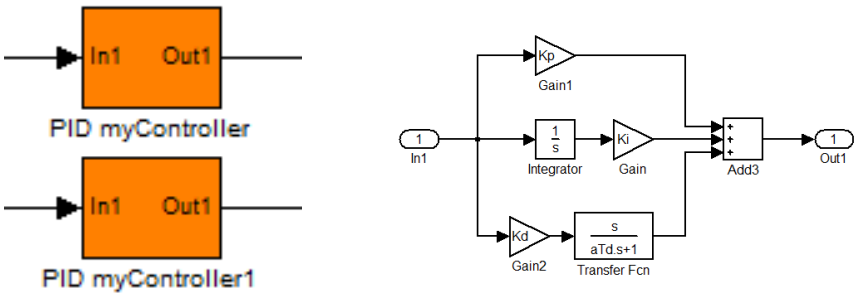

Fig. 5.9. Diagram of the PID controllers

The parameter aTd in the derivative branch is a time constant which permits to set the duration of the transitional regime. The output of the PIDs gives the *y*- and *z*-components of the force, necessary to stabilize the rotor.

C) Force Controller Block

The input stadium transforms the components of the force from cartesian representation to polar, providing the modulus Fr and the spatial phase fi_Fr. In addition, the angular position of the rotor theta is a required input variable. As said above, the **Force Controller** determines the modulus and the phase of the levitation current space vector $\bar{i}_{sv2}$ (respectively identified by the output variables Irms_ and fi_In_), required to generate the input force. These values result approximate because the analytic relationship that allows the calculation of the current space vector parameters from the value of the force, is invertible only considering the interaction between the main harmonic of the stator levitation field and the main one of the rotor field. In this way, all the higher harmonic orders are neglected. However, this is not a problem because the consequent block takes into account all the possible interactions between the magnetic fields, and the PID controllers provide to stabilize the system with their feedback action; but, the function of the **Force Controller** is necessary to give some initial values of the $\bar{i}_{sv2}$ parameters, in absence of which would not be possible to implement the regulation process.

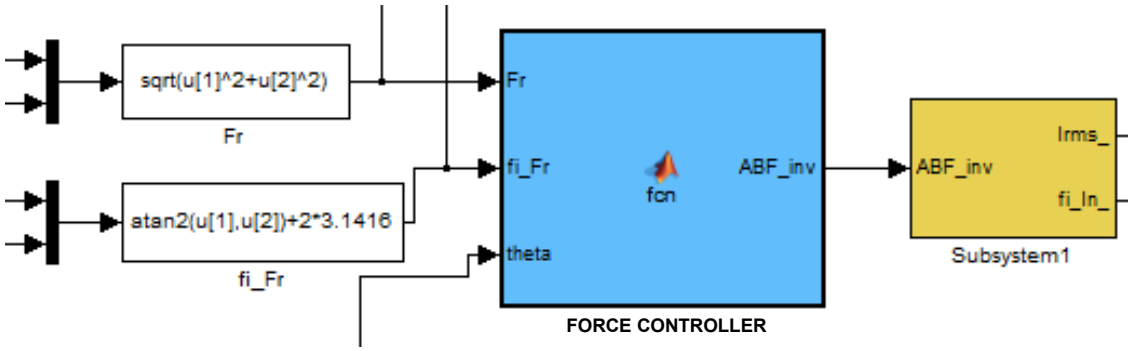

Fig. 5.10. The Force Controller of the model

In the following, the programming code of the **Force Controller** is shown, being a *"Matlab function"*.

```
function ABF_inv = fcn(Fr,fi_Fr,theta)

 %definizione costanti
 Pi = 3.141592654;
 muzero = 0.000001256;

%*********************************************************************************
%INPUT DATI (begin)
%*********************************************************************************

%%modulo della forza radiale
% Fr = 2620.06;
%%fase spaziale della forza radiale, misurata rispetto all'asse y (FEMM)
% fi_Fr = -90 * Pi / 180;
%%massimo ordine armonico indagato
 k_max = 2;

 Br_=zeros(1,1);
 Bs_=zeros(1,1);
 Irms_=zeros(1,1);
 fi_In_=zeros(1,1);
 k_=zeros(1,1);
 hn_=zeros(1,1);
 hp_=zeros(1,1);
%dichiarazione array
 ctr=zeros(k_max,1);
 rot=zeros(k_max,1);
 Kd=zeros(k_max,1);
 Bs_hp=zeros(k_max,1);
 Bs_hn=zeros(k_max,1);
 Br_hp=zeros(k_max,1);
 Br_hn=zeros(k_max,1);
 fi_In_hp=zeros(k_max,1);
 fi_In_hn=zeros(k_max,1);
 Fq=zeros(k_max,1);
 Fd=zeros(k_max,1);
 %Fr=zeros(k_max,1);
 %fi_Fr=zeros(k_max,1);
 Irms_hp=zeros(k_max,1);
 Irms_hn=zeros(k_max,1);
 hp=zeros(k_max,1);
 hn=zeros(k_max,1);

 %angolo meccanico fra asse M ed asse fase 1 (gr.mecc.)
  % deltath = 90;
  % deltath = deltath * Pi / 180;
 %numero di cave sottese dalla bobina
  nac = 10;
 %numero di fasi
  m = 5;
 %numero di cave/polo/fase
  q = 6;
 %numero di conduttori in cava
  n = 2;
 %numero cave statoriche
  %Ncv = 30;
 %coppie polari STATORE (riferite al campo PRINCIPALE)
  N_ = 1;
 %coppie polari ROTORE
  M_ = 1;
```

```
 %angolo descritto dal magnete (rad.mecc.)
  alfa_mag = 172;
  alfa_mag = alfa_mag * Pi / 180;
 %spessore del magnete
  Lm = 0.002;
 %spessore del traferro
  g = 0.001;
 %permeabilità relativa magnete
  mu_mr = 1.045;
 %fattore di Carter
  kc = 1;
 %induzione residua magnete
  Bres = 1.05;
 %profondità di macchina
  L = 0.18;
 %raggio medio al traferro
  Rg = 0.0595;
 %angolo di cava (rad.el.)
  alfa_c = 12;
  alfa_c = alfa_c * Pi / 180;
  %alfa_c = Pi / m / q
  %alfa_c = 2 * Pi / Ncv * N_
  %alfa_c = 2 * Pi / Ncv * M_
 %sequenza temporale di corrente
  st = 2;
 %angolo elettrico correnti (pulsazione * tempo - gr.el.)
  wt = 0;
  wt = wt * Pi / 180;

%*******************************************************************************************
%INPUT DATI (end)
%*******************************************************************************************

%spessore traferro complessivo
 deltag = Lm + g;
%semiampiezza di una bobina (rad.el.)
 gamma = nac * alfa_c / 2;
%induzione al traferro generata dal magnete
 BgM = Lm / (Lm + mu_mr * kc * g) * Bres;
%passo polare (al traferro)
 %Taup = Pi * Rg / N_;

%ordine massimo sequenza di corrente
 st_max = m - 1;
 if st > st_max
  return
 end

  for k = 1 : k_max
   ctr(k) = 0;
   rot(k) = ' ';
   Kd(k) = 0;
  %componenti della forza radiale definite rispetto all'asse y (d) (FEMM)
   Fq(k) = Fr * sin(fi_Fr);
   Fd(k) = Fr * cos(fi_Fr);
  end

  for k = 1 : k_max

   if (k + st) / m == int32((k + st) / m)
    ctr(k) = 1;
    rot(k) = 'I';
   elseif (k - st) / m == int32((k - st) / m)
    ctr(k) = 2;
    rot(k) = 'D';
   else
    ctr(k) = 0;
    rot(k) = ' ';
   end
```

```
if ctr(k) == 1 || ctr(k) == 2
%fattore di distribuzione
 Kd(k) = sin(q * k * alfa_c / 2) / q / sin(k * alfa_c / 2);
%valore h positivo
 hp(k) = (1 + k * N_) / M_;
%valore h negativo
 hn(k) = (-1 + k * N_) / M_;

%CASO hp INTERO e DISPARI
% (sovrapponibile con hn INTERO)
 if hp(k) == int32(hp(k)) && hp(k) / 2 ~= int32(hp(k) / 2)
  Br_hp(k) = 4 / hp(k) / Pi * BgM * sin(hp(k) * M_ * alfa_mag / 2);
  Bs_hp(k)= 2 * muzero / Pi / L / Rg / Br_hp(k) * Fr;
  Irms_hp(k) = 2 * k * Pi * 2 * deltag / muzero / m / 4 / n / sqrt(2) / q / Kd(k) /
               sin(k * gamma) * Bs_hp(k);
  if ctr(k) == 2
   fi_In_hp(k)= hp(k) * M_ * theta - wt - atan2(Fq(k),Fd(k));
  elseif ctr(k) == 1
   fi_In_hp(k)= -hp(k) * M_ * theta - wt + atan2(Fq(k),Fd(k));
  end
 end

%CASO hn INTERO e DISPARI
% (sovrapponibile con hp INTERO)
 if hn(k) == int32(hn(k)) && hn(k) / 2 ~= int32(hn(k) / 2)
  Br_hn(k) = 4 / hn(k) / Pi * BgM * sin(hn(k) * M_ * alfa_mag / 2);
  Bs_hn(k)= 2 * muzero / Pi / L / Rg / Br_hn(k) * Fr;
  Irms_hn(k) = 2 * k * Pi * 2 * deltag / muzero / m / 4 / n / sqrt(2) / q / Kd(k) /
               sin(k * gamma) * Bs_hn(k);
  if ctr(k) == 2
   fi_In_hn(k)= hn(k) * M_ * theta - wt + atan2(Fq(k),Fd(k));
  elseif ctr(k) == 1
   fi_In_hn(k)= -hn(k) * M_ * theta - wt - atan2(Fq(k),Fd(k));
  end
 end

%il ciclo si interrompe quando l'ordine armonico di rotore è INTERO, DISPARI ed
%assume il valore INFERIORE tra i due: hn, hp (in realtà questo è sempre 'hn'
%per definizione)
 if (hn(k) == int32(hn(k)) && hn(k) / 2 ~= int32(hn(k) / 2)) && (hn(k) < hp(k))
  Br_=Br_hn(k);
  Bs_=Bs_hn(k);
  Irms_=Irms_hn(k);
  fi_In_=fi_In_hn(k);
  k_=k;
  hn_=hn(k);
  hp_=(1 + k_ * N_) / M_;
  break
 elseif (hp(k) == int32(hp(k)) && hp(k) / 2 ~= int32(hp(k) / 2)) && (hp(k) < hn(k))
  Br_=Br_hp(k);
  Bs_=Bs_hp(k);
  Irms_=Irms_hp(k);
  fi_In_=fi_In_hp(k);
  k_=k;
  hn_=(-1 + k_ * N_) / M_;
  hp_=hp(k);
  break
 else
  Br_=0;
  Bs_=0;
  Irms_=0;
  fi_In_=0;
  k_=0;
  hn_=0;
  hp_=0;
 end

 end

end %(for k = 1 : k_max)
```

```
ABF_inv = [Br_,Bs_,Irms_,fi_In_,k_,hn_,hp_];
```

Note that the code goes to a "break" when the first value of an existing harmonic order is found, both for the magnetic field produced by levitation current space vector $\bar{i}_{sv2}$, both for the magnetic field produced by rotor magnets, taking in this way into account only the main orders.

D) Electromagnetic Model Block

The **Electromagnetic Model** block represents a complete model of the motor, by the electrical point of view. It determines the effective radial force necessary to support the rotor, in terms of the *y*- and *z*-components Fy and Fz, taking into account all the possible interactions between the harmonic orders of stator and rotor magnetic fields, according to the conditions of existence already seen in chapter 4 and revived hereunder (5.35)-(5.39):

$$\frac{k_1 \mp s_{v1}}{m} \in N_0, \quad \frac{k_2 \mp s_{v2}}{m} \in N_0, \quad \frac{k_2^{'} \mp s_{v2}}{m} \in N_0, \quad h \in N_{odd} \tag{5.35}$$

$$hp_r - k_1 p_s = \pm 1 \tag{5.36}$$

$$hp_r - k_2 p_s = \pm 1 \tag{5.37}$$

$$k_2 p_s - k_1 p_s = \pm 1 \tag{5.38}$$

$$k_2^{'} p_s - k_2 p_s = \pm 1 \tag{5.39}$$

This model also considers the effects of both space vectors $\bar{i}_{sv1}$, $\bar{i}_{sv2}$ (respectively, torque and levitation), thus provides an accurate prediction of the radial force and torque generated by the motor. The drive maintains the current space vector $\bar{i}_{sv1}$ in leading by 90 electrical degrees with respect to the magnet axis, so that the motor produces the requested torque in each operating condition of the $\bar{i}_{sv2}$ space vector: particularly, this task is performed by the block

represented in the following Fig. 5.11, which adds an angle of 90 electrical degrees to the electrical angle corresponding to theta, angular position of the magnet axis. The obtained result, together with the value of Irms1 block, completely defines the current space vector $\bar{i}_{sv1}$.

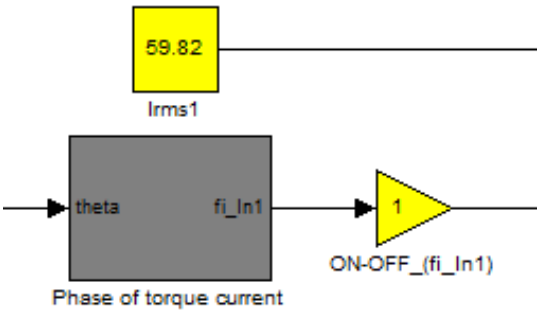

Fig. 5.11

The input of **Electromagnetic model** block is given by the $\bar{i}_{sv1}$ modulus and phase Irms1 and fi_In1, the $\bar{i}_{sv2}$ modulus and phase Irms2 and fi_In2, the rotor position deltath (it is the same variable theta used in the Force Controller, its name changed only because of formal reasons), Fig. 5.12.

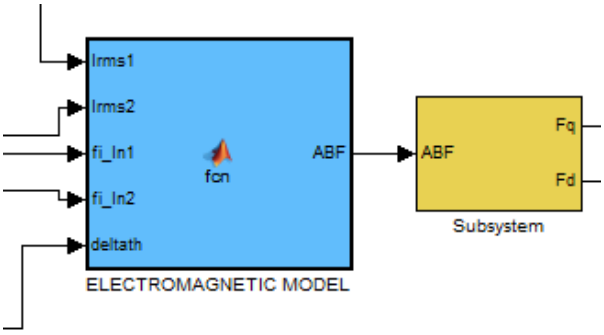

Fig. 5.12

In the following, the programming code of the **Electromagnetic Model** is shown, being a *"Matlab function"*.

```
%ALGORITMO COMPLETO
% interazioni st1-rotore, st2-rotore, st1-st2, st2-st2 descritte tramite
% sviluppo in serie di Fourier

function ABF = fcn(Irms1,Irms2,fi_In1,fi_In2,deltath)

 %Irms=zeros(1,1);
 %fi_In=zeros(1,1);
 %st=zeros(1,1);

 %sequenze di corrente
 st1=1;
 st2=2;

%definizione costanti
 Pi = 3.141592654;
 muzero = 0.000001256;
%numero di cave sottese dalla bobina
  nac = 10;
 %numero di fasi
  m = 5;
 %numero di cave/polo/fase
  q = 6;
 %numero di conduttori in cava
  n = 2;
 %coppie polari STATORE (riferite al campo PRINCIPALE)
  N_ = 1;
 %coppie polari ROTORE
  M_ = 1;
 %angolo descritto dal magnete (rad.mecc.)
  alfa_mag = 172;
  alfa_mag = alfa_mag * Pi / 180;
 %spessore del magnete
  Lm = 0.002;
 %spessore del traferro
  g = 0.001;
 %permeabilità relativa magnete
  mu_mr = 1.045;
 %fattore di Carter
  kc = 1;
 %induzione residua magnete
  Bres = 1.05;
 %profondità di macchina
  L = 0.18;
 %raggio medio al traferro
  Rg = 0.0595;
 %angolo di cava (rad.el.)
  alfa_c = 12;
  alfa_c = alfa_c * Pi / 180;
 %massimo ordine armonico indagato
  k_max = 30;
  k1_max = k_max;
  k2_max = k_max;
 %angolo elettrico correnti (pulsazione - gr.el.)
  wt = 0;
  wt = wt * Pi / 180;

%*****************************************************************************************
%INPUT DATI (end)
%*****************************************************************************************

%spessore traferro complessivo
 deltag = Lm + g;
%semiampiezza di una bobina (rad.el.)
 gamma = nac * alfa_c / 2;
%induzione al traferro generata dal magnete
 BgM = Lm / (Lm + mu_mr * kc * g) * Bres;
```

```
%passo polare (al traferro)
 Taup = Pi * Rg / N_;

 ctr=zeros(k_max,1);
 rot=zeros(k_max,1);
 Kd=zeros(k_max,1);
 Bs=zeros(k_max,1);
 Br=zeros(k_max,1);

 Fq_hp1=zeros(k1_max,1);
 Fd_hp1=zeros(k1_max,1);
 Fq_hn1=zeros(k1_max,1);
 Fd_hn1=zeros(k1_max,1);
 Fnq_hp1=zeros(k1_max,1);
 Fnd_hp1=zeros(k1_max,1);
 Fnq_hn1=zeros(k1_max,1);
 Fnd_hn1=zeros(k1_max,1);
 fi_Frp1=zeros(k1_max,1);
 fi_Frn1=zeros(k1_max,1);

 Fq_hp2=zeros(k2_max,1);
 Fd_hp2=zeros(k2_max,1);
 Fq_hn2=zeros(k2_max,1);
 Fd_hn2=zeros(k2_max,1);
 Fnq_hp2=zeros(k2_max,1);
 Fnd_hp2=zeros(k2_max,1);
 Fnq_hn2=zeros(k2_max,1);
 Fnd_hn2=zeros(k2_max,1);
 fi_Frp2=zeros(k2_max,1);
 fi_Frn2=zeros(k2_max,1);

 Fq_s12=zeros(k1_max,1);
 Fd_s12=zeros(k1_max,1);
 Fq_s22=zeros(k2_max,1);
 Fd_s22=zeros(k2_max,1);


 Torque1=zeros(k_max,1);
 Torque2=zeros(k_max,1);
 Fq=zeros(1,1);
 Fd=zeros(1,1);

%*******************************************************************************************
  % SEQUENZA DI CORRENTE ST1

  for i = 1 : k1_max
   ctr(i) = 0;
   rot(i) = ' ';
   Kd(i) = 0;
   Bs(i) = 0;
   Fq_hp1(i) = 0;
   Fd_hp1(i) = 0;
   Fq_hn1(i) = 0;
   Fd_hn1(i) = 0;
   fi_Frp1(i) = 0;
   fi_Frn1(i) = 0;
  end

  for k1 = 1 : k1_max

   if (k1 + st1) / m == int32((k1 + st1) / m)
    ctr(k1) = 1;
    rot(k1) = 'I';
   elseif (k1 - st1) / m == int32((k1 - st1) / m)
    ctr(k1) = 2;
    rot(k1) = 'D';
   else
    ctr(k1) = 0;
    rot(k1) = ' ';
   end
```

```
   if ctr(k1) == 1 || ctr(k1) == 2
   %fattore di distribuzione
    Kd(k1) = sin(q * k1 * alfa_c / 2) / q / sin(k1 * alfa_c / 2);
   %ampiezza della k1-esima armonica di campo
    Bs(k1) = muzero * m / 2 * 4 / k1 / Pi * n * sqrt(2) * Irms1 / 2 / deltag * q *
             Kd(k1) * sin(k1 * gamma);
   %valore h positivo
    hp = (1 + k1 * N_) / M_;
   %valore h negativo
    hn = (-1 + k1 * N_) / M_;
   %CASO hp INTERO
   % (sovrapponibile con hn INTERO)
    if hp == int32(hp) && hp / 2 ~= int32(hp / 2)
     Br_hp = 4 / hp / Pi * BgM * sin(hp * M_ * alfa_mag / 2);
     if ctr(k1) == 2
      Fnq_hp1(k1) = Pi * L * Rg / 2 / muzero * Bs(k1) * Br_hp * sin(hp * M_ * deltath -
                    wt - fi_In1);
      Fq_hp1(k1) = Fnq_hp1(k1); %+ Ftq_hp1(k1) - Fttq_hp1(k1);
      Fnd_hp1(k1) = Pi * L * Rg / 2 / muzero * Bs(k1) * Br_hp * cos(hp * M_ * deltath -
                    wt - fi_In1);
      Fd_hp1(k1) = Fnd_hp1(k1); %+ Ftd_hp1(k1);
     elseif ctr(k1) == 1
      Fnq_hp1(k1) = Pi * L * Rg / 2 / muzero * Bs(k1) * Br_hp * sin(hp * M_ * deltath +
                    wt + fi_In1);
      Fq_hp1(k1) = Fnq_hp1(k1); %+ Ftq_hp1(k1) - Fttq_hp1(k1);
      Fnd_hp1(k1) = Pi * L * Rg / 2 / muzero * Bs(k1) * Br_hp * cos(hp * M_ * deltath +
                    wt + fi_In1);
      Fd_hp1(k1) = Fnd_hp1(k1); %+ Ftd_hp1(k1);
     end
    end
   %CASO hn INTERO
   % (sovrapponibile con hp INTERO)
    if hn == int32(hn) && hn / 2 ~= int32(hn / 2)
     Br_hn = 4 / hn / Pi * BgM * sin(hn * M_ * alfa_mag / 2);
     if ctr(k1) == 2
      Fnq_hn1(k1) = -Pi * L * Rg / 2 / muzero * Bs(k1) * Br_hn * sin(hn * M_ * deltath -
                    wt - fi_In1);
      Fq_hn1(k1) = Fnq_hn1(k1); %+ Ftq_hn1(k1) - Fttq_hn1(k1);
      Fnd_hn1(k1) = Pi * L * Rg / 2 / muzero * Bs(k1) * Br_hn * cos(hn * M_ * deltath -
                    wt - fi_In1);
      Fd_hn1(k1) = Fnd_hn1(k1); %+ Ftd_hn1(k1);
     elseif ctr(k1) == 1
      Fnq_hn1(k1) = -Pi * L * Rg / 2 / muzero * Bs(k1) * Br_hn * sin(hn * M_ * deltath +
                    wt + fi_In1);
      Fq_hn1(k1) = Fnq_hn1(k1); %+ Ftq_hn1(k1) - Fttq_hn1(k1);
      Fnd_hn1(k1) = Pi * L * Rg / 2 / muzero * Bs(k1) * Br_hn * cos(hn * M_ * deltath +
                    wt + fi_In1);
      Fd_hn1(k1) = Fnd_hn1(k1); %+ Ftd_hn1(k1);
     end
    end
   else
    Fq_hp1(k1) = 0;
    Fd_hp1(k1) = 0;
    Fq_hn1(k1) = 0;
    Fd_hn1(k1) = 0;
   end

  end %(next k1)

%RISULTANTE
  for i = 1 : k1_max
   Fq = Fq + Fq_hp1(i);
   Fq = Fq + Fq_hn1(i);
   Fd = Fd + Fd_hp1(i);
   Fd = Fd + Fd_hn1(i);
  end

%*******************************************************************************
 % SEQUENZA DI CORRENTE ST2
```

```
for i = 1 : k2_max
 ctr(i) = 0;
 rot(i) = ' ';
 Kd(i) = 0;
 Bs(i) = 0;
 Fq_hp2(i) = 0;
 Fd_hp2(i) = 0;
 Fq_hn2(i) = 0;
 Fd_hn2(i) = 0;
 fi_Frp2(i) = 0;
 fi_Frn2(i) = 0;
end

for k2 = 1 : k2_max

 if (k2 + st2) / m == int32((k2 + st2) / m)
  ctr(k2) = 1;
  rot(k2) = 'I';
 elseif (k2 - st2) / m == int32((k2 - st2) / m)
  ctr(k2) = 2;
  rot(k2) = 'D';
 else
  ctr(k2) = 0;
  rot(k2) = ' ';
 end

 if ctr(k2) == 1 || ctr(k2) == 2
 %fattore di distribuzione
  Kd(k2) = sin(q * k2 * alfa_c / 2) / q / sin(k2 * alfa_c / 2);
 %ampiezza della k2-esima armonica di campo
  Bs(k2) = muzero * m / 2 * 4 / k2 / Pi * n * sqrt(2) * Irms2 / 2 / deltag * q *
           Kd(k2) * sin(k2 * gamma);
 %valore h positivo
  hp = (1 + k2 * N_) / M_;
 %valore h negativo
  hn = (-1 + k2 * N_) / M_;

  %CASO hp INTERO
  % (sovrapponibile con hn INTERO)
   if hp == int32(hp) && hp / 2 ~= int32(hp / 2)
    Br_hp = 4 / hp / Pi * BgM * sin(hp * M_ * alfa_mag / 2);
    if ctr(k2) == 2
     Fnq_hp2(k2) = Pi * L * Rg / 2 / muzero * Bs(k2) * Br_hp * sin(hp * M_ * deltath -
                   wt - fi_In2);
     Fq_hp2(k2) = Fnq_hp2(k2); %+ Ftq_hp2(k2) - Fttq_hp2(k2);
     Fnd_hp2(k2) = Pi * L * Rg / 2 / muzero * Bs(k2) * Br_hp * cos(hp * M_ * deltath -
                   wt - fi_In2);
     Fd_hp2(k2) = Fnd_hp2(k2); %+ Ftd_hp2(k2);
    elseif ctr(k2) == 1
     Fnq_hp2(k2) = Pi * L * Rg / 2 / muzero * Bs(k2) * Br_hp * sin(hp * M_ * deltath +
                   wt + fi_In2);
     Fq_hp2(k2) = Fnq_hp2(k2); %+ Ftq_hp2(k2) - Fttq_hp2(k2);
     Fnd_hp2(k2) = Pi * L * Rg / 2 / muzero * Bs(k2) * Br_hp * cos(hp * M_ * deltath +
                   wt + fi_In2);
     Fd_hp2(k2) = Fnd_hp2(k2); %+ Ftd_hp2(k2);
    end
   end

 %CASO hn INTERO
 % (sovrapponibile con hp INTERO)
  if hn == int32(hn) && hn / 2 ~= int32(hn / 2)
   Br_hn = 4 / hn / Pi * BgM * sin(hn * M_ * alfa_mag / 2);
   if ctr(k2) == 2
    Fnq_hn2(k2) = -Pi * L * Rg / 2 / muzero * Bs(k2) * Br_hn * sin(hn * M_ * deltath -
                  wt - fi_In2);
    Fq_hn2(k2) = Fnq_hn2(k2); %+ Ftq_hn2(k2) - Fttq_hn2(k2);
    Fnd_hn2(k2) = Pi * L * Rg / 2 / muzero * Bs(k2) * Br_hn * cos(hn * M_ * deltath -
                  wt - fi_In2);
    Fd_hn2(k2) = Fnd_hn2(k2); %+ Ftd_hn2(k2);
```

```
     elseif ctr(k2) == 1
      Fnq_hn2(k2) = -Pi * L * Rg / 2 / muzero * Bs(k2) * Br_hn * sin(hn * M_ * deltath +
                    wt + fi_In2);
      Fq_hn2(k2) = Fnq_hn2(k2); %+ Ftq_hn2(k2) - Fttq_hn2(k2);
      Fnd_hn2(k2) = Pi * L * Rg / 2 / muzero * Bs(k2) * Br_hn * cos(hn * M_ * deltath +
                    wt + fi_In2);
      Fd_hn2(k2) = Fnd_hn2(k2); %+ Ftd_hn2(k2);
     end
    end
   else
    Fq_hp2(k2) = 0;
    Fd_hp2(k2) = 0;
    Fq_hn2(k2) = 0;
    Fd_hn2(k2) = 0;
   end

  end % Next k2

 %RISULTANTE
  for i = 1 : k2_max
   Fq = Fq + Fq_hp2(i);
   Fq = Fq + Fq_hn2(i);
   Fd = Fd + Fd_hp2(i);
   Fd = Fd + Fd_hn2(i);
  end

%*************************************************************************************
 %INTERAZIONE fra i due campi STATORICI di sequenza ST1, ST2

  for k1 = 1 : k1_max
  %campo k1 INVERSO
   if (k1 + st1) / m == int32((k1 + st1) / m)
    %ampiezza della k1-esima armonica di campo
    Kd_k1 = sin(q * k1 * alfa_c / 2) / q / sin(k1 * alfa_c / 2);
    Bs_k1 = muzero * m / 2 * 4 / k1 / Pi * n * sqrt(2) * Irms1 / 2 / deltag * q * Kd_k1
            * sin(k1 * gamma);
    k2p = (1 + k1 * N_) / N_;
    k2n = (-1 + k1 * N_) / N_;
    if (k2p + st2) / m == int32((k2p + st2) / m)
      Kd_k2p = sin(q * k2p * alfa_c / 2) / q / sin(k2p * alfa_c / 2);
      Bs_k2p = muzero * m / 2 * 4 / k2p / Pi * n * sqrt(2) * Irms2 / 2 / deltag * q *
               Kd_k2p * sin(k2p * gamma);
     Fq_s12(k1) = Pi * L * Rg / 2 / muzero * Bs_k1 * Bs_k2p * sin((wt + fi_In1) - (wt +
                  fi_In2));
     Fd_s12(k1) = Pi * L * Rg / 2 / muzero * Bs_k1 * Bs_k2p * cos((wt + fi_In1) - (wt +
                  fi_In2));
     Fq = Fq + Fq_s12(k1);
     Fd = Fd + Fd_s12(k1);
    end
    if (k2p - st2) / m == int32((k2p - st2) / m)
      Kd_k2p = sin(q * k2p * alfa_c / 2) / q / sin(k2p * alfa_c / 2);
      Bs_k2p = muzero * m / 2 * 4 / k2p / Pi * n * sqrt(2) * Irms2 / 2 / deltag * q *
               Kd_k2p * sin(k2p * gamma);
     Fq_s12(k1) = Pi * L * Rg / 2 / muzero * Bs_k1 * Bs_k2p * sin((wt + fi_In1) + (wt +
                  fi_In2));
     Fd_s12(k1) = Pi * L * Rg / 2 / muzero * Bs_k1 * Bs_k2p * cos((wt + fi_In1) + (wt +
                  fi_In2));
     Fq = Fq + Fq_s12(k1);
     Fd = Fd + Fd_s12(k1);
    end

    if (k2n + st2) / m == int32((k2n + st2) / m)
      Kd_k2n = sin(q * k2n * alfa_c / 2) / q / sin(k2n * alfa_c / 2);
      Bs_k2n = muzero * m / 2 * 4 / k2n / Pi * n * sqrt(2) * Irms2 / 2 / deltag * q *
               Kd_k2n * sin(k2n * gamma);
     Fq_s12(k1) = -Pi * L * Rg / 2 / muzero * Bs_k1 * Bs_k2n * sin((wt + fi_In1) - (wt +
                  fi_In2));
     Fd_s12(k1) = Pi * L * Rg / 2 / muzero * Bs_k1 * Bs_k2n * cos((wt + fi_In1) - (wt +
                  fi_In2));
     Fq = Fq + Fq_s12(k1);
```

```
    Fd = Fd + Fd_s12(k1);
   end
   if (k2n - st2) / m == int32((k2n - st2) / m)
     Kd_k2n = sin(q * k2n * alfa_c / 2) / q / sin(k2n * alfa_c / 2);
     Bs_k2n = muzero * m / 2 * 4 / k2n / Pi * n * sqrt(2) * Irms2 / 2 / deltag * q *
              Kd_k2n * sin(k2n * gamma);
    Fq_s12(k1) = -Pi * L * Rg / 2 / muzero * Bs_k1 * Bs_k2n * sin((wt + fi_In1) + (wt +
                 fi_In2));
    Fd_s12(k1) = Pi * L * Rg / 2 / muzero * Bs_k1 * Bs_k2n * cos((wt + fi_In1) + (wt +
                 fi_In2));
    Fq = Fq + Fq_s12(k1);
    Fd = Fd + Fd_s12(k1);
   end
  end
 %campo k1 DIRETTO
  if (k1 - st1) / m == int32((k1 - st1) / m)
   %ampiezza della k1-esima armonica di campo
   Kd_k1 = sin(q * k1 * alfa_c / 2) / q / sin(k1 * alfa_c / 2);
   Bs_k1 = muzero * m / 2 * 4 / k1 / Pi * n * sqrt(2) * Irms1 / 2 / deltag * q * Kd_k1
           * sin(k1 * gamma);
   k2p = (1 + k1 * N_) / N_;
   k2n = (-1 + k1 * N_) / N_;
   if (k2p + st2) / m == int32((k2p + st2) / m)
     Kd_k2p = sin(q * k2p * alfa_c / 2) / q / sin(k2p * alfa_c / 2);
     Bs_k2p = muzero * m / 2 * 4 / k2p / Pi * n * sqrt(2) * Irms2 / 2 / deltag * q *
              Kd_k2p * sin(k2p * gamma);
    Fq_s12(k1) = Pi * L * Rg / 2 / muzero * Bs_k1 * Bs_k2p * sin(-(wt + fi_In1) - (wt +
                 fi_In2));
    Fd_s12(k1) = Pi * L * Rg / 2 / muzero * Bs_k1 * Bs_k2p * cos(-(wt + fi_In1) - (wt +
                 fi_In2));
    Fq = Fq + Fq_s12(k1);
    Fd = Fd + Fd_s12(k1);
   end
   if (k2p - st2) / m == int32((k2p - st2) / m)
     Kd_k2p = sin(q * k2p * alfa_c / 2) / q / sin(k2p * alfa_c / 2);
     Bs_k2p = muzero * m / 2 * 4 / k2p / Pi * n * sqrt(2) * Irms2 / 2 / deltag * q *
              Kd_k2p * sin(k2p * gamma);
    Fq_s12(k1) = Pi * L * Rg / 2 / muzero * Bs_k1 * Bs_k2p * sin(-(wt + fi_In1) + (wt +
                 fi_In2));
    Fd_s12(k1) = Pi * L * Rg / 2 / muzero * Bs_k1 * Bs_k2p * cos(-(wt + fi_In1) + (wt +
                 fi_In2));
    Fq = Fq + Fq_s12(k1);
    Fd = Fd + Fd_s12(k1);
   end

   if (k2n + st2) / m == int32((k2n + st2) / m)
     Kd_k2n = sin(q * k2n * alfa_c / 2) / q / sin(k2n * alfa_c / 2);
     Bs_k2n = muzero * m / 2 * 4 / k2n / Pi * n * sqrt(2) * Irms2 / 2 / deltag * q *
              Kd_k2n * sin(k2n * gamma);
    Fq_s12(k1) = -Pi * L * Rg / 2 / muzero * Bs_k1 * Bs_k2n * sin(-(wt + fi_In1) - (wt
                 + fi_In2));
    Fd_s12(k1) = Pi * L * Rg / 2 / muzero * Bs_k1 * Bs_k2n * cos(-(wt + fi_In1) - (wt +
                 fi_In2));
    Fq = Fq + Fq_s12(k1);
    Fd = Fd + Fd_s12(k1);
   end
   if (k2n - st2) / m == int32((k2n - st2) / m)
     Kd_k2n = sin(q * k2n * alfa_c / 2) / q / sin(k2n * alfa_c / 2);
     Bs_k2n = muzero * m / 2 * 4 / k2n / Pi * n * sqrt(2) * Irms2 / 2 / deltag * q *
              Kd_k2n * sin(k2n * gamma);
    Fq_s12(k1) = -Pi * L * Rg / 2 / muzero * Bs_k1 * Bs_k2n * sin(-(wt + fi_In1) + (wt
                 + fi_In2));
    Fd_s12(k1) = Pi * L * Rg / 2 / muzero * Bs_k1 * Bs_k2n * cos(-(wt + fi_In1) + (wt +
                 fi_In2));
    Fq = Fq + Fq_s12(k1);
    Fd = Fd + Fd_s12(k1);
   end
  end

end %Next k1
```

```
%*************************************************************************************
  %INTERAZIONE fra diversi ordini armonici della sequenza ST2

  for k2 = 1 : k2_max
  %campo k2 INVERSO
   if (k2 + st2) / m == int32((k2 + st2) / m)
    %ampiezza della k2-esima armonica di campo
    Kd_k2 = sin(q * k2 * alfa_c / 2) / q / sin(k2 * alfa_c / 2);
    Bs_k2 = muzero * m / 2 * 4 / k2 / Pi * n * sqrt(2) * Irms2 / 2 / deltag * q * Kd_k2
            * sin(k2 * gamma);
    k2p = (1 + k2 * N_) / N_;
    k2n = (-1 + k2 * N_) / N_;
    if (k2p + st2) / m == int32((k2p + st2) / m)
     Kd_k2p = sin(q * k2p * alfa_c / 2) / q / sin(k2p * alfa_c / 2);
     Bs_k2p = muzero * m / 2 * 4 / k2p / Pi * n * sqrt(2) * Irms2 / 2 / deltag * q *
              Kd_k2p * sin(k2p * gamma);
     Fq_s22(k2) = Pi * L * Rg / 2 / muzero * Bs_k2 * Bs_k2p * sin((wt + fi_In2) - (wt +
                  fi_In2));
     Fd_s22(k2) = Pi * L * Rg / 2 / muzero * Bs_k2 * Bs_k2p * cos((wt + fi_In2) - (wt +
                  fi_In2));
     Fq = Fq + Fq_s22(k2);
     Fd = Fd + Fd_s22(k2);
    end
    if (k2p - st2) / m == int32((k2p - st2) / m)
     Kd_k2p = sin(q * k2p * alfa_c / 2) / q / sin(k2p * alfa_c / 2);
     Bs_k2p = muzero * m / 2 * 4 / k2p / Pi * n * sqrt(2) * Irms2 / 2 / deltag * q *
              Kd_k2p * sin(k2p * gamma);
     Fq_s22(k2) = Pi * L * Rg / 2 / muzero * Bs_k2 * Bs_k2p * sin((wt + fi_In2) + (wt +
                  fi_In2));
     Fd_s22(k2) = Pi * L * Rg / 2 / muzero * Bs_k2 * Bs_k2p * cos((wt + fi_In2) + (wt +
                  fi_In2));
     Fq = Fq + Fq_s22(k2);
     Fd = Fd + Fd_s22(k2);
    end

    if (k2n + st2) / m == int32((k2n + st2) / m)
     Kd_k2n = sin(q * k2n * alfa_c / 2) / q / sin(k2n * alfa_c / 2);
     Bs_k2n = muzero * m / 2 * 4 / k2n / Pi * n * sqrt(2) * Irms2 / 2 / deltag * q *
              Kd_k2n * sin(k2n * gamma);
     Fq_s22(k2) = -Pi * L * Rg / 2 / muzero * Bs_k2 * Bs_k2n * sin((wt + fi_In2) - (wt +
                  fi_In2));
     Fd_s22(k2) = Pi * L * Rg / 2 / muzero * Bs_k2 * Bs_k2n * cos((wt + fi_In2) - (wt +
                  fi_In2));
     Fq = Fq + Fq_s22(k2);
     Fd = Fd + Fd_s22(k2);
    end
    if (k2n - st2) / m == int32((k2n - st2) / m)
     Kd_k2n = sin(q * k2n * alfa_c / 2) / q / sin(k2n * alfa_c / 2);
     Bs_k2n = muzero * m / 2 * 4 / k2n / Pi * n * sqrt(2) * Irms2 / 2 / deltag * q *
              Kd_k2n * sin(k2n * gamma);
     Fq_s22(k2) = -Pi * L * Rg / 2 / muzero * Bs_k2 * Bs_k2n * sin((wt + fi_In2) + (wt +
                  fi_In2));
     Fd_s22(k2) = Pi * L * Rg / 2 / muzero * Bs_k2 * Bs_k2n * cos((wt + fi_In2) + (wt +
                  fi_In2));
     Fq = Fq + Fq_s22(k2);
     Fd = Fd + Fd_s22(k2);
    end
   end

  %campo k2 DIRETTO
   if (k2 - st2) / m == int32((k2 - st2) / m)
    %ampiezza della k2-esima armonica di campo
    Kd_k2 = sin(q * k2 * alfa_c / 2) / q / sin(k2 * alfa_c / 2);
    Bs_k2 = muzero * m / 2 * 4 / k2 / Pi * n * sqrt(2) * Irms2 / 2 / deltag * q * Kd_k2
            * sin(k2 * gamma);
    k2p = (1 + k2 * N_) / N_;
    k2n = (-1 + k2 * N_) / N_;
    if (k2p + st2) / m == int32((k2p + st2) / m)
     Kd_k2p = sin(q * k2p * alfa_c / 2) / q / sin(k2p * alfa_c / 2);
```

```
     Bs_k2p = muzero * m / 2 * 4 / k2p / Pi * n * sqrt(2) * Irms2 / 2 / deltag * q *
              Kd_k2p * sin(k2p * gamma);
     Fq_s22(k2) = Pi * L * Rg / 2 / muzero * Bs_k2 * Bs_k2p * sin(-(wt + fi_In2) - (wt +
                  fi_In2));
     Fd_s22(k2) = Pi * L * Rg / 2 / muzero * Bs_k2 * Bs_k2p * cos(-(wt + fi_In2) - (wt +
                  fi_In2));
     Fq = Fq + Fq_s22(k2);
     Fd = Fd + Fd_s22(k2);
    end

    if (k2p - st2) / m == int32((k2p - st2) / m)
     Kd_k2p = sin(q * k2p * alfa_c / 2) / q / sin(k2p * alfa_c / 2);
     Bs_k2p = muzero * m / 2 * 4 / k2p / Pi * n * sqrt(2) * Irms2 / 2 / deltag * q *
              Kd_k2p * sin(k2p * gamma);
     Fq_s22(k2) = Pi * L * Rg / 2 / muzero * Bs_k2 * Bs_k2p * sin(-(wt + fi_In2) + (wt +
                  fi_In2));
     Fd_s22(k2) = Pi * L * Rg / 2 / muzero * Bs_k2 * Bs_k2p * cos(-(wt + fi_In2) + (wt +
                  fi_In2));
     Fq = Fq + Fq_s22(k2);
     Fd = Fd + Fd_s22(k2);
    end
    if (k2n + st2) / m == int32((k2n + st2) / m)
     Kd_k2n = sin(q * k2n * alfa_c / 2) / q / sin(k2n * alfa_c / 2);
     Bs_k2n = muzero * m / 2 * 4 / k2n / Pi * n * sqrt(2) * Irms2 / 2 / deltag * q *
              Kd_k2n * sin(k2n * gamma);
     Fq_s22(k2) = -Pi * L * Rg / 2 / muzero * Bs_k2 * Bs_k2n * sin(-(wt + fi_In2) - (wt
                  + fi_In2));
     Fd_s22(k2) = Pi * L * Rg / 2 / muzero * Bs_k2 * Bs_k2n * cos(-(wt + fi_In2) - (wt +
                  fi_In2));
     Fq = Fq + Fq_s22(k2);
     Fd = Fd + Fd_s22(k2);
    end
    if (k2n - st2) / m == int32((k2n - st2) / m)
     Kd_k2n = sin(q * k2n * alfa_c / 2) / q / sin(k2n * alfa_c / 2);
     Bs_k2n = muzero * m / 2 * 4 / k2n / Pi * n * sqrt(2) * Irms2 / 2 / deltag * q *
              Kd_k2n * sin(k2n * gamma);
     Fq_s22(k2) = -Pi * L * Rg / 2 / muzero * Bs_k2 * Bs_k2n * sin(-(wt + fi_In2) + (wt
                  + fi_In2));
     Fd_s22(k2) = Pi * L * Rg / 2 / muzero * Bs_k2 * Bs_k2n * cos(-(wt + fi_In2) + (wt +
                  fi_In2));
     Fq = Fq + Fq_s22(k2);
     Fd = Fd + Fd_s22(k2);
    end
   end

  end %Next k2


%CALCOLO RISULTANTI

 %modulo della forza radiale
  Fr1 = sqrt(Fd ^ 2 + Fq ^ 2);
 %angolo misurato rispetto all'asse y (FEMM)
  fi_Fr = atan2(Fq, Fd);

%*************************************************************************************
  % sequenza ST1: CALCOLO COPPIA Torque1(k)

  for k = 1 : k_max

   if (k + st1) / m == int32((k + st1) / m)
    ctr(k) = 1;
    rot(k) = 'I';
   elseif (k - st1) / m == int32((k - st1) / m)
    ctr(k) = 2;
    rot(k) = 'D';
   else
    ctr(k) = 0;
    rot(k) = ' ';
   end
```

```
  if ctr(k) == 1 || ctr(k) == 2
  %fattore di distribuzione
   Kd(k) = sin(q * k * alfa_c / 2) / q / sin(k * alfa_c / 2);
  %ampiezza della k-esima armonica di campo
   Bs(k) = muzero * m / 2 * 4 / k / Pi * n * sqrt(2) * Irms1 / 2 / deltag * q * Kd(k) *
           sin(k * gamma);
   if k / 2 ~= int32(k / 2)
    Br(k) = 4 / k / Pi * BgM * sin(k * M_ * alfa_mag / 2);
    if ctr(k) == 1
     Torque1(k) = 1 / muzero * deltag * L * N_ ^ 2 * Taup * Bs(k) * Br(k) * sin(k * M_
                  * deltath + wt + fi_In1);
    elseif ctr(k) == 2
     Torque1(k) = 1 / muzero * deltag * L * N_ ^ 2 * Taup * Bs(k) * Br(k) * sin(k * M_
                  * deltath - wt - fi_In1);
    else
     Torque1(k) = 0;
    end
   else
    Br(k) = 0;
    Torque1(k) = 0;
   end
  else
   Kd(k) = 0;
   Bs(k) = 0;
  end

 end

%CALCOLO RISULTANTE
 Torque1sum = 0;
 for k = 1 : k_max
  Torque1sum = Torque1sum + Torque1(k);
 end

% sequenza ST2: CALCOLO COPPIA Torque2(k)

 for k = 1 : k_max

  if (k + st2) / m == int32((k + st2) / m)
   ctr(k) = 1;
   rot(k) = 'I';
  elseif (k - st2) / m == int32((k - st2) / m)
   ctr(k) = 2;
   rot(k) = 'D';
  else
   ctr(k) = 0;
   rot(k) = ' ';
  end

  if ctr(k) == 1 || ctr(k) == 2
  %fattore di distribuzione
   Kd(k) = sin(q * k * alfa_c / 2) / q / sin(k * alfa_c / 2);
  %ampiezza della k-esima armonica di campo
   Bs(k) = muzero * m / 2 * 4 / k / Pi * n * sqrt(2) * Irms2 / 2 / deltag * q * Kd(k) *
           sin(k * gamma);
   if k / 2 ~= int32(k / 2)
    Br(k) = 4 / k / Pi * BgM * sin(k * M_ * alfa_mag / 2);
    if ctr(k) == 1
     Torque2(k) = 1 / muzero * deltag * L * N_ ^ 2 * Taup * Bs(k) * Br(k) * sin(k * M_
                  * deltath + wt + fi_In2);
    elseif ctr(k) == 2
     Torque2(k) = 1 / muzero * deltag * L * N_ ^ 2 * Taup * Bs(k) * Br(k) * sin(k * M_
                  * deltath - wt - fi_In2);
    else
     Torque2(k) = 0;
    end
   else
    Br(k) = 0;
    Torque2(k) = 0;
```

```
    end
   else
    Kd(k) = 0;
    Bs(k) = 0;
   end

  end %(for k = 1 : k_max)

%CALCOLO RISULTANTE
  Torque2sum = 0;
  for k = 1 : k_max
   Torque2sum = Torque2sum + Torque2(k);
  end

ABF = [Fq,Fd,Fr1,fi_Fr,Torque1sum,Torque2sum,Irms1,fi_In1,Irms2,fi_In2,deltath];
```

Note that the variables Fq, Fd, restituted as output arguments of the *"Matlab function"*, correspond to the searched Fy, Fz components of the radial force.

E) Forces To Moments Matrix Block

This block simply provides to calculate the moments given by the resultant radial force in the absolute reference system, by means of the contributions of its components (5.40)-(5.41):

$$\overline{M}_{F_y} = -F_y \frac{L_{sh}}{2} sin\,\varphi\hat{i} + F_y \frac{L_{sh}}{2} cos\,\varphi\, cos\,\psi\hat{k} \tag{5.40}$$

$$\overline{M}_{F_z} = F_z \frac{L_{sh}}{2} cos\,\varphi\, sin\,\psi\hat{i} - F_z \frac{L_{sh}}{2} cos\,\varphi\, cos\,\psi\hat{j} \tag{5.41}$$

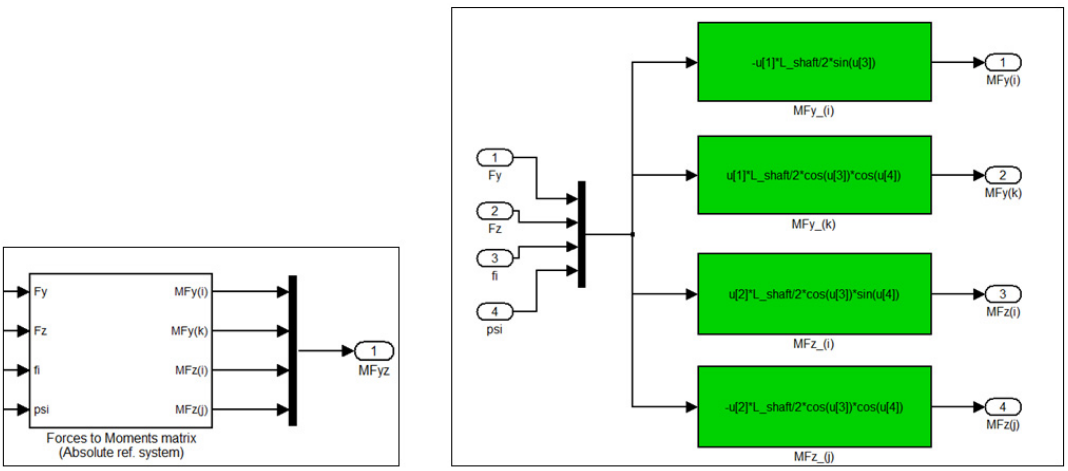

Fig. 5.13

The relationships were implemented in SIMULINK® by describing every single term, as shown in Fig. 5.13.

5.4.2 Euler's Equations Block

A) Applied Moments Block

In the **Applied Moments** block, the moments of the resultant radial forces are recalculated from the ***abs*** to the ***ftr*** reference system. The important feature in this block, is the *"ABSOLUTE to FTR"* function which provides to realize the above action; other blocks are used for auxiliary functions, as the signals scope.

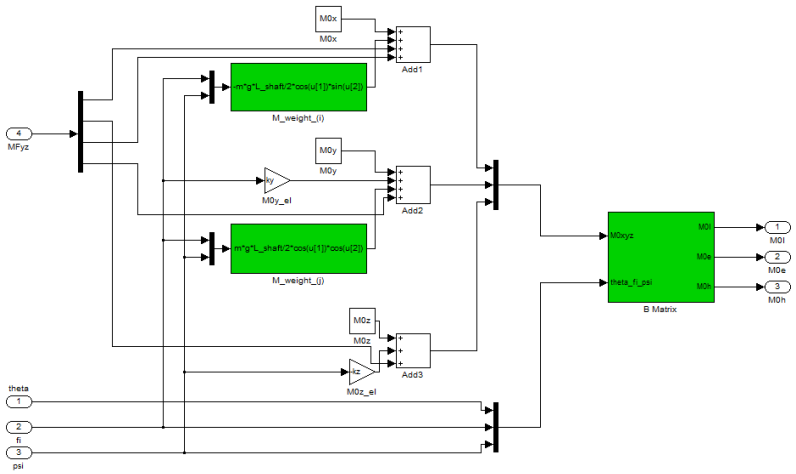

Fig. 5.14

The array MFyz represents the moments already calculated in the **Levitation Forces** block, which are added in summation to the moment produced by the weight force, given in (5.42) with respect to the ***abs*** reference system.

$$\overline{M}_g = \begin{vmatrix} \hat{i} & \hat{j} & \hat{k} \\ \frac{L_{sh}}{2}\cos\varphi\cos\psi & \frac{L_{sh}}{2}\cos\varphi\sin\psi & \frac{L_{sh}}{2}\sin\varphi \\ 0 & 0 & -mg \end{vmatrix} = \tag{5.42}$$

$$= mg\frac{L_{sh}}{2}\left(-\cos\varphi\sin\psi\hat{i} + \cos\varphi\cos\psi\hat{j}\right)$$

Consider the mass m of the rotor and the shaft, the center of gravity located on the axis with a fixed point at the origin O of the system at a distance $L_{sh}/2$ from the latter. The total moment is then expressed, by means of the $\overline{\overline{B}}(\theta,\varphi,\psi)$ matrix (5.31), with respect to the ***ftr*** reference system and passed to the next block.

B) Euler's Equations Block

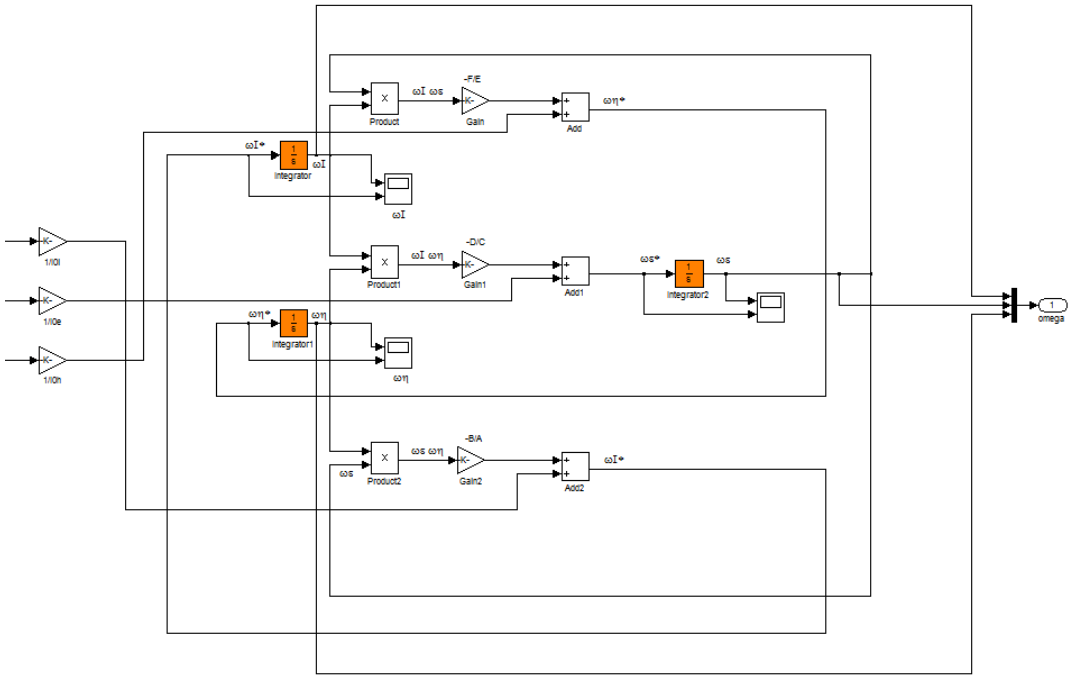

Fig. 5.15

This part of the system implements the Euler's equations, seen in (5.20) as rearranged in (5.33): the output of the block is constituted by the angular speed vector with respect to the ***ftr*** reference system (Fig. 5.15). The variables marked with a capital letter which compare in Fig. 5.15 correspond to the moments of inertia seen in (5.33).

5.5 The setting of PID controllers

To set up the PID controllers, firstly the system was analyzed by disabling the **Force Controller** and **Electromagnetic model** blocks, because of the high complexity of these Matlab functions which introduce the Fourier harmonic series distribution of the various magnetic fields: in fact, considering the whole harmonic contributions, it would be very difficult to define the corresponding transfer function. On the contrary, in this way the PID controllers output gives directly the F_y, F_z components of the resultant force. Obviously, this represents only an intermediate step to produce some provisional values of the PID coefficients K_i, K_p and K_d, being not the original system, but it permitted to obtain the actual values in an easier way. In fact, after having calibrated the values of the PID coefficients by means of this simplified analysis, the two functions were reintroduced to set up and recalculate the coefficients in the actual, original configuration.

The analytical approach to the problem was formulated by expressing the force, resultant of the interactions between magnetic fields by means of its *y*- and *z*-components, as the direct result of the PID controllers regulation, thus as a combination of proportional, integral and derivative actions (5.43), (5.51). Also, the rotor is considered subject to the weight force, obviously acting along the *z*-axis:

A) Equilibrium along the *y*-axis:

$$f_y(t) = K_p \Delta y(t) + K_i \int_0^t \Delta y(\tau) d\tau + K_d \frac{d[\Delta y(t)]}{dt} \tag{5.43}$$

Where Δy represents the error with respect to y coordinate, as defined in (5.45). Applying the Laplace transformation, it gives:

$$F_Y(s) = K_p \Delta Y(s) + \frac{K_i}{s} \Delta Y(s) + K_d \left[s \Delta Y(s) - \Delta y(0) \right] \tag{5.44}$$

$$\Delta y(t) = y(t) - y(0) \quad \Rightarrow \quad \Delta Y(s) = Y(s) - \frac{y(0)}{s} \tag{5.45}$$

By substituting (5.45) in (5.44) it gives:

$$F_Y(s) = K_p Y(s) - K_p \frac{y(0)}{s} + \frac{K_i}{s} Y(s) - \frac{K_i}{s^2} y(0) + K_d s Y(s) - K_d y(0) \tag{5.46}$$

By applying the second law of motion along the *y* axis:

$$m\ddot{y}(t) - f_y(t) = 0 \quad \Rightarrow \quad mL\left[\frac{d^2 y}{dt^2} \right] = L\left[f_y(t) \right] \tag{5.47}$$

By substituting the respective *L*-transforms in the equation (5.47) it gives:

$$\begin{aligned} & m\left[s^2 Y(s) - s y(0) - \dot{y}(0) \right] = \\ & \quad = K_p Y(s) - K_p \frac{y(0)}{s} + \frac{K_i}{s} Y(s) - \frac{K_i}{s^2} y(0) + K_d s Y(s) - K_d y(0) \end{aligned} \tag{5.48}$$

Considering that $y(0) = \dot{y}(0) = 0$, by substituting into (5.48) it gives:

$$m s^2 Y(s) = K_p Y(s) + \frac{K_i}{s} Y(s) + K_d s Y(s) \tag{5.49}$$

By collecting the common terms in (5.49), it gives the trivial solution (5.50):

$$Y(s) = 0 \tag{5.50}$$

Similarly, proceed to writing the equation along the *z*- axis:

B) Equilibrium along the *z*-axis:

$$f_z(t) = K_p \Delta z(t) + K_i \int_0^t \Delta z(\tau) d\tau + K_d \frac{d\left[\Delta z(t) \right]}{dt} \tag{5.51}$$

$$F_z(s) = K_p \Delta Z(s) + \frac{K_i}{s} \Delta Z(s) + K_d \left[s \Delta Z(s) - \Delta z(0) \right] \tag{5.52}$$

$$\Delta z(t) = z(t) - z(0) \quad \Rightarrow \quad \Delta Z(s) = Z(s) - \frac{z(0)}{s} \tag{5.53}$$

$$F_z(s) = K_p Z(s) - K_p \frac{z(0)}{s} + \frac{K_i}{s} Z(s) - \frac{K_i}{s^2} z(0) + K_d s Z(s) - K_d z(0) \tag{5.54}$$

This time the equation includes the weight force, as said above:

$$m\ddot{z}(t) = f_z(t) - mg \quad \Rightarrow \quad mL\left[\frac{d^2 z}{dt^2} \right] = L\left[f_z(t) \right] - \frac{mg}{s} \tag{5.55}$$

$$\begin{aligned} & m\left[s^2 Z(s) - s z(0) - \dot{z}(0) \right] = \\ & \quad = K_p Z(s) - K_p \frac{z(0)}{s} + \frac{K_i}{s} Z(s) - \frac{K_i}{s^2} z(0) + K_d s Z(s) - K_d z(0) - \frac{mg}{s} \end{aligned} \tag{5.56}$$

$$m s^2 Z(s) = K_p Z(s) + \frac{K_i}{s} Z(s) + K_d s Z(s) - \frac{mg}{s} \tag{5.57}$$

By collecting the common terms in (5.57), it gives (5.58), (5.59):

$$Z(s)\left[m s^3 - K_d s^2 - K_p s - K_i \right] = -mg \tag{5.58}$$

$$Z(s) = \frac{-mg}{m s^3 - K_d s^2 - K_p s - K_i} = \frac{-g}{s^3 - \frac{K_d}{m} s^2 - \frac{K_p}{m} s - \frac{K_i}{m}} \tag{5.59}$$

The *L*-transform of the *z* coordinate (5.59) describes the height of the shaft ending point with respect to the centre of the motor. By studying the stability of the equation (5.59) is possible to obtain the order of magnitude of the PID coefficients. It is not the exact solution because, as mentioned before, a simplified system configuration is examined. To find the correlation between the three poles and the coefficients of the polynomial equation in *s*, given by putting the denominator of (5.59) equal to zero, a generic expression of a third degree

polynomial is written:

$$\begin{aligned}&(s-p_1)(s-p_2)(s-p_3)=\\&\quad=s^3-(p_1+p_2+p_3)s^2+(p_1p_2+p_1p_3+p_2p_3)s-p_1p_2p_3=0\end{aligned} \tag{5.60}$$

By equating the coefficients of the polynomial (5.60) to those of the denominator in the equation (5.59), it gives:

$$\begin{cases}p_1+p_2+p_3=\dfrac{K_d}{m}\\ p_1p_2+p_1p_3+p_2p_3=-\dfrac{K_p}{m}\\ p_1p_2p_3=\dfrac{K_i}{m}\end{cases} \tag{5.61}$$

To solve the problem, the easiest way is to choose only one pole of multiplicity equal to three and of negative value if real or, if complex, having a real part of negative value (5.62), to assure the stability of the system:

$$p_1=p_2=p_3=p \quad \begin{cases}p<0 \quad \text{if } p\in\Re\\ \Re e\{p\}<0 \quad \text{if } p\in C\end{cases} \tag{5.62}$$

Finally, by substituting (5.62) in (5.61) and developing the equations, it's possible to obtain the relationships between the PID coefficients and the pole; choosing suitably its value, are determined K_i, K_p and K_d:

$$\begin{cases}3p=\dfrac{K_d}{m} & \Rightarrow \quad K_d=3mp\\ 3p^2=-\dfrac{K_p}{m} & \Rightarrow \quad K_p=-3mp^2\\ p^3=\dfrac{K_i}{m} & \Rightarrow \quad K_i=mp^3\end{cases} \tag{5.63}$$

In the next, p is chosen as a real number: the general criterion is to vary the value of p until the maximum excursion of the motor shaft ending point falls within the

desired tolerance, which can be reasonably fixed in one-tenth of the amplitude of the airgap, or less if necessary.

5.6 Simulations and results

The software SIMULINK® was used in order to complete the simulations; the analyzed machine is characterized by the following parameters (Tab. I):

TABLE I. DATA OF THE MACHINE

Param.	Description	Value
N_{sl}	number of slots	30
p	pole pairs of the machine	1
m	number of phases	5
I_n	rated phase current (A_{rms})	59.82
T_n	rated torque (Nm)	30.29
g	airgap width (mm)	1
D_e	stator outer diameter (mm)	230
D_s	stator inner diameter (mm)	120
D_m	mean diameter of the magnet (mm)	116
D_{cv_ext}	diameter at the bottom of the slot (mm)	170
D_{cv_int}	diameter at the top of the slot (mm)	126.3
D_r	rotor outer diameter (mm)	114
D_{ri}	rotor inner diameter (mm)	60
α_{cv}	slot pitch angle	12°
a_{dt}	stator slot height (mm)	25
h_{cl}	slot opening height (mm)	1
L	axial length of the machine (mm)	180
L_{sh}	total length of the shaft (mm)	320
D_{sh}	shaft diameter (mm)	40
L_m	magnet width (mm)	2
L_{dt}	tooth-body width (mm)	8
L_{cl}	slot opening width (mm)	2
L_{tc}	slot width at the top slot radius (mm)	5.23
L_{fc}	slot width at the bottom slot radius (mm)	9.7
τ_{cv}	slot pitch at the inner stator radius (mm)	12.57
m	rotor and shaft mass (kg)	16.75
I_{0I}	moment of inertia, I axis (kg m^2)	$2.7 \cdot 10^{-2}$
$I_{0\varepsilon}$	moment of inertia, ε axis (kg m^2)	$50.6 \cdot 10^{-2}$
$I_{0\eta}$	moment of inertia, η axis (kg m^2)	$50.6 \cdot 10^{-2}$

Using the method described in the previous section, a list of values for K_i, K_p and K_d is obtained, shown in Tab. II. By applying these values in the simulation, it can be seen that by increasing the absolute value of p, the maximum excursion of the motor shaft ending point is progressively reduced.

TABLE II. VALUES OF PID COEFFICIENTS

p	K_d	K_p	K_i
-20	-1.005E+03	-2.01E+04	-1.34E+05
-40	-2.01E+03	-8.04E+04	-1.072E+06
-80	-4.02E+03	-3.216E+05	-8.576E+06

In the following, will be analyzed the simulation results for p = -80 by representing in the Figs. 5.17, 5.18, the positions of the shaft ending point and of the axis point corresponding to the rotor stack length in the y, z coordinates of the absolute reference system (Fig. 5.1). It is important to note that, with reference to the constrained extremity of the shaft, the rotor stack length extends up to 250 mm and its corresponding axis point position represents the parameter to be verified. The shaft ending point extends up to 320 mm, thus its excursion will be obviously greater than the latter (Fig. 5.16).

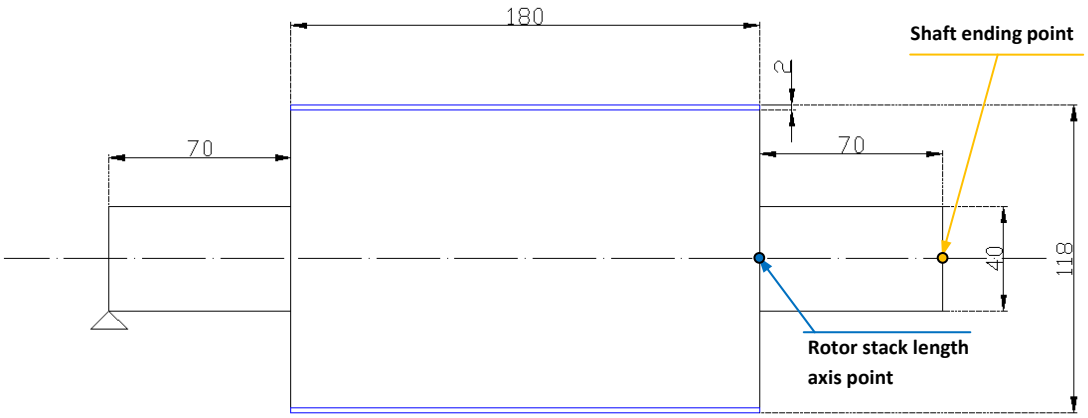

Fig. 5.16

The simulations were performed at a rotor angular speed ω_1 = 1004.8 rad/s, corresponding to 9595.13 rpm and the torque current has the rated value of 59.82 A_{rms}.

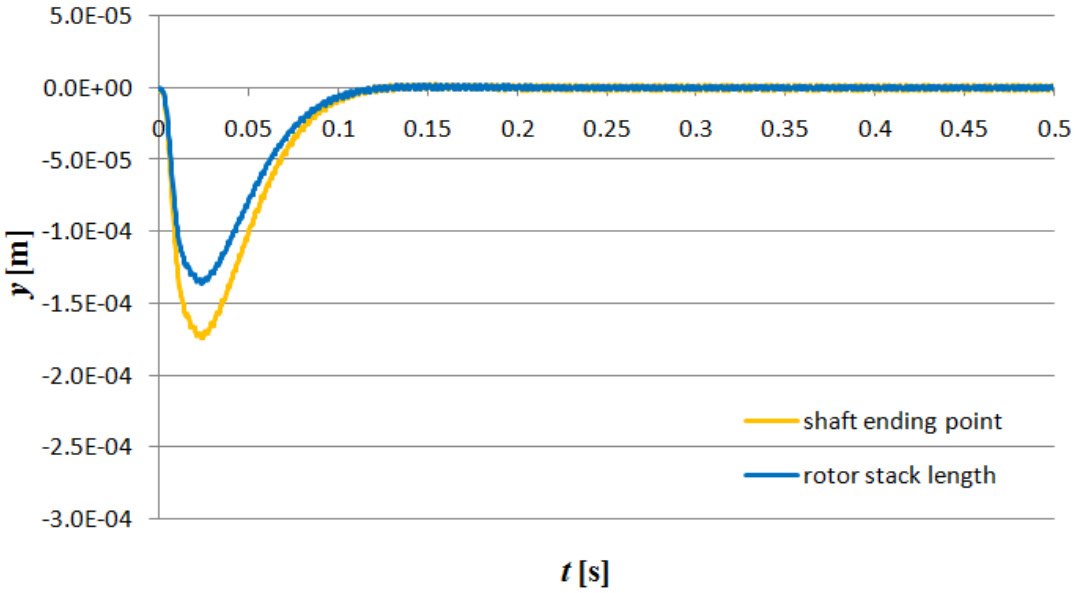

Fig. 5.17

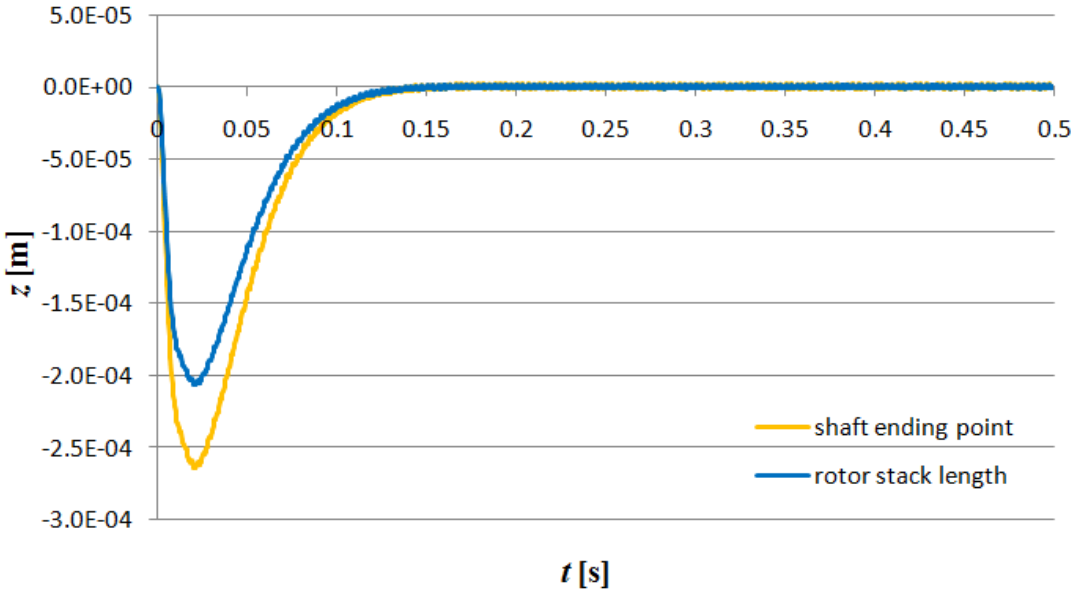

Fig. 5.18

As explained above, all the possible interactions between magnetic fields acting in the airgap are considered, by means of the "Electromagnetic model". Thus, the analyzed situation can be considered as a complete and realistic operating condition of the bearingless machine. In addition, the locus occupied by the same points on the *y*-*z* plane, represented in Fig. 5.19, provides a clearer representation of the rotor axis position. It is also interesting to observe the behavior of the torque and levitation current space vectors, $\bar{i}_{sv1}$ and $\bar{i}_{sv2}$, in terms of rms value and phase, Figs. 5.20-5.21:

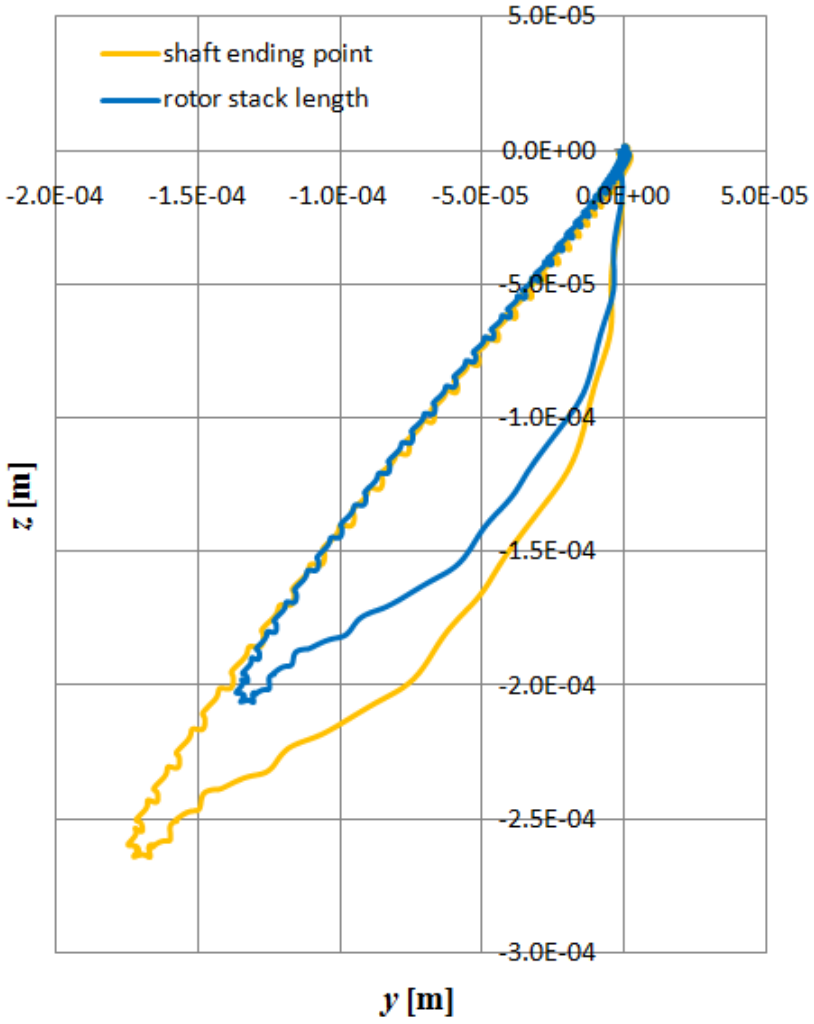

Fig. 5.19

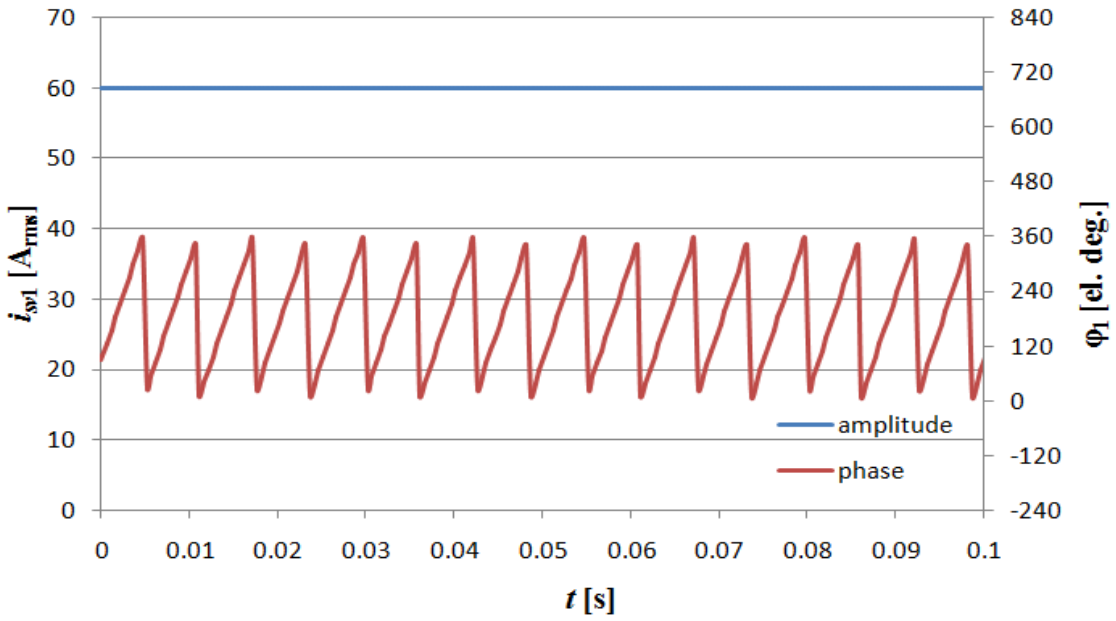

Fig. 5.20

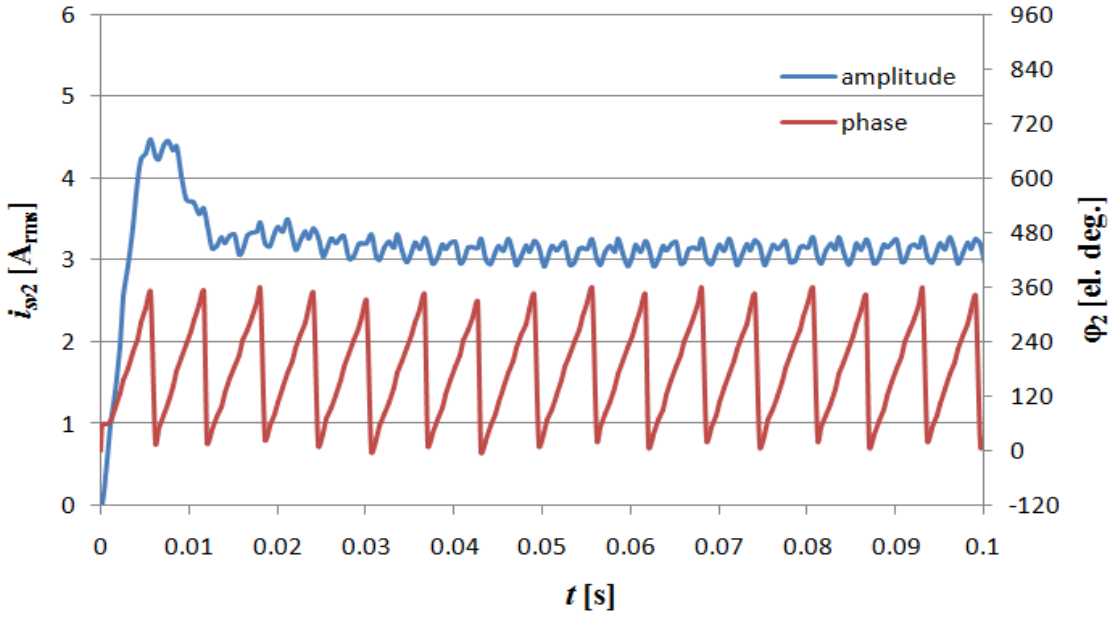

Fig. 5.21

The current space vector 1 has an imposed constant rms value (59.82) to generate continuously the requested torque, its phase which varies remaining in leading by 90 electrical degrees with respect to magnet axis.

The modulus of current space vector 2, after having reached a maximum value of almost 4.5 Amps rms in the early instants of time, oscillates between 3 and 3.3 Amps, while the phase continuously changes its value in the whole range (0 to 360 electrical degrees), having to follow the spatial phase of the required force necessary to counterbalance the weight and the other forces generated by the interactions between harmonic orders of the magnetic fields. To give a more realistic idea, the resultant force vector acting on the rotor, in the time interval from 0 ms to 100 ms, changes its position on the yz plane as shown in Fig. 5.22.

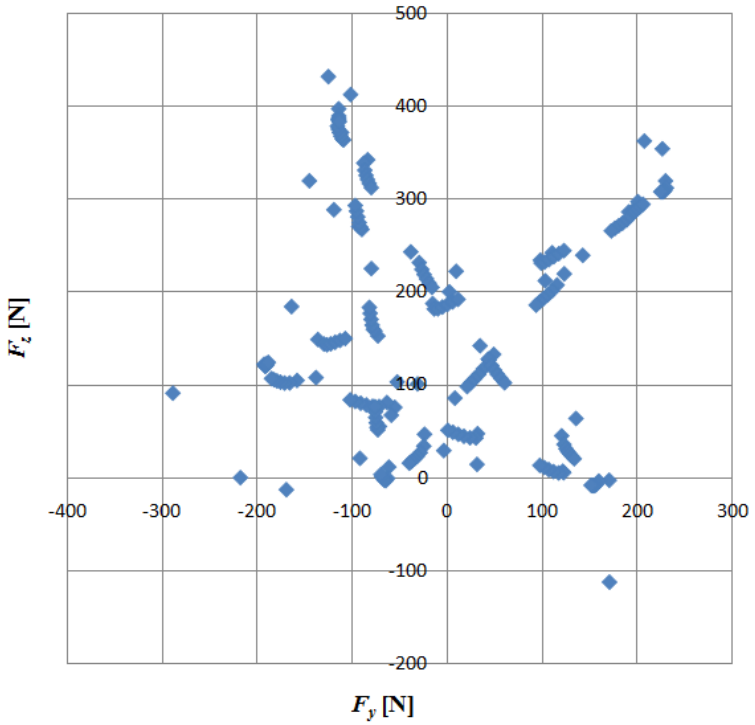

Fig. 5.22

As can be seen by comparing the Figs. 5.17-5.19, the maximum value of the excursion of the rotor stack length axis point is about 2 tenth of millimeter in the

negative z-axis direction and 1.5 tenth of millimeter in the negative y-axis direction, over the prefixed value of 1 tenth, which represents 1 tenth of the airgap width. So, it is necessary to set a different calibration of the PID controllers. The first attempt, based on the values of Tab. II corresponding to p = -80, is made by varying the coefficients K_d, K_p, K_i and verifying the result. Proceeding in this way there is no more correlation with general criterion (5.63), but lower absolute values for parameters could be found with, consequently, an easier way to practically realize the controller. A good compromise is found by acting only on K_p, multiplying by three its value in Tab. II. Thus, the values of Tab. III were used and the simulation results are shown in the following:

TABLE III. VALUES OF PID COEFFICIENTS

K_d	K_p	K_i
-4.02E+03	-9.648E+5	-8.576E+06

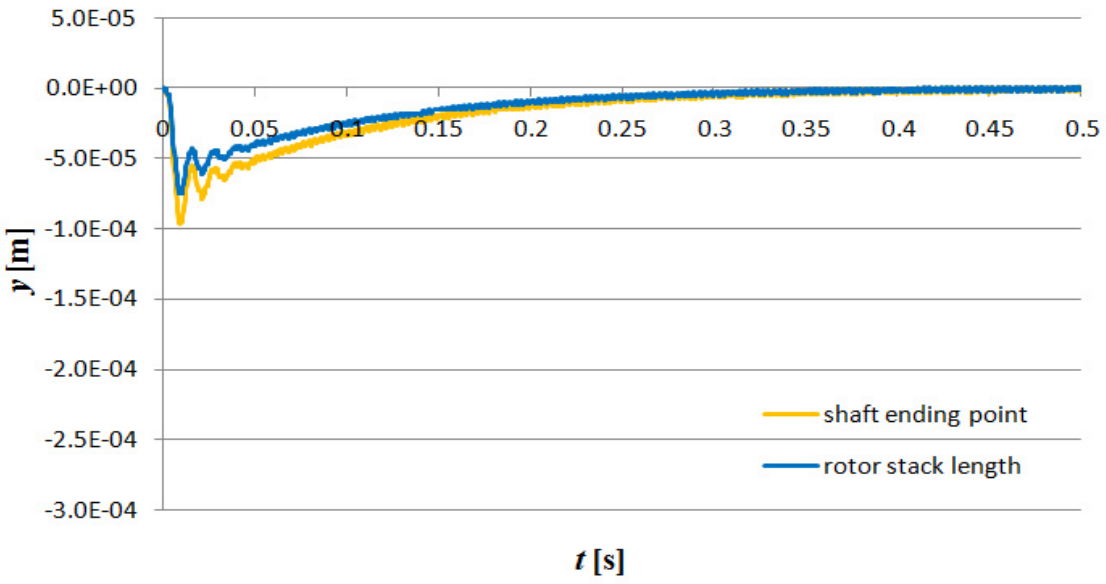

Fig. 5.23

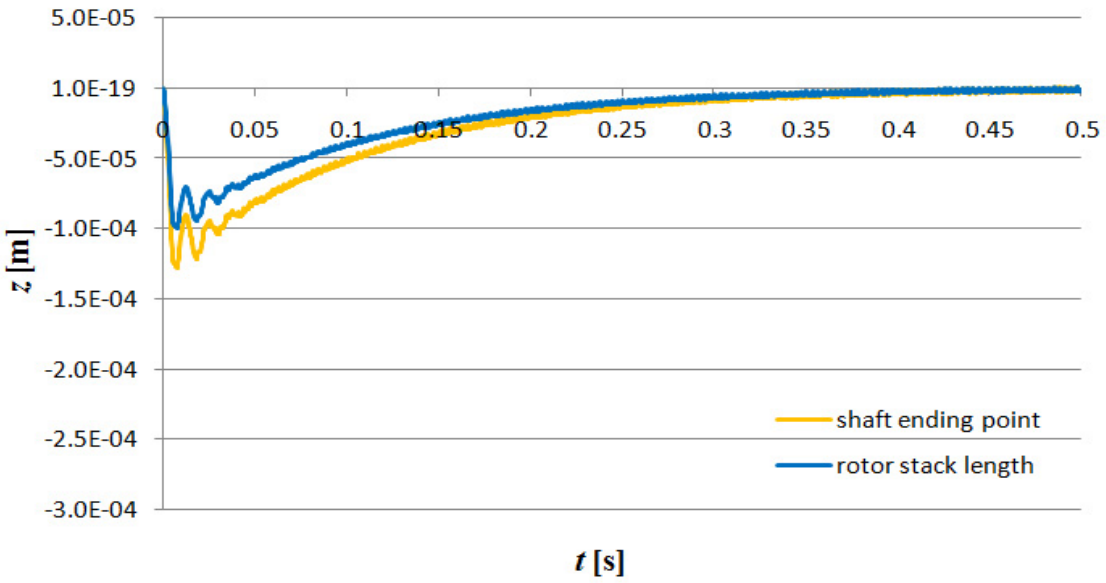

Fig. 5.24

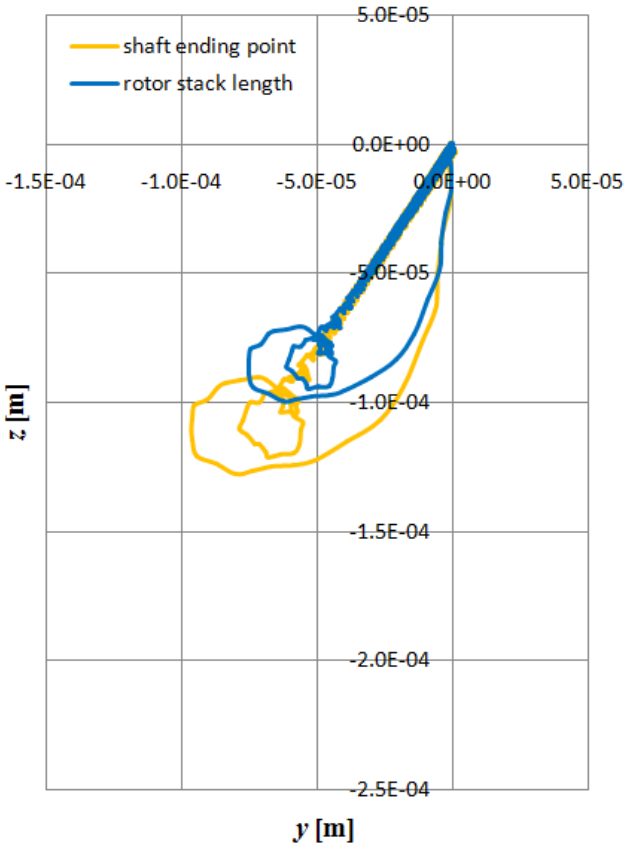

Fig. 5.25

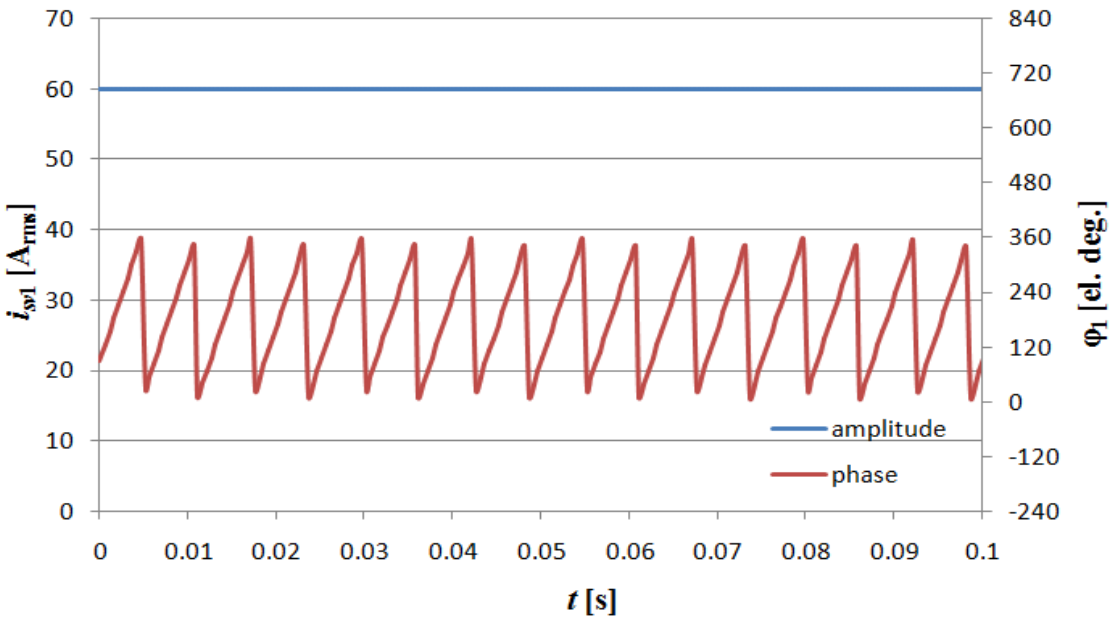

Fig. 5.26

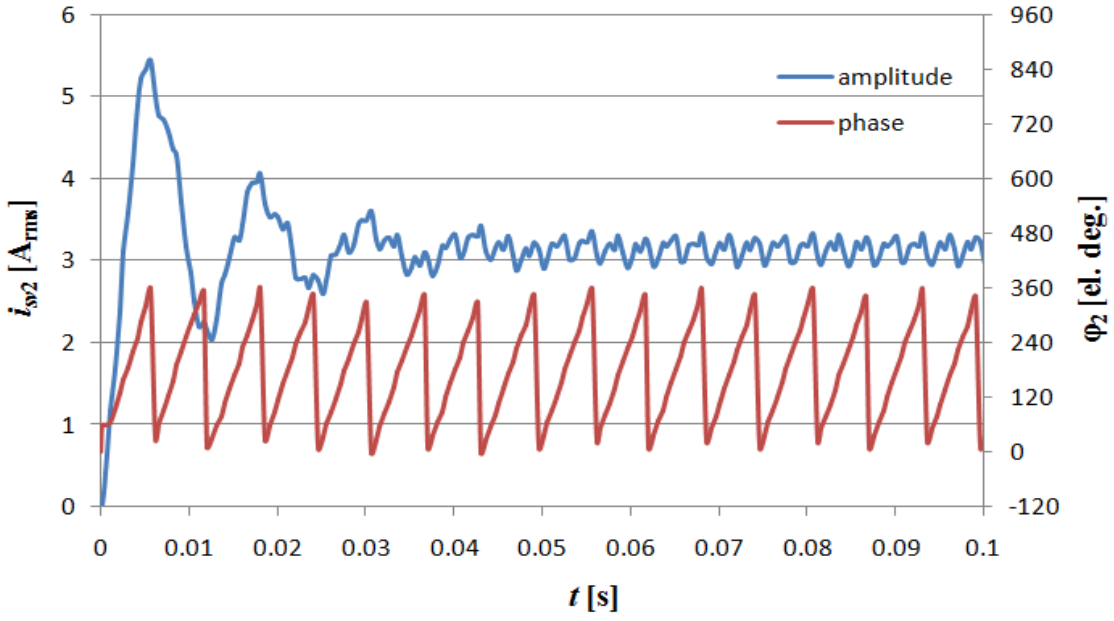

Fig. 5.27

The modulus of current space vector 2 has an oscillating behavior with a progressive reduction tending to the regime, standing in the range of 3 to 3.4 Amps, as can be noted in Fig. 5.27 and, clearly, in Fig. 5.28 where the same function is represented with an extended time axis.

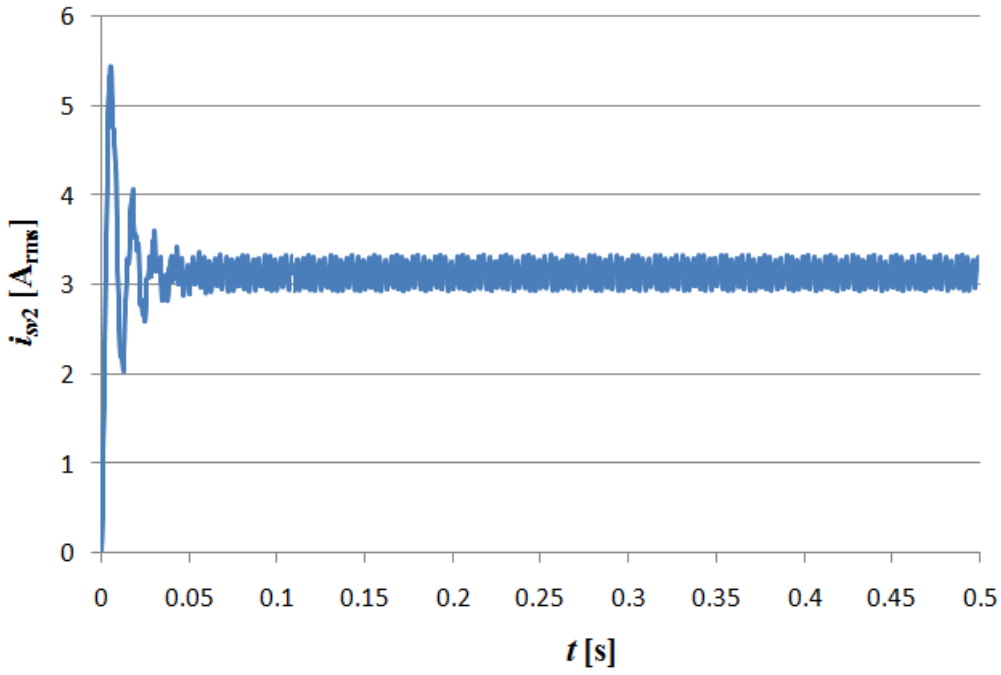

Fig. 5.28

As can be seen by comparing the Figs. 5.23-5.25, now the maximum excursion of the rotor stack length axis point is about 1 tenth of millimeter in the negative z-axis direction and about 0.75 tenth of millimeter in the negative y-axis direction. Thus, it is possible to say that the target has been achieved. As done before, in Fig. 5.29 is shown the succession of the different positions occupied by the resultant force vector on the yz plane in the time interval from 0 ms to 100 ms. In the Figs. 5.30, 5.31 the time axis has been scaled up to the value of 1 second with respect to Figs. 5.23-5.24, to highlight the stable state achieved by the system.

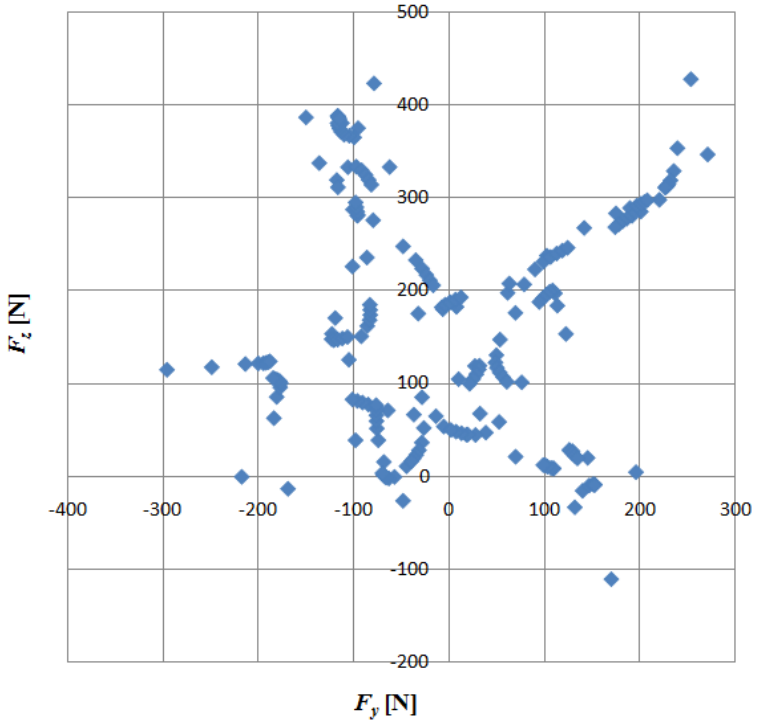

Fig. 5.29

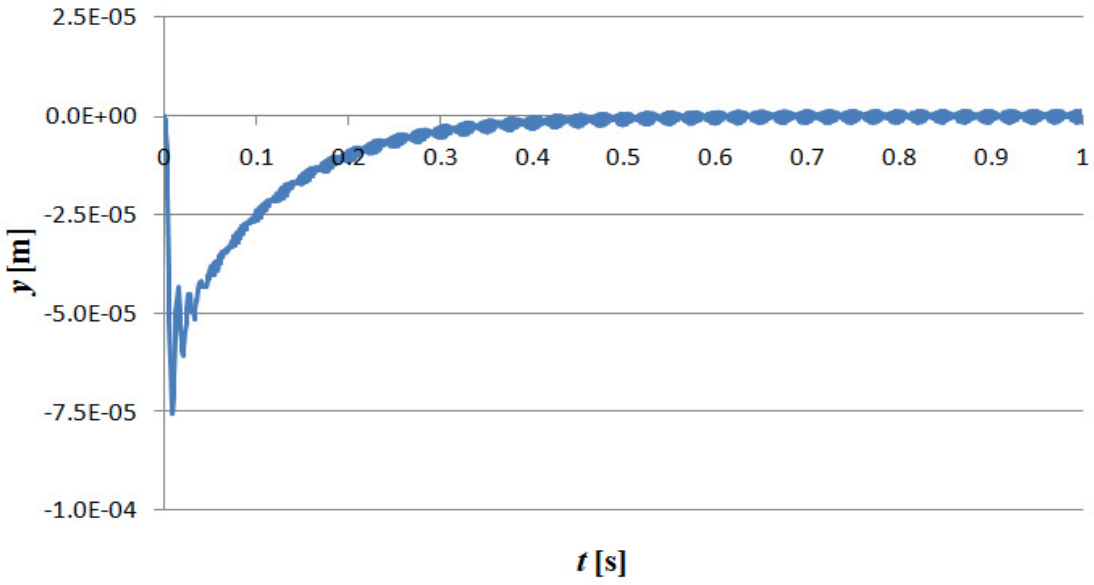

Fig. 5.30

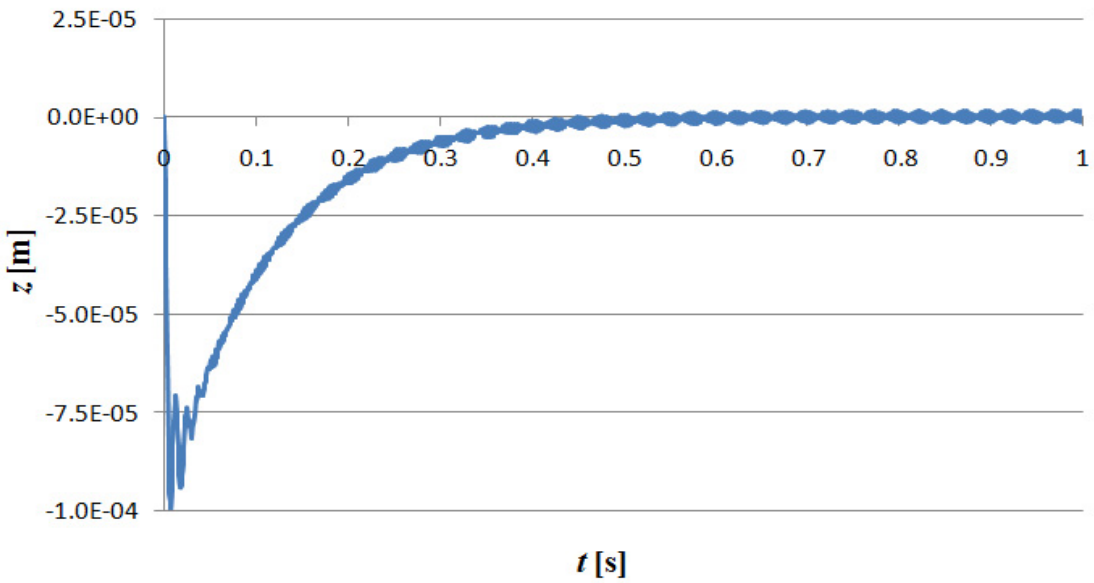

Fig. 5.31

The second way to proceed is by continuing to use the general criterion (5.63), which would probably permits a finest regulation of the PID coefficients. Finally, the values in Tab. IV were found with p = -120:

TABLE IV. VALUES OF PID COEFFICIENTS

p	K_d	K_p	K_i
-120	-6.03E+03	-7.236E+05	-2.8944E+07

The results of the simulation are shown in the following, from Fig. 5.32 to Fig. 5.37.

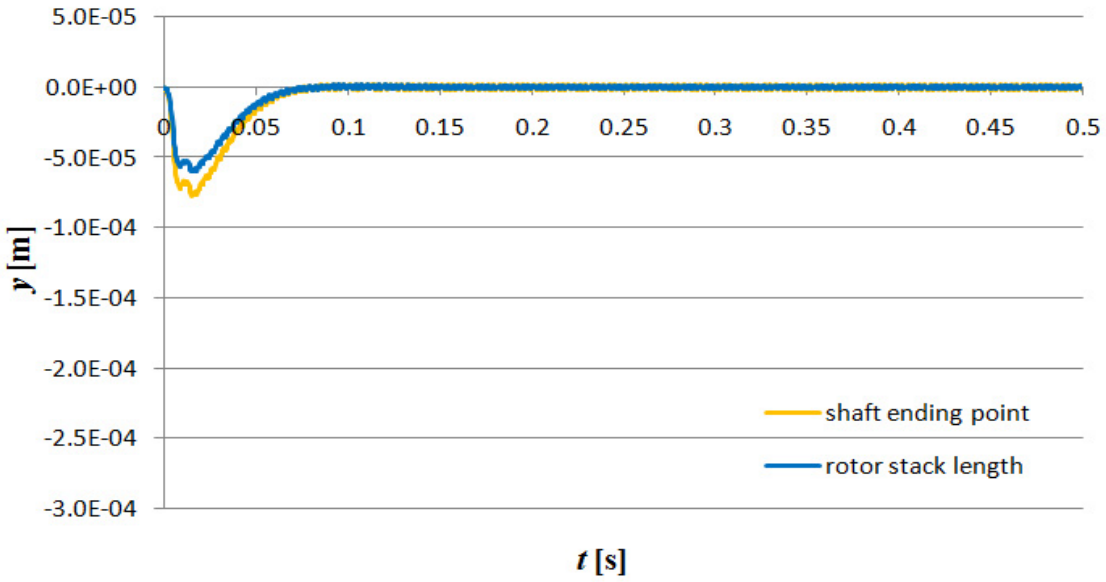

Fig. 5.32

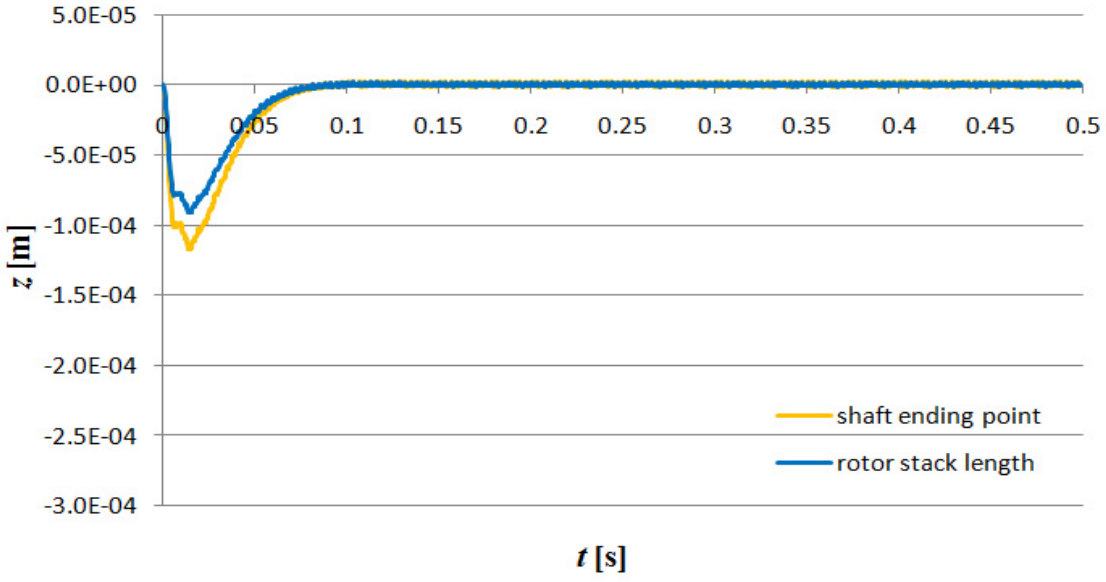

Fig. 5.33

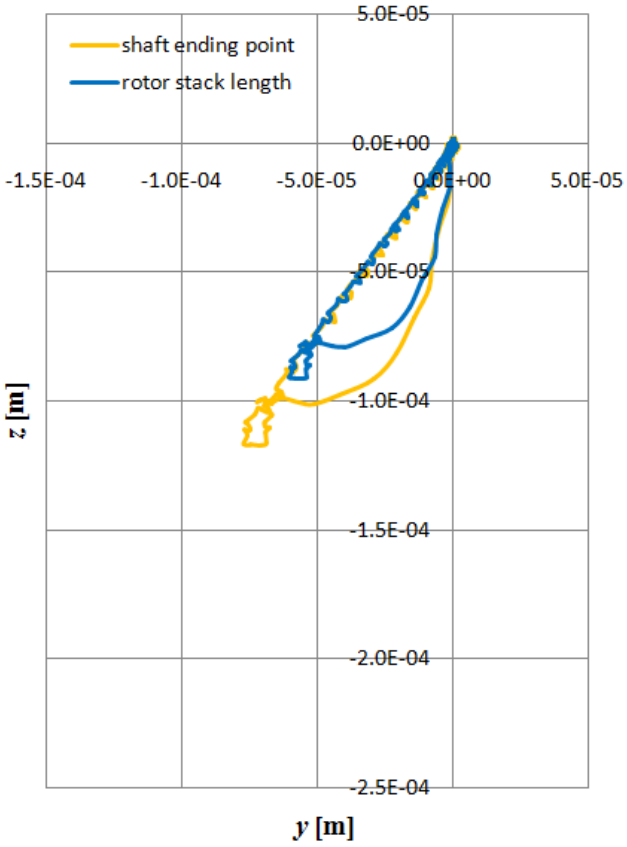

Fig. 5.34

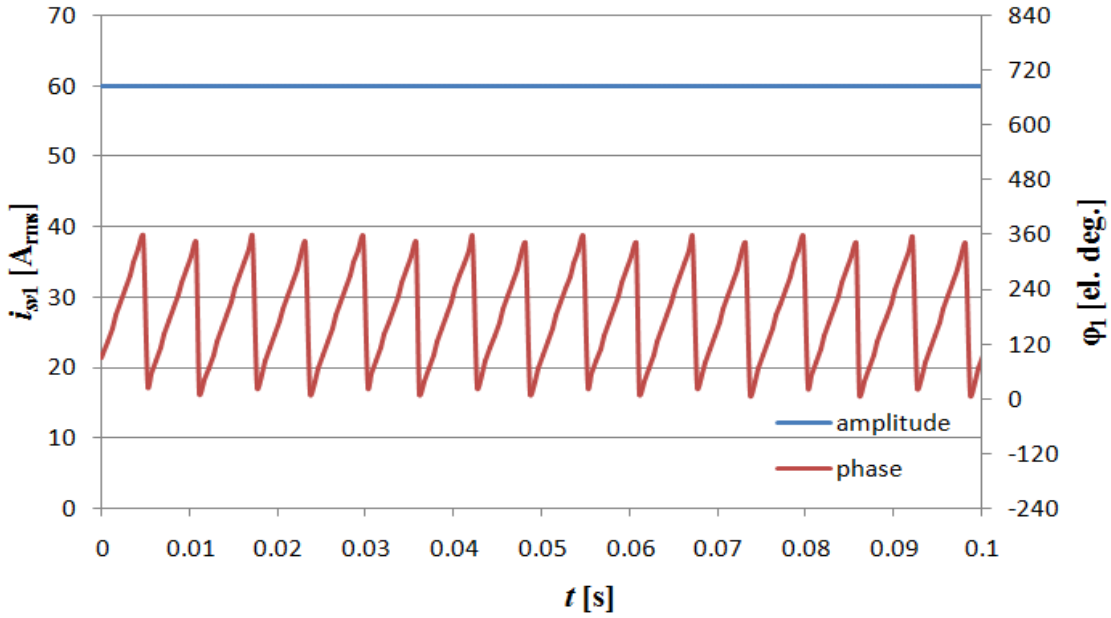

Fig. 5.35

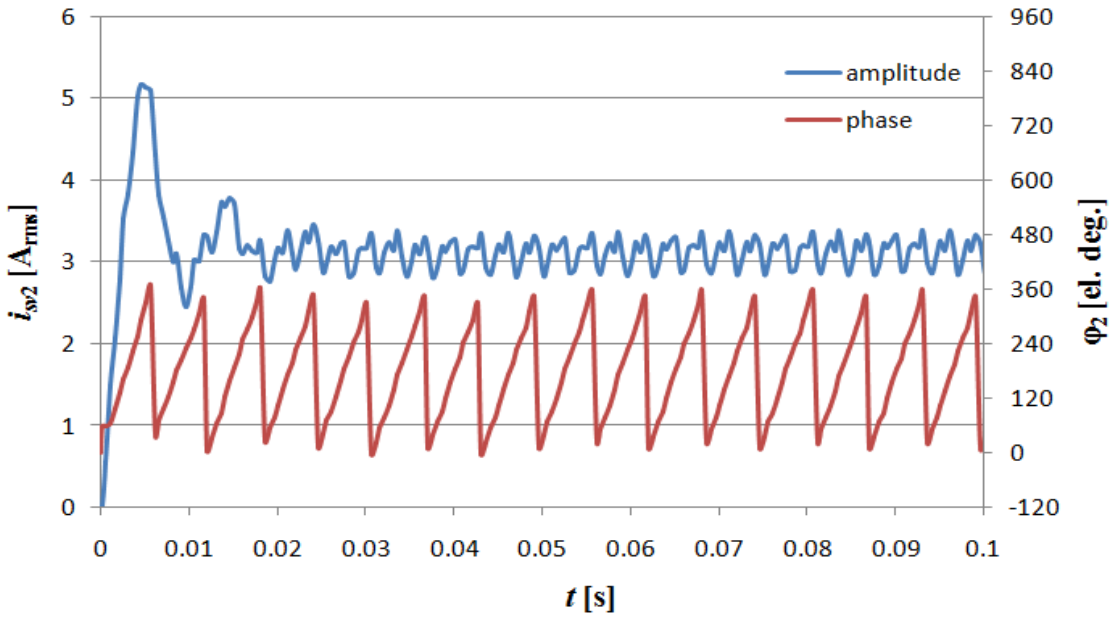

Fig. 5.36

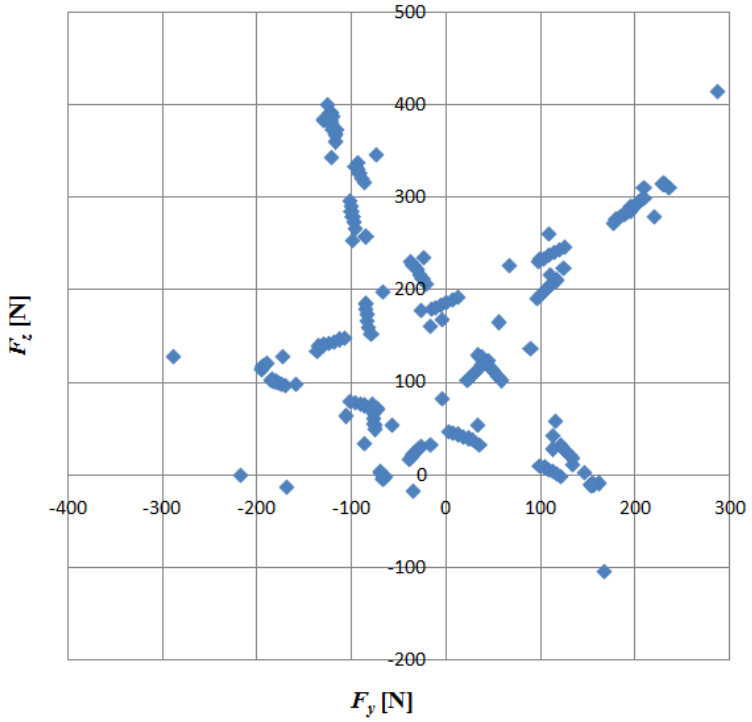

Fig. 5.37

As can be seen by comparing the obtained results with the previous, a sensible reduction of the overshoot and a faster attainment of regime condition are achieved, even if the absolute values of the PID coefficients are in general greater than in the previous attempt. It can be noted that the system behaves as if in the instant $t = 0^-$ the rotor would be perfectly centered and the motor is off; in the instant $t = 0^+$ the weight force and the other forces, produced by the interactions between stator and rotor magnetic fields, begin their action on the rotor, with the control system trying to bring it in the requested position. In the Figs. 5.38, 5.39 is shown the analyzed 5-phase bearingless motor.

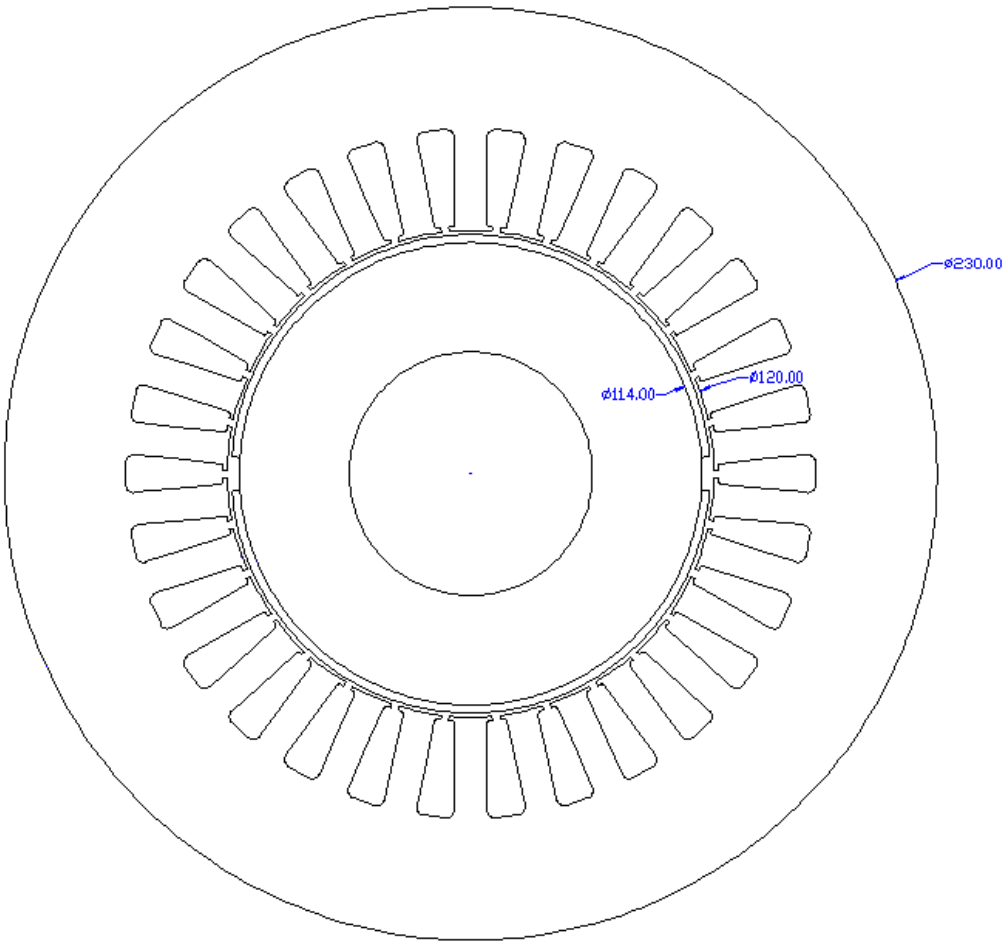

Fig. 5.38

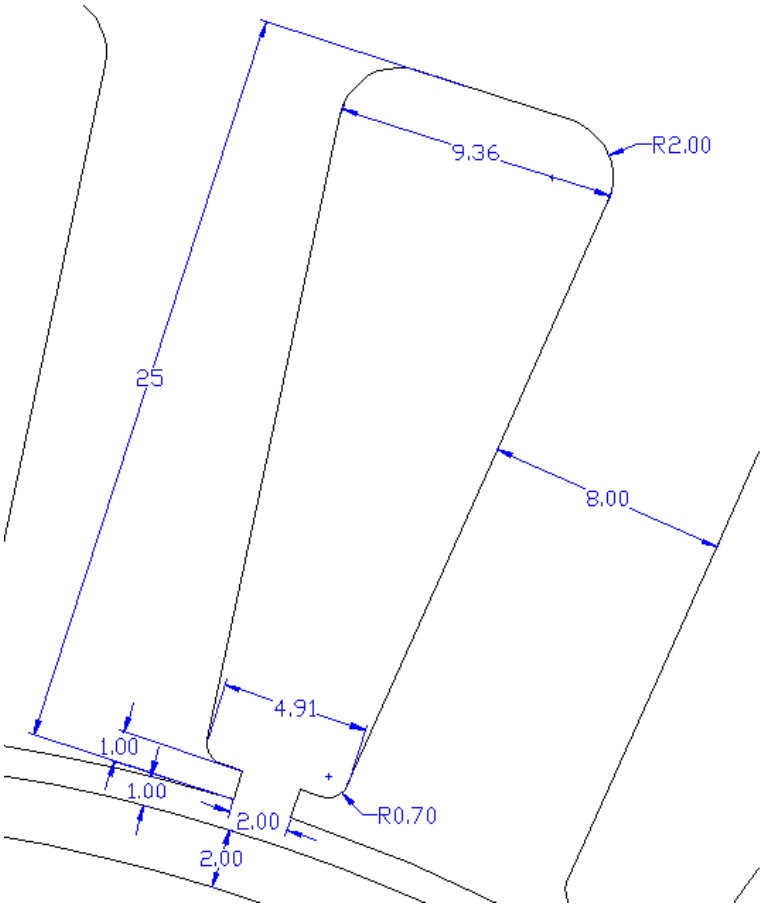

Fig. 5.39

5.7 Conclusion

In this chapter a control system for bearingless multiphase synchronous PM machines is presented, integrated by a three-dimensional mechanical model based on the Euler's equations.

The electromagnetic model of the machine, seen in Chapter 4, takes into account all the possible interactions between harmonic orders of the magnetic fields produced by the current space vector $\bar{i}_{sv1}$, which gives the torque, produced by the current space vector $\bar{i}_{sv2}$, which gives the levitation forces, and produced by rotor magnets.

Differently from other authors, which propose models that take into account only the main harmonic orders interactions between magnetic fields, the developed system is a complete one, giving in this way a more accurate modeling of the mechanical and electromagnetic phenomena.

For these reasons, it constitutes an important tool for the design of a bearingless multiphase synchronous PM machines control system and represents the design of the experimental device with related control system to realize in a test bench application.

Conclusion

The main scope of this Ph.D thesis is constituted by the non linear analysis and design of bearingless multiphase machines and drives.

The thesis work began with the development of a method to analyze the distributions of the magnetic vector potential, magnetic field and flux density in the airgap of a permanent magnet electrical machines by applying a two-dimensional model. The original contribution of the approach, inspired by a literature paper, consisted in the complete calculations to get the solution of the problem, conducted by using the techniques of mathematical analysis applied to physical and engineering problems. This model is characterized by a linear analysis.

The previous constraint of magnetic linearity is overcome by the second chapter of this Thesis, where an algorithm for the non-linear magnetic analysis of multiphase surface-mounted PM machines with semi-closed slots has been presented. Previous papers proposed the analysis of open-slot configurations with a prefixed structure of the motor, with a given number of poles and slots, or by studying only a particular position of the rotor with respect to the stator. In this work, the PM machine is represented by using a modular structure geometry. The basic element of the geometry is duplicated allowing to build up and analyze whatever typology of windings and ampere-turns distribution in a pair of poles.

In the third chapter the theme of the bearingless machines has been introduced, analyzing and describing the main concepts and ideas developed in the literature.

The fourth chapter presents an analytical model for radial forces

calculation in multiphase bearingless Surface-Mounted Permanent Magnet Synchronous Motors (SPMSM). The model allows to predict amplitude and direction of the force, depending on the values of the torque current, of the levitation current and of the rotor position. It is based on the space vectors method, letting the analysis of the machine not only in steady-state conditions but also during transients. The calculations are conducted by developing the analytical functions in Fourier series, taking all the possible interactions between stator and rotor mmf harmonic components into account. The proposed method allowed to emphasize the effects of electrical and geometrical quantities like the coil pitch, the width and length of the magnets, the rotor position, the amplitude and phase of current space vector, etc.

In the last chapter a three-dimensional mechanical model model of a bearingless multiphase synchronous PM machines has been analized. The mechanical model is based on the Euler's equations, while the electromagnetic model of the machine, developed in the previous chapter, takes into account all the possible interactions between harmonic orders of the magnetic fields produced by the current space vector mainly responsible for the torque, and by the current space vector injected for producing levitation forces. In the control model, implementd in MATLAB SIMULINK, the errors in the rotor position are used in order to calculate the components of the radial forces necessary to control the rotor axis position of the machine.

The performances of the proposed non linear model of SPMSM have been compared with those obtained by FEA software in terms of linkage fluxes, co-energy, torque and radial force. The obtained results for a traditional three-phase machine and for a 5-phase machine with unconventional winding distribution showed that the values of local and global quantities are practically coinciding, for values of the stator currents up to rated values. In addition, they are very similar also in the non-linear behavior even if very large current values are

injected. The relevant edge of the method consists in the possibility of defining the machine characteristics in a simple user interface. Then, by duplicating an elementary cell, it is possible to construct and analyze whatever typology of windings and ampere-turns distribution in a pole-pair. Furthermore, it is possible to modify the magnet width-to-pole pitch ratio analyzing various configurations in order to minimize the cogging torque, or simulating the rotor movement in sinusoidal multiphase drives or in a user-defined current distribution.

When developing a new machine design the proposed method is useful not only for the reduction of computing time, but mainly for the simplicity of changing the values of the design variables, being the numerical inputs of the problem obtained by changing some critical parameters, without the need for re-designing the model in a CAD interface. For a given rotor position and for given stator currents, the output torque as well as the radial forces acting on the moving part of a multiphase machine can be calculated. The latter feature makes the algorithm particularly suitable in order to design and analyze bearingless machines. For these reasons, it constitutes a useful tool for the design of a bearingless multiphase synchronous PM machines control system.

With reference to the control system for bearingless machines the presented model allows to calculate the radial force avoiding the errors introduced by the use of only the basic mmf harmonic components. In fact, when designing a control system for bearingless machines, many authors considered only the interaction between the main harmonic orders of the stator and rotor mmfs. In multiphase machines this can produce mistakes in determining both the module and the spatial phase of the radial force, due to the interactions between the higher harmonic orders. In addition, the proposed algorithm permits to study whatever configuration of SPMSM machine, being parameterized as a function of the electrical and geometrical quantities, like the coil pitch, the width and length of the magnets, the rotor position, the amplitude and phase of current

space vector, etc. Finally, the results of the proposed method have been compared with those of a most used FEA software, obtaining very similar values of the analyzed quantities.

In conclusion, this thesis aims to be a complete reference for the design methodologies of multiphase bearingless machines and drives, in the linear and non-linear fields of application.

List of papers

List of papers by Stefano Serri

[1] **S. Serri**, A. Tani, G. Serra, "A Method for Non-linear Analysis and Calculation of Torque and Radial Forces in Permanent Magnet Multiphase Bearingless Motors", *Proc. of SPEEDAM 2012, International Symposium on Power Electronics, Electrical Drives, Automation and Motion*, Sorrento, Italy 20-22 June, 2012, IEEE Cat. No. CFP1248A-CDR, ISBN 978-1-4673-1300-1, pp. 75-82.

[2] **S. Serri**, A. Tani, G. Serra, "Analytical Model of Radial Forces Considering Mutual Effects Between Torque and Levitation Current Space Vectors in 5-phase PM Bearingless Motors", accepted for presentation in *IECON 2013, 39th Annual Conference of the IEEE Industrial Electronics Society*, Wien, Austria, 10-13 Nov., 2013.